



Thapar University

CERTIFICATE

Certified that the thesis “**Calcifying bacteria mediated cementation for improvement of building materials**” which is submitted by **Ms. Navdeep Kaur Dhami**, in fulfillment of the requirement for the award of the degree of **Doctor of Philosophy** in the **Department of Biotechnology and Environmental Sciences**, Thapar University, Patiala, is a record of the candidate’s own independent and original research work carried out by her under our supervision and guidance. The matter embodied in this thesis has not been submitted in part or full to any other University or Institute for the award of any degree.

A handwritten signature in black ink, appearing to read 'M. Sudhakara Reddy'.

(Dr. M. Sudhakara Reddy)
Professor & Head
DBTES,
Thapar University,
Patiala – 147004
Punjab

A handwritten signature in black ink, appearing to read 'Abhijit Mukherjee'.

(Dr. Abhijit Mukherjee)
Professor
Department of Civil Engineering,
Indian Institute of Technology,
Gandhinagar - 382424
Gujarat



Thapar University

DECLARATION

I hereby declare that the work which is being presented in this thesis **“*Calcifying bacteria mediated cementation for improvement of building materials*”** submitted by me for the award of the degree of *Doctor of Philosophy* in the Department of Biotechnology and Environmental Sciences, Thapar University, Patiala, is true and original record of my own independent and original research work carried out under the supervisions of Dr. M. Sudhakara Reddy, Professor, Department of Biotechnology and Environmental Sciences, Thapar University, Patiala, India and Dr. Abhijit Mukherjee, Professor, Department of Civil Engineering, Indian Institute of Technology, Gandhinagar, Gujarat, India. The matter embodied in this thesis has not been submitted in part or full to any other university or institute for the award of any degree in India or Abroad.

Navdeep Kaur Dhani

(Navdeep Kaur Dhani)

ACKNOWLEDGEMENT

This thesis is the end of my journey in obtaining my Ph.D, probably the most challenging activity of my life yet. It was a long journey that I finished, not alone!! One of the joys of completion is to look over the past and remember all people who supported me along this long, but fulfilling road. It has been a great privilege to spend several years in the Department of Biotechnology and Environmental Sciences at Thapar University, Patiala and its members will always remain dear to me. I feel lot of nostalgia to look back on the last four years of my PhD but it's time to express my thanks to all those who contributed in many ways to the completion of this thesis and made it an unforgettable experience for me. Without these supporters, especially the selected few I'm about to mention, I may not have gotten to where I am today, at least not sanely.

I will forever be thankful to the person who made the biggest difference in my life, my supervisor, **Dr. M. Sudhakara Reddy**, Professor and Head, Department of Biotechnology and Environmental Sciences, Thapar University, Patiala. He has always been there to help me at every single step for the past four years, motivating me, guiding me and encouraging me to take up new challenges every day and tackle them with determination with optimistic attitude. It was his support which made me thrive for excellence and nothing less. His intelligent ideas, thought provoking discussions and pertinent guidance helped me sail through this tedious journey. Though during the initial times I was little apprehensive of my decision to join PhD but Dr. Reddy was always there with intelligent ideas, comprehensive understanding, serendipitous observation and vision of converting the ideas into scientific possibilities which always kept me moving forward. Besides being a supportive advisor throughout, he gave me full freedom to pursue independent work to inculcate great confidence in me. Not only has he been a great scientist, but a very kind and helpful human being. He taught me another aspect of life that “goodness

can never be defied and good human beings can never be denied”. I really feel privileged to be associated with a person like him during my life. His association with this endeavor of mine will remain a beacon light to me throughout my life. Though I will never find words to tell what I owe to him, and if I start doing it, I would not know where to stop...thanks for everything Sir...to me, professionally and personally, you are “perfection personified”.

My heart-felt gratitude goes to my second supervisor **Dr. Abhijit Mukherjee**, Professor, Department of Civil Engineering, Indian Institute of Technology, Gandhinagar, Gujarat for his expert supervision, motivation and guidance. His endless enthusiasm for research has been inspirational beyond measure during my PhD journey. I warmly thank you for your scientific inputs, valuable advice, constructive criticism and extensive discussions around my work sir!! I will remain grateful to you forever.

My special word of thanks should also go to my doctoral committee members **Dr. Maneek Kumar**, Professor, Department of Civil Engineering, Thapar University, **Dr. N. Tejo Prakash**, Professor, School of Energy and Environment, Thapar University and **Dr. N. Das**, Associate Professor, Department of Biotechnology and Environmental Sciences, Thapar University for their patient advice, valuable suggestions and motivation during every progress presentation of my PhD course. I could always look back on them for any support during for my study.

Constant motivation, constructive suggestions, meticulous approach toward science and encouragement from **Dr. Anil Kumar Dutta**, Assistant Professor, Department of Biotechnology and Environmental Sciences, Thapar University, Patiala and **Dr. Shaveta Goyal**, Associate Professor, Department of Civil Engineering, Thapar University, Patiala throughout my tenure in PhD is gratefully acknowledged. I am also indebted to all faculty members of the Department of Biotechnology and Environmental Sciences for their help and suggestions during my experimental work.

I extend my sincere word of thanks to **Dr. K. K. Raina**, Director, Thapar University, **Dr. P.K. Bajpayee**, Dean (Research and Sponsored projects) and **Dr. Sanjay Saxena**, Associate Professor, Department of Biotechnology and Environmental Sciences for their encouragement and support during the course of my PhD.

I am also grateful to **Late Dr. R.K. Jain**, Senior Scientist, Institute of Microbial Technology, Chandigarh whose association with me in the initial stages of research was a great help in accomplishing my goal.

Words fail me to express my appreciation to **Dr. M. Vasundhara**, Assistant Professor, Department of Biotechnology and Environmental Sciences for her consistent encouragement, generous care, blessing and elderly support. She was always beside me during many happy and hard moments of life to push me and motivate me. Words are short to express my gratitude to you mam!! I would also like to extend my love to **Khushi** and **Jayanth**, her kids, who have been so close to me.

My sincere thanks are to all the teachers I learnt from since my childhood. I would not have been here without their guidance, blessing and support. I would never be able to pay back the love and affection showered upon me by all my teachers.

My acknowledgement will never be complete without the special mention of all my lab seniors Dr. Pankaj, Dr. Achal, Dr. Deepika, Dr. Giri, Dr. Santosh, Dr. Himani, Dr. Harpreet and Dr. Diwakar who have taught me the lab culture and willingly devoted their valuable time whenever I needed their help.

I would like to thank all my fellow lab mates Shanky, Sakshi, Gurdeep, Balwant and Sanjay for keeping a healthy atmosphere during wonderful days of my PhD. I would like to acknowledge Sanjog and Mahima separately for being greatest friends before lab mates. I remember the times when they showed faith in me and my intellect even when I felt like digging hole and crawling into one because I didn't have faith in myself. These past several years have not been an easy ride, both academically and personally but you all stood

by my side in the thicks and thins of life and made me come out victorious at every step. I could not have asked for more than what I got from you all.

A sincere token of gratitude is also paid to my friends for their moral support and motivation whenever I was low. Dr. Puja Tandon, Shaveta, Nidhi, Bhawna, Meenu, Aditi, Seema, Gurpreet, Prerna, Charu, Aviank, Harman, Shashi, Dhakshi, Neha, Swati... the list is endless..... thanks to one and all. I really find myself lucky to have friends like them in my life. The cooperation received through my juniors Roohi, Rabia, Himani, Othima, Ishita and Manpreet is thankfully acknowledged.

Most of the results described in this thesis would not have been obtained without a close collaboration with few laboratories. I am thankful to Department of Microbiology at University of Delhi, Advanced instrumentation research facility at Jawaharlal Nehru University, National Institute of Pharmaceutical Education and Research at SAS Nagar, Punjab and Department of Civil Engineering, Indian Institute of Sciences, Bangalore, India for providing necessary facilities to carry out my research work.

I acknowledge Department of Science and Technology, Govt. of India and Council of Scientific and Industrial Research, Govt. of India for providing me with the necessary funding and fellowship to pursue my research. I would like to thank TIFAC CORE, Thapar University for providing me necessary equipments and facilities to carry out work.

I am grateful to Dr. BVV Reddy, Professor, Department of Civil Engineering, Indian Institute of Sciences, Bangalore, India for giving me an opportunity to work in his lab.

I am very thankful to Mr. Manmeet, Mr. Naminder and Mr. Vijay for their timely help and cooperation.

Most of the work would have been incomplete without the sincere support of Lab assistants. So, I owe a word of thanks to Mr. Lallan Yadav, Mr. Joga, Mr. Babban and Ms. Lalita.

I would like to recompense my veneration to the Almighty for giving me strength and patience to work through all these years so that today I can stand proud with my head held high.

Finally, I feel lacunae of words to acknowledge the people who mean the world to me, my parents and my brother. I extend my respect to my parents, my brother, my paternal and maternal grand parents and all elders to me in the family. I don't imagine a life without their love and blessings. I thank you mom and dad for showing faith in me and giving me liberty to choose what I desired. I owe you everything and wish I could show how much I love and appreciate you. I would also like to pay homage to my late maternal and paternal grandfather, who left me too soon. I wish you could have been with me for some more time. I consider myself the luckiest in the world to have such a supportive family, standing behind me with their love and support.

Date: 13 March 2014

Navdeep Kaur Dhani

Place: Patiala

(Navdeep Kaur Dhani)

I dedicate this thesis to

My parents for their constant support and unconditional love!!

The following publications are the outcome of the present research work:

1. **Dhami NK**, Mukherjee A, Reddy MS (2013). Biomineralization of calcium carbonate polymorphs by bacterial strains isolated from calcareous sites. *Journal of Microbiology and Biotechnology* 23: 707- 714.
2. **Dhami NK**, Mukherjee A, Reddy MS (2013). *Bacillus megaterium* mediated mineralization of calcium carbonate as biogenic surface treatment of Green building materials. *World Journal of Microbiology and Biotechnology*. 29: 2397 – 2406.
3. **Dhami NK**, Mukherjee A, Reddy MS (2013). Viability of calcifying bacterial formulations in fly ash for applications in restoration of building materials. *Journal of Industrial Microbiology and Biotechnology* 40: 1403 – 1412
4. **Dhami NK**, Mukherjee A, Reddy MS (2012). Improvement in strength properties of ash bricks by bacterial calcite. *Journal of Ecological Engineering* 9: 31- 35.
5. **Dhami NK**, Mukherjee A, Reddy MS (2014). Synergistic role of bacterial urease and carbonic anhydrase in carbonate mineralization. *Journal of Applied Biochemistry and Biotechnology* DOI 10.1007/s12010-013-0694-0.
6. **Dhami NK**, Mukherjee A, Reddy MS (2013). Enhancing urease production for ameliorating microbial carbonate precipitation. *Enzyme and Microbial Technology* (Communicated).
7. **Dhami NK**, Mukherjee A, Reddy MS. Biofilm and Microbial applications in Biomineralized concrete (2012). In *Advanced Topics in Biomineralization* (Ed. Jong Seto), Publisher: InTech, pp.137-164 (acknowledged amongst most highly downloadable book chapter in 2012).
8. **Dhami NK**, Mukherjee A, Reddy MS (2013). Biomineralization of calcium carbonates and their engineered applications: a review. *Frontiers of Microbiology*.

International conferences

1. **Dhami NK**, Mukherjee A, Reddy MS. Bacterial calcite as sealant of flyash mortar substrates. *Proceedings Cement and Concrete Science Conference, September 12-13, 2011*, Imperial College, London.
2. **Dhami NK**, Mukherjee A, Reddy MS. Bio mineralized carbonates as binders for construction materials. *International Conference on Bioinspired and Biobased Chemistry & Materials, October 3 – 5, 2012*, Nice, France.
3. **Dhami NK**, Mukherjee A, Reddy MS. Role of urease and carbonic anhydrase in the calcium carbonate biomineralization. *World Congress on Biotechnology, September 13-15, 2012*, Hyderabad, India,
4. **Dhami NK**, Mukherjee A, Reddy MS. Role of Bacterial calcite in enhancing the durability of low energy building materials. *International Conference on Advances in Materials Research, August 26 – 30, 2013*, COEX, Seoul, Korea,
5. **Dhami NK**, Reddy MS. Role of Bacterial urease and carbonic anhydrase and their synergism in calcium carbonate mineralization. *54th Annual Conference of Association of Microbiologists of India, November 17 – 20, 2013*, Maharishi Dayanand University, Rohtak, India.

ABSTRACT

Microbially induced calcium carbonate precipitation (MICCP) is a naturally occurring biological process in which microbes produce inorganic materials as part of their basic metabolic activities. The hydrolysis of urea by microbial urease has been found to generate carbonate ions without an associated production of protons. In the presence of calcium rich environment, calcium carbonate crystals are produced which form solid crystalline material. The evidence of ureolytic bacterial involvement in precipitation of carbonates is a new revolution in the field of industrial microbiology. The application of these bacteria for production of calcium carbonates has recently emerged as a method for protecting and consolidating decayed construction materials as carbonate crystals precipitated are highly coherent and durable. The objective of the present study was to explore calcifying bacterial diversity from alkaline soils, understand the actual function and role of bacteria in carbonate precipitation, investigate the survival of bacterial cells within the building materials and finally develop a technology for enhancing the durability of energy efficient, low cost building materials.

Ubiquitous nature of bacteria makes them ideal candidates for isolating them from extreme environments. The bacteria were isolated from calcareous soils so that they have the ability to survive in alkaline environment of various building materials. In the present work, five ureolytic and calcifying bacteria were isolated and characterized for production of various polymorphs of calcium carbonates. Role of enzymes urease and carbonic anhydrase in calcium carbonate precipitation were investigated and most efficient calcifying bacteria *Bacillus megaterium* SS3 was employed to improve the durability of various energy efficient building materials and building materials produced from industrial by products. An attempt was also made to investigate the potential of fly ash as carrier for calcifying bacterial cells for industrial applications of these builder bacteria. Optimum conditions for carbonate precipitation were also explored.

Several calcifying bacterial strains were isolated from different soils and it was found that along with urease, carbonic anhydrase enzyme also plays important role in calcium carbonate precipitation. Different bacterial isolates precipitated different carbonate polymorphs revealing strain specific precipitation by these builder bacteria. The supplementation of calcifying bacterial

cells led to positive effect on strength, porosity, permeability and durability of various low energy building materials and building materials produced from industrial by - products. The coherent and impervious nature of biological carbonates has been established from the present work. The results of present study also proved the potential of fly ash as a carrier for calcifying bacterial isolates.

The current study uncovered several aspects of the bacterially induced carbonate precipitation and elucidated that production of “carbonate crystals” by calcifying bacteria is environmentally safe and novel technology to improve the durability of low energy buildings and answer to long quest for efficient building materials.

TABLE OF CONTENTS

Chapters	Page No.
Acknowledgement	iv
List of Publications	ix
Abstract	xi
Contents	xiii
List of Figures	xxii
List of Tables	xxxii
Abbreviations	xxxv
1. Introduction	1 - 11
1.1. General Introduction	1
1.2. Gaps in the study	5
1.3. Microbial carbonate precipitation	6
1.4. Specific objectives of the thesis	11
2. Review of literature	12 - 65
2.1. Microbial biomineralization	12
2.2. Calcium carbonate precipitation	14
2.2.1. Microbially induced calcium carbonate precipitation (MICCP)	16
2.2.2. Enzyme Urease	20
2.3. Bacterial isolation source and characterization of bacterial isolates	28 - 34
2.3.1. Isolation source	28

2.3.2. <i>Phenotypic characterization</i>	32
2.3.3. <i>Molecular characterization</i>	33
2.4. Carbonic anhydrase	34 - 38
2.5. Role of Enzymes in bacterial carbonate precipitation	39 - 44
2.5.1. <i>Characteristics of bacterial ureases</i>	39
2.5.2. <i>Characteristics of bacterial Carbonic anhydrases</i>	41
2.5.3. <i>Activity Staining for Enzymes</i>	42
2.5.4. <i>Enzyme inhibitors</i>	43
2.6. Biofilm and EPS (Extracellular polymeric substances)	45- 48
2.7. Polymorphism of carbonate crystals	49 - 51
2.8. Applications of microbial carbonates in building materials	52 - 61
2.8.1. <i>Microbial calcite in cementitious materials</i>	52
2.8.2. <i>Microbial calcite in crack remediation</i>	53
2.8.3. <i>Microbial calcite in restoration of stone buildings</i>	54-56
2.8.4. <i>Microbial calcite in consolidation of sand columns</i>	57
2.8.5. <i>Microbial calcite in varying grain sized and density sand columns, low energy and industrial by-product building materials</i>	57- 61
2.9. Fly ash as a carrier material for calcifying bacterial cells	
2.9. 1. <i>Cell viability studies by Fluorescent dyes</i>	62
2.10. Response Surface Methodology (RSM) for optimization of conditions for maximum carbonate precipitation	63-65
3. Materials and methods	66 - 104
3.1. Isolation and identification of calcifying bacteria	66 - 79
3.1.1. <i>Sample collection</i>	66
3.1.2. <i>Characterization of soils</i>	66
3.1.2.1. <i>Determination of pH and electrical conductivity (EC)</i>	66
3.1.2.2. <i>Total Organic Carbon in soil (Walkley-Black method, 1934)</i>	67
3.1.2.3. <i>Elemental analysis of soils</i>	67
3.1.3. <i>Isolation and enrichment of ureolytic bacterial species</i>	67

3.1.4. Urease Assay	68
3.1.5. Precipitation on agar plates	68
3.1.6. Morphological, biochemical and physiological characterization of bacterial isolates	68
3.1.6.1. Growth kinetics of bacterial isolates	69
3.1.6.2. Gram staining	69
3.1.6.3. Capsule Staining	69
3.1.6.4. Catalase test	69
3.1.6.5. Oxidase test	70
3.1.6.6. Nitrate reduction test	70
3.1.6.7. Starch hydrolysis test	70
3.1.6.8. Alkalinity, salinity and temperature test	70
3.1.6.9. Fermentation of carbon substrate by bacterial isolates	71
3.1.6.10. Antibiotic profiling of bacterial isolates	71
3.1.7. Biofilm production	71
3.1.8. Extracellular polymeric substances production	72
3.1.9. Molecular characterization	73
3.1.9.1. Isolation of genomic DNA	73
3.1.9.2. DNA Purification	73
3.1.9.3. Electrophoresis of DNA on agarose gels	74
3.1.9.4. Spectrophotometric quantification of DNA	74
3.1.9.5. Ethidium bromide fluorescent DNA quantification	74
3.1.9.6. DNA amplification by polymerase chain reaction (PCR)	74
3.1.9.6.1. REP-PCR based DNA fingerprinting	74
3.1.9.6.2. BOX- PCR amplification	75
3.1.9.6.3. Amplification and purification of 16S rDNA	75
3.1.9.7. Ligation of 16S rDNA in pTZ57R/T vector	76
3.1.9.8. Genetic Transformation using CaCl ₂	76
3.1.9.9. Blue/white screening for recombinant plasmids	77

3.1.9.10. Isolation and purification of plasmid DNA from recombinant bacteria by alkaline lysis method	78
3.1.9.10.1. Size screening for recombinant plasmids	78
3.1.9.10.2. Restriction analysis of DNA samples by agarose gel electrophoresis	79
3.1.9.11. Sequencing	79
3.1.9.11.1. Analysis of sequence data	79
3.2. Optimum conditions and role of enzymes in CaCO ₃ precipitation	80
3.2.1. Optimization of conditions for Urease activity	80
3.2.2. Characterization of UA enzyme	81
3.2.2.1. Preparation of crude enzyme extract	81
3.2.2.2. Total protein estimation (Folin-Lowry Method) (Lowry et al., 1951)	81
3.2.2.3. Enzyme kinetics	81
3.2.2.4. SDS PAGE	82
3.2.2.5. Zymogram analysis (In gel detection of urease activity)	82
3.2.3. Estimation of Ureolytically induced calcium carbonate precipitation	82
3.2.4. Protease assay	83
3.2.5. Carbonic anhydrase activity	83
3.2.6. Optimum conditions for Carbonic anhydrase production	84
3.2.7. Characterization of CA enzyme	85
3.2.7.1.1. Preparation of crude enzyme extract	85
3.2.7.2. Enzyme kinetics	85
3.2.7.3. Activity staining	85
3.2.8. Role of Urease and Carbonic anhydrase in calcium carbonate precipitation	86
3.2.8.1. Effect of inhibitors on Enzyme activities	86
3.2.8.2. Effect of bacteria and crude enzyme extract in CaCO ₃ mineralization	87
3.2.8.3. Microbial sand plugging	88
3.2.8.4. Investigation of carbonate crystals formed by different enzyme sets	88
3.2.9. Carbonate precipitation via CA	89
3.3. Characterization of calcium carbonate crystal polymorphs	89

3.3.1. <i>Staining of crystals</i>	89
3.3.1.1. <i>Scanning electron Microscopic analysis</i>	90
3.3.1.2. <i>Confocal laser scanning microscopic analysis</i>	90
3.3.2. <i>X ray diffraction analysis</i>	91
3.3.3. <i>Fourier transform Infra red (FTIR) spectra</i>	91
3.4. <i>Evaluation of microbes for enhanced durability of various building materials</i>	91
3.4.1. <i>Preparation of varying grain sizes and density sand columns</i>	91
3.4.1.1. <i>Set up for bacterial columns</i>	91
3.4.1.2. <i>Determination of pH, EC and urea hydrolysis in bacterial and control effluents</i>	92
3.4.1.3. <i>Viability in sand columns</i>	93
3.4.2. <i>Energy efficient building materials</i>	94
3.4.3. <i>Ash bricks</i>	94
3.4.4. <i>Effect of bacterial carbonate precipitation on properties of different materials</i>	94
3.4.4.1. <i>CaCO₃ content estimation</i>	94
3.4.4.2. <i>SEM EDX and XRD</i>	94
3.4.4.3. <i>Water absorption</i>	95
3.4.4.4. <i>Rate of moisture absorption in soil cement blocks</i>	95
3.4.4.5. <i>Initial rate of absorption</i>	95
3.4.4.6. <i>Linear Expansion on saturation</i>	96
3.4.4.7. <i>Porosity</i>	96
3.4.4.8. <i>Mercury intrusion porosimetry</i>	97
3.4.4.9. <i>Wet compressive strength</i>	97
3.4.4.10. <i>Durability test of freeze thaw resistance</i>	97
3.4.4.10.1. <i>Freeze thaw resistance test</i>	97
3.5. <i>Evaluation of fly ash as carrier for calcifying bacterial cells and their viability</i>	98
3.5.1. <i>Collection of fly ash</i>	98
3.5.2. <i>Preparation of bacterial formulations</i>	98
3.5.3. <i>Stability of bacteria in formulations</i>	99
3.5.4. <i>Fluorescent dyes for studying bacterial viability</i>	99

3.5.5. <i>Scanning electron microscopic studies of bacterial formulations</i>	100
3.5.6. <i>Efficacy of Calcium Carbonate Precipitation by bacterial formulations</i>	100
3.5.6.1. <i>Calcium Carbonate Precipitation by bacterial formulations in vitro</i>	100
3.5.6.2. <i>Effect of Calcium Carbonate Precipitation by bacterial formulations in Sand plugs</i>	101
3.6. Optimization of conditions for urease and carbonate precipitation by Response surface methodology	101
3.6.1. <i>Optimization of production medium by OFAT method</i>	102
3.6.2. <i>Plackett – Burman design</i>	102
3.6.3. <i>Response surface methodology</i>	104
3.7. Statistical analysis	106
4. Results and Discussion	107 - 284
4.1. Isolation and chacterization of calcifying bacteria	105 - 128
4.1.1. <i>Isolation of CaCO₃ precipitating ureolytic bacteria</i>	107
4.1.2. <i>Calcium carbonate precipitating on agar plates</i>	111
4.1.3. <i>Morphological, biochemical & physiological characterization of bacteria</i>	112
4.1.3.1. <i>Morphological and biochemical characterization</i>	112
4.1.3.2. <i>Carbohydrate fermentation test</i>	114
4.1.3.3. <i>Antibiotic sensitivity test</i>	114
4.1.3.4. <i>Salinity, alkalinity and temperature tolerance test</i>	114
4.1.3.5. <i>Extrapolymeric substances and Biofilm production</i>	116
4.1.4 <i>Molecular characterization of bacterial isolates</i>	120
4.1.4.1. <i>BOX PCR, REP PCR and ARDRA based fingerprinting</i>	120
4.1.4.2. <i>Identification of the bacterial isolates</i>	124
<i>Conclusion and salient features</i>	128
4.2 Optimum conditions & role of enzymes in biomineralization of calcium carbonates	129 - 185
4.2.1. <i>Optimum conditions for Urease activity</i>	129
4.2.1.1. <i>Effect of different medias</i>	129
4.2.1.2. <i>Effect of varying concentrations of urea</i>	131

4.2.1.3. <i>Effect of Calcium sources and concentrations on urease activity</i>	132
4.2.1.4. <i>Effect of Nickel on urease activity</i>	137
4.2.1.5. <i>Effect of pH on urease activity</i>	139
4.2.1.6. <i>Effect of temperature on urease activity</i>	141
4.2.1.7. <i>Growth Profile</i>	143
4.2.1.8. <i>Effect of time on urease production from bacterial isolates</i>	145
4.2.1.9. <i>Specific activity of different bacterial isolates</i>	147
4.2.1.10. <i>Enzyme kinetics of Urease from different bacterial isolates</i>	148
4.2.1.11. <i>SDS PAGE of bacterial isolates</i>	150
4.2.1.12. <i>Zymography of ureases from different bacterial isolates</i>	151
4.2.2. <i>Protease activity of different bacterial isolates with time</i>	152
4.2.3. <i>Calcium carbonate precipitation via ureolytic pathway</i>	153
4.2.4. <i>Screening and characterization of carbonic anhydrase enzyme in different bacterial isolates</i>	158 - 170
4.2.4.1. <i>Carbonic anhydrase activity</i>	158
4.2.4.2. <i>Effect of time on CA activity of different bacterial isolates</i>	166
4.2.5. <i>Influence of UA and CA in calcium carbonate precipitation</i>	171 - 183
4.2.5.1. <i>Effect of inhibitors on UA and CA enzyme activity</i>	171
4.2.5.2. <i>Effect of UA and CA inhibition on CaCO₃ precipitation in vitro</i>	174
4.2.5.3. <i>Effect of UA and CA inhibition on CaCO₃ precipitation in sand plugs</i>	179
4.2.5.4. <i>Effect of UA and CA inhibition on morphology and constituents of CaCO₃ crystals</i>	180
4.2.6. <i>Calcium carbonate precipitation via CA in different bacterial isolates</i>	183
<i>Conclusion and salient features</i>	184
4.3 <i>Characterization of CaCO₃ precipitates</i>	186 – 205
4.3.1. <i>Isolation of CaCO₃ crystals</i>	186
4.3.2. <i>Characterization of CaCO₃ crystals</i>	189 - 205
4.3.2.1. <i>Methylene blue and PAS Staining of carbonate crystals</i>	189
4.3.2.2. <i>Scanning electron microscopic (SEM) and Confocal laser scanning microscopic (CLSM) analysis of carbonate crystals</i>	192

4.3.2.3. <i>Energy dispersive X ray, X ray diffraction and Fourier transmission Infra red spectroscopic analysis of carbonate crystals</i>	200
<i>Conclusion and salient features</i>	205
4.4. Application of calcifying bacteria in different building materials	207 - 259
4.4.1. <i>Evaluation of bacterial calcite in varying grain sizes and densities sand columns</i>	207- 241
4.4.1.1. <i>Effect of microbial calcite on flow rate, pH, electrical conductivity and urea hydrolysis of varying grain sizes sand columns</i>	207
4.4.1.2. <i>Effect of bacterial calcite on properties of sand columns</i>	219
4.4.1.3. <i>Effect of MICCP on varying density sand columns</i>	225
4.4.1.3.1. <i>Water absorption test</i>	227
4.4.1.3.2. <i>Compressive strength</i>	228
4.4.1.3.3. <i>Porosimetry analysis</i>	231
4.4.2. <i>Effect of Microbially induced calcium carbonate precipitation on durability of Soil cement Blocks</i>	241 - 250
4.4.2.1. <i>Absorption characteristics of Bacterial Blocks</i>	242
4.4.2.2. <i>Wet Compressive strength and linear expansion of soil cement blocks</i>	245
4.4.2.3. <i>Mercury intrusion porosimetry test</i>	247
4.4.2.4. <i>Freeze thaw resistance test and weight loss test</i>	248
4.4.2.5. <i>SEM, EDX and XRD investigations</i>	249
4.4.3. <i>Effect of Microbial calcite on properties of Ash bricks</i>	251 - 257
4.4.3.1. <i>Water absorption test</i>	252
4.4.3.2. <i>Compressive strength of bricks</i>	254
<i>Conclusion and salient features</i>	258
4.5 Efficacy of fly ash as carrier for calcifying bacterial cells	260 - 272
4.5.1. <i>Viability of calcifying bacterial cells within fly ash formulations at varying moisture and temperature till one year</i>	260 - 263
4.5.1.1. <i>Viability testing of bacterial formulations by plate count method</i>	260
4.5.1.2. <i>Viability testing of fly ash formulations via fluorescent dye 5-cyano-2,3-ditoly l tetrazolium chloride</i>	262

4.5.2. <i>Effect of time on metabolic activity of bacterial isolates, pH and moisture content of the formulations</i>	264
4.5.3. <i>Scanning electron microscopic analysis of fly ash formulations</i>	264
4.5.4. <i>Calcium carbonate precipitating efficacy of formulated bacterial cells</i>	266 - 272
4.5.4.1. <i>Efficacy of formulated bacterial cells for carbonate precipitation in vitro</i>	266
4.5.4.2. <i>Calcification efficacy of bacterial formulations within in sand plugs</i>	267
4.5.4.2.1. <i>CaCO₃ content in sand columns with formulated and control formulations</i>	267
4.5.4.2.2. <i>XRD analysis of formulated sand columns</i>	268
4.5.4.2.3. <i>Effect of formulations on properties of sand columns</i>	270
<i>Conclusion and salient features</i>	272
4.6. <i>Response Surface Methodology for enhanced urease and carbonate production</i>	273 - 284
4.6.1. <i>Selection of constituents of growth media</i>	273
<i>Conclusion and salient features</i>	284
5. Summary	285 - 290
References	291 - 322
Appendix I	323 - 331
Appendix II	332 - 341

List of Figures

- Fig. 1.1** Simplified diagram of the global carbon cycle (www.globe.gov/projects/carbon)
- Fig. 1.2** Biomineralization of calcium carbonates in natural structures a) Corals b) Ant hills c) Limestone caves (www.sciencedaily.com, www.wikipedia.org)
- Fig. 2.1** Chemical speciation of H_2CO_3 , HCO_3^- and CO_3^{2-} at 25°C
- Fig. 2.2** Coupling of urea hydrolysis and ATP generation in alkaliphilic bacteria *S. pasteurii*
- Fig. 2.3** Simplified representation of the events occurring during the microbially induced carbonate precipitation. Calcium ions in the solution are attracted to the bacterial cell wall due to the negative charge of the latter. Upon addition of urea to the bacteria, dissolved inorganic carbon (DIC) and ammonium (AMM) are released in the microenvironment of the bacteria (A). In the presence of calcium ions, this can result in a local supersaturation and hence heterogeneous precipitation of calcium carbonate on the bacterial cell wall (B). After a while, the whole cell becomes encapsulated (C), limiting nutrient transfer, resulting in cell death. Image (D) shows the imprints of bacterial cells involved in carbonate precipitation (Source: Hammes & Verstraete 2002).
- Fig. 2.4** Bacteria serving as nucleation site for CaCO_3 precipitation in the sand particles
- Fig. 2.5** pH regulation in alkaliphilic bacteria
- Fig. 2.6** Mechanism of CO_2 hydration catalyzed by CA
- Fig. 2.7** Formula of para-Nitrophenyl Acetate.
- Fig. 2.8** Regulation levels for enzyme activity. Enzymes can be regulated at transcription level or post transcription level.
- Fig. 2.9** Urease from *Bacillus pasteurii*. The green, blue and red ribbons represent α , β and γ subunits while magenta spheres are nickel ions.
- Fig. 2.10** Crystal structure of the *Neisseria gonorrhoeae* K class carbonic anhydrase. The active site Zn is shown in blue.
- Fig. 2.11** Structure of Acetohydroxamic acid

- Fig. 2.12** Structure of Acetazolamide
- Fig. 2.13** Biofilm formation (Source Montana State University Center for Biofilm Engineering)
- Fig. 2.14** Surface of a biofilm with hydrated matrix of polysaccharide and protein formed by aggregates of bacteria (<http://dujs.dartmouth.edu/fall-2009/biofilms-bacteria's-elixer-of-survival>)
- Fig. 2.15** Polymorphs of CaCO₃ (<http://www.ruhr-uni-hum.de/sediment/forschung.html>)
- Fig. 2.16** Mode of action of CTC/ DAPI fluorescent dye staining
- Fig. 3.1** Apparatus for preparing sand columns
- Fig. 3.2** Schematic illustration of moisture states of cement-based materials
- Fig. 4.1.1** Urease production by efficient ureolytic bacterial isolate on Urea agar base plate.
- Fig. 4.1.2** Comparison of urease activity (U/ml) by different bacterial isolates. Bars are mean \pm SD (n =3).
- Fig. 4.1.3** Stereomicroscopic images of CaCO₃ precipitation on carbonate precipitating plates.
- Fig. 4.1.4** EPS and Biofilm production by different bacterial isolates. Bars represent mean \pm SD (n = 3).
- Fig. 4.1.5** Protein and carbohydrate content of EPS of different bacterial isolates. Bars are mean \pm SD (n =3).
- Fig. 4.1.6** Comparison of purified genomic DNA based fingerprints generated by a) BOX-PCR and b) REP PCR for different bacterial isolates. Lane M: 1 Kb marker (Fermentas, USA).
- Fig. 4.1.7** 16S rDNA amplification of bacterial isolates. Lane M: 1 Kb marker (Fermentas)
- Fig. 4.1.8** Agarose gel electrophoresis of amplified 16S rDNA digested with restriction endonuclease a) *EcoR I* b) *Alu I* and c) *Taq I* of different bacterial strains.
- Fig. 4.1.9** Neighbor-joining tree based on bacterial 16S rDNA sequence data from different isolates of current study along with sequences available in GenBank database. Numerical values indicate bootstrap percentile from 1000 replicates.
- Fig. 4.2.1** Effect of different media on urease activity (U/ml) by bacterial isolates. Bars represent mean \pm SD (n =3)

- Fig. 4.2.2** Effect of different concentrations of urea on urease activity (U/ml) by bacterial isolates. Bars are mean \pm SD (n =3).
- Fig. 4.2.3** Effect of different calcium sources on urease activity (U/ml) by bacterial isolates. Bars are mean \pm SD (n =3)
- Fig. 4.2.4** Effect of different calcium sources on urease activity (U/ml) by bacterial isolates. Bars represent mean \pm SD (n =3)
- Fig. 4.2.5** Effect of different calcium concentrations on urease activity (U/ml) by bacterial isolates. Bars represent mean \pm SD (n =3)
- Fig. 4.2.6** Effect of varying pH on urease activity (U/ml) by bacterial isolates. Bars represent mean \pm SD (n =3)
- Fig. 4.2.7** Effect of different calcium sources on urease activity (U/ml) by bacterial isolates. Bars are mean \pm SD (n =3)
- Fig. 4.2.8** Growth profiles of bacterial isolates in NBUC media. Lines are mean \pm SD (n =3).
- Fig. 4.2.9** Urease activity by all the bacterial isolates in NBUC media at various time intervals. Lines are mean \pm SD (n =3).
- Fig. 4.2.10** Specific urease activity of all the bacterial isolates. Bars represent mean \pm SD (n =3)
- Fig. 4.2.11** SDS-PAGE bands obtained from supernatant of different isolates. M- Molecular Marker
- Fig. 4.2.12** Zymographic analysis of bacterial isolates.
- Fig. 4.2.13** Protease activity by all the bacterial isolates in nutrient media. Lines represent mean \pm SD (n =3)
- Fig. 4.2.14** Microbiologically induced CaCO₃ precipitation (a), pH (b) and urea hydrolysis (c) by different bacterial isolates NBUC media. Lines represent mean \pm SD (n =3)
- Fig. 4.2.15** Carbonic anhydrase production by bacterial isolate *B. megaterium* SS3 on p-NPA plate
- Fig. 4.2.16** Production of carbonic anhydrase by different bacterial isolates. Bars represent mean \pm SD (n =3)

- Fig. 4.2.17** Effect of different concentrations of ZnSO₄ on CA activity (U/ml) by different bacterial isolates. Bars are mean ± SD (n =3)
- Fig. 4.2.18** Effect of varying pH on carbonic anhydrase activity (U/ml) of different bacterial isolates. Lines represent mean ± SD (n =3)
- Fig. 4.2.19** Effect of varying temperature on carbonic anhydrase activity (U/ml) of different bacterial isolates. Lines represent mean ± SD (n =3)
- Fig. 4.2.20** Carbonic anhydrase activity by bacterial isolates at various time intervals. Lines represent mean ± SD (n =3).
- Fig. 4.2.21** Carbonic anhydrase activity staining of different bacterial isolates
- Fig. 4.2.22** Urease activity, Carbonic anhydrase activity and pH profile of *B. megaterium* SS3.
- Fig. 4.2.22 a** UA activity and pH profile of bacterial culture group
- Fig. 4.2.22 b** UA activity and pH profile in presence of acetohydroxamic acid (AHA)
- Fig. 4.2.22 c** CA activity and pH profile of bacterial culture group
- Fig. 4.2. 22 d** CA activity and pH profile in presence of acetazolamide (ACZ)
- Fig. 4.2. 22 e** UA activity and pH profile in presence of both AHA and ACZ
- Fig. 4.2. 22 f** CA activity and pH profile in presence of both AHA and ACZ.
- Fig. 4.2.23** Estimation of urea hydrolysis in urease induced and urease inhibited (+ AHA) bacterial culture. Lines represent mean ± SD (n =3).
- Fig. 4.2.24** Change of Ca²⁺ concentration of *Bacillus megaterium* SS3 with time under different treatments. (A) UA culture, UA culture + AHA, UA enzyme solution, UA enzyme solution + AHA (B) CA culture, CA culture + ACZ, CA enzyme solution, CA enzyme solution + ACZ (C) UA + CA culture, UA + CA culture + AHA + ACZ, UA + CA enzyme solution, UA + CA enzyme solution + AHA + ACZ.
- Fig. 4.2.25** Effect of UA inhibition (B + AHA), CA inhibition (B + ACZ) and simultaneous inhibition of UA and CA (B + AHA + ACZ) along with UA and CA induced bacterial culture (B) on calcium carbonate precipitation of *B. megaterium* SS3 in sand plugs.
- Fig. 4.2. 26** SEM images of calcium carbonate crystals (CC) associated with bacterial cells

(BC)

- Fig. 4.2.27** XRD analysis of different carbonate crystals (A) Pure calcium carbonate crystal (B) Untreated sand column (C) Bacterial treated sand column (D) Both UA and CA inhibited sand column.
- Fig. 4.2.28** Amount of Ca in a) UA and CA inhibited sand column b) bacterial treated sand column
- Fig. 4.2.29** Precipitation pattern of CaCO₃ by different CA producing bacterial isolates. Values are mean ± SD (n =3).
- Fig. 4.3.1** Precipitates of CaCO₃ crystals along the walls as well as at bottom of culture flasks inoculated with *B. megaterium* SS3, *B. cereus* SS5, *B. subtilis* SS13, *B. thuringiensis* SS15 and *L. fusiformis* SS18.
- Fig. 4.3.2** Calcium carbonate crystals precipitated by different bacterial isolates after 3 weeks. Bars represent mean ± SD.
- Fig. 4.3.3** CaCO₃ crystals of different bacterial isolates stained by Loeffler methylene blue staining (a: *B. megaterium* SS3, b: *B. cereus* SS5, c: *B. subtilis* SS 13, d: *B. thuringiensis* SS15 and e: *L. fusiformis* SS18) CC: carbonate crystals; BC: bacterial cells
- Fig. 4.3.4** CaCO₃ crystals of different bacterial isolates stained by Alcian blue PAS staining (a: *B. megaterium* SS3, b: *B. cereus* SS5, c: *B. subtilis* SS 13, d: *B. thuringiensis* SS15 and e: *L. fusiformis* SS18).
- Fig. 4.3.5** Scanning electron microscopic images of carbonate crystals precipitated by (a, b) *B. megaterium* SS3, (c, d) *B. cereus* SS5, (e, f) *B. subtilis* SS13, (g, h), *B. thuringiensis* SS15 and (i, j) *L. fusiformis* SS18. CC: carbonate crystals; BC: bacterial cells; EPS: Extra polymeric substances
- Fig. 4.3.6** Confocal laser scanning microscopic images of carbonate crystals precipitated by (a) *B. megaterium* SS3, (b) *B. cereus* SS5, (c) *B. subtilis* SS13, (d), *B. thuringiensis* SS15 and (e) *L. fusiformis* SS18.
- Fig. 4.3.7** Energy dispersive X ray spectra of carbonate crystals precipitated by (a) *B. megaterium* SS3, (b) *L. fusiformis* SS18
- Fig. 4.3.8** X ray diffraction analysis of carbonate crystals precipitated by (a) *B. megaterium*

SS3, (b) *B. cereus* SS5, (c) *B. subtilis* SS13, (d), *B. thuringiensis* SS15 and (e) *L. fusiformis* SS18.

- Fig. 4.3.9** Fourier transmission Infra red spectroscopic analysis of carbonate crystals precipitated by (a) *B. megaterium* SS3, (b) *B. cereus* SS5, (c) *B. subtilis* SS13, (d), *B. thuringiensis* SS15 and (e) *L. fusiformis* SS18.
- Fig. 4.4.1** Assembly of microbial sand columns
- Fig. 4.4.2** Estimation of flow rate in different grain sized sand columns. Bacterial sand columns (B-SC) treated with *B. megaterium* SS3 and Control sand columns (C-SC). Lines represent mean \pm SD (n = 3).
- Fig. 4.4.3** pH of the effluent from varying grain sizes sand columns. Bacterial sand columns (B-SC) treated with *B. megaterium* SS3 and Control sand columns (C-SC). Lines represent mean \pm SD (n = 3).
- Fig. 4.4.4.** Electrical conductivity of the effluent from varying grain sizes sand columns. Bacterial sand columns (B-SC) treated with *B. megaterium* SS3 and Control sand columns (C-SC). Lines represent mean \pm SD (n = 3).
- Fig. 4.4.5** Estimation of urea hydrolysis in the effluent from varying grain sizes bacterial treated and control sand columns. Lines represent mean \pm SD (n = 3).
- Fig. 4.4.6** Live viable cells in the effluent (red) of bacterial treated sand column
- Fig. 4.4.7** Layer of carbonate crystals (CC) on the surface of bacterial sand column (B-SC) treated with *B. megaterium* SS3 along with collapsed control sand column (C-SC)
- Fig. 4.4.8** Calcite content in the different layers of bacterial sand columns (B-SC) of varying grain sizes. Bars represent mean \pm SD (n = 3).
- Fig. 4.4.9** Scanning electron microscopic analysis of sand columns a,b) control sand column (C-SC) c,d) bacterial sand column (B-SC) depicting the formation of carbonate crystals (CC) and bacterial cells (BC)
- Fig. 4.4.10** Energy dispersive x ray spectra of a) Control sand column b) Bacterial sand column presenting the abundant amount of Ca
- Fig. 4.4.11** X ray diffraction spectra of a) control sand column b) microbial sand column representing the presence of calcite as well as vaterite peaks

- Fig. 4.4.12** Effect of carbonate crystal (CC) precipitation on surface of bacterial sand column (B-SC) treated with *B. megaterium* SS3 compared to control sand column (C-SC).
- Fig. 4.4.13** Influence of the bacterial treatment on water absorption of varying density sand columns. Bars represent mean \pm SD (n = 3).
- Fig. 4.4.14** Machine showing set up for measurement of Compressive strength
- Fig. 4.4.15** Influence of the bacterial treatment on water absorption of varying density sand columns. Bars represent mean \pm SD (n = 3).
- Fig. 4.4.16** Pore size distribution curve of bacterial and control specimens
- Fig. 4.4.17** Energy dispersive X ray spectrum of varying density sizes bacterial columns (a: 1.65g/cc; b: 1.70g/cc; c: 1.75g/cc)
- Fig. 4.4.18** X ray diffraction analysis of a) 1.70 g/cc density control sand column b) 1.70 g/cc density bacterial sand column
- Fig. 4.4.19** Set up for making soil cement blocks
- Fig. 4.4. 20** Effect of MICP on a) rate of water absorption b) saturated water content in soil cement blocks. Lines and bars are mean \pm SD (n = 3).
- Fig. 4.4. 21** Set up for a) compressive strength b,c,d) Linear expansion test
- Fig. 4.4. 22** Effect of MICP on a) Compressive strength b) Linear expansion of soil cement blocks. Bars are mean \pm SD (n = 3).
- Fig. 4.4. 23** Effect of MICP on a) freeze thaw strength test b) weight loss test of soil cement blocks. Values are mean \pm SD (n = 3).
- Fig. 4.4. 24** a,b) Scanning electron microscopic images c,d) Energy dispersive X ray spectrum e) X ray diffraction analysis of bacterial treated soil cement blocks.
- Fig. 4.4. 25** Deposition of CaCO₃ on the surface of Bacterial treated brick (BB) of fly ash along with untreated control brick (CB)
- Fig. 4.4. 26** Effect of MICCP on a) water absorption b) Initial rate of water absorption in ash bricks [B-RHAB: Bacterial treated rice husk ash bricks, U-RHAB: untreated rice husk ash bricks, B-FAB: Bacterial treated fly ash bricks, U-FAB: untreated fly ash bricks]. Bars represent mean \pm SD (n = 3).

- Fig. 4.4. 27** Effect of MICCP on a) Compressive strength after 3,7,14 and 28 days b) Freeze thaw resistance strength in ash bricks [B-RHAB: Bacterial treated rice husk ash bricks, U-RHAB: untreated rice husk ash bricks, B-FAB: Bacterial treated fly ash bricks, U-FAB: untreated fly ash bricks] Bars represent Mean \pm SD (n = 3).
- Fig. 4.4. 28** Scanning electron micrograph of a) control brick sample b, c) bacterially treated fly ash bricks depicting the presence of carbonate crystals (CC) and bacterial cells (BC).
- Fig. 4.4. 29** XRD analysis of a) crystals precipitated on rice husk ash bricks (collected after 4 weeks) by application of *B. megaterium* SS3 (b) control rice husk ash brick. No calcite peaks were seen.
- Fig. 4.5.1** Viability of various inoculum formulations at varying temperatures (4°C, 25°C and 37°C) and moisture contents (30%, 40%, 50%) over a period of 1 year. a, b, c) *Bacillus cereus* SS5 (BC), d, e, f) *Bacillus megaterium* SS3 (BM), g, h, i) *Lysinibacillus fusiformis* SS18 (LF)
- Fig. 4.5.2** Confocal laser scanning microscopy of bacterial formulations after staining with CTC and SYTO green where red colour indicates CTC reduction and green colour indicates total count. Different panels depict different spectra (green channel, red channel and superimposed green & red channels) a) *B. cereus* SS5, b) *B. megaterium* SS3, c) *L. fusiformis* SS18.
- Fig. 4.5.3** Scanning electron micrography of different inoculum formulations. a, b) Fly ash, c, d) *B. cereus* SS5 formulation, e, f) *B. megaterium* SS3 formulation, g, h) *L. fusiformis* SS18 formulation.
- Fig. 4.5.4** Amount of insoluble Ca²⁺ concentration in fresh bacterial cells, formulated bacterial cells and control solution at different time intervals.
- Fig. 4.5.5** CaCO₃ content in control sand column (C - SC), formulated bacterial cells sand column (For - BSC) and fresh bacterial cells sand column (F - BSC).
- Fig. 4.5.6** X ray diffraction pattern of carbonate crystals precipitated in fresh bacterial cells sand column (F - BSC), formulated bacterial cell sand column (For - BSC) and control sand column (C - SC).
- Fig. 4.5.7** Influence of microbial calcite deposition on water absorption in control sand

columns (C - SC), formulated bacterial sand columns (For - BSC) and fresh bacterial sand columns (F - BSC).

Fig. 4.6.1 a) Effect of different carbon sources b) nitrogen sources and c) bacterial inoculums concentration on urease production in *B. megaterium* SS3

Fig. 4.6.2 a) Surface plot showing the effect of Urea and glucose on urease production b) Surface plot showing the effect of Urea and NaHCO₃ on urease production c) Surface plot showing the effect of NaHCO₃ and glucose on urease production

Fig. 4.6.3 a) Contour plot between effect of Urea and glucose on urease production b) Contour plot between effect of Urea and NaHCO₃ on urease production c) Contour plot between effect of NaHCO₃ and glucose on urease production.

List of Tables

Table 2.1. Examples of precipitation through organic acid utilisation

Table 2.2: Reaction conditions reported in the literature for production of CaCO_3 via urea hydrolysis

Table 2.3. Overview of different applications where microbial calcite is used as biocement in cementitious materials.

Table 2.4. Overview of different methodologies where microbial calcite has been deposited as a layer on surface of stone.

Table 2.5. Energy in basic building materials

Table 2.6. Plackett Burman design matrix for screening the variables influencing Urease activity.

Table 2.7. Central composite design showing combinations of independent variables of medium ingredients

Table 4.1.1. Physicochemical characteristics of various soils

Table 4.1.2. Population of bacteria in different sources per gram of soil

Table 4.1.3. Comparison of urease activity (U/ml) by different bacterial isolates

Table 4.1.4. Biochemical characterization of calcifying bacterial isolates of the present study

Table 4.1.5. Fermentation of carbon substrates and antibiotic profiling of bacterial isolates of the present study

Table 4.1.6. Effect of sodium chloride concentration, temperature and pH on the growth of bacterial isolates

Table 4.1.7. Comparison of EPS and biofilm productions by the bacterial isolates

Table 4.1.8. Protein and carbohydrate content of EPS isolated from different bacterial isolates

Table 4.1.9. Percentage similarity of 16S rDNA sequences of bacterial isolates using multiple sequence alignment (ClustalW)

Table 4.1.10. Bacterial isolates and their closest relative species inferred from 16S rRNA gene sequences of NCBI database

Table 4.2.1. Optimization of growth media for maximum urease (U/ml) production by different bacterial isolates.

- Table 4.2.2** Optimization of urea concentration for maximum urease (U/ml) production by different bacterial isolates.
- Table 4.2.4** Optimization of calcium concentration for maximum urease (U/ml) production by different bacterial isolates
- Table 4.2.5** Optimization of Nickel concentration for maximum urease (U/ml) production by different bacterial isolates
- Table 4.2.6.** Effect of pH on Urease activity (U/ml) of different bacterial isolates
- Table 4.2.7.** Optimization of temperature for maximum urease (U/ml) production by different bacterial isolates
- Table 4.2.8.** Comparison of urease activity (U/ml) produced by the bacterial isolates at different time intervals
- Table 4.2.9.** Comparison of specific urease activity (U/ml) by different bacterial isolates
- Table 4.2.10.** Enzyme kinetics of Ureases from different bacterial isolates
- Table 4.2.12.** Calcium carbonate precipitation, pH profile and urea hydrolysis by ureolytic bacterial isolates at different time intervals
- Table 4.2.13.** Comparison of carbonic anhydrase activity (U/ml) produced by different bacterial isolates
- Table 4.2.14.** Optimization of Zinc for maximum CA activity (U/ml) by different bacterial isolates.
- Table 4.2.15.** Effect of pH on carbonic anhydrase activity (U/ml) of different bacterial isolates
- Table 4.2.16.** Effect of temperature on carbonic anhydrase activity (U/ml) of different bacterial isolates
- Table 4.2.17.** Comparison of carbonic anhydrase activity (U/ml) produced by the bacterial isolates at different time intervals
- Table 4.2.18.** Enzyme kinetics of crude carbonic anhydrases from different bacterial isolates
- Table 4.2.19.** Urea hydrolysis in case of bacterial culture and urease inhibited bacterial culture
- Table 4.2.20.** Amount of calcite precipitation in sand plugs treated with bacterial culture and bacterial culture supplemented with UA and CA inhibitors
- Table 4.2.21.** Amount of insoluble Ca^{2+} precipitated by different bacterial isolates over different intervals of time via CA pathway

Table 4.3.1. Calcium carbonate crystals precipitated by different bacterial isolates after 3 weeks.

Table 4.4.1. Flow rate of media from varying grain sizes bacterial treated and control sand columns

Table 4.4.2. pH of the effluent from varying grain sizes bacterial treated and control sand columns

Table 4.4.3. Electrical conductivity of the effluent from varying grain sizes bacterial treated and control sand columns.

Table 4.4.4. Estimation of urea hydrolysis in the effluent from varying grain sizes bacterial treated and control sand columns.

Table 4.4.6. Effect of microbial calcite precipitation on water absorption of varying density (1.65 g/cc, 1.70 g/cc and 1.75 g/cc) sand columns

Table 4.4.7. Effect of microbial calcium carbonate precipitation on compressive strength of varying density sand columns (1.65 g/cc, 1.70 g/cc and 1.75 g/cc)

Table 4.4.8 a) Mercury intrusion porosimetry of Control sand column (density 1.70 g/cc)

Table 4.4.8 b) Mercury intrusion porosimetry of bacterial sand column (density 1.70 g/cc)

Table.4.4.9. Mercury intrusion porosimetry analysis of control and bacteria treated blocks with 1.70g/cc density.

Table 4.4.10 a. Effect of bacterial treatment on the rate of water absorption by Soil cement blocks at different time intervals

Table 4.4.10 b. Effect of bacterial treatment on saturated water content of soil cement blocks

Table 4.4.11. Effect of microbial calcite precipitation on Compressive strength and linear expansion of soil cement blocks

Table 4.4.12. Effect of MICP on porosity of soil cement blocks by Mercury intrusion porosimetry analysis

Table 4.4.13. Effect of MICP on freeze thaw strength test and weight loss durability test of soil cement blocks.

Table 4.4.15. Effect of MICP on water absorption and Initial rate of absorption in case of rice husk ash (RHAB) and fly ash bricks (FAB)

Table 4.4.16. Effect of MICP on compressive strength (after 28 days) and freeze thaw resistance test of rice husk ash (RHAB) and fly ash bricks (FAB)

Table 4.4.16. EDX analysis of bacterial treated (B-RHAB) and untreated (U-RHAB) rice husk ash bricks and bacterial treated (B-FAB) and untreated (U-FAB) fly ash bricks.

Table. 4.5.1. Physico chemical characteristics of fly ash

Table. 4.5.2. Mercury intrusion porosimetry analysis of control sand columns (C - SC), formulated bacterial sand columns (For - BSC) and fresh bacterial sand columns (F - BSC).

Table 4.6.1. Placket Burman design matrix for screening the variables influencing Urease activity.

Table 4.6.2. Analysis of variance for urease activity by different factors using Placket Burman design.

Table 4.6.3. Experimental Design and results of CCD of response surface methodology.

Table 4.6.4. ANOVA for Urease activity using CCD of response surface methodology.

Abbreviations

Abbreviation	Word (s)
MICCP	Microbiologically Induced Calcium carbonate Precipitation
MICP	Microbially induced calcite precipitation
SEM	Scanning Electron Micrography
CSLM	Confocal laser scanning microscope
FTIR	Fourier transmission infra red spectroscope
XRD	X-Ray Diffraction
IS	Indian Standard (Code)
ASTM	American society for testing and materials
RSM	Response surface methodology
ANOVA	Analysis of Variance
EPS	Extracellular Polymeric Substances
MTCC	Microbial Type Cell Culture
DNA	Deoxyribonucleic Acid
RNA	Ribonucleic Acid

Chapter 1

Introduction

1.1 General Introduction

Several microorganisms have properties of interest for various biotechnological applications. A Japanese researcher first coined the term “Biom mineralization” in 1940s and interest began to grow in the study of this phenomenon (Watabe *et al.*, 1958; 1960). Biom mineralization of carbonates is a common and ubiquitous process, forms natural rocks, limestone, marble, calcareous sandstones and exists in environments such as marine water, fresh water, caves and soils (Hammes *et al.*, 2003). This process is considered as one of the main natural processes controlling CO₂ levels in the atmosphere both in past and present times and forms dynamic component of global carbon cycle. The carbonates account for around 78.5% of the total carbon concentration on earth (Klein and Hurlbut, 1999; Hammes and Verstraete, 2002). Most of the carbonate minerals have been found to be precipitated as calcium carbonates (CaCO₃) and amongst the various polymorphs of calcium carbonate; calcite constitutes around 4% by weight of the Earth’s crust (Hammes and Verstraete, 2002). Although the role of microbes in these mineral carbonates was absent in the initial stages but microbiological involvement in precipitation of these biominerals came to prominence since the beginning of previous century (Feldmann, 1997; Drew, 1914). Huge limestone formations on the sea bottom have to a large extent resulted from great thickness of calcareous materials from pelagic skeletal organisms (such as coccolithophores and foraminifera) (Klein and Hurlbut, 1999; Morse, 2003). The precipitation of these carbonates has been seen to occur via abiotic as well as biotic pathways. Abiotic precipitation occurs in supersaturated solutions through evaporation, temperature increases, and pressure decreases (Castanier *et al.*, 1999). Biotic precipitation can be either biotically controlled or biotically induced. When an organism exerts some sort of control over the location, size and composition of the minerals formed, like skeletons and shells, the process is said to be biotically *controlled*. If the precipitation arises as a result of the metabolic activity of an

organism, and the organism has little or no control over the mineralization, the process is biotically *induced* (Frankel and Bazylinski, 2003).

Though bacterial contribution to the extensive carbonate formations had been suspected for some time (Drew, 1910) but it remained controversial until recent investigations involving microbial pathways and required precipitation conditions, which indicated that bacteria have the potential to far exceed the abiotic contribution to calcium carbonate deposition in most environments on Earth (Castanier *et al.*, 2000) (Fig. 1.1).

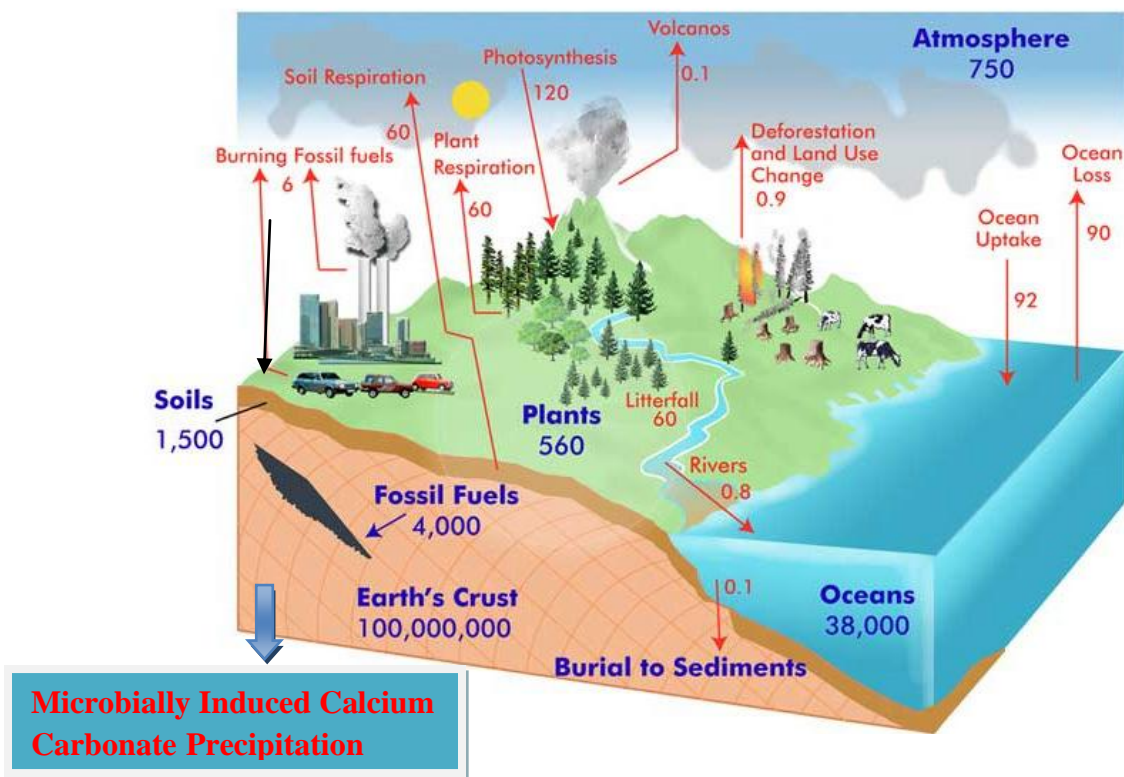


Fig.1.1. Simplified diagram of the global carbon cycle (www.globe.gov/projects/carbon)

The formation of shells in molluscs, urchin spines and fish otoliths are also results of carbonate mineralization (Rodriguez Navarro *et al.*, 2012). It has been shown that the cellular organelles that are largely responsible for the production of carbonate shells in eukaryotic organisms are the mitochondria (or chloroplasts). These organelles are widely considered as primitive endosymbiotic bacteria, which further supports the bacterial contribution to carbonate precipitation (Castanier *et al.*, 2000). Due to high surface to

volume ratio, bacteria are ideal crystal nucleation sites (Warren and Haack, 2001). Moreover, bacteria are omnipresent. Near the ground surface more than 10^{14} bacteria exist per kilogram of soil (Rodriguez Navarro *et al.*, 2012). Bacterium's ability to interact with metals is dependent on the types and densities of functional groups, which are further affected by cell wall composition, presence of S layers, sheaths, capsules or extracellular polymeric substances (Hammes *et al.*, 20003).

Naturally, bio-mineralization of calcium carbonates by microbes is also evident from formation of commonly seen structures like ant hills, coral reefs, caves etc (Fig. 1.2). These structures are not only highly durable, but also possess the property of self healing. Role of microorganisms in providing strength to these structures has paved way for exploration of this process and applications of these microorganisms in variety of fields including Biotechnology, Microbiology, Biogeochemistry, Geology, Paleobiology, Nanotechnology and Civil engineering as well. The last two decades witnessed remarkable progress in the field of biomineralization along the role of bacteria because of advanced microbiological as well as molecular research techniques (McGenity and Sellwood, 1999).

Degradation of building materials is a topic of current concern. Many beautiful historic and monumental buildings have deteriorated with time. Increased population as well as ageing infrastructure are imposing an unprecedented demand on infrastructure, which requires sustainable technologies to meet society's needs (DeJong *et al.*, 2011). The impact of durability related problems on national economies is substantial and reflected by the huge sums of money spent on maintenance and repair of such structures. Weathering, earthquakes, human activities etc. are all contributing heavily to deterioration of valuable natural and man made structures. Though synthetic agents like epoxies, silanes and siloxanes are being used since long but they come with many disadvantages like thermal expansion with time, degradation with age, disposal problems and need for constant maintenance (De Muynck *et al.*, 2010). Many a times repair is to be carried out in the area which is not easily accessible and hazardous for human beings. Under such circumstances, there is need for self healing of these materials. The technique should be such that it not only

enhances the durability of affected building, heal them in a continuous way but is also eco friendly.

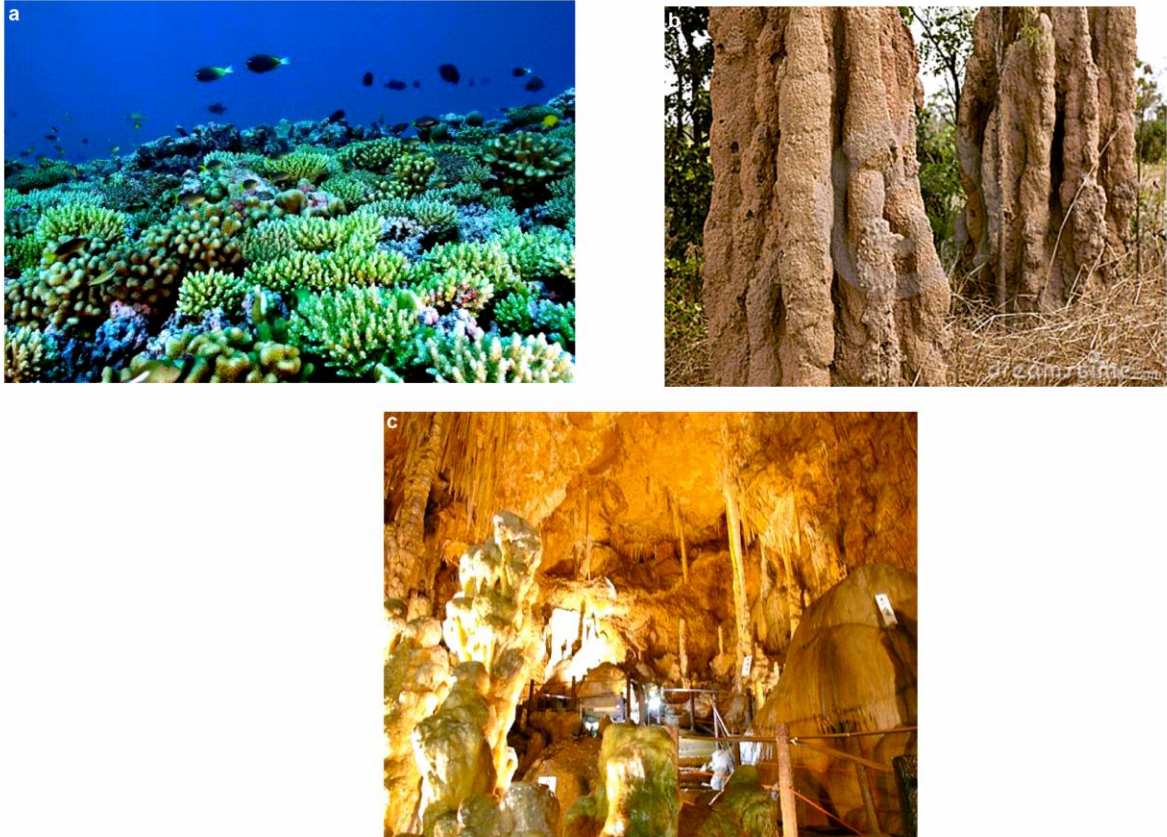


Fig. 1.2. Biomaterialization of calcium carbonates in natural structures a) Corals b) Ant hills c) Limestone caves (www.sciencedaily.com, www.wikipedia.org)

Today innovation is leadingly inspired by nature. Taking notes from *biomimicry* and *biotechnology*, the best solution for all these problems is continuous precipitation of durable carbonates by microorganisms at such places. Investigations have been carried out to synthesize calcium carbonates the way nature does as microorganisms are capable of precipitation of carbonaceous minerals, specifically calcium carbonates (CaCO_3). The fundamental microbial processes involved in precipitation of bacterial carbonates, their polymorphs have been investigated and Microbially induced calcium carbonate precipitation

(MICCP) has been developed as a potential technique to remediate and restore various building materials. This technology offers the benefit of being novel, eco-friendly and possesses the ability of self healing. Application of these calcifying builder bacteria for bioremediation purposes seems to be promising and sustainable solution for improving the properties of building materials. Though *Applied microbiology* and *Biotechnology* are long been used for applications in chemical and pharmaceutical industries, agricultural, medicine, food and feed sectors (Jargeat *et al.*, 2000; Singh and Cameotra, 2004; Gavrilesco and Chisti, 2005; Whiteley and Lee, 2006), the evidence of bacterial involvement in mineralisation of carbonates is a new revolution in the field of industrial microbiology, environment, geo technology, chemistry and civil engineering (De Jong *et al.*, 2013).

1.2. Gaps in the study

Under natural conditions, the precipitation of carbonates occurs very slowly over long geological times but in order to produce large amounts of carbonates shortly there is need to look for microorganisms with the ability to create conditions for precipitation of carbonates in shorter times. Different bacterial species precipitate carbonates in alkaline environments rich in Ca^{2+} ions and various mechanisms which could induce precipitation by bacteria in natural habitats have been proposed (Erlich, 1996; Rivadeneyra, 2004). *However, the precise role of bacteria and bacterial activities in carbonate crystallization remains unclear, although they seem to fall in 3 categories:*

- As per the first hypothesis, mineralization occurs as a byproduct of microbial metabolism involving autotrophic or heterotrophic pathways which includes enzymatic hydrolysis of urea/ dissimilatory reduction of nitrate and sulphate/ intracellular calcium metabolism (Rivadeneyra *et al.*, 1994; Douglas and Beveridge, 1998; Castanier *et al.*, 1999; Lian *et al.*, 2006);
- as per second hypothesis, carbonate nucleation takes place on the cell wall (Castanier *et al.*, 2000; Rivadeneyra *et al.*, 1998)
- third hypothesis involves role of extracellular macromolecules (Ercole *et al.*, 2007; Decho *et al.*, 2009).

Although several studies have helped in understanding contemporary settings of calcification, deciphering the biocalcification process is still at the very beginning. Among all the above processes, hydrolysis of urea by ureolytic bacteria has been found to be the most favored pathway for biotechnological applications as it can be easily controlled, allows the production of high concentration of carbonates within a short period of time, common occurrence of ureolytic bacteria in soil and aquatic environments and also because urea is fairly inexpensive substrate (De Muynck *et al.*, 2010). But before the application of such microorganisms, there is need for selection of certain parameters of bacteria as:

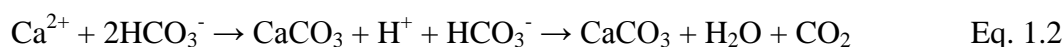
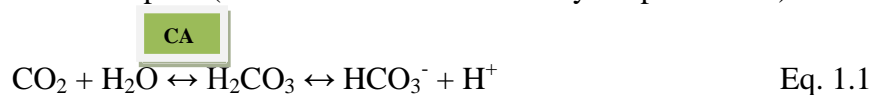
- It must be non-pathogenic and non-genetically modified
- It should not contain any transferable elements that may increase the pathogenicity of environmental strains (*e.g.* antibiotic resistance)
- It should possess high ureolytic and calcifying efficiency
- It should be alkaliphilic
- It should possess ability to deposit carbonates homogeneously on the substratum

1.3. Microbial carbonate precipitation

Ureolytic bacteria especially *Sporosarcina pasteurii* has generated lot of interest in the area of bioremediation and studied extensively (Ramakrishnan *et al.*, 1998; Fujita *et al.*, 2000; Bang *et al.*, 2001; Hammes *et al.*, 2003; Dick *et al.*, 2006; De Muynck *et al.*, 2007; Ercole *et al.*, 2007). The ureolytic bacteria uses urea as energy source to produce dissolved ammonium, dissolved inorganic carbon and CO₂. The ammonia released in the surroundings subsequently increases the pH, leading to accumulation of insoluble CaCO₃ in calcium rich environment.

Researchers from worldwide are now harnessing various such ureolytic bacteria for long term remediation of various building materials but not much alkaliphilic bacterial species have been reported. Much of the bacterial diversity capable of calcification still needs to be explored. Other species might prove to be even more efficient than already known bacterial isolates in precipitation of carbonates. The diversity of bacteria from alkaline sites will give valuable information about the microbes and their applications in calcification.

Another enzyme which has fetched the attention of various researchers in CaCO₃ precipitation studies is Carbonic anhydrase (CA). This enzyme is ubiquitously distributed in organisms (Smith and Ferry, 2000). The role of biological CA in calcification of marine invertebrates (mollusks), fish otoliths, corals and hard tissues of vertebrates has been known since long. The problem of CO₂ emissions invited researchers from around the globe who looked for efficient and economical ways for its sequestration and found that hydration of CO₂ is the slowest step in its sequestration (Bond *et al.*, 2001, Mirjafari, *et al.*, 2007). CA was found to be the most potential biological catalyst for this reaction as it aides in the CO₂ hydration reaction at fastest pace (10⁴ - 10⁶ reactions are catalyzed per second) as:



The sequestration of CO₂ into CaCO₃ by CA has paved way for application of this enzyme in biomineralization of bacterial carbonates. Though lot of work has been done on application of bovine CA in CaCO₃ precipitation, but not much has been reported on the role of bacterial CA in precipitation of carbonates which makes the investigation of this enzyme from bacterial sources quite imperative. Investigation of this enzyme from bacteria, its role in CaCO₃ precipitation and its relation to urease needs to be determined yet.

Microbial extracellular polymeric substances (EPS) and biofilm have also been reported to play important role in calcium carbonate precipitation by many researchers (Merz-Preiss and Riding, 1999; Braissant *et al.*, 2003; Dick *et al.*, 2006; Decho, 2009; Dittrich and Sibling, 2010; Ercole *et al.*, 2012). But not much work has been done on contribution of these extracellular molecules in bacterially induced calcium carbonate precipitation. Study of these macromolecules will also pave way in unfolding the details of these structures in bacterially induced CaCO₃ precipitation.

Though the process of microbially induced calcium carbonate precipitation seems fairly simple but much needs to be investigated yet. Since the discovery that MICCP can be applied for remediation of building materials, several researchers tried to optimize its performance. Most of the work has been targeted on microbial aspects like microorganisms

involved, metabolic pathways followed etc. There is need to improve the effectiveness of this technology by studying the influence of other bacterial as well as chemical aspects also. Better understanding of the fundamental principles and more suitable conditions for production of enzymes involved is required for enhanced carbonate precipitation. In nutshell, this will pave way for improved understanding of various aspects of microbiology, ecology, physiology and enzymology of this process paving way for more commercial applications.

Biomining of calcium carbonate results in the production of different phases of calcium carbonate as anhydrous polymorphs: calcite, aragonite and vaterite or two hydrated crystalline phases, monohydrocalcite ($\text{CaCO}_3 \cdot \text{H}_2\text{O}$) and ikaite ($\text{CaCO}_3 \cdot 6\text{H}_2\text{O}$) (Rodriguez Navarro *et al.*, 2012). Despite extensive studies on bacterial carbonatogenesis, little is known about these polymorphs. Besides its scientific interest, different calcium carbonate polymorphs have important technical implications as in the case of bacterial conservation of building materials, formation of coherent, durable, carbonates is required. This will not be achievable if metastable polymorphs are formed. Much more studies need to be carried out to characterize the various calcium carbonate polymorphs formed by different bacterial species which will underpin the basic biotechnological applications of these builder bacteria in various fields.

With the destruction of our ecological environment, soil and sand properties have worsened heavily to allow some infrastructure construction. Current techniques in practice include grouting via cement, chemicals, compaction, fracture and jet, micro piles, jacked piers, ground anchors, soil nailing vibro compaction etc. all of which are hazardous/toxic (De Jong *et al.*, 2010). With over 40,000 yearly projects and approximately \$6 billion/ year worldwide in the industry, new techniques for consolidation of these materials have become necessary. Application of Microbially induced calcium carbonate precipitation (MICCP) for consolidation of loose sands has been found to be the most innovative and sustainable solution by many researchers (Whiffin, 2004; van Paassen *et al.*, 2004; De Jong *et al.*, 2006). Ureolytic bacteria supplied with a solution of urea and calcium, precipitate calcite crystals within the sand column which forms cementing bridges between the existing sand

grains. The application of these ureolytic bacteria in consolidation of various sand columns has been carried out by many and these bacterial biominerals have proven promising results in improving the mechanical properties of cemented deposits (De Jong *et al.*, 2006; Achal *et al.*, 2009; Harkes *et al.*, 2010; Fujita *et al.*, 2011; Al Qabany, 2011; Thawadi, 2011).

One of the fundamental properties that determines porosity, permeability and hence strength of sand is its size distribution and grain size (Wang *et al.*, 2010). Till now, no work has been reported on optimum grain sizes and density sand columns for maximum clogging by bacterial calcite binders. The application of these builder bacteria on varying grain sizes and density sand columns needs to be studied in detail as it will elucidate the effect of microbial calcite on these columns for various commercial applications. This work will contextualize the most optimum size and densities of sand columns for maximum consolidation and strength.

Selection of materials and technologies for the building construction should satisfy the felt needs of the user as well as the development needs of the society, without causing any adverse impact on environment. Manufacturing processes of building materials contribute green house gases like CO₂ to the atmosphere. Awareness on environmental aspects is increasing in the building and construction sector and there is a great concern and emphasis in reducing the greenhouse gases emission into the atmosphere in order to control adverse environmental impacts. Cement, steel and bricks are the largest and bulk consumption items in construction industry and minimizing consumption of these materials by using alternative materials, methods and techniques can result in scope for considerable energy savings as well as reduction of CO₂ emission. Reddy and Jagdish (2003) reported that soil-cement block with 6% cement is the most energy efficient among the alternative materials for walling consuming only one-fourth of the energy of burnt clay brick. These blocks consume only 23.5% of burnt clay brick energy and have an energy content of 2.75–3.75 MJ per block of size 230 mm x 190 mm x 100 mm. These blocks are manufactured by compacting a mixture of locally available soil and sand and a small quantity of cement. The technology offers building blocks at a very low embodied energy and CO₂ emission. Moreover, it uses local materials and inexpensive equipment. Though these blocks have adequate strength and

durability, they absorb high levels of moisture. In humid conditions they become very soft and non-uniform expansion leads to excessive deformation and cracking. A barrier layer on their surface that impedes moisture ingress would significantly improve their usefulness. In order to further improve the durability of these low energy materials, new techniques need to be applied with the aim of modifying the characteristics of such sustainable low energy materials. Application of microbially induced calcite precipitation (MICP) technology may serve as the answer for long quest of durable energy efficient green building materials.

Traditional construction materials such as concrete, bricks, tiles etc. are produced from existing natural resources. This is damaging the environment due to continuous exploration and depletion of natural resources. Investigators are now looking for reusing the waste materials of various industries in economically sustainable ways. Two such industrial by products, regarded as environmental pollutants are: Fly ash (FA), generated during the combustion of coal for energy production and Rice husk ash (RHA) which is obtained from burning of rice husk. Fly ash as well as rice husk ash bricks are already available commercially but due to their lower durability, they are not preferred much. The application of calcifying bacteria on these building materials needs to be assessed for improving their performance.

So, in the present study, effect of bacterial binders as biogenic surface treatment of soil cement blocks as well as ash bricks has been determined. The results of the study might pave way not only for durable structures but also encourage applications of various other green technologies.

To date, a good many studies have investigated the potential of MICCP for durability issues of building materials but much of the work has been targeted by use of fresh bacterial cells (Rodriguez Navarro *et al.*, 2012). Although fresh cell preparations are suitable for research studies, such preparations are not applicable for long term commercial purposes. Successful commercialization of calcifying bacterial isolates has not been achieved till date because of the high cost of carrier materials (De Muynck *et al.*, 2010). The need of time is to look for economical carrier materials that can successfully support the growth of bacterial cells and

have an acceptable shelf life. Though the use of fly ash as carrier material for development of bio fertilizers has been done by many researchers (Gaiind and Gaur, 2004; Kumar and Gupta, 2010), but no work has been reported till date on the use of fly ash as carrier material for biodeposition studies. It is pre requisite to investigate optimum conditions for maximum survival and calcifying efficacy of these builder bacterial cells within the fly ash formulations. Sensitive and quick detection of bacterial cell viability is also an important aspect to be studied for checking carrier material's efficacy in sustaining bacterial populations. The use of fluorescent dyes have been used widely in recent studies on checking the viability of respiring bacterial cells (Richardson *et al.*, 2002; Adams *et al.*, 2003; Creach *et al.*, 2003; Winding *et al.*, 2004). Tetrazolium dyes like 5 cyano 2,3 ditolyl tetrazolium chloride (CTC) ease the process of visualisation of actively respiring bacterial cells through microscopy and flow cytometry. Till now, no reports have been available on the use of such dyes for studying bacterial viability with in the formulations. The present work will investigate the efficacy of fly ash as carrier material for calcifying bacterial cells at various temperatures and moisture contents for over a period of 1 year and the viability of bacterial cells within the formulations by fluorescent dye CTC.

The production of high amounts of carbonates by bacterial cells is dependent on better urease production by ureolytic bacteria. The production of enzymes is strongly influenced by the medium components such as carbon source, nitrogen source, physical parameters etc. (Deepak *et al.*, 2008; Singh and Bishnoi, 2012). It is rather difficult to search for major factors and optimize them for biotechnological processes as there are many factors that are involved. The classical method of medium optimization involves changing one factor at a time (OFAT) and keeping others fixed but it is rather laborious, time consuming and expensive. Statistical experimental design methods offer considerable advantage over the OFAT method for improved process. Optimizing all the affecting parameters by statistical experimental design, Plackett Burman and Response surface methodology (RSM) eliminates the limitations of single factor optimization process (Montgomery, 1991; Gohel *et al.*, 2006). An attempt will also be made to optimize the medium components involved in production of urease in order to enhance the production of carbonates by application of RSM.

So, with all this background, the objectives of the present work were aimed to assess and develop microbial process for efficient production of bacterial carbonates which can be harnessed for remediation of various building materials. The importance of improving fundamental understanding of various aspects of the process of MICCP also formed the major areas of this research.

1.4. The specific objectives of this thesis are:

1. Isolation and identification of efficient ureolytic and calcifying bacteria from alkaline soils by biochemical and molecular tests
2. Study of fundamental principles, enzymes, extracellular molecules involved in MICCP and investigate the optimum conditions for bacterial carbonate precipitation
3. Investigation of the diversity and characteristics of various carbonate polymorphs formed by different bacterial isolates
4. Application of calcifying bacteria on various sand columns, low energy green building materials and building materials produced by industrial by products in order to establish “proof of concept” that durable and economical cementation can be achieved via Microbially induced calcium carbonate precipitation
5. Evaluating the feasibility of using fly ash as a carrier material for long term storage of calcifying bacterial cells at varying temperatures and moistures and investigating the suitability of these formulations for commercial applications
6. Optimizing the media components for high urease and carbonate production by application of Response surface methodology

Chapter 2

Review of literature

2.1. Microbial biomineralization

Biomineralization of calcium carbonates, that is, the biologically controlled or mediated/induced mineralization of CaCO_3 , is an important and ubiquitous process resulting in biominerals produced by a range of taxa, from bacteria and archaea to eukarya (Lowenstam and Weiner, 1989; Mann, 2001; Gower, 2008; Maldrum and Colfen, 2008; Dittrich and Sibling, 2010). In case of biologically controlled mineralization (BCM), minerals are directly synthesized at a specific location within or on the cell and only under certain conditions. In most cases, BCM happens intracellularly, where the lipids, proteins, polysaccharides, etc. make a stable matrix for the cations to condense, and for the minerals to grow in a constrained space. Examples of controlled mineralization are magnetite formation in magnetotactic bacteria (Bazylinski *et al.*, 2007) and silica deposition in unicellular algae coccolithophores and diatoms, respectively (Barabesi *et al.*, 2007).

Minerals that form by biologically induced mineralization (BIM) processes generally nucleate and grow extracellularly as a result of metabolic activity of the organism and subsequent chemical reactions involving metabolic byproducts. Bacterial surfaces such as cell walls or polymeric materials (exopolymers) exuded by bacteria including slimes, sheaths, or biofilms, and even dormant spores can act as important sites for adsorption of ions, mineral nucleation and growth (Beveridge, 1989; Konhauser, 1998; Banfield and Zhang, 2001; Bäuerlein, 2003). Boquet *et al.* (1973) reported that almost all bacteria are capable of CaCO_3 precipitation while Knorre and Krumbein (2000) concluded Microbially induce calcium carbonate precipitation (MICCP) as a by product of microbial metabolic processes.

Microbially induced calcium carbonate precipitation, part of biomineralization has been the primary focus of research in biogeotechnical engineering to date as there is currently great interest in the development of mimic materials based on biomineralization. The carbonate precipitation induced by microbial metabolic activities is pollution free, natural and a continuous process. The promising results of this technology have invited researchers from worldwide to harness these carbonates for various purposes. This process proved implications for:

1. Atmospheric CO₂ fixation through carbonate sediment formation and lithification (Krumbein, 1979; Monger *et al.*, 1991; Chafetz and Buczynski, 1992; Folk, 1993) and dolomite precipitation (Vasconcelos *et al.*, 1995)
2. Solid-phase capture of inorganic contaminants (Warren *et al.*, 2001)
3. Pathological formation of mineral concretions, such as gallstones and kidney stones in humans (Keefe, 1976).
4. The possibility of understanding extraterrestrial biological processes such as Martian carbonate production by bacteria (McKay *et al.*, 1996; Thomas-Keprta *et al.*, 1998).

Number of applications involving MICCP have been attempted in various fields as in the removal of heavy metals (Warren *et al.*, 2001; Wu *et al.*, 2011; Achal *et al.*, 2011c, 2012) and radionucleotides (Fujita *et al.*, 2004), removal of calcium from wastewater (Hammes *et al.*, 2003), biodegradation of pollutants (Simon *et al.*, 2004; Chaturvedi *et al.*, 2006), remediation (fixation) of metal-contaminated soil and groundwater (Warren *et al.*, 2001; Mitchell and Ferris, 2006), polychlorinated biphenyl removal (Okwadha and Li, 2011) and atmospheric CO₂ sequestration (Dupraz *et al.*, 2009; Ramanan *et al.*, 2009; Shaffer, 2010; Mitchell *et al.*, 2010; Sharma and Bhattacharya, 2010; Yadav *et al.*, 2011). Recently, bacterial precipitation of fluorescent calcium carbonate with potential applications as filler in rubber and plastics, in stationery ink, and as fluorescent marker, has also been reported (Yoshida *et al.*, 2010).

The application of MICCP in remediation of building materials has brought another major revolution in which *Applied Microbiology and Biotechnology* have again proved their

potential for serving the problems of Civil Engineers. The use of bacteria for remediating building materials seems like a new idea but this conservation method mimics what nature has been doing for eons. This technology has offered the benefits of being novel, self healing and eco-friendly. But various factors involved in calcium carbonate precipitation needs to be unpinned before studying the role of microbes in the process.

2.2. Calcium carbonate precipitation

Calcium carbonate precipitation has been observed in a range of natural environments varying from saline aquatic environments, freshwater environments and saline soils by various researchers (Novitsky, 1981; Rivadeneyra *et al.*, 2004; Baskar *et al.*, 2005; Zamarreno *et al.*, 2009). Primarily the precipitation of calcium carbonate is governed by four major factors:

- (1) Calcium concentration
- (2) Carbonate concentration
- (3) pH of the environment (which affects carbonate speciation and calcium carbonate solubility)
- (4) Presence of nucleation sites (Hammes and Verstraete, 2002)

In the natural environments, carbonate precipitation theoretically occurs by increasing the concentration of calcium and/or carbonate in solution or by decreasing the solubility of calcium and/or carbonate. Bacterial cells have been shown to be excellent nucleation sites for growing of minerals as seen in the formation of rocks (Ferris *et al.*, 1986; 1987). So, the first three parameters form the key for microbially induced calcium carbonate precipitation.

In order for precipitation to take place, supersaturation of the precipitating species must exist (Randolph and Larson, 1988). As the solubility product (K_{sp}) of calcite is extremely low ($3.3 \times 10^{-9} \text{ mol L}^{-1}$ at 25°C), the supersaturation can be achieved straightforwardly (Sawada, 1998). The precipitation can be achieved by simply mixing together moderate concentrations of soluble Ca^{2+} and CO_3^{2-} ions. The crystals formed when the reaction happens rapidly are generally very small and powder-like with little cementation strength.

The difference between the saturation concentration and supersaturation concentration forms one of the prime factors which controls the rate of precipitation (Bodek *et al.*, 1988). In general, the higher the supersaturation concentration, the faster the rate and the smaller the crystals. The supersaturating product concentration and thus the degree of disequilibrium remains relatively low (compared to chemical example), which allows larger crystals to form over an extended period with higher cementation strength (Whiffin, 2004).

pH also influences the supersaturation level of carbonate ions (Fig. 2.1). The proportion of total carbonate that exists as CO_3^{2-} in solution at any time is highly dependent on the pH. The carbonate concentration is very low, below pH 8, which means that if desired, the size of crystals that form can be increased by decreasing the pH or vice versa (Whiffin, 2004).

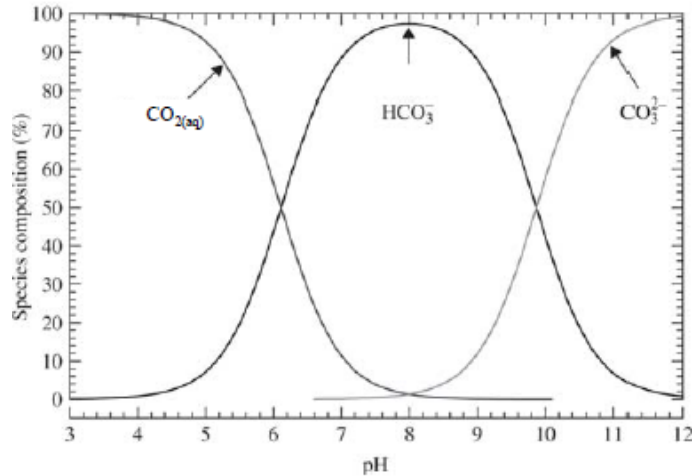


Fig.2.1. Chemical speciation of H_2CO_3 , HCO_3^- and CO_3^{2-} at 25°C (from Atkins, 2002)

Calcium carbonate precipitates also dissolve naturally or under biological influence. The precipitation and dissolution processes are equilibrium reactions governed by solubility constants. Solubility constant for CaCO_3 is temperature dependant and defined as:



$$K_{\text{so}} = [\text{Ca}^{2+}][\text{CO}_3^{2-}] = 4.83 \times 10^{-9} \quad (\text{calcite, } 25^\circ\text{C}) \quad \text{Eq. 2.2}$$

$$\text{IAP} = (\text{Ca}^{2+})(\text{CO}_3^{2-}) \quad \text{Eq. 2.3}$$

$$\Omega = \text{IAP}/K_{\text{so}} \quad \text{Eq. 2.4}$$

IAP > K : over-saturated system (precipitation is likely)

IAP = K : equilibrium

IAP < K: under-saturated system (dissolution is likely)

In calculation of the likeliness of dissolution/precipitation reactions to occur, or quantification of pH changes or in studying impact of biological process, comprehensive and detailed literature on speciation modelling is available (Morse and Arvidson, 2002; Stumm and Morgan, 1981) with speciation softwares like MINEQL (<http://www.mineql.com>), ChemEQL, CHESS, JESS, PHREEQC, Visual Minteq etc. Among the 60 different carbonate minerals comprising calcite (CaCO_3), dolomite ($\text{CaMg}(\text{CO}_3)_2$), magnesite (MgCO_3), rhodochrosite (MnCO_3), siderite (FeCO_3) etc., CaCO_3 is the most common among all (Lippmann, 1973; Rieger *et al.*, 2007; Gower, 2008; Gebauer *et al.*, 2010).

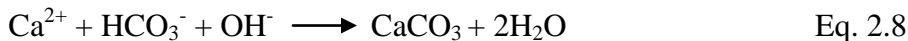
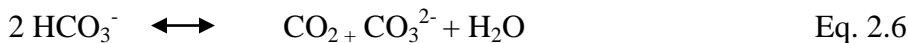
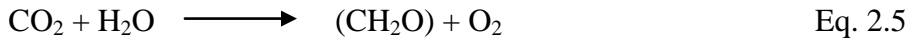
As the isolation of highly pure and coherent calcium carbonates from natural sources like shell crust is a very laborious and expensive process, so microbially induced carbonate precipitation has received much attention as an environment-friendly method of generating calcium carbonates.

2.2.1. Microbially induced calcium carbonate precipitation (MICCP)

MICCP has gained tremendous interest in the last 20 years and found to be the primary focus of research in bio geo civil engineering because of its numerous applications. Mainly four groups of microorganisms are seen to be involved in the process

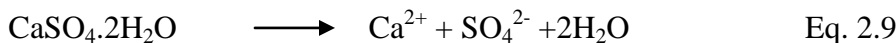
- i. Photosynthetic organisms - such as cyanobacteria and algae
- ii. Sulphate reducing bacteria- that are responsible for dissimilatory reduction of sulphates
- iii. Organisms utilizing organic acids
- iv. Organisms that are involved in nitrogen cycle (by ammonification of amino acids/ nitrate reduction/ hydrolysis of urea (Stocks - Fischer *et al.*, 1999; Hammes and Verstraete, 2002; Jargeat *et al.*, 2003).

The most common form of MICCP in aquatic environments is caused by photosynthetic organisms (McConnaughey and Whelan, 1997). The metabolic processes of algae and cyanobacteria utilize dissolved CO₂ (Eq. 2.5, which is in equilibrium with HCO₃⁻ and CO₃²⁻ (Eq. 2.6). The removal of CO₂ induces a shift in this equilibrium, and results in an increase in pH (Eq. 2.7) (Ehrlich, 1998). When this reaction occurs in the presence of calcium ions, calcium carbonate is produced (Eq. 2.8) (Hammes and Verstraete, 2002).



Calcium carbonate precipitation via this pathway occurs in sea water, geological formations (Packman *et al.*, 1999; Machel, 2001), in landfill leachates (Malava *et al.*, 2000) and even during the biological treatment of acid mine drainage (Kaufman *et al.*, 1996). Interestingly, in several of the described examples for this pathway, dolomite and aragonite, instead of calcite are the predominant minerals to precipitate (Packman *et al.*, 1999; Wright, 1999; Warthman *et al.*, 2000; Machel, 2001).

Calcium carbonates can also be precipitated by heterotrophic organisms, by the production of carbonate or bicarbonate and modification of the environment to favour precipitation (Castanier *et al.*, 1999). The abiotic dissolution of gypsum (CaSO₄·2H₂O) (Eq. 2.9) provides an environment that is rich in both sulphate and calcium ions. In the presence of organic matter and absence of oxygen, sulphate reducing bacteria can reduce sulphate to H₂S and release HCO₃⁻ (Eq. 2.10) (Castanier *et al.*, 1999; Ehrlich, 1998; Wright, 1999). If H₂S then degasses from the environment, this results in an increase in pH and favors the precipitation of calcium carbonate (Eq. 2.8) (Castanier *et al.*, 1999).





Third pathway includes bacteria using organic acids as their sole source of carbon and energy wherein some common species of soil bacteria are included. Such acids include acetate, citrate, oxalate, acetate, glyoxylate, succinate and malate. The consumption of these acids results in pH increase, thereby leading to precipitation in the presence of calcium ions (Equations 2.11-13) (Knorre and Krumbein, 2000; Braissant *et al.*, 2002)

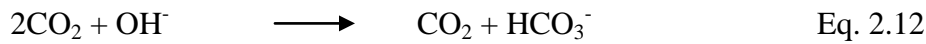
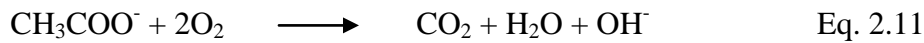
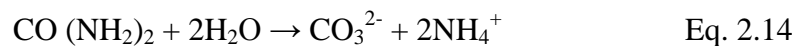


Table 2.1 summarises some of the microbial strains, crystal types and organic acids which have been reported for this mechanism during calcium carbonate precipitation. Numerous heterogenous bacterial groups are linked to this precipitation mechanism. Braissant *et al.* (2002) speculated that this pathway might be extremely common in natural environments due to the abundance of such low molecular weight acids in the soils (produced by fungi and plants).

The fourth pathway for microbially induced carbonate precipitation is by organisms involved in the nitrogen cycle, via ammonification of amino acids, nitrate reduction and the hydrolysis of urea. Hydrolysis of urea by enzyme urease is the simplest of all mechanisms described for MICCP. Calcium carbonate is readily precipitated under these conditions in the presence of calcium as:



The use of ureolytic bacteria in biotechnological applications is also appealing because of many reasons:

1. Firstly the enzyme urease is widespread amongst bacteria.
2. Another benefit of ureolytic bacteria is that urea, an important nitrogen compound found in natural environment, is a fairly inexpensive substrate (Hammes *et al.*, 2003a).
3. Also, the use of bacteria to raise the pH in the environment is preferable to the direct injection of a base because the gradual hydrolysis of urea is likely to promote a wider spatial distribution of calcite, whereas the direct addition of base is likely to cause immediate precipitation at the injection site (Ferris *et al.*, 2003).

Table 2.1. Examples of precipitation through organic acid utilisation

Microorganism	Acid	Mineral phase	Reference
<i>Pseudomonas fluorescence</i>	Citrate	Calcite and Vaterite	Anderson <i>et al.</i> , (1992)
<i>Ralstonia eutropha</i>	Ca – citrate	Calcite and Vaterite	Braissant <i>et al.</i> , (2002)
<i>Xanthobacter autrophicus</i>	Ca – oxalate		
<i>Flavobacter sp.</i>	Acetate		Ferrer <i>et al.</i> , (1988)
<i>Acinetobacter sp.</i>	Ca – acetate		
<i>Vibrio spp.</i>	Ca – acetate	Mg – calcite	Rivadeneira <i>et al.</i> , (1994)
<i>Nesterkonia halobia</i>	Ca – acetate	Dolomite, aragonite and calcite	Rivadeneira <i>et al.</i> , (2000)
<i>Halomonas eurihalina</i>	Ca – acetate	Aragonite, calcite and Mg – calcite	Rivadeneira <i>et al.</i> , (1998)
Heterotrophic microbial mat isolates	Ca – acetate	Calcite	Knorre and Krumbein, (2000)

2.2.2. Enzyme Urease

Urease (UA; EC 3.5.1.5) is a nickel-containing metalloenzyme which is found in a wide range of microorganisms and plants, some of which produce this enzyme in large quantities (Mobley *et al.*, 1989). Urease from Jack bean (*Canavalia ensiformis*) was the first enzyme to be crystallized and the first enzyme found to contain nickel (Sumner, 1926). Work of James B. Sumner on this enzyme eventually got him Noble prize in Chemistry in 1946.

The commercial demand for urease is not high and currently, urease is only available in industrial quantities from Roche for use in the diagnostic and high technology specialist ceramics fields (Gauckler and Baader, 1999; Roche, 2001). It is thus expensive and is of a higher purity than is required for applications in biocementation. The ability to produce urease is widespread amongst microbial populations and the enzyme has been well studied from a clinical perspective as it can indicate increased virulence properties in pathogenic bacteria (Collins and D'Orazio, 1993; Mobley *et al.*, 1995; Lee and Calhoun, 1997; Provorov and Vorobyov, 2000) and as a general nitrogen volatilisation phenomenon in agricultural soils (Pettit *et al.*, 1976; Sloan and Anderson, 1995; Nielsen *et al.*, 1998). Four modes of regulation have been reported to exist for the synthesis of urease in microbial systems (Mobley and Hausinger, 1989; Mobley *et al.*, 1995):

- (i) Constitutive, where a constant enzyme activity is expressed per cell, independent of external conditions.
- (ii) Inducible, where a background level of enzyme activity is expressed per cell which can be induced by the presence of an inducer molecule (e.g. urea) or other environmental condition.
- (iii) Repressible, by the presence of ammonia or ammonia precursors including urea. This synthesis is de-repressed (i.e. enzyme activity increases) under nitrogen limiting conditions.
- (iv) Developmental, where an organism in different developmental stages (*e.g.* swarming versus non-swarming) has variable expression of urease (Falkinham III and Hoffman, 1984).

An ideal microbial source of urease for production of carbonate binders must be tolerant to high concentrations of urea and calcium. The organism should also have a high level of

urease activity that is either constitutively produced (*i.e.* a constant amount of enzyme is expressed per cell) or can be reliably induced.

In general, ureolytic bacteria can be divided into two distinct groups according to their urease response to ammonium; those whose urease activity is not repressed (*Sporosarcina pasteurii*, *Proteus vulgaris* and *Helicobacter pylori*) and those whose urease activity is repressed *e.g.* *Pseudomonas aeruginosa*, *Alcaligenes eutrophus* (Kaltwasser *et al.*, 1972) and *Klebsiella aerogenes* (Friedrich and Magasanik, 1977). In *K. aerogenes*, the presence of ammonium inside the cell induces the production of glutamine, which prevents further hydrolysis of urea (Mulrooney *et al.*, 2001). As high concentrations of urea are hydrolysed during production of calcium carbonate, only those microorganisms whose urease activity is not repressed by ammonium are useful. The organism must also meet the needs for safe environmental application. In order to safely release an organism into the environment, it must be non-pathogenic, non-genetically modified, and not contain any transferable elements that may increase the pathogenicity of environmental strains (*e.g.* antibiotic resistance). *Sporosarcina pasteurii* follows all these conditions and has been used extensively by various researchers (Stocks - Fischer *et al.*, 1999; De Muynck *et al.*, 2010).

As urea is widespread in the environment and requirement for nitrogen is also universal, a diverse section of the biota has evolved with the ability to hydrolyse urea, through the action of urease. The occurrence of urease is found commonly in bacteria, several species of yeast and a number of higher plants including jack beans (*Canvalia ensiformis*) (Dixon *et al.*, 1980), soybean leaf and seed (*Glycine max*) (Kerr *et al.*, 1983), pigweed (*Chenopodium album*) (El-Shora, 2001) and mulberry leaf (*Morus alba*) (Hirayama *et al.*, 2000).

Organisms with ureolytic ability mostly use urea as a source of nitrogen and transport urea actively or by passive diffusion into the cell cytoplasm, where urease hydrolyses urea releasing two ammonium molecules. These products can then be directly assimilated into biomass via the glutamine synthetase-glutamate synthase (GS-GOGAT) pathway or by the action of glutamate dehydrogenase (GDH) (Tyler, 1978). To ensure this process is energy efficient, the production of urease in organisms such as *Pseudomonas aeruginosa*,

Alcaligenes eutrophus (Kaltwasser *et al.*, 1972) and *Klebsiella aerogenes* (Friedrich and Magasanik, 1977), is repressed by the presence of ammonium. There are however some exceptions to this regulation, such as *Proteus vulgaris*, which can produce urease even in the presence of high concentrations of ammonium (Mörsdorf and Kaltwasser, 1989). Some specialist organisms exist that have additional uses for urease, beyond nitrogen assimilation. *Helicobacter pylori*, an inhabitant of low pH gastric juices in the stomach, not only has intracellular but also extracellular urease that is located on the cell surface. The extracellular urease plays a protective role from the low pH environment of the stomach, by providing a microenvironment of more neutral pH, generated from production of ammonium near the cell surface (Marshall *et al.*, 1990; Dunn and Grütter, 2001; Ha *et al.*, 2001).

Sporosarcina pasteurii is a moderately alkaliphilic organism with a growth optimum at pH 9.25. Alkaliphiles present a special problem for the generation of ATP due to reversed chemiosmotic proton gradient. In neutrophilic organisms, ATP is produced from proton motive force that is generated by pumping protons out of the cell from the electron transport chain. This generates a proton concentration gradient (high outside/low inside) and causes protons to be driven back into the cell through the ATP-synthase, resulting in ATP generation (Prescott *et al.*, 1993). When the external environment is highly alkaline, the proton concentration gradient is reversed and the gradient favours protons to be fluxed out of the cell, but not back into it. Alkaliphilic organisms must create a high membrane potential (charge difference across the membrane) by pumping out cations, to drive protons back into the cell against the concentration gradient (Ivey *et al.*, 1998) (Fig. 2.2). For *S. pasteurii*, the effluxed cation used to create a high membrane potential to drive ATP synthesis is ammonium, which can be supplied directly as ammonium or indirectly as urea (Jahns, 1996).

For biocementation purposes, an ideal microbial source of urease should have the following properties:

- i. High urease production capacity
- ii. Non pathogenic

- iii. Ability to produce urease in the presence of ammonium
- iv. Consistent production (reliable)
- v. High stability (robust)

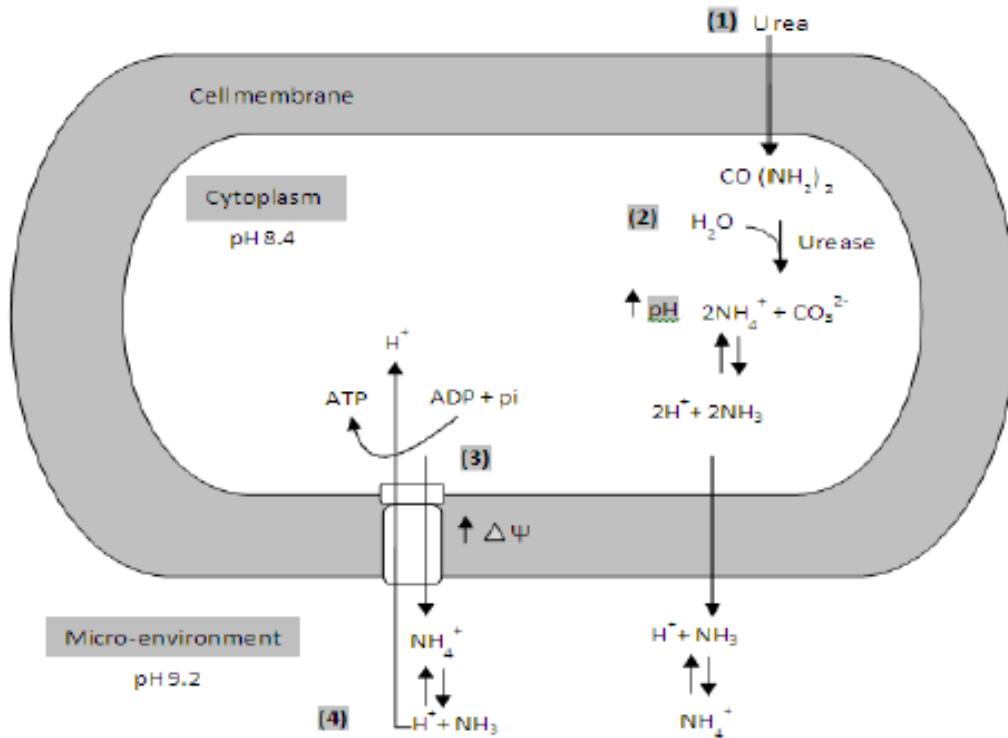


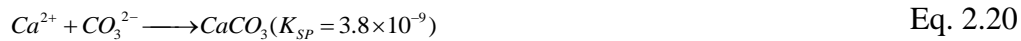
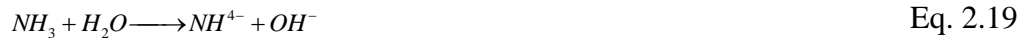
Fig. 2.2: Coupling of urea hydrolysis and ATP generation in alkaliphilic bacteria *S. pasteurii* (Thawadi 2011)

2.2.3. Microbially induced calcium carbonate precipitation via urea hydrolysis

The precipitation of carbonates via urea hydrolysis by ureolytic bacteria is the simplest and most easily controlled mechanism of MICCP with potential to produce high amounts of carbonates in short period of time (Fig. 2.3). During microbial urease activity, 1 mol of urea is hydrolyzed intracellularly to 1 mol of ammonia and 1 mol of carbonate (Eq. 2.16), which spontaneously hydrolyzes to form additional 1 mol of ammonia and carbonic acid (Eq. 2.17) as follows:



These products equilibrate in water to form bicarbonate, 1 mol of ammonium and hydroxide ions which give rise to pH increase



K_{SP} is the solubility product in Eq. 2.20

The primary role of bacteria has been ascribed to their ability to create an alkaline environment through various physiological activities.

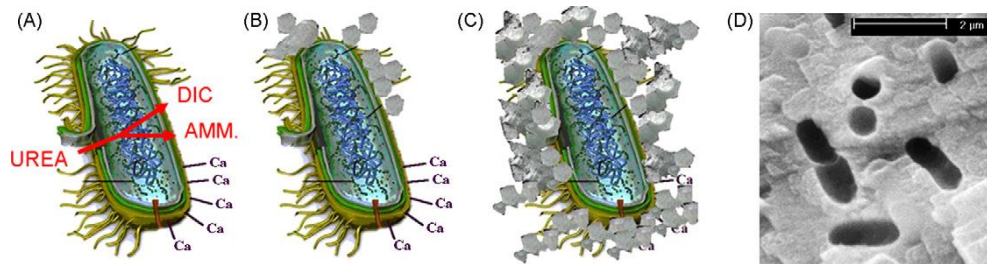


Fig. 2.3. Simplified representation of the events occurring during the microbially induced carbonate precipitation. Calcium ions in the solution are attracted to the bacterial cell wall due to the negative charge of the latter. Upon addition of urea to the bacteria, dissolved inorganic carbon (DIC) and ammonium (AMM) are released in the microenvironment of the bacteria (A). In the presence of calcium ions, this can result in a local supersaturation and hence heterogeneous precipitation of calcium carbonate on the bacterial cell wall (B). After a while, the whole cell becomes encapsulated (C), limiting nutrient transfer, resulting in cell death. Image (D) shows the imprints of bacterial cells involved in carbonate precipitation (Source: Hammes & Verstraete 2002).

Bacterial surfaces also play an important role in calcium precipitation (Fortin *et al.*, 1997). Due to the presence of several negatively charged groups, at a neutral pH, positively charged metal ions could be bound on bacterial surfaces, favouring heterogeneous nucleation

(Douglas, 1998; Bauerlein, 2003). Ferris and Stehmeier (1993) suggested that there is considerable evidence that microorganisms might function as crystal nucleating agents during mineral precipitation. As bacteria have high surface to volume ratio, they are ideal crystal nucleation sites (Warren and Haack, 2001). Bacterium's ability to interact with metals is dependent on the types and densities of functional groups, which are in turn affected by cell wall composition, presence of S layers, sheaths, capsules or extracellular polymeric substances (EPS). Gram negative bacteria's cell membranes are dominated by presence of carboxylate groups, as well as phosphate moieties resulting in net negative charge (Schultze-Lam *et al.*, 1996) while gram positive bacteria have lipopolysaccharide (LPS) and peptidoglycan having net negative charge. The overall anionic nature of bacterial cells in most aquatic environments is result of pKa values of carboxyl and phosphoryl groups (Warren and Haack, 2001; Ferris and Beveridge, 1985). Under normal conditions, divalent cations (Ca^{2+} ; Mg^{2+}) contribute to the stability of teichoic and teichuronic acid polymers, lipopolysaccharides (LPS) and S-layers. This reaction (binding of divalent cations to the cell wall) forms the beginning of crystallization (Southam, 2000). Formation of CaCO_3^- moieties on the cell surface correlates with the moieties on CaCO_3 crystal surface (Nilsson and Sternbeck, 1999), so that the heteronucleus (bacteria) does indeed match up with the crystal. Not only the cell surface features of bacteria contribute to crystal nucleation site formation, but also influence cellular processes on immediate surroundings of the bacteria (Schultze-Lam *et al.*, 1996). Microorganisms are always surrounded by thin watery layer, which physically creates micro environment (Warren and Haack, 2001; Schultze-Lam *et al.*, 1996). This layer forms the interface between microbial cell and outside environment, in which the concentration of chemical species different to those of outside environment can prevail. Both Wright (1999) and McConnaughey and Whelan (1997) reported the potential of microorganisms to concentrate cations, while EPS are known to slow down diffusion of ions (HCO_3^- , CO_3^{2-} , Ca^{2+}), thus resulting in elevated localized concentrations (Kawaguchi and Decho 2002). Commonly, carbonate precipitates develop on the external surface of bacterial cells by successive stratification (Pentecost and Bauld, 1988; Castanier *et al.*, 1999) and bacteria can be embedded in growing carbonate crystals (Rivadeneira *et al.*, 1998;

Castanier *et al.*, 1999). Possible biochemical reactions in urea-CaCl₂ medium to precipitate CaCO₃ at the cell surface can be summarized as follows:

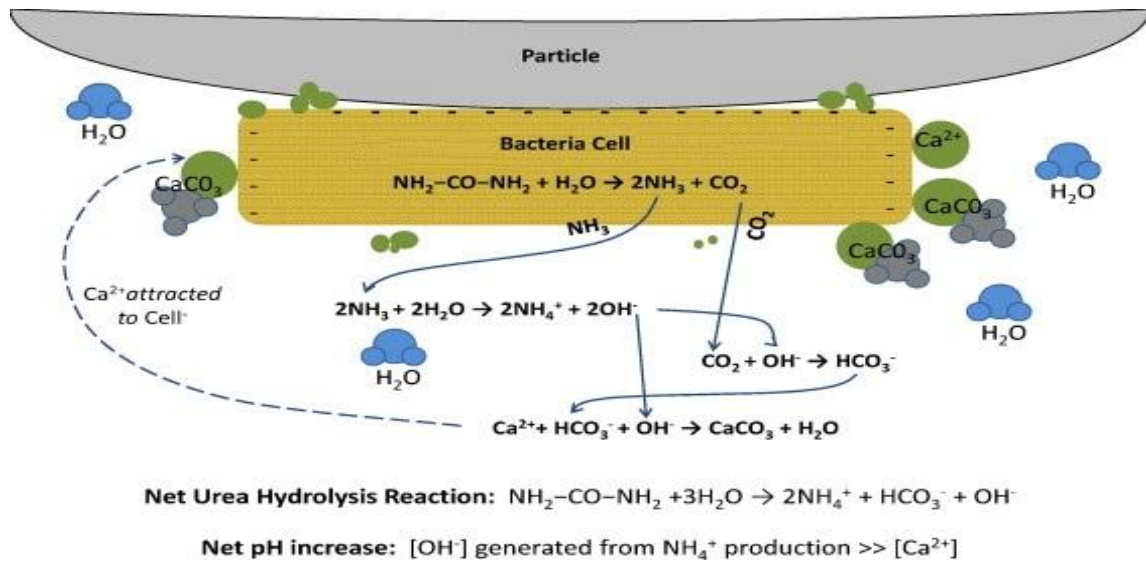
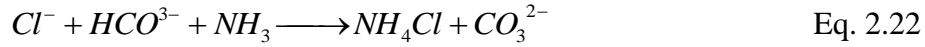
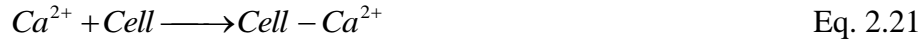


Fig. 2.4. Bacteria serving as nucleation site for CaCO₃ precipitation in the sand particles

Several authors have investigated various conditions for calcium carbonate precipitation via Urea hydrolysis (Table 2.2). The actual role of the bacteria in the precipitation remains, however, a matter of debate. Some authors believe this precipitation to be an unwanted and accidental by-product of the metabolism (Knorre and Krumbein, 2000) while others think that it is a specific process with ecological benefits for the precipitating organisms (Ehrlich, 1996; Mc Connaughey and Whelan, 1997).

Several researchers applied different ureolytic bacteria for carbonate precipitation studies. These bacteria included *Bacillus pasteurii*, *Pseudomonas sp.*, *Variovorax sp.*, *Leuconostoc mesenteroides*, *Micrococcus sp.*, *Bacillus subtilis*, *Deleya halophila*, *Halomonas eurihalina* and *Myxococcus Xanthus* (Mobley and Hausinger, 1989; Rivadeneyra *et al.*, 1991; 1996; 1998; Ferris and Stehmeier, 1992, Tiano *et al.*, 1999; Stocks - Fischer *et al.*, 1999; Castanier *et al.*, 2000; Fujita *et al.*, 2000; Fujita *et al.*, 2000; Rodrigues-Navarro *et al.*, 2003).

Table 2.2: Reaction conditions reported in the literature for production of CaCO₃ via urea hydrolysis

Purpose	Urea (mM)	Ca ²⁺ (mM)	Urease Activity (mM/min)	Reference
Sr⁹⁰ sequestration	333	25	0.045	Fujita <i>et al.</i> , 2000
Sr⁹⁰ sequestration	330	0.025	0.042	Warren <i>et al.</i> , 2001
Removal of Ca²⁺ from waste water	16	14	0.293	Hammes <i>et al.</i> , 2003c
Removal of Ca²⁺ from waste water	8	15	0.032	Hammes <i>et al.</i> , 2003a
Stone remediation	333	12-50	0.110	Stocks - Fischer <i>et al.</i> , 1999
	333	340	0.02- 0.12	De Muynck <i>et al.</i> , 2011
Stone remediation	66	25	0.041	Bachmeier <i>et al.</i> , 2002
Portland cement remediation	333	50	n/s	Ramachandran <i>et al.</i> , 2001
Plugging of rock pores	333	0.25	n/s	Gollapudi <i>et al.</i> , 1995
Biocementation	1500	1500	4-18	Whiffin <i>et al.</i> , 2004
Sand column cementation	333	25	0.65	Achal <i>et al.</i> , 2009; Van Paassen <i>et al.</i> , 2009
Soil cementation	1000	1000	n/s	Cheng and Ruwisch, 2012
Biodeposition	333	340	n/s	De Belie and De Muynck, 2008
Carbonate precipitation	666	250	n/s	Okwadha <i>et al.</i> , 2010

2.3. Bacterial isolation source

Microorganisms are omnipresent. Near the ground surface more than 10^{14} bacteria exist per kilogram of soil (Rodriguez Navarro *et al.*, 2012).

"Microbial organisms are much more diverse than we ever imagined. We are just beginning to understand how vast that diversity might be." Dr. Cheryl Kuske

A variety of microorganisms inhabit extreme environments i.e. these organisms thrive in physically or geochemically extreme conditions that are detrimental to most life on earth. These are known as extremophiles and are divided into various classes corresponding to their environmental niche. e.g. Acidophiles (with optimal growth at pH levels of 3 or below), Alkaliphiles (with optimal growth at pH levels of 9 or above), Anaerobes (which do not require oxygen for growth), Cryptoendoliths (which live in microscopic spaces within rocks, pores between aggregate grains, fissures, aquifers etc.), Halophiles (organisms requiring at least 0.2M concentrations of salt (NaCl) for growth), Hyperthermophiles (organisms that can thrive at temperatures between 80–122°C), Metallotolerants (which are capable of tolerating high levels of dissolved heavy metals such as copper, cadmium, arsenic, and zinc), Oligotrophs (which are capable of growth in nutritionally limited environments), Thermophiles (which can thrive at temperatures between 45–122 °C) and many more. Culture-dependent and culture-independent (molecular) methods have been employed for understanding the diversity of microbes in these environments. Microbial diversity is expressed by monitoring species richness and species evenness. Species richness is the number of different types of species present in a community while evenness is the number of organisms of each species present in the community (Vigdis and Ovreas, 2002; Kassen and Rainy, 2004). Extensive global research efforts have revealed the novel diversity of extremophilic microbes. These organisms have evolved several structural and chemical adaptations, which allow them to survive and grow in extreme environments. Extreme environments, such as acidic or hot springs, saline and/or alkaline lakes, deserts and the ocean beds found in nature are too harsh for normal life to exist. A variety of microorganisms, however, survive and grow in such environments. These

extremophiles, not only tolerate specific extreme condition(s), but usually require these for survival and growth. Most extremophiles are found in microbial world. The range of environmental extremes tolerated by microbes is much broader than other life forms. The limits of growth and reproduction of microbes are, -12° to more than $+100^{\circ}\text{C}$, pH 1 to 13, hydrostatic pressures up to 1400 atm and salt concentrations of saturated brines. Besides natural extreme environments, there are manmade extreme conditions such as cool houses, steam heated buildings and acid mine waters (Satyanarayana *et al.*, 2005).

The major impetus that has driven extensive and intensive research efforts on extremophiles during the last decades is the potential biotechnological applications associated with these microbes and their products. The likely potential has been increasing exponentially with the isolation of new microbial strains, the identification of novel compounds and pathways, and the molecular and biochemical characterization of cellular components. Examples of extremozymes that are now commercially used include: Alkaline proteases, cellulases, xylanases, nitrilases, lipases in detergents; pectinases in Paper, waste treatment, degumming; elastases, keritinases in hide dehairing; alkaliphilic halophiles in oil recovery along with many others (Satyanarayana *et al.*, 2005; Chaudhary *et al.*, 2006; Khandelwal *et al.*, 2007; Rastogi *et al.*, 2009).

Although microorganisms are perhaps the most diverse (Torsvik *et al.*, 2002; Venter *et al.*, 2004) and abundant (Whitman *et al.*, 1998) type of organisms on Earth, the distribution of microbial diversity at continental scales is poorly understood. Ecologists describing microbial biogeography typically invoke Beijerinck (1913) from a century ago: “Everything is everywhere, the environment selects.” However, few studies have attempted to verify this statement or specify which environmental factors exert the strongest influences on microbial communities in nature (Papke and Ward, 2004).

For applications in biocementation of building materials, there is need to isolate microorganisms which can tolerate high pH (as in case of cementitious materials which have pH around 11) i.e. the microbes needed to be looked upon should be from alkaline environments. There are two kinds of naturally occurring stable alkaline environments in the

world. First, high Ca^{2+} environments (groundwaters dominated by CaOH) and second low Ca^{2+} environments (lakes, deserts, soils dominated by sodium carbonate) (Grant *et al.*, 1989; 1992). Microbial studies pertaining to the alkaline environments such as calcareous soils are very scarce. Bacterial diversity of such alkaline sites will give valuable information about the predominant microbes, which could possibly be used for production of calcium carbonate crystals for microbial remediation of building materials.

Cells face many challenges in an alkaline environment. Of greatest significance is the ability to maintain internal pH. If cells are to survive in an alkaline environment, they must either possess specific cellular machinery that works best in the alkaline range, or they must have methods of acidifying the cytosol in relation to the extracellular environment. Studies have demonstrated that alkaliphilic enzymes possess relatively normal pH optimum. The determination that these enzymes function most efficiently near physiologically neutral pH ranges (about 7.5-8.5) was one of the primary steps in elucidating how alkaliphiles survive intensely basic environments (Higashibata *et al.*, 1998). It has been reported that the cell wall of alkaliphilic bacterial isolates also play key role in protecting the cell from alkaline environments. The cells have primarily two barriers to reduce pH values:

- Cell walls containing acidic polymers function as negatively charged matrix and may reduce the pH value at the cell surface. The surface of plasma membrane must be kept below pH 9, because plasma membrane is very unstable at alkaline pH values (pH 8.5 to 9.0).
- Plasma membranes may also maintain pH homeostasis by using Na^+/H^+ antiporter system ($\Delta\Psi$ dependent and ΔpH dependent), the K^+/H^+ antiporter and ATPase driven H^+ expulsion (Fig. 2.5).

Components of the cell walls of several alkaliphilic *Bacillus* spp. were investigated in comparison with those of the neutrophilic *B. subtilis* and it was found that in addition to peptidoglycan, alkaliphilic *Bacillus* sp. contain certain acidic polymers, such as galacturonic acid, gluconic acid, glutamic acid, aspartic acid, and phosphoric acid (Aono and Horikoshi, 1983). The negative charges on acidic non peptidoglycan components may assist cells to grow in alkaline environments.

The peptidoglycans of alkaliphilic *Bacillus* spp. appeared to be similar to that of neutrophilic *Bacillus subtilis*. Although some variation in the amide content among the peptidoglycans from alkaliphilic *Bacillus* strains was found, the variation in pattern was similar to that known in neutrophilic *Bacillus* species. The first reported alkaliphilic bacterial species is *Bacillus pasteurii* (Chester, 1889).

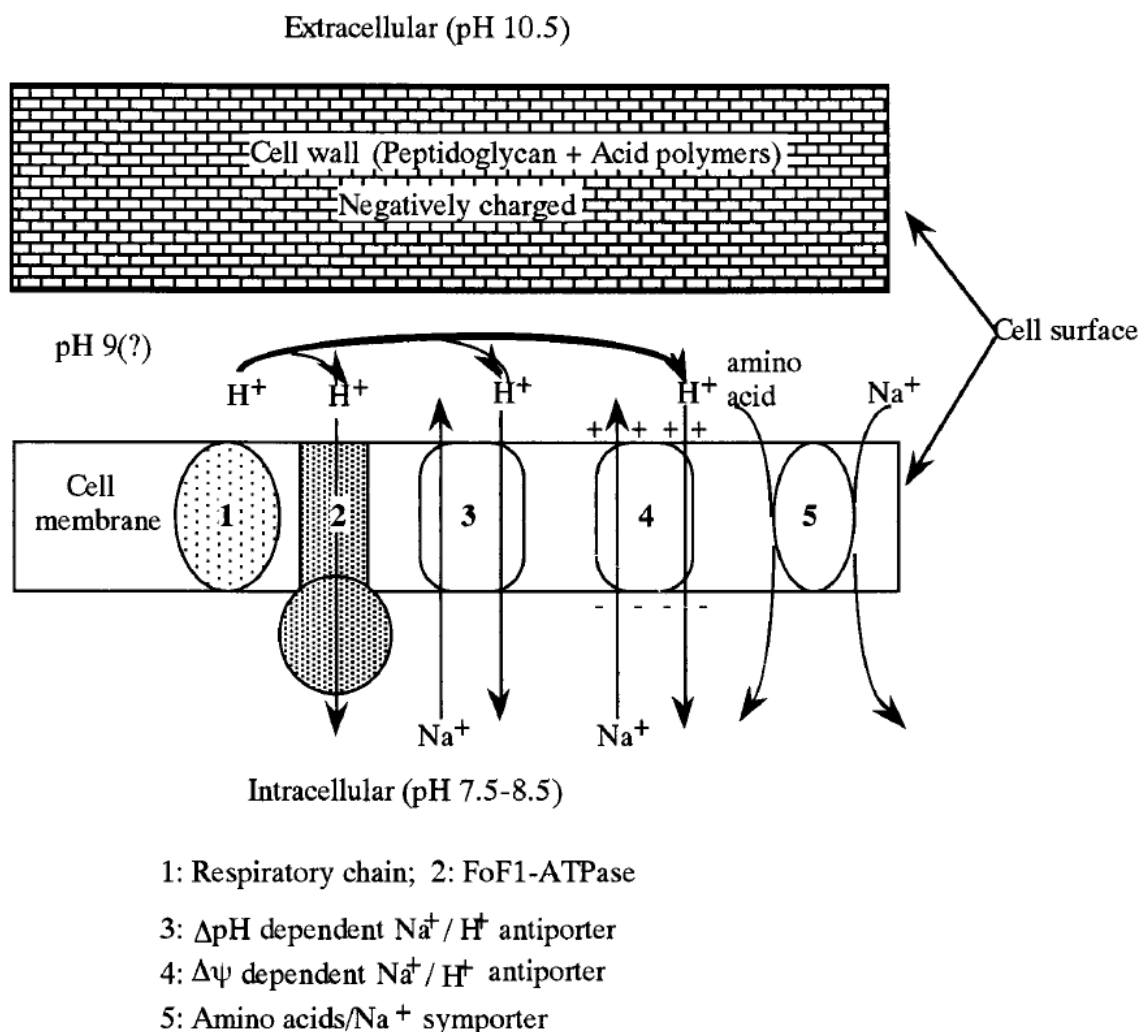


Fig. 2.5. pH regulation in alkaliphilic bacteria (Horikoshi, 1999)

The extensive and intensive efforts world over in understanding the diversity of extremophilic microbes have indicated that what we know today is just the tip of the

iceberg. Many more novel and useful extremophilic microbes are expected to be discovered in the near future.

2.3.1. Phenotypic characterization

Reliable identification of bacteria remains an important task in environmental microbiology. Isolates are characterized by a range of methods. Traditionally, morphological and physiological characteristics were used for classification and identification. Phenotypic approaches using either conventional or commercial systems are still used in the majority of laboratories. Phenotypes are defined as observable characteristics of cells. The historic way to characterize bacteria is to its phenotypic properties such as morphology, structure, cultivation, nutrition, biochemical metabolism, pathogenicity, antigenic properties and ecology. Though this characterization is carried widely but it has several limitations. Phenotypic similarities do not necessarily indicate phylogenetic relationships (relationship based on the ancestry of organisms) (Gillis and De Leg, 1992). It does not serve as a basis for sound classification and reliable identification because mutations and environmental conditions affect these traits. Thus, until very recently, microbial identification required the isolation of pure cultures (or defined co-cultures) followed by testing for multiple physiological and biochemical traits (Amann *et al.*, 1995). Cultural methods reveal only those physiological and nutritional types which are compatible with the cultural environment. The potential limitations of this approach are widely acknowledged and accepted (Torsvik *et al.*, 1996).

Diversity of microbes has remained elusive, yet it is critical to understand the adaptation of microbes to different environments and their function in those environments. Integrating information from environmental surveys, however, has thus far been a formidable obstacle to a global understanding of microbial ecology. Determining physical and chemical factors, such as temperature, pH, or geography, that correlate with differences between diverse microbial communities will reveal how easily microbes tolerate different kinds of environmental changes and will increase our understanding of microbial ecology and evolution.

2.3.2. Molecular characterization

Till 1980s the diversity of bacteria was assessed by identification with phenotypic tests and numerical taxonomy from collections of isolates obtained from plating on nutrient media and liquid enrichments traditionally. However, it was known that plate counts of bacteria from natural habitats are much lower than direct total counts and <1 % of these bacteria are culturable. Non culturable habit of these bacteria was the biggest hurdle in studying the true diversity of these habitats (Fry, 2000). In 1990, Stephen Giovannoni and David Ward's research groups first investigated bacterial diversity in the Sargasso Sea and in hot springs using molecular approaches based on sequence analysis of the highly conserved 16S rRNA gene. This was achieved in the Sargasso Sea study by extracting community DNA, PCR amplification of 16S rRNA genes, sequencing and identification of the source of these genes by phylogenetic analysis. This brought a new revolution in studying the true bacterial diversity by genotypical studies. Since protein synthesis is a very ancient process and present in all living cells, rRNA molecules are excellent targets to estimate evolutionary relationships.

Ribosomal RNA has been used by Woese *et al.* (1990) for his studies on bacterial evolution. Major properties of rRNA are: 1) these are old molecules present in the ribosomes, 2) they are functionally constant, 3) have a wide distribution, 4) are well conserved over large phylogenetic distances, 5) they occur in large number in cells (10^4 - 10^5 /cells). In bacteria, three types of rRNA molecules are present with different chain length and sedimentation rate(s): 5S rRNA (about 120 nucleotides), 16S rRNA (~ 1600 nucleotides) and 23S rRNA (~3000 nucleotides). The 5S molecule is too small and only suitable to distinguish major phylogenetic groups. 23S rRNA is excellent for phylogenetic studies, but so far few studies are available while 16S rRNA has been given most attention. Bacterial species can be identified by generating clone libraries of the 16S rRNA followed by sequencing and comparison with databases containing thousands of ribosomal cells. Analysis of 16S rRNA gene is now widely used for analysis of bacterial populations. The macromolecules that are most suitable for this would require the following prerequisites: i) generally present, ii)

functionally homologous in all organisms and iii) the sequence in the molecule should equally change during the evolutionary process.

Since rDNA-based fingerprinting lays too much emphasis on a single locus for deciphering phylogenetic affinities, multi-locus analysis by BOX-PCR, ERIC-PCR and random amplification of polymorphic DNA (RAPD) is also being investigated now a days. The BOX-PCR, in contrast to Amplified Ribosomal DNA Restriction Analysis (ARDRA), is multi-locus analysis and produces higher degree of resolution among the isolates. The repetitive sequences in the form of BOX elements are randomly located within the whole genome and the BOX primers amplify genomic regions between the two BOX elements. The distribution of these repetitive sequences (BOX and ERIC) is nearly a true reflection of genomic structure and amplification of inter-REP elements often detects similarities in a given group of bacteria. It is anticipated that REP- and ERIC-like sequences are virtually ubiquitous in bacteria and facilitate a rapid molecular characterization by PCR-based fingerprinting (Selenska-Pobell *et al.*, 1995).

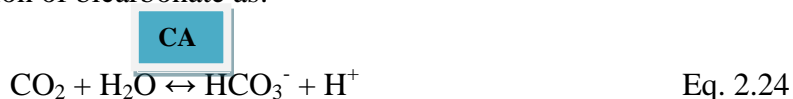
Recently, the development of culture-independent molecular techniques, like fluorescence *in situ* hybridization (FISH), polymerase chain reaction (PCR) or denaturing gradient gel electrophoresis (DGGE) improved the analysis of environmental samples. Beside fluorescent probes for the major groups of bacteria, species-specific probes are also being applied for filamentous bacteria (Eschenhagen *et al.*, 2003).

2.4. Carbonic anhydrase

The exponentially growing concentrations of Carbon dioxide in the environment invited researchers from worldwide to deal with the problem. Different ways were proposed to reduce the emission of CO₂ into the atmosphere and earlier strategies developed were:

- ✓ Reduce its production and release into the atmosphere (by use of less carbon intensive energy sources like wind, solar and nuclear energy)
- ✓ Increase efficiency of energy use from production to its end use

But both these options were not possible practically, so researchers shifted to capturing/sequestering the CO₂ in a safe manner. The alternative for CO₂ disposal in sequestration form paved way for fixing it in the form of carbonate minerals such as calcite, magnesite, and dolomite. This method came out to be safe and permanent method of disposing off the CO₂ as these carbonate minerals are environmentally benign and stable. But hydration of CO₂ to form carbonic acid is the rate-limiting step in the conversion of CO₂ into carbonate ions, which has a forward reaction constant of 6.2×10^{-3} s at 25 °C (Bond *et al.*, 1999; Sullivan *et al.*, 1993). The biological catalyst for this reaction came out to be Carbonic anhydrase (Ho and Sturtevant, 1963) which is one of the fastest enzymes that catalyses CO₂-hydration reaction with typical rates between 10⁴ and 10⁶ reactions per second for different forms of this enzyme (Heck *et al.*, 1994). It catalyzes the hydration of carbon dioxide and the dehydration of bicarbonate as:



The significant role of this enzyme in CO₂ sequestration studies paved way for exploring the properties of this enzyme and investigating its applications in other processes of carbonate precipitation.

Carbonic anhydrase (EC4.2.1.1) is a zinc-containing metalloenzyme that is widespread in animals, plants and micro organisms (Karlsson *et al.*, 1998; Smith and Ferry, 2000; Sharma *et al.*, 2009). This enzyme is fundamental to many eukaryotic biological processes such as photosynthesis, respiration, CO₂ and ion transport, calcification and acid base balance (Smith *et al.*, 1999; Smith and Ferry, 2000). The mode of action of this enzyme (Fig. 2.6) within the blood cells is as follows:

1. The binding of zinc lowers the pKa of water from 15.7 to 7, generating a hydroxide ion (OH⁻) to attack carbon dioxide. Zinc releases a proton from a water molecule to generate this hydroxide ion. pH decreases as a result from the decrease in the pKa. According to Le Chatelier's principle, this drives the reaction towards deprotonation.
2. The carbon dioxide substrate binds to the enzymes active site and is positioned for optimal interaction.

3. The hydroxide ion (being a great nucleophile) attacks the carbonyl of carbon dioxide, converting it to bicarbonate ion through the nucleophilic attack. Oxygen on the carbon dioxide molecule forms an intermediate bond with the Zn metal during the conversion process.

4. The enzyme is regenerated and the bicarbonate ion is released. The enzyme is ready for another reaction to occur. This regenerative ability of this enzyme allows this reaction to be highly efficient and kinetically fast to constantly process carbon dioxide within the blood cells.

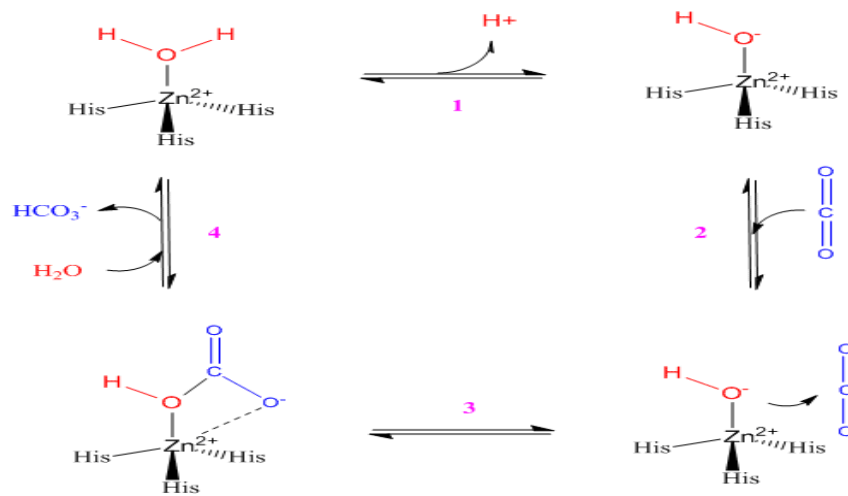
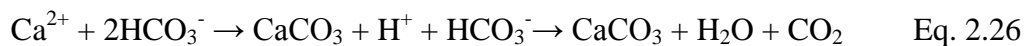


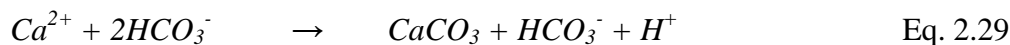
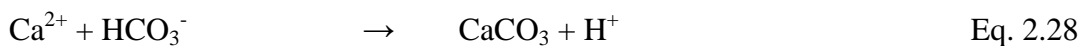
Fig. 2.6. Mechanism of CO₂ hydration catalyzed by CA (Prabhu *et al.*, 2011)

Quite a few studies have reported the precipitation of carbonates by CAs. Liu *et al.* (2005) used bovine CA in brines and reported that the enzyme increased the rate of precipitation of CaCO₃. Mirjafari *et al.* (2007) also observed that bovine CA could promote the formation of CaCO₃. CA aids in the precipitation of CaCO₃, by the following equations:



After successful applications of bovine CAs, several researchers looked for carbonic anhydrases from bacterial sources for biomimetic CO₂ sequestration studies (Bond *et al.*, 2001; Bhattacharya *et al.*, 2003, 2004; Liu *et al.*, 2005; Mirjafri *et al.*, 2007; Favre *et al.*, 2009; Raymond, 2009; Sharma and Bhattacharya, 2010; Wanjari *et al.*, 2011). Recently Li *et al.* (2011) reported that bacterial CA could also promote CaCO₃ precipitation as an activator. The role of bacterial CA in CO₂ sequestration encouraged its applications in carbonate biomineralization studies.

In enzyme catalyzed reactions increase in the rate of removal of CO₂ from the solution facilitated by CA increases the rate of production of NH₃ consequent from urea dissociation (Botre and Botre, 1989). Hydrolysis of urea results in accumulation of both bicarbonate and ammonia in the cell, which favors the physiological and regulatory links between urea and bicarbonate metabolism (Stahlet *et al.*, 2005). Also, the incorporation of nickel into the active site of urease is dependent on CO₂/ HCO₃⁻ metabolism which is in turn regulated by carbonic anhydrase (Park and Hausinger, 1995). It is thus reasonable to expect that along with urease, carbonic anydrase might also be involved in calcium carbonate precipitation in bacterial system. This enzyme might be playing a synergic role with urease. Achal and Pan (2011) also reported the involvement of bacterial CA in CaCO₃ precipitation. Li *et al.* (2011) hypothesized following reactions involving UA and CA that might be taking place during CaCO₃ precipitation:



Though lot of work on bacterially induced carbonate precipitations has been carried out with urease as the chief enzyme, there is need to understand the role of CA also in calcium

carbonate precipitation. Its relationship with Urease also needs to be elucidated along with its impact on bacterial promoted carbonate precipitation.

The activity of Carbonic anhydrase activity can be measured conveniently in aqueous phase by using nitrophenyl esters. CA catalyses the hydrolysis of nitrophenyl esters with different efficiencies depending on the structure of the acyl part of substrate. The most efficient ester substrate for CA has been found to be para-nitrophenyl acetate (p-NPA) because of short and few acyl groups (Fig. 2.7).

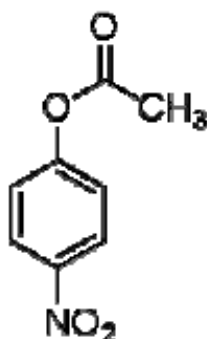


Fig. 2.7. Formula of para-Nitrophenyl Acetate.

p-NPA is bound as neutral species to the CA active site, allowing the strong nucleophilic ($\text{Zn}^{2+}(\text{OH})^-$) attack, without any electrostatic repulsions, thus effectively hydrolyzing it (Innocenti *et al.*, 2008). Purified CA from *Bacillus pumilis*, *Pseudomonas fragi* and *Micrococcus lylae* have been reported to give esterase activity of 6840 U/g, 4890U/g and 4400 U/g respectively (Prabhu *et al.*, 2011).

2.5. Role of Enzymes in bacterial carbonate precipitation

In order to achieve maximum enzyme productivity, it is important first to understand the properties of the enzymes. Its kinetics, optimum conditions and its regulation need to be explored. Enzyme kinetics is the study of the chemical reactions that are catalyzed by enzymes. Studying an enzyme's kinetics can reveal the catalytic mechanism of the enzyme, its role in metabolism, how its activity is controlled etc. Optimum conditions also need to be investigated in order to achieve the maximum product of the enzymatic reaction. As

regulation of enzyme activity is essential for energy efficient cell function, there is need to identify the parameters that maintain high enzyme activity. Many enzymes within the cell are produced constitutively; i.e they are produced under all growth conditions. Other enzymes are not required all the time and their synthesis can be turned on or off (repressed) according to metabolites present. This type of genetic control is regulated at transcriptional level by the cell where messenger mRNA, which codes for the enzyme is produced from DNA template (Fig. 2.8).

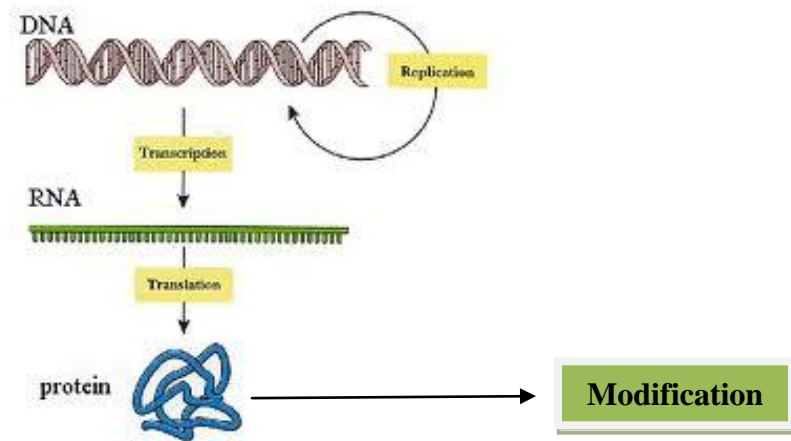


Fig. 2.8. Regulation levels for enzyme activity. Enzymes can be regulated at transcription level or post transcription level.

Enzymes that are controlled at transcription (inducible/repressible) are normally repressed under normal conditions in order to conserve energy from unnecessary protein synthesis. The presence of inducer, normally its substrate can strongly induce an enzyme upto 1000 fold its level under non induced conditions (Lowe, 2000).

2.5.1. Characteristics of bacterial ureases

As far as bacterial ureases are concerned, they have been isolated and characterized by various researchers (Mobley and Hausinger, 1989; Mobley *et al.*, 1995). These ureases are composed of three distinct subunits, one large (α 60 – 76 kDa) and two small (β 8–21 kDa, γ 6–14 kDa) commonly forming ($\alpha\beta\gamma$)₃ trimers stoichiometry resulting in the enzyme molar masses between 190 and 300kDa (Barbara, 2009) (Fig. 2.9). *Helicobacter* species have an

exceptional urease which is composed of two subunits, α (61–66 kDa), β (26–31 kDa) (Ha *et al.*, 2001).

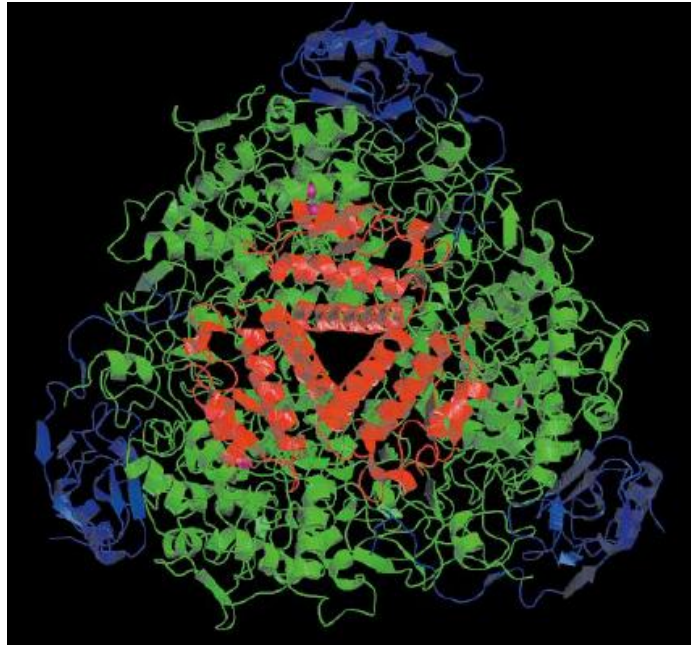


Fig. 2.9. Urease from *Bacillus pasteurii*. The green, blue and red ribbons represent α , β and γ subunits while magenta spheres are nickel ions (Benini *et al.*, 1999).

Stocks - Fischer *et al* (1999) in their studies on Urease from *B. pasteurii* reported pH 8.0 to be the best for maximum activity of this enzyme though it increased from 6 to 10. Substantial activity remained at pH 9, but it started decreasing afterwards. Balan *et al.* (2012) reported 35°C as the optimum temperature for production of Urease in *Klebsiella* sp. Similar results were reported by Yang *et al* (2008) in *Enterobacter* spp. For urease, the K_m and V_{max} values at pH 7.0 were found to be 41.6 mM and 3.55 mM min⁻¹ mg⁻¹ while at pH 7.7, the kinetic constants decreased to 26.2 mM for K_m and 1.72 mM min⁻¹ mg⁻¹ for V_{max} (Stocks - Fischer *et al.*, 1999). This study reported higher affinity of the enzyme at increased pH. Bachmeier *et al.* (2002) reported K_m and V_{max} for *B. pasteurii* as 17.3 mM and 1.57 mM min⁻¹ mg⁻¹ protein whereas after immobilization of urease in polyurethane, K_m was found to increase to 22.99 mM while V_{max} decreased to 0.73 mM min⁻¹ mg⁻¹.

2.5.2. Characteristics of bacterial Carbonic anhydrases

Many researchers have studied CA from several bacterial sp. Three evolutionarily distinct classes of carbonic anhydrase namely α class, β class and γ class have been identified. All the three classes have been found in prokaryotes (Smith and Ferry, 2000; Tripp *et al.*, 2001). In case of bacterial system, Carbonic anhydrase activity was first reported in *Neisseria sicca* by Veitch and Blankenship (1963) and this enzyme was the first carbonic anhydrase purified from a prokaryote (Silverman and Lindskog, 1988) (Fig. 2.10). The *N. sicca* enzyme is a monomer with a molecular mass of 28.6 kDa (Adler *et al.*, 1972). The molecular weight of the purified CA from *C. freundii* SW3 sp. has been reported to be 24 kDa which added it in the β class (Ramanan *et al.*, 2009). While in case of *E. gergoviae*, *E. taylorae*, *A. hydrophila* and *A. caviae*, subunit molecular weight of CA was determined to be ~ 29 kDa which suggested it to be of α type (Sharma *et al.*, 2008).

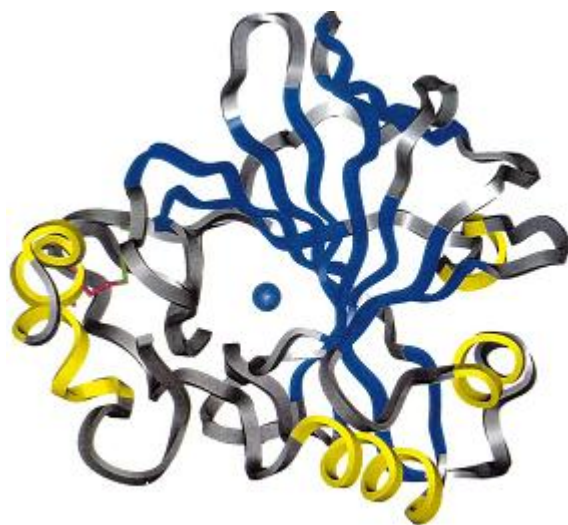


Fig. 2.10. Crystal structure of the *Neisseria gonorrhoeae* K class carbonic anhydrase. The active site Zn is shown in blue (Smith and Ferry, 2000).

Buzolyova and Somov (1999) reported the presence of CA in *Yersinia pseudotuberculosis* and *Listeria monocytogenes*, the pathogens isolated from soil and water. Recently, CA from *Bacillus pumilis*, *B. mucilaginous*, *B. megaterium*, *B. subtilis*, *Citrobacter freundii*, *Methanothermobacter thermoautotrophicum*, *Enterobacter gergoviae*, *E. taylorae*, *Aeromonas hydrophila*, *A. caviae*, *Pseudomonas fragii*, *Stenotrophomonas acidophilia* and

Micrococcus lylae has also been reported (Sharma *et al.*, 2009; Ramanan *et al.*, Wanjari *et al.*, 2009).

Sharma *et al.* (2008a) reported the maximum CA activity to be in the range of pH 8.0 to 8.5 and at a temperature of 40 - 45°C by various bacterial isolates. However the enzyme stability was found to be from pH 7.5 – 8.5 and from 35 - 40°C in bacterial isolates of *E. gergoviae*, *E. taylorae*, *A. hydrophil* and *A. cavia*. Zhang *et al.* (2011) reported that in case of *B. mucilaginosus* K02 the optimum pH for CA production is 5.5 - 6.5 whereas 32 – 36°C was found to be the optimum temperature. The Km and Vmax of purified CA from *B. pumilis* was reported to be 0.87 mM and 0.93μ moles/min while that of immobilized enzyme as 2.36 mM and 0.54 μ moles/min by Wanjari *et al.* (2011). The study of enzyme properties needs to be investigated in order to understand the best conditions for its reaction.

2.5.3. Activity Staining for Enzymes

Zymography and activity staining is a widely used electrophoretic technique for the detection of hydrolytic enzymes, based on the substrate repertoire of the enzyme. For detection of urease, Sharma *et al.* (2008b) reported a simple zymographic method in non-denaturing polyacrylamide gels in case of *Canavalia ensiformis*. In this method, the protein samples subjected to polyacrylamide are incubated with a solution of urea, followed by incubation with β-mercaptoethanol–nitroprusside solution. Presence of urease is detected by formation of purple bands corresponding to the site of urease activity. In the process, sodium nitroprusside reacts with thiols and forms purple coloured complex in alkaline medium (Szacilowski *et al.*, 2002) which is produced if the protein sample has ureolytic activity. Bergdale *et al.* (2012) recently reported zymography analysis of urease enzyme from *Sporosarcina pasteurii* and urease cloned strains of *Pseudomonas*.

In case of CA, Hou *et al.* (2000) suggested protein electrophoretic method based on SDS PAGE. In this method, CA containing protein samples of dioscorins, tuber Storage proteins of Yam (*Dioscorea batatas Decne*) were subjected to 15% SDS PAGE followed by bromothymol blue staining. This method relies on dehydration activity of CA where bromothymol blue gives yellow colour upon being reduced to pH 6.5 – 7.0 depicting the presence of CA. Ramanan *et al.* (2009) got positive activity staining results in case of

several bacterial isolates as *Proteus vulgaris* RS7, *Bacillus subtilis* SA3, *Enterobacter sp* RS1 and *Citrobacter freundii* SW3.

2.5.4. Enzyme inhibitors

Hydroxamic acids are the family of compounds presenting the strong chelating properties towards various metal ions (Kurzak *et al.*, 1992). The coordination phenomenon is responsible for many biochemical actions in which naturally occurring hydroxamic acids participate. The compounds containing the hydroxamic group have been shown to inhibit activity of various metalloproteinases such as urease (Stemmler *et al.*, 1995), oxidases (Ikeda-Saito *et al.*, 1991), zinc proteinases involved in cancers (Hajduk *et al.*, 1997; Groneberg *et al.*, 1999). One of the simplest hydroxamic acids is acetohydroxamic acid (CH_3CONHOH), which has been extensively studied by theoretical methods (Ventura *et al.*, 1993; Bagno *et al.*, 1994; Muñoz-Caro *et al.*, 2000; Niño *et al.*, 2000) (Fig. 2.11).

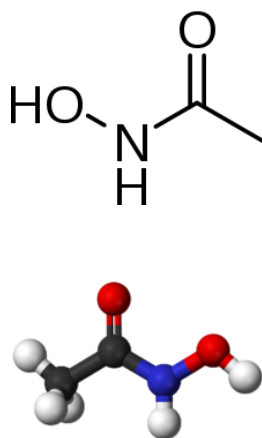


Fig. 2.11. Structure of Acetohydroxamic acid

The molecule is similar to urea, chelates the nickel atoms at the active site of urease and acts as competitive inhibitor of urease enzyme (Fishbein and Carbone, 1965). It has been successfully used for inhibition of urease activity in *Helicobacter pylori* as well as *B. pasteurii* (Krishnamurthy *et al.*, 1998; Bachmeier *et al.*, 2002) and also for treatment of urinary tract infections (Mushner *et al.*, 1974) as it prevents alkalinisation of urine by inhibiting urease and thereby preventing hydrolysis of urea and subsequent production of

ammonia. It was also reported by Bachmeier *et al.* (2002) that addition of AHA in the bacterial culture does not affect its growth.

Acetazolamide (2-acetylamino-1,3,4-thiadiazole-5-sulfonamide), which belongs to the family of sulfonamide drugs has been a known inhibitor of CA. The compound has a molecular formula of $C_4H_6N_4O_3S_2$ (Coleman, 1967; Wingard *et al.*, 1991) (Fig. 2.12) and first used as a diuretic in clinical use. X-ray crystallographic investigations have revealed the binding nature of acetazolamide to the active site of carbonic anhydrase (Supuran and Scozzafava, 2001; Abbate *et al.*, 2004). The inhibitory effect of sulfonamides on carbonic anhydrase activity was reported by many (Lindskog and Wistrand, 1987; Supuran, 1994, 2001a,b; Supuran and Scozzafava, 2002). Though all the unsubstituted members of sulfonamide family inhibit the activity of carbonic anhydrase, but acetazolamide has been most widely studied among them (Wingard *et al.*, 1991; Burnham *et al.*, 2001). It has been used successfully for inhibition of bacterial CA in *Neisseria gonorrhoeae*, *Aeromonas* sp., *Enterobacter* sp., *Shigella* sp. and *Klebsiella* sp (Huang *et al.*, 1998; Sharma *et al.*, 2008a).

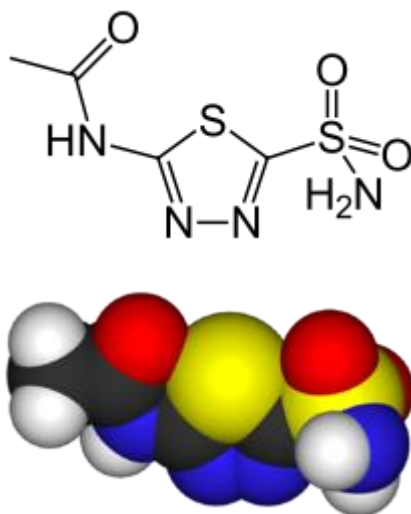


Fig. 2.12. Structure of Acetazolamide

Though lot of studies have been carried out to investigate bacterial ureases and carbonic anhydrases but no work has been reported on inhibiting both the enzymes in bacterial system and determine the impact of these enzymes in calcium carbonate precipitation. It is mandatory to inhibit both the enzymes by specific inhibitors and elucidate the effect of both enzymes on the production of carbonates in bacterial system.

2.6. Biofilm and EPS (Extracellular polymeric substances)

Various mechanisms that induce precipitation by bacteria in natural habitats, have been proposed and discussed above (Ehrlich, 1996; Rivadeneyra *et al.*, 2004; Dittrich *et al.*, 2010). The precise role of bacteria and bacterial activities in the process of carbonate crystallization seem to fall categorically into three different tracks.

1. As a by-product of microbial metabolism
2. Due to carbonate nucleation on the cell wall
3. Due to extracellular macromolecules.

The extracellular polymeric materials i.e., exopolysaccharides (EPS) and capsular polysaccharides (CPS) produced by bacteria form a large class of polymers implicated in various processes such as the formation of structure and architecture of biofilm matrices and calcium carbonate precipitation (Ercole *et al.*, 2007; Decho, 2009; Dittrich & Sibling, 2010). Biofilm is an assemblage of microbial cells irreversibly associated with a surface and usually enclosed in a matrix of polysaccharide material. It is composed primarily of microbial cells and extracellular polymeric substances (EPS) which play role in structure and function of different biofilm communities (Kokare *et al.*, 2009). It is now widely recognized that in natural settings bacterial cells are most often found in close association with surfaces and interfaces, in the form of multicellular aggregates referred to as biofilms. This proclivity towards multicellularity makes bacterial cells similar to many other types of living cells: capable of unicellular existence and yet generally residing within multicellular communities. Biofilms offer their member cells several benefits, of which protection from environmental insults and assaults is foremost (Davey and O'Toole, 2000).

The formation of biofilm occurs step by step, such as attachment of bacterial cell to a surface, colonization and development (Fig. 2.13). Biofilms exist on all types of surfaces from soil to food products (Kokare *et al.*, 2009).

Biofilm formation can occur by at least three mechanisms. One is by the redistribution of attached cells by surface motility. A second mechanism is from the binary division of

attached cells (Heydorn *et al.*, 2000). As cells divide, daughter cells spread outward and upward from the attachment surface to form cell clusters, in a similar manner to colony formation on agar plates. A third mechanism of aggregation is the recruitment of cells from the bulk fluid to the developing biofilm (Neilson *et al.*, 2000). The relative contribution of each of these mechanisms will depend on the organisms involved, the nature of the surface being colonized, and the physical and chemical conditions of the environment. In oligotrophic environments mature biofilms may consist of little more than a sparse covering of cells with relatively little structural complexity. Biofilms can take over 10 days to reach structural maturity, based on microscopically measured physical dimensions and visual comparison (Stoodley *et al.*, 1999).

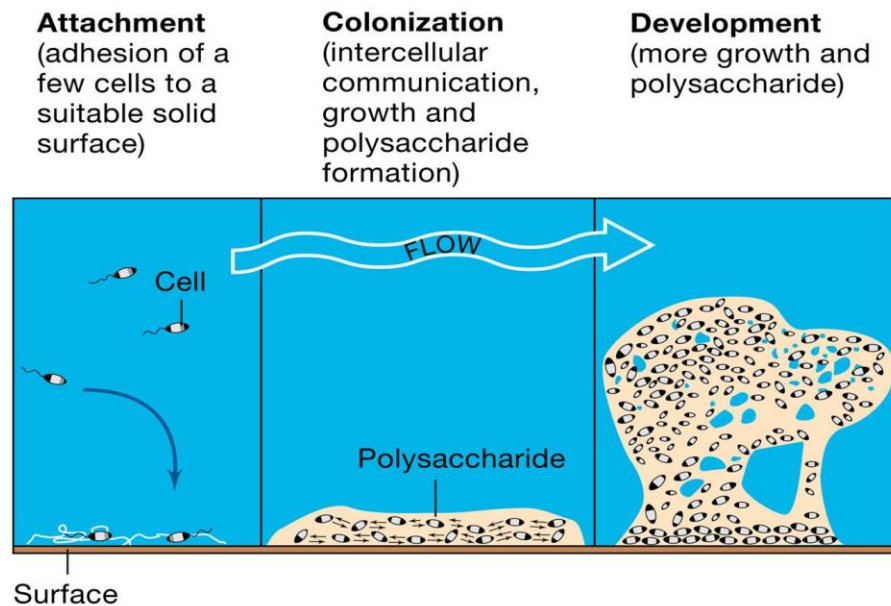


Fig. 2.13. Biofilm formation (Source Montana State University Center for Biofilm Engineering)

The biofilm structure appears to be largely determined by the production of slime-like matrix of extracellular polymeric substances (EPS), which provides the structural support for the biofilm (Flemming *et al.*, 2000) (Fig. 2.14). Microbial biofilms are often sufficiently thick and extensive to be visible to the unaided eye, and they may contain millions of prokaryotic (and sometimes some eukaryotic) cells in arrangements that facilitate the stable juxtaposition of physiologically cooperative organisms (Stoodley *et al.*, 2003).

Microorganisms in biofilms produce extracellular polymeric substances (EPS) that hold the cell aggregates together and form the structural biofilm matrix scaffold (Merz-Preiss & Riding, 1999; Dick *et al.*, 2006). In case of bioprecipitation, researchers have made attempts to investigate the role of bacterial Biofilms and Extrapolymeric substances. The matrix of extracellular polymeric secretions has been described to influence the calcium carbonate precipitation in a positive way (Kawaguchi and Decho, 2002). The bacterial extra polymeric substances can trap calcium ions at a given pH or serve as growth modifiers controlling crystallization and influencing the polymorphic development of CaCO_3 during mineralization, as observed in cyanobacteria (Kawaguchi and Decho, 2002; Braissant *et al.*, 2003; Dupraz *et al.*, 2009). EPS has been reported to play an important role in the coverage of the surface by biofilms, cell adhesion and precipitation, either through trapping and concentration or through the action of specific proteins that influence precipitation (Tsuneda *et al.*, 2003; Rodriguez – Navarro *et al.*, 2012). Number of studies also clarified that mutants unable to synthesize EPS are unable to form biofilms (Sutherland, 2001). Hammes *et al.* (2003) also suggested that specific proteins present in biological extracellular polymeric materials may cause the formation of different polymorphs of CaCO_3 bioliths.

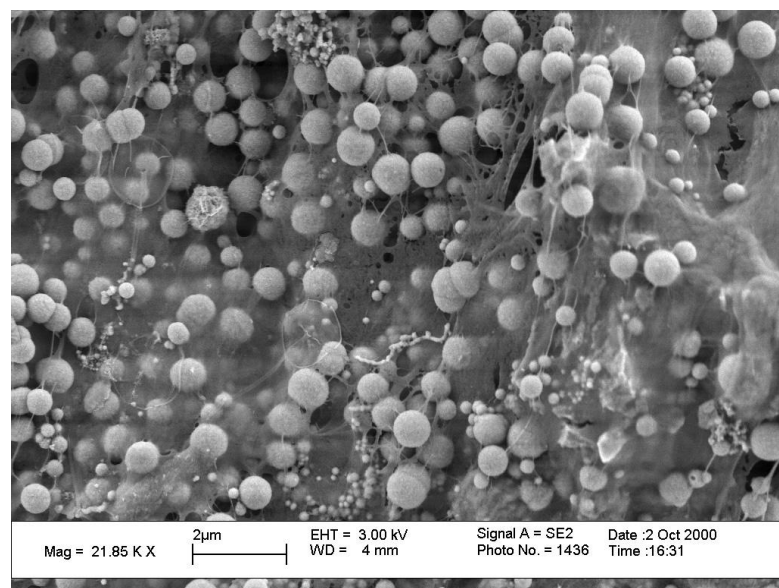


Fig. 2.14. Surface of a biofilm with hydrated matrix of polysaccharide and protein formed by aggregates of bacteria (<http://dujs.dartmouth.edu/fall-2009/biofilms-bacteria's-elixer-of-survival>)

Merz-Preiss and Riding (1999) showed that a biofilm formed on the surface of the stones acts as nucleation site for extracellular calcium carbonate precipitation. Ercole *et al.* (2012) also reported that deposition of carbonate crystals is promoted by Extracellular polymeric materials. The same group recently reported that presence of calcium ions increases the production of biofilms. In the presence of calcium ions, SDS PAGE analysis revealed overexpression of some proteins in both EPS and capsular polymeric substances (CPS) fractions of *Bacillus firmus* and *Neisseria calcarea*. It suggested that calcium ions modulate the protein composition of extracellular fraction which further impacts bioprecipitation. The shape of the crystals precipitated by CPS fraction from *N. calcarea* was similar to the crystals precipitated by living cells.

Given their ubiquity and importance in the microbial world, it is hardly surprising that biofilms have attracted the attention of the scientific community as they might play a major role as a protective agent to combat adverse conditions inside building materials. It is imperative to understand the involvement of these extracellular molecules in bacterial calcium carbonate biomineralization.

2.7. Polymorphism of carbonate crystals

After determining the fundamental principles and enzymes involved in MICCP, studies were carried to investigate the different CaCO_3 polymorphs formed by bacterial cells. Researchers have reported that calcium carbonate forms three anhydrous polymorphs: calcite, aragonite and vaterite, two hydrated crystalline phases, monohydrocalcite ($\text{CaCO}_3 \cdot \text{H}_2\text{O}$) and ikaite ($\text{CaCO}_3 \cdot 6\text{H}_2\text{O}$), and various amorphous phases (ACC) with differences in short range order and degree of hydration (Lippmann, 1973; Rieger *et al.*, 2007; Gower, 2008; Gebauer *et al.*, 2010) (Fig. 2.15). Bacterial induced calcium carbonate precipitation results in the production of many of these varying CaCO_3 phases (Rodriguez Navarro *et al.*, 2012). Although vaterite and calcite are the most common bacterial calcium carbonate polymorphs (Ben Chekroun *et al.*, 2004; Rodriguez Navarro *et al.*, 2007; González-Muñoz *et al.*, 2011), mineralization of monohydrocalcite (Krumbein, 1975) and aragonite (Krumbein, 1974, Sánchez-Navas *et al.*, 2009) have also been reported. The evidence that bacterial mineralization of calcium

carbonate involves the formation of ACC precursor phases is also growing (Hammes *et al.*, 2003; Benzerara *et al.*, 2006; Chen *et al.*, 2009).

Barabesi *et al.* (2007) reported plausible genetic link in calcium carbonate production by *Bacillus subtilis*, suggesting that bacterial precipitation of carbonate minerals brings some evolutionary advantage to the microorganisms. For instance, it may help fixating excess/toxic Ca (Obst *et al.*, 2009) or help bacteria to survive unfavorable conditions in a cryptobiotic state (Yoshida *et al.*, 2010). Polymorphism is not the only aspect bringing about differentiation amongst CaCO₃ crystals. Even in case of calcite, there are more than 300 different crystal forms which combine to produce thousand different crystal variations (<http://mineral.galleries.com>).

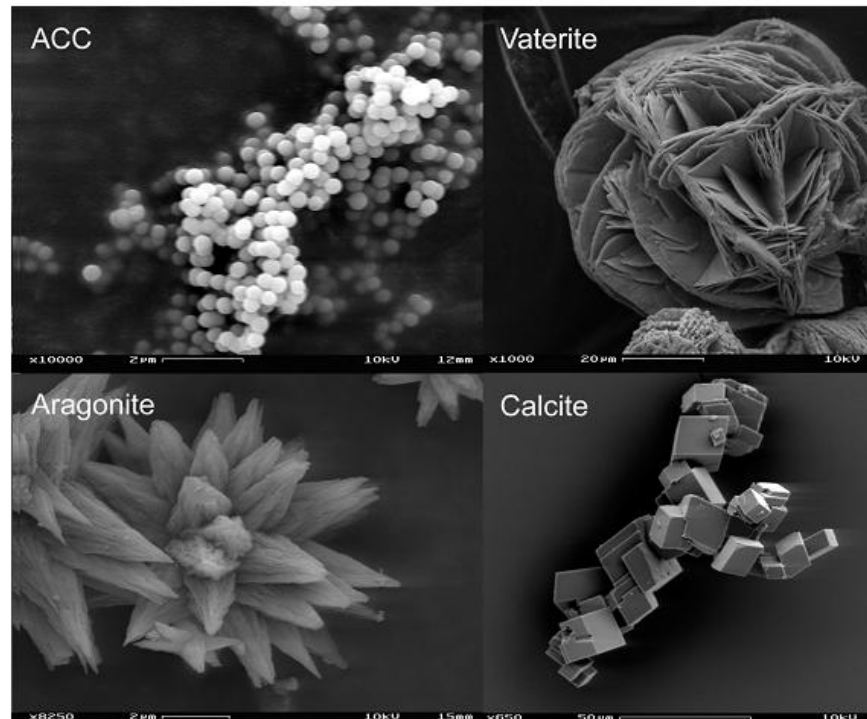


Fig. 2.15. Polymorphs of CaCO₃ (<http://www.ruhr-uni-hum.de/sediment/forschung.html>)

Despite extensive studies on bacterial carbonatogenesis, little is known on what is the cause(s) of polymorph selection during bacterial calcium carbonate mineralization. Very little is known about the kinetic or thermodynamic control determining which polymorph

develops upon bacterial carbonatogenesis (Zamarreno *et al.*, 2009). It has been suggested that specific proteins in extracellular polymeric substances (EPS) produced by different bacteria control aragonite or calcite polymorph selection (Kawaguchi and Decho, 2002). Briassant *et al.* (2003) have associated polymorph selection (vaterite vs. calcite) during bacterial carbonatogenesis with the characteristics of EPS. Lian *et al.* (2006) reported that *Bacillus megaterium* cells and EPS induce calcite and vaterite precipitation respectively. However, Ercole *et al.* (2007) showed that EPS isolated from *Bacillus firmus* and *Bacillus sphaericus* induce the precipitation of calcite.

Studies suggested that phase, amount and morphology of calcium carbonate minerals depend on supersaturation, temperature, pH and $[Ca^{2+}] / [CO_3^{2-}]$ ratio. The saturation index, $SI = \log \Omega = \log IAP/K_s$; where Ω is the saturation state of the system, IAP is the ion activity product and K_s is the thermodynamic solubility product of the relevant phase. Calcium carbonate precipitation in microbial systems typically occurs when the saturation index (with respect to calcite) is above 1 (Arp *et al.*, 2001; Mitchell *et al.*, 2006). Along with this, organics also play important role in the carbonate precipitation. The organics act as crystallization inhibitors (when in solution) and prevent the nucleation of calcium carbonate even at high SI values (Rodriguez Navarro *et al.*, 2007). It follows that bacterial presence and activity are a prerequisite for the precipitation of calcium carbonate. The bacterial metabolic activity produces necessary increase in supersaturation to induce the heterogeneous crystallization of calcium carbonate.

Under far from equilibrium conditions (i.e., high supersaturation) where kinetics rather than thermodynamics control crystallization (Kitamura, 2002), the crystallization of $CaCO_3$ typically follows the Ostwald's rule of steps (Ogino *et al.*, 1987; Meldrum and Colfen, 2008). This rule dictates that the less stable (more soluble) phase(s) will precede the crystallization of the more stable one(s). In the case of calcium carbonate, the crystallization sequence according to the Ostwald's rule is: ACC – vaterite – aragonite (Temperature > 30-35°C) – calcite (Ogino *et al.*, 1987; Rieger *et al.*, 2007; Meldrum and Colfen, 2008). At room temperature and alkaline pH (8.5-10.5), formation of vaterite is favored (Tai and Chen, 1998). This phase typically appears as spherulites made up of radial fibrous crystals

elongated along their c-axis (Rodriguez Navarro *et al.*, 2007). Vaterite may eventually transform into stable calcite via a dissolution/precipitation process (Spanos and Koutsoukos, 1998). Conversely, at room temperature and pH close to neutrality, as well as $\text{pH} > 11$, the development of calcite is promoted (Tai and Chen, 1998).

Besides its scientific interest, calcium carbonate polymorph selection can have important technical implications (Meldrum and Colfen, 2008). For instance, the bacterial conservation of building materials requires the formation of a coherent, durable, calcium carbonate cement i.e. calcite. This is not fully achieved if metastable vaterite (more soluble than calcite) is formed during a bacterial conservation treatment (Rodriguez Navarro *et al.*, 2003). The same principle may apply for soil strengthening, cement and concrete protection, solid phase capture of groundwater metal contaminant, and/or the effective (long term) CO_2 sequestration via bacterial calcium carbonate mineralization. So, there is growing need to characterize various carbonate polymorphs formed by different bacteria under similar conditions.

2.8. Applications of microbial carbonates in building materials

Microbial metabolic activities lead to production of relatively insoluble organic and inorganic compounds intra- and/or extracellularly, which remain in the environment for a long time even after cell death. Few microorganisms produce glycocalyx and a variety of organic polymers outside the cell wall (Lappin-Scott *et al.*, 1988; MacLeod *et al.*, 1988), while others accumulate inorganic compounds such as phosphorites, carbonates, silicates, iron, and manganese oxides in cytoplasm (Beveridge *et al.*, 1983; Ghiorse, 1984; Knoll, 1985; Ruiz *et al.*, 1988; Rivadeneya *et al.*, 1991).

Application of bacterial carbonates lead to decrease in the permeability of building materials due to *in situ* growth and metabolism of microorganisms (Raiders *et al.*, 1989). The potential of MICCP technology in restoration of cement mortar cubes, sand consolidation and limestone monument repair, reduction of water and chloride ion permeability in concrete, filling of pores and cracks in concrete, enhanced strength of red bricks via urea hydrolysis pathway has been investigated by many researchers (Stocks – Fischer *et al.*, 1999; Bang *et*

al., 2001; Bachmeier *et al.*, 2002; Dick *et al.*, 2006; Ramakrishnan 2007; De Muynck *et al.*, 2008a,b; Van Paassen *et al.*, 2009; Sarda *et al.*, 2009; Achal *et al.*, 2009a,b; 2011a,b; Achal *et al.*, 2010; Chu *et al.*, 2011, Al Qabany 2011).

2.8.1. Microbial calcite in cementitious materials

The applicability of microbial calcite to improve the compressive strength of mortar and concrete has been proved by several studies (Bang *et al.*, 2001; Ramachandran *et al.*, 2001; Ghosh *et al.*, 2005; De Muynck *et al.*, 2007a,b; Park *et al.* 2010; Jonkers *et al.*, 2010; Achal *et al.*, 2011a,b) where different micro organisms have been applied in the concrete mixture (Table 2.3). In all these, microbial calcite successfully improved the properties of the cement concrete specimens.

De Muynck *et al.* (2008b) improved the permeability characteristics of mortar by *B. sphaericus* Ramakrishnan *et al.* (1998) reported the increase in resistance of concrete towards alkali, freeze thaw attack, drying shrinkage and reduction in permeability upon application of bacterial cells. Achal *et al.* (2011) treated mortar cubes with *Bacillus* sp. CT-5 and reported nearly six times less absorption of water as compared to untreated specimens. The same group in 2010b studied the effect of *Bacillus pasteurii* on water impermeability in concrete cubes and found the reduction in penetration of water which was more significant on the top side as compared to sides because of better compaction and closing of pores at the top surface.

2.8.2. Microbial calcite in crack remediation

Use of microbial calcite has exhibited high potential for remediation of cracks in various structural formations such as concrete and granite (Gollapudi *et al.*, 1995; Stocks- Fisher *et al.*, 1999). Microbiologically enhanced crack remediation has been reported by Bang and Ramakrishnan (2001) where *Bacillus pasteurii* was used to induce calcium carbonate precipitation. Ramachandran *et al.* (2001) proposed microbiological remediation of cracks in concrete. Polyurethanes have also been used as vehicle for immobilization of calcifying enzymes and whole cells because of its mechanically strong and biochemically inert nature

(Klein and Kluge, 1981; Wand and Ruchenstein, 1993). Bang *et al.* (2001) investigated the encapsulation of bacterial cells in polyurethanes and reported positive potential of Microbiologically enhanced crack remediation by PU immobilized bacterial cells.

De Belie and De Muynck (2008) reported positive potential of microbiologically induced carbonate precipitation for the repair of cracks in concrete by *B. sphaericus* while Ramachandran *et al.* (2001) observed the effect of microbial calcite on compressive strength values in Portland cement mortar cubes by *B. pasteurii* and found 61% increase. Qian *et al.* (2010a) also reported that compressive strength of treated specimens could be restored to 84%.

Table 2.3. Overview of different applications where microbial calcite is used as biocement in cementitious materials.

Application	Author	Organism	Solution
Cement mortar	Calcite bioconcept (Le Metayer-Leverel <i>et al.</i> , 1999)	<i>Bacillus cereus</i>	Nutrical
Remediation of cracks in concrete	Ramachandran <i>et al.</i> , (2001)	<i>Bacillus pasteurii</i>	SF*
	De Belie <i>et al.</i> , (2008)	<i>Bacillus sphaericus</i>	Growth and biocementation medium
Concrete	Ramachandran <i>et al.</i> , (2001)	<i>Bacillus pasteurii</i>	SF
	Ghosh <i>et al.</i> , (2005)	<i>Shewanella</i>	
	Mukherjee <i>et al.</i> , (2010)	<i>Sporosarcina pasteurii</i>	CSL urea medium, LML urea medium NB urea medium
Self Healing	Jonkers <i>et al.</i> , (2007)	<i>Bacillus pseudifirmus</i> <i>Bacillus cphnii</i>	- Calcium lactate

*Stocks - Fischer *et al.* (1999)

2.8.3. Microbial calcite in restoration of stone buildings

Bacterially induced carbonate precipitation has also been checked for reducing the permeation properties and enhancing the durability properties of ornamental stone by various researchers (Le Me´tayer *et al.*, 1999; Rodriguez-Navarro *et al.*, 2003; Dick *et al.*, 2006). Overview of different methodologies for deposition of microbial calcite layer on stone surfaces is given in table 2.4.

Bacterially induced calcium carbonate was compatible with the substrate and significantly reduced the water sorptivity of the treated stone (Le Me´tayer-Levrel *et al.*, 1999). Rodriguez- Navarro *et al.* (2003) proposed the use of *Myxococcus Xanthus*, an abundant Gram-negative, non-pathogenic aerobic soil bacterium. This bacterium has been known to induce the precipitation of carbonates, phosphates and sulfates in a wide range of solid and liquid media (González-Muñoz *et al.*, 1993, 1996; Ben Omar *et al.*, 1995, 1998; Ben Chekroun *et al.*, 2004; Rodriguez-Navarro *et al.*, 2007). Calcium carbonate cementation in this case was observed upto a depth of several hundred micrometers (>500µm) without any plugging or blocking of the pores. Another research group led by Tiano *et al.* (1999) studied the consolidating effect of microbial calcite crystals on Pietra di Lecce bioclastic limestone by use of *Micrococcus* spp. and *Bacillus subtilis*. Dick *et al.* (2006) reported 50% reduction in water absorption by treating limestone cubes with two strains of *B. sphaericus*. Capitelli *et al.* (2006) investigated the positive potential of Carbogel as a delivery system for bacteria. Zamarreno *et al.* (2009) investigated the application of calcite crystals precipitated by fresh water bacteria on limestone and found significant reduction in pore sizes of the substrate in treated specimens.

2.8.4. Microbial calcite in consolidation of sand columns

Many researchers have evaluated the potential of bacterial calcite in consolidation of sand plugs (Stocks – Fischer *et al.*, 1999; Bachmeier *et al.*, 2002; Dick *et al.*, 2006; Whiffin *et al.*, 2007; Achal *et al.*, 2009b; van Paassen *et al.*, 2009). Kantzas *et al.* (1992) reported that sand consolidation by *Bacillus pasteurii* reduced the porosity by up to 50% and permeability by up to 90% in the areas where the cementation took place. Improvement in strength of sand

columns upon bacterial carbonates was also reported by Ferris and Stehmeier (1992), DeJong *et al.* (2006) and Whiffin *et al.* (2004). Recent research initiatives (Whiffin *et al.*, 2004, 2005; Mitchell and Santamarina, 2005; DeJong *et al.*, 2006; Ivanov and Chu, 2008; Van Paassen *et al.*, 2009; Al Qabany *et al.*, 2011; Cheng *et al.*, 2013) have shown that the calcite crystals form cohesive “bridges” between existing sand grains, thereby leading to increase in the stiffness of sand with limited decrease in permeability. From the above mentioned applications, microbial concrete seems to bring a new revolution in the civil industry. Promising results on the use of micro organisms for improvement of the durability of building materials have drawn the attention of research groups all over the world.

Though the use of a microbial calcite as biosealant for concrete, stone and sand has proved its potential in various building materials, but there are many areas where applications of this wonder metabolic product needs to be explored. Major among those are varying grain sizes & density sand columns, low energy building materials and building materials manufactured from industrial by products.

2.8.5. Microbial calcite in varying grain sized and density sand columns, low energy and industrial by-product building materials

Sand is one of the most common materials being used worldwide for most of the building structures. The most important role in structural properties of sand is dependent upon the grain size, which plays a crucial role. Trask (1959) studied the effect of grain size on strength of sand, clay and water. Their work concluded that for given water content and clay-sand ratio, the strength increases as the grain size of the sand decreases. Ozgurel and Vipulanandan (2005) studied the effect of grain size and distribution on permeability and mechanical behavior of acrylamide grouted sand. Their investigation revealed that particle size distribution influenced the strength, modulus and stress-strain relationship but had minimal effect on the failure strain and permeability of grouted sand. Wang *et al.* (2010) studied the effect of grain size distribution and structure on mechanical behaviour of silty sand and concluded that the grain size distribution affects the mechanical properties of mixed sand. But no report till date has been made on the effect of bacterial calcite on sand

with varying grain sizes. Along with varying grain sizes, varying densities of sand columns also need to be evaluated for application of bacterial calcite.

Table 2.4. Overview of different methodologies where microbial calcite has been deposited as a layer on surface of stone.

Authors	Experimental methods		Application procedure	
	Inoculum	Bacteria	Nutrients	Evaluation procedures
Le Metayer-Leverel <i>et al.</i> (1999)	Culture in exponential phase: 10^7 to 10^9 cells/ ml	Spraying	Spraying (5 times)	Water absorption, SEM analysis, surface roughness, colorimetry and plate count
Tiano <i>et al.</i> (1999)	Overnight culture 10^6 cells cm^{-2}	Brushing on water saturated specimens	Wetting every day for 15 days	Water absorption, colorimetric measurements, stone cohesion
Rodriguez <i>et al.</i> (2003)	2% inoculums	Immersion in growing bacterial culture (shaking or stationary conditions) for 30 days		Stone cohesion, weight increase, XRD and SEM analysis, porosimetry analysis
Dick <i>et al.</i> (2006)	1% inoculums	Immersion in growing bacterial culture (intermediate wetting) for 28 days		Water absorption, SEM analysis
Biobrush	10^8 cells ml^{-1}	Spraying	In Carbogel	Water absorption and drying due to evaporation
Tiano <i>et al.</i> (2009)	n.d.	n.d.	Immersion in test solution or spraying (in situ) tests	Water absorption, colorimetric measurements, stone cohesion, staining of newly formed calcite with Alizarin Red S and Calcein
De Muynck <i>et al.</i> (2008)	Overnight culture 10^7 to 10^9 cells ml^{-1}	Immersion for 1 day	Immersion for 4 days	Weight increase, water absorption, gas permeability, chloride migration, carbonation, freezing and thawing, SEM and XRD analysis

*n.d. = Not defined

Conventional building materials like cement, bricks and steel are the bulk consumption items in construction industry. But manufacturing processes of all these materials at very high temperatures contribute huge greenhouse gases into the atmosphere. It is estimated that cement production alone contributes 7% to global anthropogenic CO₂ emissions, what is particularly due to the sintering of limestone and clay at a temperature of 1500°C (Worrell *et al.*, 2001). Energy requirements for production and processing of different building materials, CO₂ emissions and the implications on environment have been studied by many researchers (Buchnan and Honey, 1994; Oka *et al.*, 1993; Suzki *et al.*, 1995; Debnath *et al.*, 1995) and given in table 2.5.

Table 2.5. Energy in basic building materials (Reddy and Jagadish, 2001)

Type of material	Thermal energy (MJ/kg)
Cement	5.85
Lime	5.63
LP	2.33
Steel	42
Aluminium	236.8
Glass	25.8

Energy consumed during production of basic building materials has been studied by Reddy and Jagadish (2003). The major players for contributing to the energy cost of building constructions are bricks, cement and steel. In order to reduce indirect energy use in buildings, alternatives for bricks, steel and cement were looked upon and unprocessed earth constructions came into picture. Use of earth made construction materials like sand, mud, soils, stones, unprocessed timber etc. not only offer low energy but also low cost and environmental friendly characteristics. Among all these, soil cement blocks served as the answer to long quest for low energy buildings (Reddy and Jagadish, 2003).

Soil–cement blocks are produced by employing manually operated machines in a highly decentralised fashion and have become increasingly popular in India and elsewhere

(Mukerji, 1986; Jagadish, 1988; Walker *et al.*, 2000). Detailed information on production, properties and masonry using soil cement blocks can be obtained from studies of Reddy and Jagadish (1989), Reddy (1991) and Rao *et al.* (1995). Soil–cement blocks used for the load bearing masonry buildings have cement content of about 6–8%. The blocks with 6% cement consume only 23.5% of burnt clay brick energy. Such blocks have an energy content of 2.75–3.75 MJ per block of size 230mm x 190mm x 100 mm and have been found to be most energy efficient blocks. Commonly known as compressed earth blocks (CEB), these blocks are used for load bearing masonry of 2-3 stories height buildings. Though these structures have good strength and durability, but during changes of temperatures and humidity etc. ingress of moisture leads to inhomogeneous expansions and contractions of building structures that ultimately leads to cracks. These cracks not only influence the service durability of building structure, but are also harmful for the structural safety also. In order to further improve the durability of these low energy materials, new techniques need to be applied with the aim of modifying the characteristics of such sustainable low energy materials. Most of the work in concrete and stone has focussed on the bioclogging activity of microbially induced calcite precipitation (MICP) as a protective surface layer. There is need to evaluate the feasibility of use of bacterial calcite as bioclogging agent for surface permeability reduction of energy efficient soil cement blocks. This may lead to improvement in the durability properties of these energy efficient buildings and pave way for more buildings with low embodied energy and low carbon emissions.

The traditional construction materials such as concrete, bricks, hollow blocks, solid blocks, pavement blocks and tiles are being produced from the existing natural resources. This is damaging the environment due to continuous exploration and depletion of natural resources. Many authorities and investigators are now working to have the privilege of reusing the wastes in environmentally and economically sustainable ways (Aubert *et al.*, 2006).

Fly ash generated during the combustion of coal for energy production is another industrial by product that is recognized as an environmental pollutant. An estimated 600 million tonnes of fly ash was produced in the world in 2000 (Malhotra, 1999). For the purpose of energy, economic developing and environmental ecosystem conserving, many research

works and development investigations have been conducted in its utilization as a starting material, such as using coal fly ash to produce artificial reef (Kuo, 1994), as an addition materials for concrete (Lai, 1994; Yang, 1997), raw materials of ceramic (Wang *et al.*, 1994), element extraction, environmental engineering, agriculture, paint and plastic industry but the utilization amount of fly ash is still limited.

Rice husk is one of the major agricultural byproduct and available in all parts of the world except Antarctica (FAO, 2002). It accounts for 20% of the 649.7 million tons of rice produced annually worldwide (FAO, 2008). Rice husk ash (RHA) is obtained from burning of rice husk. Traditionally, rice husk has been considered a waste material and is generally disposed off by dumping or burning, although some has been used as a low-grade fuel. The produced partially burnt husk from the milling plants when used as a fuel contributes to pollution and efforts are being made to overcome this environmental issue by utilizing this material as a supplementary cementing material (Chandrashekar *et al.*, 2006). Nevertheless, RHA has been successfully used as a pozzolana in commercial production in a number of countries including Columbia, Thailand and India.

Bricks are the basic building blocks for many civil structures and around 70 billion bricks are produced in India alone annually. Manufacturing processes of building materials contribute greenhouse gases like CO₂ to the atmosphere. Now a days there is a great concern and emphasis in reducing the greenhouse gases emission into the atmosphere in order to control adverse environmental impacts (Reddy and Jagadish, 2001). The utilization of above mentioned by-products as partial replacement of clay in bricks can serve important economical, environmental and technical benefits such as the reduced amount of waste materials, cleaner environment, reduced energy requirement, durable service performance during service life and cost effectiveness. But few problems associated with ash bricks are low strength, higher water adsorption, low resistance to abrasion, low fire resistance and high porosity compare to normal red bricks (Kumar and Palit, 1994). So in order to equalize the durability parameters of ash bricks, we need to enhance their strength by application of bacterial calcite. To the best of our knowledge, there is no work reporting on improvement in properties of ash bricks by microbially induced calcite precipitation.

2.9. Fly ash as a carrier material for calcifying bacterial cells

The application of calcifying bacterial cells for production of biogenic carbonate minerals has brought revolution in various fields of applied microbiology, geo technical sciences, environment and civil engineering (De Jong *et al.*, 2013). Although fresh cell preparations of bacterial cells are suitable for research studies, such preparations are not applicable for commercial purposes where these calcifying agents need to be applied in a simplified manner. To be acceptable, there must be suitable formulations of bacterial cells that can be easily handled and used. Formulations contain one or more beneficial bacterial strains (or species) in an easy-to-use carrier material. Use of suitable carrier capable of supporting high viable microbial population for a prolonged duration is utmost important along with the nature of bacterial isolate and optimum conditions for storage. Till now, successful commercialization of calcifying bacterial isolates has not been achieved because of the high cost of carrier materials like sepiolite, high density poly ethylene sheets (costs around 3 \$ m⁻²) and carbogel (costs around 39 \$ kg⁻¹) (De Muynck *et al.*, 2010). Commercial success of any technology is dependent upon its cost effectiveness. Hence, there is a need to look for economical carrier materials that can successfully support the growth of bacterial cells and have an acceptable shelf life. Also, the conditions for maintaining survival and efficacy of bacterial isolates need to be worked upon. Along with the above parameters, size of bacterial inoculum and survival of bacterial cells inside the formulations could have serious implications for the use of bacterial calcification as a method of consolidation.

2.9. 1. Cell viability studies by Fluorescent dyes

Sensitive detection of cell viability is an important aspect for bacterial applications for various biotechnological processes. Even in case of application of calcifying bacteria to building materials, it is imperative to check their viability at various intervals of time to determine their effectiveness. Measurement of cellular metabolic activity provides a very sensitive assay for vitality and viability.

All living cells require energy to grow and multiply, for synthesis of enzymes, nucleic acids, polysaccharides, and other cell components, for cell maintenance and repair of damage, for

motility, and for numerous other processes (Breeuwer and Abee, 2004). In case of microbial cells, energy is generated via electron transfer systems. These systems are composed of a series of electron carriers, which are usually membrane bound, such as NADH dehydrogenases, cytochromes, quinines etc. that can accept electrons from an electron donor and can transfer them to an electron acceptor. The energy released during this process is used to extrude protons to the external environment. The net result is the generation of a proton motive force, which can *e.g.* be used to generate ATP. O₂ is generally used as the external electron acceptor and the respiration of bacteria is therefore determined by measurement of the oxygen consumption (Breeuwer and Abee, 2004). Tetrazolium dyes are now a days used widely for the measurement of bacterial respiration. These dyes act as an alternative electron acceptor (Altman, 1976). The respiring bacterial cells reduce tetrazolium dyes to their respective formazan products.

In 1984, Stellmach described the synthesis of the non-fluorescent redox dye 5-cyano-2,3-ditolyl tetrazolium chloride (CTC), and Rodriquez *et al.* (1992) demonstrated that respiring bacterial cells can reduce CTC to the red fluorescent, water-insoluble formazan product 3-cyan-1,5-di-tolyl-formazan (CTF) (Fig. 2.16). CTF has an absorption peak at 450 nm, and the fluorescence of the crystals is in the red region (approx. 570–650 nm).

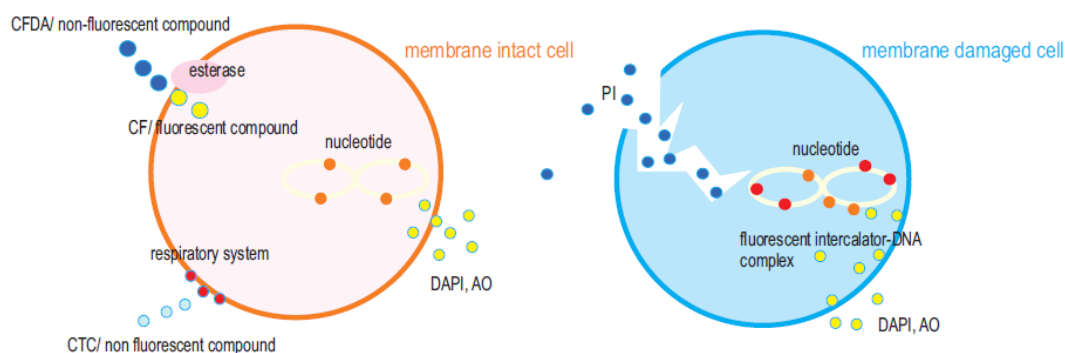


Fig. 2.16. Mode of action of CTC/ DAPI fluorescent dye staining

The procedure commonly used for tetrazolium reduction assays involves incubation of the cells (20 minutes to several hours) in the presence of the tetrazolium dye followed by fixation using formaldehyde, paraformaldehyde or formalin, and mounting with paraffin oil

or immersion oil on a microscope slide for examination. This is typically combined with counterstaining with DAPI/SYTO for determination of the total cell count. DAPI/SYTO stains both membrane damaged as well as membrane intact cells simultaneously (Leuko *et al.*, 2004; Zamarreno *et al.*, 2009). Detection of bacterial viability via CTC has been found to be very quick and convenient method of studying actively respiring bacterial populations. This method has been recently used for the detection of viable bacterial populations by many researchers worldwide (Adams, 2003; Creach *et al.*, 2003; Richardson *et al.*, 2002; Winding *et al.*, 1994). In the present work, we have made an attempt to check the viability of bacterial cells within fly ash formulations and determine their calcification efficacy.

2.10. Response Surface Methodology (RSM) for optimization of conditions for maximum carbonate precipitation

Production of various biotechnological products required at large scale often needs to be optimized for conditions which provide their maximum level. It is prerequisite to find all the factors and conditions involved in a process and optimize the parameters so that their response reaches the optimum level. In order to develop a process for maximum carbonate precipitation also there are several factors that need to be optimized. Several conventional methods for optimization of a process exist but they are based on ‘one variable at time’ (OVAT) approach i.e. information regarding that variable alone can be provided. These methods have many drawbacks as:

- They are time consuming
- Require huge sets of experiments to be conducted
- Are uneconomical
- Lack mutual interactions among variables (Rathi *et al.*, 2002; Kunamneni, 2005)

Response surface methodology (RSM) is an ideal tool consisting of experimental strategies, mathematical methods and statistical inference for constructing and exploring relation between a response variable and set of design variables (Khuri and Cornell, 1987; Plackett and Burman, 1946; Myers and Montgomery, 1995; Murthy *et al.*, 2000; Xin *et al.*, 2005). This method simplifies the optimization of a product by studying the mutual interactions

among the variables over a large range of values in a statistically valid manner. Many researchers have applied this process for optimization of medium constituents and other variables for production of various enzymes, fermentation products and biomolecules (Vohra and Satyanarayana, 2002; Saxena and Saxena, 2004; Xiong *et al.*, 2004; Himabindu *et al.*, 2006; Deepak *et al.*, 2008; Lv *et al.*, 2008; Singh and Bishnoi, 2012).

The multivariate approach of RSM eases the evaluation and interactions of different parameters involved in the process (Khuri and Cornell, 1987; Myers and Montgomery, 1995). In the first phase, this method simplifies the otherwise huge number of factors as it first screens different variables affecting the process and shortlists most effective and important amongst those (Plackett and Burman, 1946). Next, it determines what settings of the independent variables results in a value of optimum response. This phase makes considerable use of the first-order model. The true response surface usually exhibits curvature near the optimum and second-order model (or perhaps some higher-order polynomial) is then used. Once the required model has been obtained, it is analyzed to determine the optimum conditions for the process. In this, the response surface is expressed in the form of the second degree polynomial equation as:

$$Y_i = \beta_0 + \sum \beta_i X_i + \sum \beta_{ii} X_i^2 + \sum \beta_{ij} X_i X_j$$

where Y_i is the response variable, $X_i X_j$ are input variables which influence the response variable Y ; β_0 is the interception coefficient; β_i is the i th linear coefficient; β_{ii} is the i th quadratic coefficient and β_{ij} is the ij th interaction coefficient.

The significant terms in the model are found by analysis of variance (ANOVA) for each response. Level of significance is judged by determining the probability level of the F -statistic calculated from the data less than 5%. After performing the model fitting, residual analysis is conducted to validate the assumptions used in the ANOVA. Maximization and minimization of the polynomials fitted is performed by desirability function method, and mapping of the fitted responses is achieved using computer software such as Design Expert 8.0.

Though lot of studies have proved the successful application of RSM in production of various enzymes, fermentation products and biomolecules by optimizing various parameters and interactions involved in the final product but till now, not much has been done on the standardization of conditions for maximum carbonate production by RSM. So, there is need to investigate and optimize the major factors involved in production of enzymes involved in carbonate precipitation so as to enhance the production of these biominerals.

Chapter 3

Materials and methods

3.1. Isolation and identification of calcifying bacteria

3.1.1. Sample collection

Alkaline soils were collected randomly from Anantapur District, Andhra Pradesh (site 1), Ropar District Punjab (site 2), Samrala, District Ludhiana Punjab (site 3) and Patiala District, Punjab (site 4). The samples were collected from depth of 0-30 cm by alcohol sterilized implements in sterile containers. The samples were transported to laboratory at 4°C. Portion of soils were air dried, crushed and sieved to < 2mm for physico chemical characteristics.

3.1.2. Characterization of soils

3.1.2.1. Determination of pH and electrical conductivity (EC)

Air-dried soil (20 g) was taken in 100 mL beaker and 50 mL of distilled water was added to it and thoroughly stirred for 2-3 min using a glass rod. Further, it was kept in shaking condition (120 rpm) for 3 hrs. Suspension was allowed to settle for 30 min. The instrument was calibrated with two buffer solutions of known pH viz. one acidic and other alkaline. The electrode was rinsed with distilled water and carefully wiped with filter paper. The pH of the soil was measured by immersing the electrode in supernatant solution. The pH value was recorded when the reading was stabilized (usually after 1 min). The soil sample was mixed with water and stirred as described previously. KCl solution (0.01 M; EC = 1.413 mS m⁻¹) was used to calibrate the meter. The electrode was dipped in the supernatant solution and recorded the EC.

The pH and electric conductivity was determined in 1:2.5 (w/v) water extract using Deluxe water and Soil Analysis kit (Model 191E).

3.1.2.2. Total Organic Carbon in soil (Walkley-Black method, 1934)

Dried soil (1.0 g) was transferred into a 150 mL conical flask and 10 mL of 1N $K_2Cr_2O_7$ was added and mixed well. The blank was prepared in which all reagents except soil were added. The conical flasks were kept on teflon / asbestos sheet and 20 mL of concentrated H_2SO_4 from the sides of the flask was added. The flask was swirled during addition. The flask was allowed to stand for 30 min and there after 70 mL of water was added. These flasks were swirled thoroughly and allowed the soil particles to settle overnight. The supernatant was decanted and read the color intensity using red filter at 660 nm. For standard, 0, 10, 20, 30, 40 and 50 mg of anhydrous sucrose crystals was weighed into a 100 mL volumetric flask and repeated the same procedure.

Calculation

The quantities of sucrose (0, 10, 20, 30, 40 and 50 mg) were multiplied by 0.4207 and found the quantities (%) of carbon present. Because 10 mg sucrose contained 4.207 mg C and if suppose 4.207 mg C was found in 1000 mg of soil, it meant 100 mg sample contained = $(4.207 \times 100) / 1000$ mg carbon; Organic carbon (%) = Colorimetric reading \times 0.0042.

3.1.2.3. Elemental analysis of soils

One gram of soil sample was taken and oven dried at 105°C for 24 hours. The sample was removed from oven and kept into desiccator and ground in analytical mill to get particles having particle size of about 0.1mm size. 10 to 100 mg of the dried soil samples were taken for the elemental analysis by Energy dispersive X ray analyzer (Thermo Scientific USA).

3.1.3. Isolation and enrichment of ureolytic bacterial species

All the samples were first enriched for ureolytic bacteria by inoculating one-gram of respective sample in 50 mL nutrient broth (Hi-Media, Mumbai, India) (pH 8.0) containing 2% urea and incubated at 37°C for 120 hrs under shaking condition (120 rpm). For isolation and enumeration of cultivable bacteria, all the samples were serially diluted in saline (0.85%) and plated on alkaline nutrient agar (Casein hydrolysates 15.0 g/L; Peptone 5.0 g/L, NaCl 5.0 g/L and Agar 20.0 g/L having pH 9). The plates were then incubated at two temperatures (28°C and 37°C). The grown bacterial colonies from the plates were sub cultured several times on the same medium from where it was picked. Finally for selection

of ureolytic bacteria, the colonies were randomly selected and transferred onto Urea Agar base medium (HiMedia, India) to check the production of urease based on the intensity of pink color. This was followed by quantitative urease production test.

3.1.4. Urease Assay

For estimation of urease activity in urease positive isolates, the bacterial cells (1% , OD₆₀₀ = 1.0) of each strain were inoculated into 250 mL flasks containing autoclaved Nutrient broth (Appendix I) media supplemented with 1% urea (pH 8.0) and incubated under shaking conditions at 37°C. 1 ml culture broths from each flask were taken at an interval of 24 hrs, centrifuged (8000 rpm for 5 mins) and the supernatant was collected. The amount of ammonia released from urea was then determined according to the phenol-hypochlorite assay method of Natarajan (1995). The culture supernatant (250 µl) was added to a mixture containing 1 ml of 0.1 M potassium phosphate buffer (pH 8.0) and 2.5 ml of urea (0.1 M). The mixture was incubated at 37°C for 5 minutes followed by addition of phenol nitroprusside and alkaline hypochlorite, 1 ml each and the assay mixture was then incubated at 37°C for 25 minutes. Optical density was measured at 626 nm. Ammonium chloride (50-1000 µM) was used as the standard. One unit of urease is defined as the amount of enzyme hydrolyzing one µmole urea per min.

3.1.5. Precipitation on agar plates

The isolated ureolytic bacterial strains were then plated on precipitation agar (Appendix I). The plates were incubated at 37°C and colonies were assessed for visual crystal formation within 10 days.

3.1.6. Morphological, biochemical and physiological characterization of bacterial isolates

The characterization of all the bacterial isolates was done by conventional physiological and biochemical tests described in Bergey's Manual of Systematic Bacteriology (Holt *et al.*, 1994).

3.1.6.1. Growth kinetics of bacterial isolates

The growth profile of bacterial isolates in all media were tested by taking the absorbance (OD₆₀₀) at regular time intervals for 30 hrs and corresponding colony forming units (cfu/mL) were counted after incubation at 37°C.

3.1.6.2. Gram staining

Bacterial smear prepared from actively growing cells was spread on a glass slide and fixed by heating. Crystal violet was flooded for 10 sec. It was followed by brief washing in water to remove excess crystal violet. Gram iodine was flooded for ten seconds and washed with water. Further, it was decolourised with ethyl alcohol until the moving dye front has passed the lower edge of the section and washed immediately in tap water. Safranin was used to counter stain for 15 sec and washed with water to remove the excessive stain. The slides were visualized under microscope at different magnifications.

3.1.6.3. Capsule Staining

The capsule stain is a differential stain, which selectively stains external capsules surrounding bacterial cells. Capsules are highly ordered polymers of sugars and proteins that surround some bacterial cells, and can be easily dislodged by heat or water. The primary stain applied is crystal violet, which stains both the bacterial cell and the surrounding capsule. A 20% copper sulfate solution is then applied, which serves a dual function as both decolorizer and counterstain. It removes and replaces the crystal violet in the capsule only. At the end of the staining procedure, the capsule appears as a faint blue or white halo around a purple cell observed under microscope.

3.1.6.4. Catalase test

Small amount of bacterial cells were placed onto a clean microscope slide. A few drops of H₂O₂ (3%) were added onto the smear. Rapid evolution of O₂ bubble was considered as the positive result. Either no bubble or only a few scattered bubbles indicate negative result.

3.1.6.5. Oxidase test

Small amount of bacteria from an agar slant or plate was obtained with a sterile swab. One drop of N,N,N',N'-tetramethyl phenylenediamine dihydrochloride reagent was placed onto the culture on the swab. Positive reactions turned the bacteria violet to purple immediately or within 10 to 30 seconds.

3.1.6.6. Nitrate reduction test

Nitrate media (Appendix I) was used to determine the ability of an organism to reduce nitrate (NO_3) to nitrite (NO_2) using the enzyme nitrate reductase. It also tests the ability of organisms to perform nitrification of nitrate to nitrite. Nitrate broth contained potassium nitrate as a source of nitrate. Bacteria were grown in nitrate agar plate. After sufficient growth of bacteria, 2-3 drops of sulfanilic acid and α -naphthylamine were added. If the organism had reduced nitrate to nitrite, the nitrites in the medium will form nitrous acid. Sulfanilic acid reacts with the nitrous acid to produce diazotized sulfanilic acid. This reacts with the α -naphthylamine to form a red-colored compound. Therefore, if the medium turns red after the addition of the nitrate reagent, it was considered a positive result for nitrate reduction.

3.1.6.7. Starch hydrolysis test

Starch hydrolysis was checked on starch agar plate by making a streak over the surface of agar plate, incubated at 37°C. After growth of the culture, iodine was added to the surface of the agar. Iodine turns blue-black in the presence of starch. Absence of the blue-black color indicates that starch is no longer present in the medium. Bacteria, which show a clear zone around the growth, produce the extracellular enzyme amylase.

3.1.6.8. Alkalinity, salinity and temperature test

Different sodium chloride concentrations (0, 2, 5, 7, 10, 12 and 15%) were amended in the alkaline nutrient broth (pH 10) to determine the survival of the bacterial isolates in saline conditions. Growth of bacterial isolates was recorded by measuring the absorbance at 600

nm of 24 hrs grown cells. Four temperatures (25, 30, 37 and 45°C) were chosen to test the growth pattern of bacterial isolates. Bacterial isolates were grown in liquid and solid media and incubated at different temperatures as stated above.

3.1.6.9. Fermentation of carbon substrate by bacterial isolates

Total of 35-carbohydrate fermentation tests were performed with isolated bacterial species according to the manufacturer's direction (Himedia Lab., Mumbai, India). Inoculum was prepared by growing the cells in nutrient broth at 37°C in shaking condition until the inoculum turbidity was ≥ 0.5 OD at 600nm. Citrate utilization, lysine, ornithine, TDA, nitrate reduction, acid phosphatase, urease and H₂S production tests were performed with all bacterial isolates by standard methods.

3.1.6.10. Antibiotic profiling of bacterial isolates

Bacterial isolates were grown in nutrient broth until the absorbance reached to 1.0 at 600 nm. The grown bacterial cells were spread on nutrient agar and antibiotic discs were kept on it. These plates were incubated at 37°C and the inhibition zone was noted. Ready precoated twenty antibiotic discs (Himedia Lab., India) were used to check the sensitivity of the bacterial isolates. These were: Norfloxacin (10 µg), Gentamicin (10 µg), Chloramphenicol (30 µg), Cefuroxime (30 µg), Ciprofloxacin (5 µg), Cefaperazone (75 µg), Ceftazidime (30 µg), Roxithromycin (30 µg), Calaritmomycin (15 µg), Co-Trimoxazole (25 µg), Netillin (30 µg), Cefaclor (30 µg), Cephataxime (30 µg), Cephadroxil (30 µg), Azithromycin (15 µg), Ampicillin/Cloxacillin (10/10 µg), Penicillin (10 units), Amikacin (30 µg), Sparfloxacin (5 µg) and Ampicillin/sublactam (10/10 µg).

3.1.7. Biofilm production

Biofilm production from all the isolates was established aseptically in nutrient broth containing calcium chloride and urea on glass plates (25×75 mm) using crystal violet (CV) staining method as described by Morikawa *et al.* (2006) with slight modifications. Briefly, an overnight culture of all the bacteria were diluted to an OD₆₀₀ of 0.5 and 1 µl was added to 99 µl nutrient medium onto the glass plate and incubated at 37°C for 24 hrs. Then, media

and loosely bound cells were removed from the glass plate by gently rinsing with sterile milliQ water and the remaining cells and matrices were stained with 150 μ l of 1% CV solution for 25 min at room temperature. After washing twice with distilled water, the CV attached to the biofilm was solubilized in 150 μ l DMSO, quantified by measuring its absorbance at 570 nm and expressed in cfu/mm².

3.1.8. Extracellular polymeric substances production

For production of EPS, the bacterial culture was inoculated into 100 ml modified EPS Basal Medium (Appendix I). It was then incubated at 37 °C for 72 hrs. After incubation, culture broths containing EPS were centrifuged at 13,200 *g* at 4°C for 25 min and the supernatants were stored at – 20°C. The method used for EPS extraction was modified method of Cerning *et al.* (1994). EPS in 50 ml supernatant were precipitated by the addition of three volumes of chilled absolute ethanol. The mixture was held at 4°C overnight and then subjected to centrifugation at 13,200 *g* at 4°C for 15 min. The resulting pellet was dried at room temperature for 6 hours in laminar air flow followed by drying at 100 °C till constant weight and dry weight was measured.

Once the EPS was extracted, the resulting EPS suspension (resuspended in 10 mL DI water) was evaluated for the total amounts of sugar and protein using previously developed methods. Specifically, the sugar quantification was performed with Phenol-Sulfuric Acid (PSA) method (Dubois *et al.*, 1956), and the protein was quantified using the Lowry method (Lowry *et al.*, 1951). The PSA method involved adding 50 mL 80% (w/w) phenol solution (Fisher Scientific), followed by 5mL of highly concentrated sulfuric acid 95.5% (Fisher Scientific) to 2 mL of resuspended EPS solution. The phenol, acid, and EPS suspension was incubated at room temperature (22–25°C) for 10 min, followed by incubation in a water bath for 20 min at 25–30°C. Total protein amount quantification was performed with the Lowry method using bovine serum albumin (BSA; 1mg/mL) (Fisher BioReagents, Fisher Scientific) as the standard and measured spectroscopically (BioSpec-mini) at a wavelength of 500 nm. Next, 0.3 mL of resuspended EPS solution (in 10mL DI water) was put in a glass vial (20mL in volume) and 1.5 mL alkaline copper reagent (made by combining 1mL 2%

Na₂C₄H₄O₆, 1 mL 1% CuSO₄·5H₂O and 98mL 2% NaCO₃ in 10·1 M NaOH) followed by the addition of 75 mL Folin reagent (Folin and Ciocalteu's Phenol Reagent, MP Biomedicals, LLC, Germany). The subsequent mixture was incubated at room temperature for 30 min and measured in the spectrometer at 500 nm. The absorbance reading was compared to the standard curve for BSA to determine the concentration of protein in each EPS sample.

3.1.9. Molecular characterization

3.1.9.1. Isolation of genomic DNA

A single colony of bacterial isolate was inoculated into 25 ml of nutrient broth in a 250 ml flask and incubated for 14-18 hours at 37°C under shaking condition (120 rpm). Liquid cultures (2.0 ml) were harvested by centrifugation (Eppendorf microfuge) at 8,000 rpm for 1 min. The cell pellets were resuspended with 800 µl saline-EDTA, and approximately 10 µg crystalline lysozyme were added. During incubation at 37°C for 30 min, the cell suspension was mixed thoroughly by inverting the Eppendorf tube several times. After addition of 200 µl SDS (10%), the cell suspension was incubated again at 65°C for 15 min. The cell suspension was extracted with organic solvents to remove proteins and cell debris: first, with an equal volume phenol:chloroform:isoamyl alcohol (25:24:1) solution, and centrifuged 10 min at 12,000 rpm. The upper aqueous phase was then extracted with an equal volume of phenol:chloroform:isoamyl alcohol (25:24:1). To precipitate extracted nucleic acids, 0.7 volume isopropanol was added to the aqueous phase, followed by 10 min centrifugation at 12,000 rpm. The DNA pellets were washed with 750 µl EtOH (70%) and microfuged another 10 min. Finally, the pellets were resuspended in 40 µl TE buffer/milliQ water and stored at 4°C.

3.1.9.2. DNA Purification

The DNA was purified by elution through the Wizard DNA Clean up system (Promega) according to manufacturer's instructions in order to remove contaminants, which can hamper in manipulation of DNA.

3.1.9.3. Electrophoresis of DNA on agarose gels

DNA was loaded on agarose gels (0.7 % w/v) prepared in 1X TAE, pH 8.0 using a 6X loading dye (appendix I). Ethidium bromide (0.5 µg/ml) was added to stain the gel prior to pouring. The nucleic acids were then electrophoresed at 3 volts/cm for 45-60 minutes and visualized on a U.V. transilluminator.

3.1.9.4. Spectrophotometric quantification of DNA

The concentration of extracted DNA in suspension was estimated by spectrophotometric measurement at A_{260} . For double-stranded DNA suspensions, an OD of 1.0 at a wavelength of 260 nm and using a cuvette with 1 cm light path, is equal to a concentration of 50 µg/ml. The quality of the DNA was evaluated by measurement of the A_{260}/A_{280} and the A_{230}/A_{260} ratios. Ideally, the A_{260}/A_{280} ratio should be 1.8-2.0 while the A_{230}/A_{260} ratio should be 0.3-0.9. Ratios (A_{260}/A_{280}) less than 1.8 indicate protein or phenol contamination, while ratios greater than 2.0 indicate the presence of RNA.

3.1.9.5. Ethidium bromide fluorescent DNA quantification

DNA was migrated electrophoretically in an agarose gel containing ethidium bromide (0.5 µg/ml). The quantity of DNA was visually determined with reference to a known DNA concentration of lambda phage (Fermentas, USA) by comparing the intensity of fluorescence.

3.1.9.6. DNA amplification by polymerase chain reaction (PCR)

3.1.9.6.1. REP-PCR based DNA fingerprinting

Reaction mixture for the Repetitive element palindromic (REP) PCR contained 1X PCR buffer (Invitrogen, USA), each deoxynucleotide triphosphate at a concentration of 200 µM, 1.5 mM MgCl₂, each primer at a concentration of 0.1 µM and 2.5 U of Taq DNA polymerase (Invitrogen, USA) in a final volume of 100 µl. DNA amplification was

performed with Genamp 2700 PCR system (Applied Biosystem, USA) by using the following program; initial denaturation at 95°C for 2 min, 35 cycles at 92°C for 30 sec, at 38°C for 80 sec and at 60°C for 200 sec, final extension at 68°C for 8 min and final soak at 4°C. The REP PCR primers were REP F 5'- III ICG ICG ICA TCI GGC -3' and REP R 5'- ICG ICT TAT CIG GCC TAC-3'.

3.1.9.6.2. BOX- PCR amplification

BOX-PCR (based on primers targeting the highly conserved repetitive DNA sequences of the BOXA subunit of the BOX element) was conducted to obtain the genomic fingerprinting of the all efficient bacteria. 5'CTACGGCAAGGCGACGCTGACG-3' sBOXA1R: primer was used to study distinctly different species. The reaction procedure was: an initial denaturation at 95°C for 5 min, followed by 40 cycles of denaturation at 90°C for 30 sec, annealing at 50°C for 30 sec, extension at 72°C for 8 min and a final extension at 72°C for 10 min. PCR products were then examined through electrophoresis in 2% agarose gel containing ethidium bromide at 40 V in 0.5XTBE buffer.

3.1.9.6.3. Amplification of 16S rDNA and Purification of PCR products

The polymerase chain reaction (PCR) provides a rapid and highly sensitive method for the primer-mediated enzymatic amplification of specific target sequences in genomic DNA resulting in the exponential increase of target DNA copies.

For amplification of 16S rRNA gene the following primers were used: Forward primer 5'-AGAGTTTGATCCTGGCTCAG-3' and reverse primer 5'-ACGGGCGGTGTGTTC-3' (Weisberg *et al.*, 1991). The amplification of 16S rDNA from isolates was carried out with a GenAmp thermocycler (Applied Biosystem, USA). Reaction mixture for the PCR contained 1X PCR buffer (Fermentas, USA), each dNTPs at a concentration of 200 µM, 1.5 mM MgCl₂, each primer at a concentration of 0.1 µM and 2.5U of Taq DNA polymerase (Fermentas, USA) in a final volume of 50 µl. PCR conditions were as follows: Preheating at 92°C for 120 s, 36 cycles of 92°C for 60 s, 48°C 30 s and 72°C for 120 s and final extension

72°C for 370 s. Successful amplifications were confirmed by agarose gel (0.8% w/v) electrophoresis and ethidium bromide staining.

Amplified 16S rDNA was purified using the QIAquick PCR purification kit (Qiagen, USA), following the instructions of the manufacturer. Purified PCR products were eluted from the purification columns by the addition of 50 µl 10 mM Tris buffer (pH 8.0). PCR products, as they resulted from amplification of total DNA from environmental samples, were purified by agarose gel (0.8 %) electrophoresis prior to cloning. After staining with ethidium bromide, a defined band was visualized under UV irradiation and excised. Besides removing surplus primers, nucleotides, and salts, this method possessed the advantage that incomplete (shorter) amplification fragments are also removed prior to cloning. Subsequently, the DNA was extracted from the gel matrix material, using the QIAEX gel extraction kit (Qiagen), whereby the DNA is bound to silica gel particles, in the presence of high salt concentrations. Finally purified PCR products were eluted with 30 µl TE buffer (pH 8.0). In this manner, purified PCR products were applied directly for the cloning in T-vector.

3.1.9.7. Ligation of 16S rDNA in pTZ57R/T vector

The 16S rDNA PCR products were cloned using the restriction independent InsTA Cloning Kit, following the manufacturer's protocol (Fermentas, USA). The 16S rDNA amplicon was ligated into pTZ57R/T vector. The reaction mixture was prepared as described below and incubated overnight at 4°C.

Plasmid pTZ57R/T (55ng/µl)	3 µl
Insert (75ng/µl)	4 µl
Buffer (5X)	6 µl
T4 Ligase	1 µl
H ₂ O	16 µl

3.1.9.8. Genetic Transformation using CaCl₂

A single colony of *E. coli* DH5 α from a freshly grown plate was inoculated into 25 ml of LB broth in a 250 ml flask and incubated the culture for 16-20 hrs at 37°C under shaking condition (120 rpm). Aseptically 200 μ l of the above-saturated culture was transferred into 25 ml of fresh LB broth in a 250 ml flask. The culture was further incubated with vigorous shaking at 37°C for 2-3 hrs. To monitor the growth of the culture, the OD₅₉₀ was determined at every one-hour (OD₅₉₀ should be ~ 0.5). The above culture was transferred to sterile, disposable, ice-cold 50 ml polypropylene tubes. The culture was cooled to 0°C by storing the tubes on ice for 10 min. The cells were harvested by centrifugation at 8,000 rpm for 10 minutes at 4°C. The pellet was resuspend in 10 ml of ice-cold 0.1 M CaCl₂ and store on ice for 15 min. Further the cells were recovered by centrifugation at 8,000 rpm for 10 min at 4°C. The cell pellet was resuspended in 1 ml of ice-cold 0.1 M CaCl₂. The cells in this stage may be stored on ice for 12-24 hours. CaCl₂ treatment for 2 hours induces considerably a transient state of “competence” in the *E. coli* cells. One hundred micro liter of the suspension of competent cells was transferred to a sterile and prechilled microfuge tube (1.5 ml capacity). The plasmid DNA sample (~100 ng in a volume of 5 μ l or less) was added to each tube. The content of the tubes were mixed gently and stored the tubes on ice for 30 minutes. The tubes were incubated in a circulating water bath that has been preheated to 42°C for exactly 2 minutes without shaking. The tubes were rapidly transferred to an ice bath and chill the cells for 1-2 minutes. One ml of LB broth was added to each tube and incubated the cultures for 45-60 minutes at 37°C to allow the bacteria to recover and to express the antibiotic resistance marker encoded by the plasmid. One hundred micro liters of transformed cells was spreaded on each 90 mm Luria agar-Ampicillin-X-Gal-IPTG plates and incubated at 37°C. Transformed colonies should appear in 12-16 hours.

3.1.9.9. Blue/white screening for recombinant plasmids

After transformation of the ligated product, the *E. coli* DH5 α (Lac Z⁻) bacterial host cells were plated on Luria agar medium containing 50 μ g/ml ampicillin, for selection of transformants. X-Gal and IPTG were used to screen for colonies containing a recombinant

plasmid. The cloning site in the pTZ57R/T vector is located in the multiple cloning site (mcs) of the plasmid's lacZ α gene; if no insert is present, functional β -galactosidase is produced, and the transformed bacterial colony is blue. These few blue colonies occur due to the presence of supercoiled vector molecules, which have escaped linearization. However, if the host cell receives a recombinant plasmid containing a 16S rDNA insert in the lacZ α gene, the resulting transformant colony is white (Lac Z⁻).

3.1.9.10. Isolation and purification of plasmid DNA from recombinant bacteria by alkaline lysis method

The plasmid DNA was isolated based on the alkaline lysis method. A single transformed *E. coli* white colony was transferred into 2 ml of Luria broth medium containing appropriate antibiotic (ampicillin, used in a final concentration of 50 μ g/ml) in a loosely capped 15-ml tube and incubated the culture overnight at 37°C with vigorous shaking. 1.5-2.0 ml of the above-saturated culture was poured into a microfuge tube and cells were harvested by centrifugation at 8,000 rpm for 1 min. The bacterial pellet was resuspended in 200 μ l of ice-cold Solution I (Appendix I) by vigorous vortexing to ensure that the bacterial pellet is completely dispersed in this solution. Further 200 μ l of freshly prepared Solution II (Appendix I) was added and the contents were mixed by gentle inversion of the tubes, five to ten times. Vortexed is avoided here. The tubes were stored on ice for 5 min. Finally 300 μ l of ice-cold Solution III (Appendix I) was added and mixed by inversion to disperse Solution III (Appendix I) through the viscous bacterial lysate. The tubes were stored on ice for 10 min. The tubes were centrifuged at 12,000 rpm for 10 min in a microfuge. The upper aqueous phase was then extracted with an equal volume of phenol:chloroform:isoamyl alcohol (25:24:1). To precipitate extracted plasmid DNA, 0.7 volumes isopropanol were added to the aqueous phase, followed by 10 min centrifugation at 12,000 rpm. The DNA pellets were washed with 750 μ l EtOH (70%) and microfuged another 10 min. Finally, the pellets were resuspended in 40 μ l TE buffer/milliQ water and stored at 4°C for further use.

3.1.9.10.1. Size screening for recombinant plasmids

Clones containing approximately 1.5 Kb 16S rDNA inserts were identified by PCR screening, using the rapid protocol for preparation of template DNA from single bacterial colonies and M13-forward/M13-reverse plasmid primers. The amplification products were checked by agarose gel (0.8-1.0% w/v) electrophoresis.

3.1.9.10.2. Restriction analysis of DNA samples by agarose gel electrophoresis

DNA 17 µl (500 ng) was added in a sterile microfuge tube. The appropriate 10x restriction enzyme assay buffer was added and mixed thoroughly by tapping the tube. 1 µl (2-5 units) of the restriction enzyme was added, mixed by tapping the tube. The mixture was incubated at the 37 °C for 1-2 hr. To stop the reaction, 4-5 µl gel-loading buffer was added, mixed by vortexing briefly (as the DNA samples need to be analyzed directly on agarose gel).

3.1.9.11. Sequencing

The 16S rDNA inserts were sequenced for both strands using M13 forward and reverse primers, used for pTZ57R/T vectors. The sequence was generated by chain termination method (Sanger *et al.*, 1977) using an Applied Biosystems automatic sequencer (DNA Sequencing Facility, Department of Biochemistry, South Campus, Delhi University, New Delhi, India).

3.1.9.11.1. Analysis of sequence data

Sequences were submitted to the CHECK-CHIMERA program of the RDP II (Maidak *et al.*, 2001), in order to detect the presence of possible chimeric artefacts generated by PCR. Similarities were calculated for nearly complete 16S rDNA sequences using only unambiguously determined nucleotide positions. The 16S rDNA gene sequences of all the isolates were compared with those available in GenBank/ EMBL databases using BLAST program (Altschul *et al.*, 1997) and at RDP-II (Cole *et al.*, 2003). The sequences of closely related strains and uncultured bacteria were retrieved from RDP-II and aligned using multiple alignments CLUSTALW program (Thompson *et al.*, 1997). The evolutionary distance was calculated by Kimura 2 parameter, phylogenetic dendograms were constructed

by neighbor-joining method by the use of MEGA 5 package (Tamura *et al.*, 2007). For analysis, 1000 bootstrap replicates were performed to assess the statistical support for the tree.

3.2. Optimum conditions and role of enzymes in CaCO₃ precipitation

3.2.1. Optimization of conditions for Urease activity

The next aim of the work was to optimize the conditions for maximum urease activity by different bacterial isolates. For this, *Sporosarcina pasteurii*, Sp P (previously known as *Bacillus pasteurii*) which is a well known urease producing and model bacterium used by researchers for ureolytically induced carbonate precipitation (Ramakrishnan *et al.*, 1998; Stocks - Fischer *et al.*, 1999; Ramachandran *et al.*, 2001) was procured from IMTech (Institute of Microbial Technology), Chandigarh, India and selected for optimization of the parameters for maximum urease production. With the objective of obtaining high yield of urease production, various factors influencing the production were studied. 1% bacterial inoculum (OD₆₀₀ = 1.0) of each strain along with *S. pasteurii* (Sp P) was inoculated into 250 ml flasks containing autoclaved media and incubated at 37°C for 24 hours. The supernatants were collected by centrifugation and analyzed for urease activity as described in section 3.1.4. The varying parameters selected were: different medias (Nutrient broth, Tryptic soya, Yeast extract, B4 media, Appendix I supplemented with 1 % urea), different concentrations of urea (1-5%), varying calcium sources and concentrations (calcium chloride, calcium acetate, calcium sulphate, calcium lactate, calcium nitrate from 10 mM – 100 mM) and NiCl₂ (5-100 µM). In order to find the pH profiling of urease activity, potassium phosphate buffer (pH 6-7), tris-HCL buffer (pH 7-9) and glycine-NaOH buffer (pH 10) were selected (Appendix I). All the buffers were at 0.1M concentration. The assay mixture was incubated at 37°C for 2 hours in different pH values of above buffers and the enzyme activity was determined by spectrophotometric urease assay. The optimum temperature for urease activity was determined by incubating the assay mixture described above at different temperatures between 25°C and 65°C for 2 hours and the resulting enzyme activity was measured. The urease production efficacy of all the isolates of present study was compared

with *Sporosarcina pasteurii* Sp P. The efficacy of urease production was also evaluated with time (upto 144 hrs).

3.2.2. Characterization of Urease enzyme

3.2.2.1. Preparation of crude enzyme extract

To study the properties of urease enzyme from all the bacterial isolates, 1% bacterial inoculum ($OD_{600} = 1.0$) of each strain along with *S. pasteurii* (Sp P) was inoculated into sterilized NBU media (Appendix I) and grown for a period of 3 - 5 days depending on the time of maximum activity. The culture broths were then centrifuged (x 5000 rpm) at 4°C and supernatants were collected by filtration.

3.2.2.2. Total protein estimation (Folin-Lowry Method) (Lowry et al., 1951)

BSA (Bovine serum albumin) standard solutions were prepared in the range of concentrations 0.05, 0.1, 0.2, 0.4, 0.6, 0.8, 1.0 mg/ ml. From these solutions, 0.2 ml protein solutions were pipetted out into different test tubes. Simultaneously bacterial samples were also taken. 2 ml of alkaline copper sulphate reagent [prepared by (a) 50 ml of 2% sodium carbonate mixed with 50 ml of 0.1 N NaOH solution (0.4 gm in 100 ml distilled water) (b) 10 ml of 1.56% copper sulphate solution mixed with 10 ml of 2.37% sodium potassium tartarate solution. Prepared analytical reagents by mixing 2 ml of (b) with 100 ml of (a)] was then added and the solutions were mixed well. The final volume in each of the test tubes was 5 ml. These solutions were incubated at room temperature for 10 min. This was followed by addition of 0.2 ml of Folin Ciocalteau reagent solution (1N) to each tube and incubation for 30 mins. The absorbance was measured at 660 nm. The absorbance was plotted against protein concentration to get a standard calibration curve. The absorbance of sample was checked and concentration of the sample was determined from the standard curve.

3.2.2.3. Enzyme kinetics

The enzyme kinetics (K_m and V_{max}) of crude enzyme extracts were determined by measuring the activity of UA in the presence of varying concentrations urea substrate (5 - 50 mM).

Michaelis–Menten constant (K_m) and the maximum velocity (V_{max}) was determined using the Lineweaver–Burk double reciprocal plot (Lineweaver and Burk, 1934).

3.2.2.4. SDS PAGE

Sodium dodecyl sulphate-polyacrylamide gel electrophoresis (SDS-PAGE) was carried out to check proteins in the supernatant from all the bacterial isolates as described by Laemmli (1970), using a 5% (w/v) stacking and a 10% (w/v) separating gels. Samples were heated at 100°C for 5 min before electrophoresis. The compositions of reagents used in SDS-PAGE are provided in Appendix I.

3.2.2.5. Zymogram analysis (*In gel detection of urease activity*)

Electrophoresis was carried out at room temperature under non-denaturing conditions using an Hoeffer (USA) electrophoresis unit. The stacking and separating gels contained 5% and 8% acrylamide solution, respectively. The buffer system of Laemmli (1970) was used. Sodium dodecyl sulphate (SDS) was replaced in each electrophoretic solution by double-distilled water and the urease samples were not heated. The crude supernatants of all the isolates were mixed with sample buffer and electrophoresis was performed overnight at constant voltage.

At the end of electrophoresis, the gel was washed with double–distilled water for 10 min and then three times with 0.01 and 0.005 M acetate buffer (pH 6.0) for 15 min each with gentle shaking. The washed gel was then immersed in 5 M urea solution and incubated at 37°C for 5 min without shaking. The gel was then transferred to a 1.5% sodium nitroprusside solution and kept for 5 min. A volume (200 μ L) of freshly prepared 1 M β -mercaptoethanol was added immediately and mixed to obtain a final concentration of 10 mM β -mercaptoethanol for the staining solution. The gel was gently shaken and a dark purple red colour developed, which became intense within 5 min. Photographs were taken on a BioRad (CA, USA) and were processed with Quantity One software (BioRad, USA).

3.2.3. Estimation of Ureolytically induced calcium carbonate precipitation

For investigation of bacterially induced CaCO_3 precipitation via ureolytic pathway, bacterial cells of each strain were inoculated into 250 ml flasks containing 100 ml Nutrient broth media supplemented with 2% urea and 25 mM CaCl_2 (NBUC media) to a final concentration of 5×10^7 cells mL^{-1} (pH 8.0) and incubated at 37 °C with shaking (120 rpm). All samples were prepared in triplicate flasks that were pre-washed with 6 M HCl. Control sets were prepared without any bacterial inoculum. At every 2 hr for the first 12 hr and longer intervals afterwards, the replicates were terminated to determine the pH and amount of insoluble Ca^{2+} in the pellets and soluble Ca^{2+} in the supernatant by centrifuging the broth and quantifying the Ca^{2+} content according to the EDTA titration method (APHA *et al.*, 1998). Culture pellet of each sample was dissolved with 3N hydrochloric acid. Four ml of Sodium hydroxide (5N) was added to the precipitate so that final pH reaches 12-13. Few drops of hydroxyl naphthol blue were added as an indicator and the mixture was finally titrated against 0.05M EDTA. End point was noted from pink to blue which is easily visualized. 1ml of EDTA used for titration is equivalent to 5.004 mg of CaCO_3 precipitated.

3.2.4. Protease assay

The Alkaline protease activity was estimated as per the method of Fukumoto *et al.* (1971) with little modifications. All the bacterial isolates were inoculated into Nutrient broth media and incubated at 37°C for 120 hrs. Aliquots were taken from all the flasks after every 24 hours. One ml of each bacterial culture was added to 5 ml of 0.6% casein and incubated at 37°C for 10 minutes. The reaction was stopped thereafter by adding 5 ml of a TCA mixture containing 36 ml of 50% (w/v) TCA solution, 220 ml of 1 M sodium acetate solution, 330 ml of 1 M acetic acid solution in a total volume of 1000 ml. The unreacted casein was precipitated, and the resulting precipitate was filtered off using Whatman filter paper No. 1. The optical density of the filtrate was measured at 275 nm against a blank. A standard graph was generated using standard tyrosine solutions of 5–50 $\mu\text{g ml}^{-1}$. One unit of protease activity was defined as the amount of enzyme, which liberated 1 μg tyrosine per min at 37°C.

3.2.5. Carbonic anhydrase activity

Another enzyme which has been recently shown to play a role in carbonate precipitation is Carbonic anhydrase (CA). In order to investigate the presence of this enzyme, the selected ureolytic bacterial isolates were checked for qualitative production of CA on Nutrient agar media supplemented with 1mM para nitrophenyl acetate (p-NPA) plates along with *Bacillus pumilus* (Bc P), which is a known producer of carbonic anhydrase. This isolate was procured from Department of Biochemistry, Delhi University, South campus.

The carbonic anhydrase activity of all bacterial isolates was then investigated for quantitative production. The bacterial cells (1%, OD₆₀₀ = 1.0) of all the isolates were inoculated into Nutrient broth media supplemented with 5µM ZnSO₄ and incubated at 37°C under shaking condition (130 rpm) for 24 hours. The CA production was then estimated by measuring the amount of p-nitrophenol produced according to spectrophotometric assay of Smith and Ferry (1999). After an interval of 24 hours, the culture was centrifuged at 8000 rpm for 5 minutes (4°C) and the supernatant comprising extracellular CA was collected by filtration. The culture filtrate (200 µl) was added to a mixture containing 1.80 ml of 100 mM phosphate buffer, pH 7.0 and 1 ml of 3 mM p-nitrophenyl acetate solution. The increase in A_{348 nm} was recorded for 5 minutes. The $\Delta A_{348 \text{ nm}} / \text{minute}$ was computed using the maximum linear rate for both the test and blank. One unit of carbonic anhydrase activity is defined as the amount of enzyme required to form 1 µmole of p-nitrophenol per minute. p-nitrophenol was used as standard.

3.2.6. Optimum conditions for Carbonic anhydrase production

In order to optimize the conditions for production of CA, all bacterial isolates were subjected to varying concentrations of Zinc sulphate (0 - 50µM) along with *Bacillus pumilus* Bc P. The efficacy of Bc P was then compared with the isolates of present study in terms of CA production. The effect of pH, temperature and time on the production of CA was also determined as in the case of urease. It was seen that the maximum CA activity in all the isolates was found at the same time as that of UA activity.

3.2.7. Characterization of Carbonic Anhydrase enzyme

3.2.7.1.1. Preparation of crude enzyme extract

To study the properties of CA enzyme from all the bacterial isolates, 1% bacterial inoculum ($OD_{600} = 1.0$) of each strain along with *B. pumilus* BcP was inoculated into sterilized Nutrient broth medium supplemented $10 \mu\text{M}$ ZnSO_4 and grown for a period of 3 - 4 days depending on the time of maximum activity. The culture broths were then centrifuged ($\times 8000$ rpm) at 4°C and supernatants were collected by filtration and used as crude enzyme extracts. Protein contents were estimated as described before.

3.1.7.2. Enzyme kinetics

The enzyme kinetics (K_m and V_{max}) of crude enzyme extracts were determined by measuring the activity of CA in the presence of varying concentrations of p-NPA substrate (1 - 5 mM). Michaelis–Menten constant (K_m) and the maximum velocity (V_{max}) was determined using the Lineweaver–Burk double reciprocal plot (Lineweaver and Burk, 1934).

3.2.7.3. Activity staining

Carbonic anhydrase activity staining of crude enzyme extracts was performed in 15% SDS–PAGE gels followed by color change with bromothymol blue stain. CA activity reveals yellow bands against the blue background of bromothymol blue according to the procedure from Ramanan *et al.* (2002). The samples were mixed with sample buffer (50 mM Tris–HCl, pH 6.8, 2% SDS, 1% bromophenol blue and 10% glycerol) and kept at 37°C overnight. After electrophoresis, the gel was washed in Buffer A containing 25% isopropanol in 10 mM of Tris–HCl buffer, pH 8.0, to remove SDS ahead of activity staining. The gel was washed again in Buffer B containing 100 mM Tris–HCl buffer, pH 8.3, and stained overnight using 0.25% bromothymol blue and destained using Buffer B.

As it was confirmed that all the Ureolytic bacteria were also efficient producers of CA, the next step was to investigate the role of bacterial CA in calcium carbonate precipitation.

3.2.3. Role of Urease and Carbonic anhydrase in calcium carbonate precipitation

3.2.3.1. Effect of inhibitors on Enzyme activities

In order to determine the role of both urease and carbonic anhydrase enzymes in CaCO_3 precipitation, bacterial isolate *Bacillus megaterium* SS3 was selected for detailed investigation as it produced both the enzymes efficiently. 1% bacterial inoculum of *B. megaterium* SS3 was inoculated into 100 ml nutrient broth supplemented with 2% Urea + $5\mu\text{M}$ NiCl_2 + $10\mu\text{M}$ ZnSO_4 for 72 hours. The culture broth was then centrifuged at 5000 rpm for 10 mins (4°C). The bacterial cells were harvested and washed with saline. The cells were then suspended into 100 ml of Nutrient broth media (to final concentration of 5×10^7 cells/ml) supplemented with various combinations:

1. $5\mu\text{M}$ Nickel chloride (NiCl_2) along with 2% urea for Urease induced set
2. 5 mM Acetohydroxamic acid (AHA) along with 2% urea for Urease inhibited set
3. $10\mu\text{M}$ zinc sulfate (ZnSO_4) for Carbonic anhydrase induced set
4. $5\mu\text{M}$ Acetazolamide (ACZ) + $10\mu\text{M}$ zinc sulfate (ZnSO_4) for Carbonic anhydrase inhibited set
5. $5\mu\text{M}$ Nickel chloride (NiCl_2) + 2% urea + 5 mM AHA + $5\mu\text{M}$ ACZ
6. $10\mu\text{M}$ zinc sulfate (ZnSO_4) + 5 mM AHA + $5\mu\text{M}$ ACZ

Each set was prepared in triplicate and the initial pH of all the sets was adjusted to 8.0. The sets were then incubated at 37°C in rotating shaker at 120 rpm for 96 hrs. Changes in enzyme activity and pH were determined by taking the culture broth at different time intervals (0, 2, 4, 6, 8, 10, 12, 24, 48, 72, 96 hrs).

Urea hydrolysis rate in case of urease inhibited set 2 was also estimated and compared to urease induced set 1 by colorimetric urea analysis method of Knorst *et al.* (1997). 2 ml of the crude enzyme supernatant was mixed with 0.5 ml of mixture containing 4% w/v p-dimethylbenzaldehyde and 4% v/v sulphuric acid in pure ethanol. The mixture was incubated at room temperature for 10 mins. Standard urea solutions were prepared in the range of 10 – 500 mM. The absorbance of the standards was taken at 422 nm and concentration of urea in the samples was determined against the standard solutions.

3.2.3.2. Effect of bacteria and crude enzyme extract in CaCO_3 mineralization

After investigating the positive potential of both inhibitors in inhibiting the enzyme activities, the next aim was to check the effect of inhibition of both the enzymes on CaCO₃ precipitation and also to check efficacy of bacterial cells in comparison to only crude enzymes in CaCO₃ precipitation.

For comparing the efficacy of enzyme induced as well as inhibited system for carbonate precipitation, two types of experimental systems were designed; with and without the bacteria. For bacterial system, the harvested bacterial inoculums of various sets prepared above were supplemented with 25 mM CaCl₂ while in case of only enzyme extracts without bacteria, the culture supernatants of harvested bacterial cells were taken and supplemented with 25 mM CaCl₂. Briefly, following combinations for CaCO₃ precipitation were designed:

1. 5 μM Nickel chloride (NiCl₂) along with 2% urea + 25 mM CaCl₂ (UA induced)
2. 5 μM Nickel chloride (NiCl₂) along with 2% urea + 5 mM Acetohydroxamic acid (AHA) + 25 mM CaCl₂ (UA inhibited)
3. 10 μM zinc sulfate (ZnSO₄) + 25 mM NaHCO₃ + 25 mM CaCl₂ (CA induced)
4. 5 μM Acetazolamide (ACZ) 25 mM NaHCO₃ + 25 mM CaCl₂ for Carbonic anhydrase inhibited set (CA inhibited)
5. 5 μM Nickel chloride (NiCl₂) + 2% urea + 10 μM zinc sulfate (ZnSO₄) for simultaneous induction of Urease and Carbonic anhydrase (UA + CA induced)
6. 5 μM Nickel chloride (NiCl₂) + 2% urea + 10 μM zinc sulfate (ZnSO₄) + 5 mM Acetohydroxamic acid (AHA) + 5 μM Acetazolamide (ACZ) for simultaneous inhibition of Urease and Carbonic anhydrase (UA + CA inhibited)

The pH of all the sets was adjusted to 8.0. The flasks were incubated at 37°C on a rotating shaker at 120 rpm and the samples were taken at different time intervals (0, 2, 4, 6, 8, 10, 12, 18 and 24 hrs). After each sampling period, the samples were centrifuged and the supernatant was analyzed for Ca²⁺ concentration along with the pH profile.

3.2.3.3. Microbial sand plugging

Microbial sand plugging experiments were performed as per methodology of Achal *et al.* (2010). Briefly, 50 ml of bacterial cultures from all 5 combinations prepared above i. e.

a) bacterial culture + both UA + CA induced

- b) bacterial culture + AHA
- c) bacterial culture + ACZ
- d) bacterial culture + AHA + ACZ

were mixed with 100 g sterilized river sand and packed into plastic columns (height = 15 inch; diameter = 5 inch). The bottom side of each column was blocked by using Whatman filter paper. All the columns were fed with 30 ml respective media till 10 days. The experiment was stopped after 10 days. The upper layer of the columns was cut, ground, dried at 50°C for overnight and sieved through 45µm diameter mesh prior to calcium carbonate estimation. Precipitated CaCO₃ from each layer was measured by EDTA titration method (AHPA, 1989). Briefly, one gram of sand sample was dissolved with 3N hydrochloric acid. Followed by this, 4 ml of Sodium hydroxide (5N) was added to the precipitate and final volume was made up to 50 ml using deionized water. Few drops of hydroxyl naphthol blue were added as an indicator and the mixture was finally titrated against 0.05M EDTA. End point was noted from pink to blue which is easily visualized and the amount of CaCO₃ formed was calculated by the volume of EDTA used × 0.005004 × 1,000/gm of sample used.

3.2.3.4. Investigation of carbonate crystals formed by different enzyme sets

The carbonate crystals precipitated on the surface of all sand plugs were then investigated for morphological and mineralogical constituents by Scanning electron microscopy, X ray diffraction analysis and Energy dispersive X ray analyzer.

3.2.4. Carbonate precipitation via Carbonic anhydrase

After investigating the role of CA of *Bacillus megaterium* SS3 in CaCO₃ precipitation, carbonate precipitation efficacy of all other isolates via CA pathway was also investigated. Bacterial cells of each strain were inoculated into 250 ml flasks containing 100 ml Nutrient broth media supplemented with 10 µM ZnSO₄ + 25 mM NaHCO₃ + 25 mM CaCl₂ to a final concentration of 5 × 10⁷ cells mL⁻¹ (pH 8.0) and incubated at 37 °C with shaking (120 rpm).

All samples were prepared in triplicate flasks that were pre-washed with 6 M HCl. Control sets were prepared without any bacterial inoculum. At every 2 hr for the first 12 hr and longer intervals afterwards, the replicates were terminated to determine the pH and amount of insoluble Ca^{2+} in the pellets and soluble Ca^{2+} in the supernatant by centrifuging the broth and quantifying the Ca^{2+} content according to the EDTA titration method (APHA *et al.*, 1998).

3.3. Characterization of calcium carbonate crystal polymorphs

In order to assess the applicability of different calcium carbonate polymorphs for different biotechnological applications, it is pre requisite to gather information on the various polymorphs produced by different calcifying bacteria. All the five CaCO_3 precipitating bacterial strains were grown in Nutrient broth ($\text{OD}_{600} = 1.0$) and then 1% of each bacterial isolate was inoculated into 250 ml flasks containing 100 ml NBUC media (pH 8.0) and incubated at 37 °C with shaking (120 rpm) for 3 weeks. After 3 weeks, the carbonate crystals precipitated at the bottom of each flask were filtered on Whatman No.1 filter paper (90 mm in diameter) and collected after washing with sterile distilled water. The crystals were air dried at 37°C for 48 hrs. The filters were weighed before and after collection of crystals to estimate the amounts of carbonate crystals precipitated by the different isolates. This was followed by analysis of the crystals for morphological and chemical constituents.

3.3.1. Staining of crystals

The crystals were mounted on glass slides and stained with Loeffler's methylene blue (methylene blue, 3 g; potassium hydroxide, 10 mg; 95% ethanol; 300 ml per liter of dH_2O) for 1 min, rinsed with dH_2O , dried by blotting, and observed with white light by the use of 1,000 X magnification and immersion oil. The bacteria inside and around the crystals were observed.

To investigate the polysaccharides associated with carbonate crystals, the crystals were stained with alcian blue – periodic acid - Schiff stain (PAS). Firstly, 100% ethanol was applied on the crystals for 5 min followed by rinsing with dH_2O for 5 min, application of

alcian blue for 5 min followed by 1% Schiff's reagent for 5 min. The final rinsing was done with dH₂O for 5 min.

3.3.1.1. Scanning electron Microscopic analysis

The precipitated bacterial crystals were analyzed using Scanning Electron Microscopy, SEM (ZEISS EVO 50) equipped with EDX. For SEM analysis, the crystals were fixed over night in 2.5% glutaraldehyde in 0.1 M sodium phosphate buffer at 4°C, rinsed in 0.2 M phosphate buffered saline (pH 7.4) for 1 hour and dehydrated in series of graded ethyl alcohol. The SEM observation was done under the following analytical condition: EHT = 20.00 kv, WD = 10 -11 mm. Elemental analysis was done with energy dispersive X-ray analyzer (Bruker AXS, Quan Tax 200).

3.3.1.2. Confocal laser scanning microscopic analysis

In order to determine the morphological features of different crystals by confocal scanning laser microscope (CSLM), fluorescent dye CTC (5-cyano-2,3-ditolyl tetrazolium chloride; Polysciences Inc.) was used. The crystals were fixed for 30 min with 4% paraformaldehyde-phosphate-buffered saline. The slides were flooded with freshly prepared 1.5 mM (final concentration) CTC solution. The stain solution was left to react overnight at room temperature in the dark, and the slides were stored at 20°C for 30 min to stop the reaction. Before visualization with a confocal scanning laser microscope (LSM 510 Meta; Carl Zeiss), the slides were covered with a cover slip and fixed with DPX mountant (Hi Media). The stain was excited at 453 nm by the use of a 590-nm long-pass filter.

3.3.2. X ray diffraction analysis

XRD spectra were obtained using an X' Pert PRO diffractometer with a Cu anode (40kV and 30mA) and scanning from 3⁰ to 60⁰ 2 θ . The components of the sample were identified by comparing them with standards established by the International Center for Diffraction Data.

3.3.3. Fourier transform Infra red (FTIR) spectra

The FTIR spectrum of all the crystals was recorded on a Bruker Vertex- 70 apparatus by the diffuse reflectance accessory technique. The spectra of the crystals were scanned in the range of 400 - 4000 cm^{-1} .

3.4. Evaluation of microbes for enhanced durability of various building materials

3.4.1. Preparation of varying grain sizes and density sand columns

3.4.1.1. Set up for microbial sand plugging

Locally available clean, dry, well graded, natural river sand was procured. The sand was sieved in varying sized meshes (0.2 – 1.5 mm) and each fraction was collected separately and autoclaved to remove the indigenous bacterial flora. In the meantime, for determining the efficacy of bacterially induced calcium carbonate precipitation in varying grain sized sand columns, the most efficient calcifying bacterial isolate *Bacillus megaterium* SS3 was inoculated into 1000 ml conical flasks containing 500 ml autoclaved Nutrient broth media supplemented with 2% urea (pH 8.0) and incubated under shaking conditions at 37°C for 72 hours. The bacterial cells were then harvested (5000 rpm X 10 mins at 4°C) and washed with saline. The cells were then suspended into 500 ml sterilized NBUC media (pH 8.0).

The sand columns were prepared by mixing the bacterial solution into the varying grain sized sand particles as described above. Briefly, 50 ml of grown culture ($\text{OD}_{600} 1.0$) was mixed with 100 g sterilized sand. Sand slurry of each grain size containing bacterial culture for each set was packed into a plastic column (height = 15cm; diameter = 5 cm) and bottom side of the column was blocked by using Whatman filter paper. A control reaction was packed in column in which sterile sand was mixed with media only (without cells). After preparation, the sand columns were vibrated to allow uniform settlement. In control set, instead of mixing bacterial slurry, only media was added. Nutrient broth media containing urea and calcium chloride was then injected to drive away extra air or voids and attain uniform mixing till 10 days. Flow rate was measured by measuring the volume of media that came out of columns per minute. The effluent was collected for investigation of pH and electrical conductivity. The experiments in all the sand columns were terminated after ten

days.

In another set, varying densities sand columns were also prepared (1.65, 1.70, 1.75 g/cc) by mixing 1:1 soil: sand along with 7% cement and mixed with 10% bacterial inoculums prepared above by column making machine (Fig. 3.1). In this case, 30 ml NBUC was sprayed daily on the surface of each set of bacterial column for 10 days.



Fig. 3.1. Apparatus for preparing sand columns

3.4.1.2. Determination of pH, EC and urea hydrolysis in bacterial and control effluents

The effluent collected from the bacterial treated as well as control sand columns with varying grain sizes was analyzed for pH, EC and urea hydrolysis in order to assess the bacterial activity within the sand columns. The pH of the effluent was recorded by Cyber Scan 510 and electrical conductivity was also analyzed at regular intervals. For estimating the hydrolyzed urea, colorimetric urea analysis method was used (Knorst *et al.*, 1997). 2 ml of the effluent was mixed with 0.5 ml of mixture containing 4% w/v p-Dimethylbenzaldehyde and 4% v/v sulphuric acid in pure ethanol. The mixture is incubated at room temperature for 10 mins and absorbance is taken at 422 nm against standard urea solutions.

3.4.1.3. Viability in sand columns

For investigating the viability of bacterial cells in the sand columns, a portion of the sand

column from the top was cut and the viability of bacterial cells within this portion was estimated by staining with fluorescent dye CTC in which actively respiring bacteria reduce it to red colour. Briefly, the specimen was crushed finely and smear of this was prepared on clean microscopic glass slide. The fixing on microscopic slides was done for 30 min with 4% paraformaldehyde 2- phosphate - buffered saline. The slides were then flooded with freshly prepared 1.5 mM (final concentration) CTC solution. The stain solution was left to react overnight at room temperature in the dark, and the slides were stored at 20°C for 30 min to stop the reaction. Before visualization with a confocal scanning laser microscope (LSM 510 Meta; Carl Zeiss), the slides were covered with a coverslip and fixed with DPX mountant (Hi Media, India). The stain was excited at 453 nm by the use of a 590-nm long-pass filter. The slides were visualized at 400 X magnifications under immersion oil.

3.4.2. Energy efficient building materials

Soil cement blocks of size 230 X 100 X 75mm were prepared by manually operated block making machine as per Reddy and Gupta, 2005. Soil: sand (1: 1) along 7% cement ratio was optimized along with 10% bacterial suspension. The bacterial culture *B. megaterim* SS3 had density of 10^8 cells/ml and block density was set at 1.8 g/cc. The specimens treated with bacteria and control blocks were subjected to various quality control tests after 28 days of curing.

3.4.3. Ash bricks

30% rice husk ash bricks and 30% fly ash bricks {composed of 3 ash : 7 clay} manufactured as per IS 2117 : 1991 were procured from a local kiln (Dharam Bricks, Ludhiana, Punjab, India). The chemical composition of rice husk ash and fly ash is presented in table 7.14. The bricks were designated as: B-RHAB for Bacteria treated rice husk ash bricks, U-RHAB for Untreated rice husk ash bricks, B-FAB for Bacteria treated fly ash bricks, U-FAB for Untreated fly ash bricks and RB for conventional red bricks. The procured bricks were oven dried at 50°C to achieve constant weight and then allowed to cool at room temperature.

3.4.4. Effect of bacterial carbonate precipitation on properties of different materials

3.4.4.1. *CaCO₃ content estimation*

For analyzing the extent of carbonate precipitation, bacterial as well as control sand columns with varying grain sizes as well as densities were grounded and sieved through a 45 μ m diameter mesh. Precipitated carbonates were measured by EDTA titration method (AHPA, 1989) as mentioned above in section 3.2.3.3.

3.4.4.2. *SEM EDX and XRD*

The morphology and chemical constituents of bacterial carbonate consolidated specimens were analysed with Alizarin Red staining, SEM - EDX and XRD. Samples were completely dried at room temperature, then examined by SEM (Zeiss EVO50) at accelerating voltages ranging from 15 to 35 kV, which was equipped with an energy-dispersive X-ray analyzer (Bruker-AXS, QuanTax 200) for elemental analysis. Samples were gold coated with a sputter coating Emitech K575 prior to examination. Consolidated bacterial treated samples were cut open prior to examination. XRD-spectra were obtained using an X'Pert PRO diffractometer with a Cu anode (40 kV and 30 mA) and scanning from 3 to 60° 2 θ . Each consolidated sample was crushed and grinded using motor pestle before mounting on to a glass fiber filter using a tubular aerosol suspension chamber (TASC). The components of the sample were identified by comparing them with standards established by the International Center for Diffraction data.

3.4.4.3. *Water absorption*

For studying water absorption, bacterial treated and control blocks were dried in oven at 50°C and dry weight was measured ($W_{oven\ dried}$) as per IS 3495 (1992). The samples were then saturated overnight in water and weighed again ($W_{saturation}$). Water absorption was calculated by using following formula:

$$\% \text{ Water absorption} = \frac{W_{saturation} - W_{oven\ dried}}{W_{oven\ dried}} \times 100 \quad \text{Eq. 3.1}$$

3.4.4.4. Rate of moisture absorption in soil cement blocks

In order to determine the rate of water absorption, the specimens were dried in an oven at 60°C until they attained constant weight. The weights of dried blocks were recorded.

To calculate the rate of moisture absorption, the blocks were immersed in water for different intervals of time (0, 0.5, 1, 1.5, 2, 3, 4, 5, 6, 7, 8, 9, 10, 15, 20, 25, 30, 35, 40, 50, 60, 70, 80, 90, 100, 120, 140, 160, 180, 210, 240, 600, 720, 960, 1220 and 1440 mins) and the weight of wet block was measured. The percentage saturation of the block was calculated with respect to dry weight.

3.4.4.5. Initial rate of absorption

For conducting the initial rate of water absorption (IRA), four weeks bacterial treated and untreated bricks were immersed in water tray with water level up to 3 mm as per ASTM C67. Bricks were taken out after one minute and the rate of absorption was calculated as grams of water absorbed /min/194cm² or 30 in² of bed surface area by the following equation:

$$S = (W_1 - W) * 194 \text{ cm}^2 / A \quad \text{Eq. 3.2}$$

Where S = Suction in grams per min per 194 cm², W₁ = Weight of brick after 1 min immersion in 3mm water, W = Dry weight of the brick and A = Cross sectional area of the surface of brick in cm².

3.4.4.6. Linear Expansion on saturation

Experiments were performed to determine the linear expansion on saturation of soil cement blocks. Length comparator fabricated in the lab was used. Initial length of the oven dried blocks was determined and then soaked in water for 24 h. Length of saturated blocks was determined. The difference in the initial and final readings gave linear expansion of the block, which was expressed as percentage of actual length in dry state to get linear expansion value.

3.4.4.7. Porosity

The simplest of total porosity measurements is based upon the Archimedes' Principle which states a body wholly or partially immersed in a fluid is buoyed by a force equal to the mass of the fluid displaced (Lide, 1999). The total porosity (P) is calculated from their water saturated surface dry mass (m_{sat}), their mass suspended in water (m_{water}), and their oven dry mass² (m_{dry}).

$$P (\%) = (m_{sat} - m_{dry} / m_{sat} - m_{water}) \times 100 \quad \text{Eq. 3.3}$$

These moisture states are schematically illustrated in Figure 3.2.

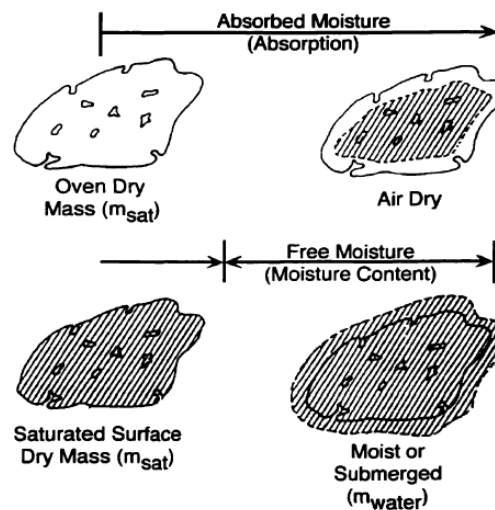


Fig. 3.2. Schematic illustration of moisture states of cement-based materials (Neville, 1973)

All specimens were immersed in tap water for 24 hours prior to measuring their water-saturated surface-dry mass, and their mass in water. Each sample rested on a mesh stand in approximately 100 ml of water per sample. These conditions ensured that all sides of the sample were exposed to water and that sufficient water was present to enable complete saturation. The water-saturated surface-dry mass was determined by removing each specimen from the water, wiping the excess water off with a damp towel, and immediately weighing the section. Its mass in water was determined by placing the water-saturated surface dry sample in a wire basket which was immersed in water. The mass of the section was calculated by subtracting the mass of the basket in the water alone from the mass of the basket in the water with the section in it. After the weighing was completed, the samples

were dried at 50°C for 24 hours to remove all of the evaporable water. This time period was determined from monitoring the mass of water lost with time from ten similar samples. Reweighing these dried specimens provided the oven dry mass. From all these measurements, the total porosity was calculated for each specimen using Equation 3.3.

3.4.4.8. Mercury intrusion porosimetry

Changes in porosity and pore size determination following biomineralization were studied using mercury intrusion porosimetry (MIP) (with a Micromeritics Autopore 5510 device). Cubes with 1cm³ geometric volume were cut from the upper layer of both bacterial treated and control specimens and dried over night in an oven at 80°C. The samples were degassed under vacuum at pressure of 50 µm Hg. Mercury surface tension value of 485 dynes/cm and contact angle of 130° was used, respectively. Mean pore size in the range of 0.006 µm to 338 µm was determined. Porosity (% total porosity) was then determined as weight normalized volume of mercury intruded in the sample.

3.4.4.9. Wet compressive strength

The compressive strength of bacterial treated and control (columns, bricks and blocks) was obtained as per IS 3495 using automatic compression testing machine COMPTEST 3000. The frogs for bricks were filled with rich cement mortar. Specimens were soaked in water for 48 hours prior to testing. Saturated specimens of bricks and blocks were mounted in compression testing machine such that there is thin plywood sheet on both faces of the block between thick rigid platens. The ultimate crushing load was noted down to calculate wet compressive strength of the specimens.

3.4.4.10. Durability test of freeze thaw resistance

3.4.4.10.1. Freeze thaw resistance test

Freeze thaw test was also performed for bacterial treated and untreated bricks. The bricks were subjected to 15 freeze thaw cycles as per modified ASTM C67. The bricks were subjected to 16 hours freezing at 4 ± 1 °C in tray containing 0.5 inch depth of water followed

by 8 hours of thawing at room temperature. This was continued for 15 cycles and after 15 days, compressive strength was calculated as per the procedure explained above.

3.5. Evaluation of fly ash as carrier for calcifying bacterial cells and their viability

3.5.1. Collection of fly ash

Fly ash samples were collected (0–40 cm depth) randomly from fly ash sedimentation pond of National Aluminium Company Ltd. (NALCO), Damnjodi (18°46'22" N 082°53'23" E), Orissa, India. The samples were mixed thoroughly, and a portion of the fly ash was used to analyze various physicochemical characteristics.

3.5.2. Preparation of bacterial formulations

Three efficient calcifying bacterial isolates *Bacillus megaterium* SS3, *Bacillus cereus* SS5 and *Lysinibacillus fusiformis* SS18 were used in this study. These strains were maintained in Nutrient broth media (5.0 g peptone, 1.5 g beef extract, 1.5 g yeast extract and 5.0 g sodium chloride per litre). Pure cultures of all the three bacterial isolates were cultivated in nutrient broth media by inoculating 1% pure culture in 1000 ml flask containing 500 ml Nutrient broth media and incubated at 37°C in a rotating shaker at 120 rpm for 3 days. The bacterial cultures were then centrifuged at 5000 rpm for 10 mins (4°C) to obtain the bacterial pellet. The pellet was washed twice with phosphate buffer saline. The bacterial pellets of all the cultures were resuspended in 20% sterilized distilled water to make bacterial slurry.

The fly ash was autoclaved prior to use. Three different sets of fly ash (250 g each) in triplicates for each bacterial isolate were prepared by adjusting the moisture content of fly ash to 30%, 40% and 50% (w/v) by adding known volume of sterilized distilled water. Finally, the bacterial slurry of SS3, SS5 and SS18 prepared above was mixed thoroughly with varying moisture fly ash sets so that the initial cfu load in all the sets was around 5×10^8 cells/ g. All the formulations were mixed well for uniform distribution of bacterial cells in fly ash and all the formulations were then packed in sterile polythene bags (Hi Media,

India) and stored at different temperatures (4°C, 25°C and 37°C). Control fly ash bags without bacterial inoculation were also prepared.

3.5.3. Stability of bacteria in formulations at various moisture content and temperatures

The viability, stability and purity of the bacterial isolates within the formulations was determined monthly. 1 g of the formulation was sampled monthly in sterile conditions from all the packets incubated at different temperatures and was processed separately. Before sampling, the packets were shaken carefully and thoroughly to ensure uniform distribution of bacterial cells. After that, 1 g of the formulation was suspended in 10 ml sterile distilled water and serial dilutions were made. 100 µl aliquot was then plated onto nutrient agar plates and incubated at 37°C for 48 hours. The plate count was carried out in triplicates and final value of colony forming units (cfu/ml) expressed as log cfu /g fly ash was average of three readings. The pH of the fly ash in the formulations was also recorded at regular intervals. The whole process was carried till 1 year over an interval of 1 month.

3.5.4. Fluorescent dyes for studying bacterial viability

The viability of bacterial formulations was also checked by florescent dye CTC (5-cyano - 2, 3 - ditolyl tetrazolium chloride; Polysciences Inc.). 1g formulated cells were taken after 1 year and inoculated into 100 ml nutrient broth for 2 hrs and then fixed on microscopic slides for 30 min with 4% paraformaldehyde 2- phosphate - buffered saline. The slides were flooded with freshly prepared 1.5 mM (final concentration) CTC solution. The stain solution was left to react overnight at room temperature in the dark, and the slides were stored at 20°C for 30 min to stop the reaction. Counter staining was done with 2 µm SYTO[®] 24 nucleic acid stain. Before visualization with a confocal scanning laser microscope (LSM 510 Meta; Carl Zeiss), the slides were covered with a coverslip and fixed with DPX mountant (Hi Media, India). The stain was excited at 453 nm by the use of a 590-nm long-pass filter. The slides were visualized at 400 magnification under immersion oil.

3.5.5. Scanning electron microscopic studies of bacterial formulations

The bacterial formulations after 1 year were subjected to Scanning electron microscopic analysis. One gram from each formulation was randomly sampled and analyzed using SEM. For SEM analysis, the samples were fixed over night in 2.5% glutaraldehyde in 0.1 M sodium phosphate buffer at 4°C, rinsed in 0.2 M phosphate buffer saline (pH 7.4) for 1 hour and dehydrated in series of graded ethyl alcohol. The SEM observation was done under the following analytical condition: EHT = 20.00 kv, WD = 10 -11 mm.

3.5.6. Efficacy of Calcium Carbonate Precipitation by bacterial formulations

3.5.6.1. Calcium Carbonate Precipitation by bacterial formulations in vitro

In order to check the efficacy of bacterial formulations, 1 gm inoculum formulation (10^6 cfu/g) of *Bacillus cereus* (as it had maximum viability after 1 year) was inoculated into 50 ml Nutrient broth media supplemented with 2% urea and 25mM CaCl_2 (NBUC) as described earlier. In another set, fresh bacterial cells (10^6 cfu/ml) were inoculated into NBUC media along with a control where no bacterial inoculation was done. All the three sets were incubated at 37°C in rotating shaker at 120 rpm for 72 hours for precipitation of CaCO_3 . The aliquots from flasks were taken at regular time intervals and the broth was centrifuged to quantify soluble Ca^{2+} in the supernatant by EDTA titration method as described before (section 3.2.3).

3.5.6.2. Effect of Calcium Carbonate Precipitation by bacterial formulations in Sand plugs

For studying the efficacy of formulated bacterial cells, Microbial sand plugging experiments were performed as per Reddy and Gupta (2005) with little modification. 10% NBUC media was added to 1 : 1 : 0.5 soil : sand : flyash (formulated) along with 7% cement content and labelled as Formulated bacterial sand columns (For - BSC). Sand, soil, fly ash and cement were sterilized prior to use to eliminate the indigenous microflora by autoclaving at 121°C for 1 h. The columns were packed as cylinders with diameter 3.8 cm and height 7.6 cm. In second set, similar columns as described above were prepared along with addition of fresh bacterial cells (5×10^6 cfu/g) to fly ash and mixed with 10% NBUC media, labelled as

Fresh bacterial sand columns (F - BSC). In control set, the columns were prepared with only NBU media and designated as Control sand columns (C - SC).

All the columns were kept at room temperature for 24 hrs followed by their curing for 28 days by spraying 30 ml NBUC media/day on the surface of the columns. After 28 days of curing, the specimens were allowed to dry at room temperature and CaCO₃ precipitated on the surface of all types of columns was determined as described in section 3.2.3.3. Micrographic and chemical characterization of the carbonates formed was done through Scanning electron microscope, Energy dispersive X ray and X ray diffraction studies as described earlier (3.4.4.2.)

In order to test the efficacy of bacterial columns, it is imperative to study the consolidating effect of biodeposition on porosity of the substrate material. For this characterization, water absorption and mercury intrusion porosimetry analysis was done as reported in section 3.4.4.3 and 3.4.4.8.

3.6. Optimization of conditions for urease and carbonate precipitation by Response surface methodology

In order to optimize the production of CaCO₃ for maximal precipitation, there is need to standardize the media for maximum urease production. For this, it is crucial to optimize the medium constituents. Basal media (2 g glucose, 1 g yeast extract, 2 g urea, 0.21 g NaHCO₃, 0.5 g NH₄Cl, 0.005g MgSO₄. 7H₂O, 0.27 g CaCl₂, 0.5 g KH₂PO₄ per 100 mL) was optimized for urease production in *Bacillus megaterium* SS3 using one factor at a time. After this, in order to find the most significant media parameters for urease production by *B. megaterium* SS3, Placket Burman design was used to screen the significantly affecting variables in order to evaluate the relative importance of various factors affecting urease production. Different sets of *B. megaterium* SS3 inoculated with variable ranges of media components were investigated for urease production after incubation at 37°C and 130 rpm for 72 hrs.

3.6.1. Optimization of production medium by OFAT method

Growth conditions and chemical components were varied one at a time to check their impact on urease production. Various parameters such as inoculum size, source of carbon and nitrogen were optimized. *B. megaterium* SS3 was inoculated into different basal media with varying carbon, nitrogen and inoculum concentrations. Various carbon sources tested were: glucose, sucrose, fructose, lactose, starch and mannitol. Different nitrogen sources tested were beef extract, peptone, casein, ammonium sulphate and sodium nitrate. The initial inoculum concentrations were investigated from a range of 5×10^6 cells/ml to 5×10^9 cells/ml.

3.6.2. Plackett – Burman design

Plackett Burman design is a powerful and efficient mathematical approach to determine the effect of medium constituents on enzyme activity (Kaur and Satyanarayana, 2005). At the first stage, screening the factors by Plackett – Burman design involves both the determination of parameters that have a positive influence on production and the elimination of those that have a negative or no influence. Once the components critical to production are screened, the second step involves the determination of optimum concentration of each component for maximum product formation. The variables selected in this study were glucose, peptone, urea, calcium chloride, NiCl_2 , NaCl , MgSO_4 and agitation. The variables were investigated and experiments were carried out at 37°C and 130 rpm for 72 hrs. Each variable was set at two levels, high level and low level. The experimental design is given in table (2.6).

Table 2.6. Plackett Burman design matrix for screening the variables influencing Urease activity.

Std	Run	Factor 1 Urea	Factor 2 Glucose	Factor 3 NaHCO ₃	Factor 4 Peptone	Factor 5 NH ₄ Cl	Factor 6 MgSO ₄ ·7H ₂ O	Factor 7 CaCl ₂	Factor 8 KH ₂ PO ₄	Response Urease activity (U/ml)
4	1	1	3	0.1	1.5	1.5	0.002	0.3	0.6	
9	2	3	3	0.3	0.5	0.5	0.002	0.3	0.2	
3	3	3	1	0.3	1.5	0.5	0.006	0.3	0.6	
12	4	1	1	0.1	0.5	0.5	0.002	0.1	0.2	
5	5	1	1	0.3	0.5	1.5	0.006	0.1	0.6	
2	6	1	3	0.3	0.5	1.5	0.006	0.3	0.2	
1	7	3	3	0.1	1.5	1.5	0.006	0.1	0.2	
7	8	3	1	0.1	0.5	1.5	0.002	0.3	0.6	
6	9	1	1	0.1	1.5	0.5	0.006	0.3	0.2	
8	10	3	3	0.1	0.5	0.5	0.006	0.1	0.6	
10	11	1	3	0.3	1.5	0.5	0.002	0.1	0.6	
11	12	3	1	0.3	1.5	1.5	0.002	0.1	0.2	

Experimental runs were performed according to the design and response (enzyme activity) was recorded. Urease activity after 72 hours was recorded as per methodology given in section 3.1.4. Significant parameters were selected from the data and studied further by Response surface method.

3.6.3. Response surface methodology

The interactive effects of three significant factors *A* (Glucose), *B* (Urea), and *C* (NaHCO₃) on the response, namely, urease production were determined statistically using RSM. Central composite design (CCD) developed by the Design Expert software, version 8.0.7.1 (Stat Ease Inc. Minneapolis, USA, trial version) was adopted for this purpose.

Each one of the above independent variables *A*, *B*, and *C* was taken at a central coded value considered as zero and studied at three different levels. A matrix consisting of 20 experiments with 5 replicates at the centre point generated by the software was performed for maximizing the urease production (Table 2.7).

Production was carried out in 250 mL Erlenmeyer flasks containing 100 mL of the production medium (pH 8.0). The flasks were sterilized by autoclaving at 120°C for 20 min, inoculated with the culture under aseptic conditions, and incubated at 37°C for 72 h, in an orbital shaker set at 130 rpm. At the end of the incubation period, urease assay was performed and activity was recorded as the response (dependent variable). All experiments were carried out in triplicate and the data represent the mean. Following second-order polynomial equation describes the relationship between the dependent and independent variables. The model was statistically analyzed. Analysis of variance (ANOVA) involved Fischer's *FF* test to judge the model's overall significance, associated probability values, and coefficient of determination to measure the regression model's goodness of fit. The fitted polynomial equation was further expressed in the form of 3D and contour plots which depicted the interactions graphically.

In order to further validate and confirm the suitability of the model, verification experiments with numerically optimized levels of tested variables were performed.

Table 2.7. Central composite design showing combinations of independent variables of medium ingredients

Std	Run	Factor 1 Urea (g/100 mL)	Factor 2 Glucose (g/100 mL)	Factor 3 NaHCO ₃ (g/100 mL)
18	1	2	2	0.2
17	2	2	2	0.2
12	3	2	2.87	0.2
16	4	2	2	0.2
5	5	1.5	1.5	0.25
19	6	2	2	0.2
7	7	1.5	2.5	0.25
9	8	1.13	2	0.2
13	9	2	2	0.11
6	10	2.5	1.5	0.25
8	11	2.5	2.5	0.25
15	12	2	2	0.2
2	13	2.5	1.5	0.15
11	14	2	1.13	0.2
10	15	2.87	2	0.2
1	16	1.5	1.5	0.15
14	17	2	2	0.29
4	18	2.5	2.5	0.15
20	19	2	2	0.2
3	20	1.5	2.5	0.15

As urease activity is a direct measure of the amount of carbonate precipitation, the amount of CaCO_3 precipitated was estimated at maximum urease production by quantifying the carbonate crystals (section 3.3) and estimating the amount of calcium carbonates as per methodology given in section 3.2.3. The level of carbonate production was also compared with the carbonate production before optimization.

3.7. Statistical analysis

All the experiments were performed in triplicate and the data were analyzed by analysis of variance (ANOVA) using GraphPad prism (5.0) software followed by the Tukey's honestly significant difference test.

Chapter 4

Results and Discussion

4.1. Isolation and Characterization of calcifying bacteria

4.1.1. Isolation of CaCO₃ precipitating ureolytic bacteria

Consideration of soil as a living ecosystem offers the potential of innovative and sustainable solution to isolation of different microbes. Though ignored for centuries, bacteria are omnipresent in soils at surprisingly high concentrations. This largely unexplored soil diversity has spurred research on isolation of various microbes which play great roles in biomineralization processes and precipitate inorganic solids of great technical importance. Although, numerous studies have investigated microbial diversity in wide range of habitats, but there are still many which await exploration. Alkaline soils provide a window into the prime habitat of alkalophilic bacteria and are areas of specific interest because of being carbonate dominated habitats (Satyanarayana *et al.*, 2005). Alkaliphilic ureolytic bacteria represent the most favoured pathway for precipitation of carbonates. The bacterial urease simply hydrolyzes the urea to form bicarbonate, ammonium and hydroxide ions. These products gives rise to pH increase, which in turn results in the formation of carbonate ions, which in the presence of soluble calcium ions, precipitate as CaCO₃. Because of the carbonate precipitating ability of these alkalophilic bacteria, alkaline soils of various sites were investigated for isolation of calcifying bacteria.

Though bacterial diversity differs in different alkaline sources, but all of them are subjected to high pH environments (> 8.5). The bacterial isolates from varying alkaline/ calcareous soils (Table 4.1.1) were tested for their ability to grown in nutrient broth with 2% urea. The grown bacterial isolates were plated on nutrient agar plates supplemented with urea. The bacterial count from all the soil samples varied as given in the table 4.1.2. Most of the bacterial colonies appeared at 10⁻³ dilution. No growth was observed at 10⁻⁶ or 10⁻⁷ dilution. The results of this screening indicated that an active population of facultatively anaerobic

alkalophilic bacteria persisted in all the samples. Bacterial population was highest in alkaline soil collected from Anantapur district, Andhra Pradesh, India.

Table 4.1.1. Physicochemical characteristics of various soils

	Alkaline soil 1 (Anantapur)	Alkaline soil 2 (Ropar)	Alkaline soil 3 (Samrala)	Alkaline soil 4 (Patiala)
pH	10.3	9.1	8.9	8.6
EC	1.82	2.06	0.81	1.24
Organic C	0.58	0.67	0.38	0.44
Constituent	Percentage			
Si	71.9	62.3	67.9	76.6
Al	10.8	13.9	11.5	9.6
Ca	2.8	3.6	3.9	2.3
Mg	1.6	1.9	0.91	0.72
Fe	3.9	3.1	2.2	2.4
Mn	0.11	0.08	0.04	0.06
Zn	0.42	0.26	0.12	0.31
Na	3.06	4.13	3.21	2.81
K	3.1	2.9	3.4	3.7

Table 4.1.2. Population of bacteria in different sources per gram of soil

Sources	Bacteria (x 10 ³)
Alkaline soil 1 (Anantapur)	3.6
Alkaline soil 2 (Ropar)	2.1
Alkaline soil 3 (Samrala)	0.07
Alkaline soil 4 (Patiala)	0.003

Ubiquitous nature of bacteria makes them ideal candidates for studying their diversity and isolating them from extreme environments. Numerous bacterial colonies were present in all the plates showing their high concentrations in alkaline soils of all regions. Bacteria are diverse in all soils regardless of its type, mineralogy, pH, and other environmental factors. Though complexity in environmental conditions vary at multiple spatial scales and influences bacterial diversity (Horner - Devine *et al.*, 2004), we successfully isolated different bacteria from all the alkaline soils. The bacteria that were isolated from such calcareous soils are alkaline in habitat and certain structural components of the cell wall of these alkalophiles, such as teichuronopeptide, may contribute to pH homeostasis at high pH and aid these bacteria to survive in alkaline environments (Aono *et al.*, 1999).

After enriching the growth of ureolytic bacteria in urea enriched nutrient broth, the efficient bacteria were screened for production of urease in urease selective media i.e. Urea agar media. This media contains phenol red and the urease producing bacteria utilize the urea present in the media degrading phenol red to give pink colour in alkaline environment (Andrews *et al.*, 1995) (Fig. 4.1.1). Based on production of intense pink colour by different isolates, thirty different colonies were selected for further studies.

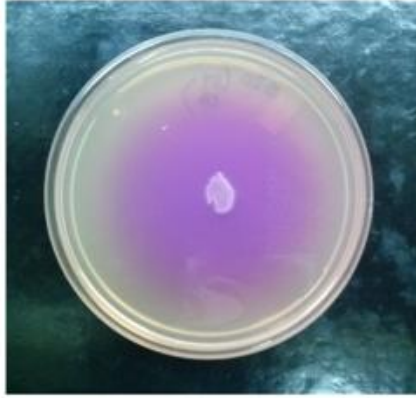


Fig. 4.1.1. Urease production by efficient ureolytic bacterial isolate on Urea agar base plate.

After the primary screening, all the 30 bacterial isolates were checked for quantitative production of urease in comparison to *S. pasteurii* (Sp P) which was used as reference strain as it has been widely recognized as high urease producing model bacterium by researchers capable of high precipitation of CaCO_3 (Ramakrishnan *et al.*, 1998; Stocks - Fischer *et al.*, 1999; Ramachandran *et al.*, 2001). This strain was procured from culture collection of Institute of Microbial technology (IMTECH), Chandigarh, India. Eight efficient bacterial isolates were further selected based on high amount of urease production and were designated as SS3, SS5, SS13, SS15, SS18, SS20, SS21 and SS22 (Table 4.1.2; Fig. 4.1.3).

Table 4.1.3. Comparison of urease activity (U/ml) by different bacterial isolates

Bacterial isolate	Soil site	Urease production (U/ml)
<i>S. pasteurii</i> (Sp P)	IMTECH	58 ± 4a
SS3	Soil site 1	62 ± 3a
SS5	Soil site 1	55 ± 6ab
SS13	Soil site 1	48 ± 4b
SS15	Soil site 1	57 ± 5a
SS18	Soil site 1	51 ± 3b
SS20	Soil site 2	45 ± 3c
SS21	Soil site 3	43 ± 5c
SS22	Soil site 4	41 ± 4c

Values bearing different letters in the same column are significant at $P < 0.05$. Values are mean ± SD (n = 3).

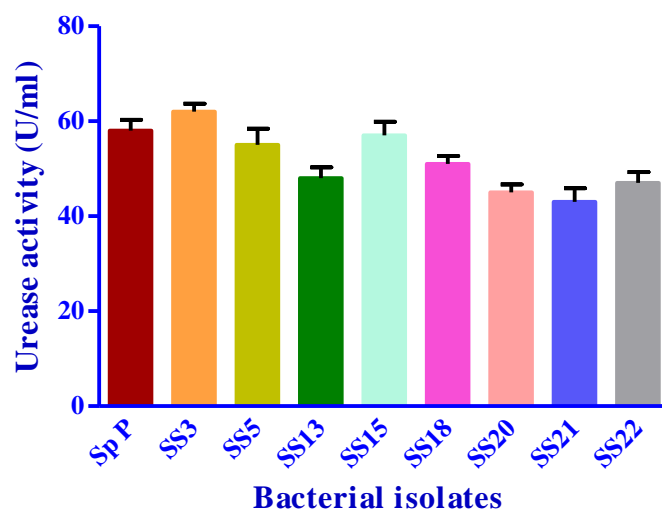


Fig. 4.1.2. Urease activity (U/ml) by bacterial isolates from different soil sites. Bars are mean \pm SD (n =3).

4.1.2. Calcium carbonate precipitating on agar plates

The ureolytic bacterial isolates selected above were further tested for their ability to induce crystallization on carbonate precipitation agar plates. The precipitation started in the centre of the bacterial colony and extended on sides with time (Fig. 4.1.3). The formation of carbonate crystals occurred in 24 to 48 hours in all the isolates. The morphological pattern of carbonate precipitation was found to be different in most of the isolates. In few cases, larger carbonate crystals were formed while in others, small, transparent, thick or amorphous aggregates were formed. After successful precipitation from all the isolated ureolytic bacterial isolates, all the bacterial isolates were subjected to their characterization. Hammes *et al.* (2003) also found variations in crystal precipitation patterns by various bacteria isolated from garden soil.

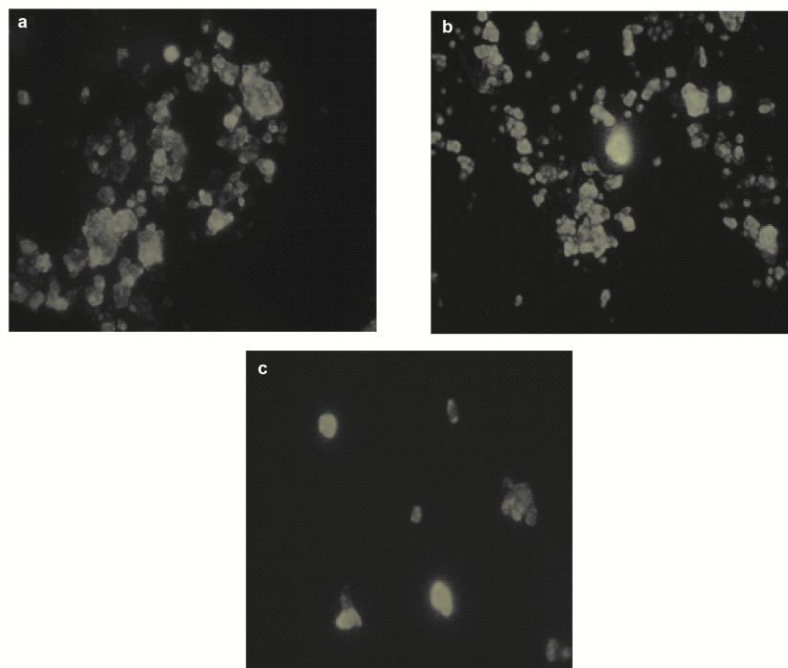


Fig. 4.1.3. Stereomicroscopic images of CaCO_3 precipitation on carbonate precipitating agar plates.

4.1.3. Morphological, biochemical and physiological characterization of bacteria

4.1.3.1. Morphological and biochemical characterization

The bacterial isolates showed diverse morphological and biochemical characteristics (Table 4.1.4). They differed in colony and cell morphology, growth pattern and biochemical tests. Seven of the bacterial isolates were Gram positive, rod shaped, catalase positive, oxidase positive and motile except SS15 which was non motile. SS20 was the only isolate that formed cocci, was oxidase negative and formed yellowish pigment. No pigment was formed in any other bacterial isolate. For capsule test, all the strains showed negative reaction. For DNase test, only SS20 and SS21 showed partial positive character while all other isolates were negative. Starch, casein and gelatin hydrolysis was noted with SS3, SS13 and SS15, whereas SS5, SS18, SS21 and SS22 hydrolyzed casein and esculin. SS20 hydrolyzed only starch. Nitrate reduction was noticed in SS3, SS5, SS18 and SS21.

Table 4.1.4. Biochemical characterization of calcifying bacterial isolates of the present study

Bacterial Isolates	Gram Staining	Capsule	Motility	Catalase	Oxidase	Dnase	Nitrate Reduction	Citrate Utilization	Malonate Utilization	Tyrosine degradation	Phenylalanine deamination	Hydrolysis of				
												Starch	Casein	Gelatin	Esculin	
SS3	+	-	+	+	+	-	+	+	+	-	+	+	+	+	+	
SS5	+	-	+	+	+	-	±	-	-	-	-	-	-	+	-	+
SS13	+	-	+	+	+	-	-	-	-	-	-	-	+	+	-	-
SS15	+	-	-	+	+	-	-	-	+	+	+	+	+	+	+	-
SS18	+	-	+	+	+	-	-	+	-	-	-	-	-	+	-	+
SS20	+	-	+	+	-	±	-	-	-	-	-	-	+	-	-	-
SS21	+	-	+	-	+	±	+	-	+	-	+	-	-	+	-	+
SS22	+	-	+	+	+	-	+	+	-	+	+	-	-	+	-	+

+ Positive; - negative and ± weak positive

4.1.3.2. Carbohydrate fermentation test

The ability to ferment different carbohydrates by these bacterial isolates was determined. Majority of the isolates were capable of fermenting different carbon substrates (Table 4.1.4). Acid production was observed with 6 carbon sources by SS3 and SS20 while SS5, SS13, SS15 and SS18 fermented only 4 carbon sources. SS21 and SS22 were able to ferment more than 7 carbon sources.

4.1.3.3. Antibiotic sensitivity test

Bacterial isolates were then tested for their sensitivity to different antibiotics (Table 4.1.5). Total of twenty different antibiotics were used. SS3 and SS5 were found to be most sensitive to many antibiotics, while all others were quite resistant. SS3 was sensitive to six, SS5 to five, SS13 and SS18 to four, SS15, SS20 and SS22 to three while SS21 was sensitive to only two antibiotics. There were noticeable variations in sensitivity patterns to antibiotics among all the bacterial isolates. There are few studies of the sensitivity of *Bacillus* species to antibiotics even though they relate to the genus taxonomy. Few *Bacillus* sp. have been reported to be resistant to penicillin G antibiotics, whereas few have been reported to show sensitivity to cephalosporin C, polymyxin B, ampicillin, bacitracin, rifampicin, tetracycline, kanamycin, streptomycin, chloramphenicol, and erythromycin (Claus and Berkeley, 1986). The antibiotic profile of all the isolates matched well with *Bacillus* species.

4.1.3.4. Salinity, alkalinity and temperature tolerance test

Upon subjecting all the bacterial isolates to salinity and temperature tests (Table 4.1.6), SS3, SS15 and SS21 were able to survive 0 – 7 % NaCl, SS5, SS18 and SS22 survived 0 – 8 % NaCl while SS13 survived 0 – 6 % and SS20 survived 0 - 9 % NaCl.

The bacterial isolates were investigated for growth in different pH buffered media. The growth was determined in liquid as well as solid media amended with different buffers. All the isolates were able to grow between pH 6.5 - 10 except SS20 which recorded to grow between pH 8-11 (Table 4.1.6). Two isolates SS3 and SS5 showed wide pH tolerance and

growth upto pH 11. When subjected to different temperatures (25, 30, 37, 45, 50 and 55°C), SS3, SS5 and SS22 were able to grow in range of 25 – 50 °C, SS13 in 28 – 45 °C, SS15 in 25 – 45 °C, SS18 in 25-55 °C, SS20 at 30 – 55 °C while SS21 in the range of 30 – 45 °C (Table 4.1.6).

Table 4.1.5. Fermentation of carbon substrates and antibiotic profiling of bacterial isolates of the present study

Bacterial isolate	Carbon substrate fermentation	Antibiotic sensitivity
SS 3	Sucrose, lactose, fructose, dextrose, raffinose, trehalose, ribose, sorbitol, ONPG, arabinose	Tetracycline, Cephalosporin C, Erythromycin, Cloxacillin, Chloramphenicol, Cefuroxime
SS 5	Sucrose, xylose, glycerol, sorbitol, glucosamine, mannitol	Amoxyclav, Cefaclor , Ceftazidime, Co-Trimoxazole, Ciprofloxacin
SS 13	Sucrose, lactose, fructose, raffinose, trehalose, ribose, sorbitol, ONPG	Clindamycin, Vancomycin, Chloramphenicol, Cephadroxil
SS 15	Sucrose, lactose, fructose, dextrose, sorbitol, ONPG	Gentamicin, Chloramphenicol, Ofloxacin
SS 18	Sucrose, lactose, fructose, dextrose, raffinose, glucosamine, ribose, sorbitol, ONPG, arabinose	Cefalexin, Vancomycin, Co-Trimoxazole, Ofloxacin
SS20	Sucrose, xylose, glycerol, sorbitol, ONPG	Ceftazidime, Tetracycline, Erythromycin
SS21	Sucrose, lactose, glycerol, trehalose, arabinose	Ofloxacin, Cephadroxil
SS22	Sucrose, lactose, fructose, trehalose, ribose, ONPG	Amoxyclav, Ceftazidime, Co-Trimoxazole

Total of 35-carbohydrate fermentation tests was performed with isolated bacterial species using HiCarbo Kit (Himedia Lab., Bombay, India).

* Total 20 antibiotics were used with isolated bacteria using ICOSA, Universal -1 Kit (Hi-Media Lab., Mumbai, India).

Table 4.1.6. Effect of sodium chloride concentration, temperature and pH on the growth of bacterial isolates

Bacterial isolate	NaCl (%)	Temp (°C)	Growth in buffered alkaline condition (pH)							
			6.5	8	9	10	10.5	11	12	
SS 3	0-7	25 – 50	++	+++	+++	+++	+++	+++	+++	-
SS 5	0-8	25 – 50	++	+++	+++	+++	+++	+++	+++	-
SS 13	0-6	28 – 45	+++	+++	+++	+++	++	++	++	-
SS 15	0-7	25 – 45	+++	+++	++	+++	++	-	-	-
SS 18	0-8	25 – 55	+++	+++	++	++	++	+	-	-
SS20	0-9	30-55	--	++	+++	+++	+++	++	-	-
SS21	0-7	30-45	++	++	+++	+++	++	+	-	-
SS22	0-8	25-50	+	+++	+++	+++	+++	++	-	-

-: no growth, +: poor growth, ++: good growth, +++: luxurious growth

Salt tolerance, growth temperature range as well as growth pH range are important taxonomic criteria which are used to differentiate species in the genus *Bacillus* (Claus and Berkeley, 1986). All the bacterial isolates of the present study thrived well in alkaline environments. Bacteria growing in alkaline environments are generally divided into two general classes: those with optimum growth ranges above pH 10, termed alkalophiles, and those with optimum growth ranges around neutral pH, but still capable of growth up to pH 9.5, termed alkaline tolerant (Sharp and Munster, 1986; Krulwich and Guffanti, 1989). So, the bacterial isolates of present study were alkalophilic in nature.

4.1.3.5. Extrapolymeric substances and Biofilm production

Both extrapolymeric substances (EPS) and biofilm have been reported to play important role in the microbial CaCO₃ precipitation (Ercole *et al.*, 2012). In the present study, all the bacterial isolates produced significant amount of EPS and biofilm. Noticeable differences were observed in the production of EPS and biofilm by different bacterial isolates. SS3, SS5, SS13, SS15, SS18, SS20, SS21 and SS22 produced 289, 360, 194, 218, 295, 255, 312, 241

and 276 mg/100 ml EPS while OD₅₉₀ for biofilm production was observed to be 0.58, 0.52, 0.35, 0.47, 0.40, 0.62, 0.51 and 0.44 respectively in case of SS3, SS5, SS13, SS15, SS18, SS20, SS21 and SS22 after 3 days (Table 4.1.7; Fig 4.1.4). Formation of monoxenic biofilms was also determined on the surface of glass plates and it was found that biofilms of SS3, SS5 and SS20 effectively covered the surface as compared to other isolates and proved the formation of mature sessile biofilms.

The isolated EPS from all the bacterial isolates was also characterized for proteins and carbohydrates (table 4.1.8; Fig. 4.1.5). The total protein content in the EPS was found to be higher than carbohydrate content in all the isolates. The hydrophobic interactions and polyvalent cation bridging promoted by proteins enhances the stability of biopolymer network (Jorand *et al.*, 1998). EPS proteins may specifically bind calcium ions and promote carbonate precipitation allowing right environmental conditions, such as alkaline pH and/ specific ion co-ordination, being a nucleation site (Ercole *et al.*, 2012). Hammes *et al.* (2003) suggested that specific proteins present in biological extracellular polymeric materials cause the formation of different polymorphs of CaCO₃.

Table 4.1.7. Comparison of EPS and biofilm productions by the bacterial isolates

Isolates	EPS Production (mg/100 ml)	Biofilm Production (OD)
SS3	360 ± 12.5a	0.58 ± 0.02a
SS5	194 ± 7.8f	0.53 ± 0.04b
SS13	218 ± 8.3e	0.36 ± 0.01e
SS15	291 ± 8.6c	0.48 ± 0.03c
SS18	255 ± 6.2	0.44 ± 0.04d
SS20	295 ± 6.7c	0.54 ± 0.06b
SS21	262 ± 3.5d	0.46 ± 0.03d
SS22	321 ± 5.6b	0.49 ± 0.05c

Values bearing different letters in the same column differ significantly (P<0.05). All values are mean ± SD (n = 3).

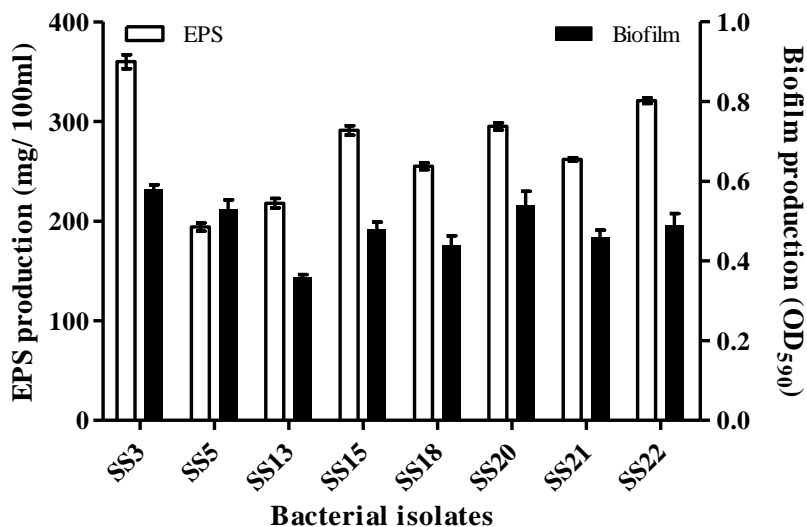


Fig. 4.1.4 EPS and biofilm production by different bacterial isolates. Bars represent mean \pm SD (n = 3).

Both extracellular polymeric secretions and biofilms have been reported to influence the calcium carbonate precipitation in a positive way (Kawaguchi and Decho, 2002). EPS has been reported to play an important role in the coverage of the surface by biofilms, cell adhesion and precipitation, either through trapping and concentration or through the action of specific proteins that influence precipitation in the natural environments (Tsuneda *et al.*, 2003; Rodriguez – Navarro *et al.*, 2012). A number of studies have cited that mutants unable to synthesize EPS are unable to form biofilms (Sutherland, 2001; Ercole *et al.*, 2012), although bacteria may still attach to the surface and form microcolonies to a limited extent. The importance of biofilm is in colonizing stone surface and reacting as nucleation site for extracellular calcium carbonate precipitation (Dick *et al.*, 2006). The structure of biofilms is largely influenced by a number of biological factors such as twitching motility, growth rate, cell signalling, and EPS production (Stoodley *et al.*, 2002). The biofilm structure appears to be largely determined by the production of slime-like matrix of EPS, which provides the structural support for the biofilm. Recently Ercole *et al.* (2012) showed that EPS associated with bacterial biofilms affect the process of CaCO₃ precipitation in *Bacillus firmus* and

Nocardia calcareae. The production of EPS and biofilms was also reported to increase in the presence of calcium ions by the same group.

Table 4.1.8. Protein and carbohydrate content of EPS isolated from different bacterial isolates

Isolates	Protein content (mg/100 ml)	Carbohydrate content (mg/100ml)
SS3	28.4 ± 1.5a	16.9 ± 1.8a
SS5	18.2 ± 0.75d	14.6 ± 1.7b
SS13	19.9 ± 1.6d	9.8 ± 0.88de
SS15	24.2 ± 2.2b	14.3 ± 1.2b
SS18	21.7 ± 1.8c	12.7 ± 0.92c
SS20	26.3 ± 2.3b	13.9 ± 0.82c
SS21	25.1 ± 1.6b	15.8 ± 1.7ab
SS22	19.2 ± 1.5d	16.8 ± 1.2a

Values bearing different letters in the same column differ significantly ($P < 0.05$). All values are mean ± SD (n = 3).

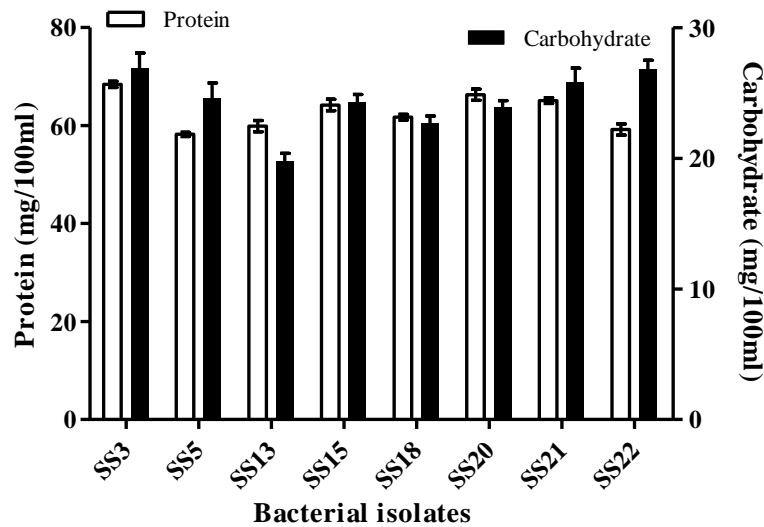


Fig. 4.1.5. Protein and carbohydrate content of EPS of different bacterial isolates. Bars are mean ± SD (n =3).

Both EPS and biofilms are correlated in bacterial carbonate precipitation. Huge amounts of EPS deposit when microorganisms form biofilms. These biopolymers serve as “glue” between the cells. Attempts have been made to use bacterial biofilms as clogging agent to decrease hydraulic conductivity *in situ* beneath and within dams and levees, to reduce infiltration from ponds, to reduce leakage at landfills and to make subsurface barriers to impacted groundwater migration (Lambert *et al.*, 2010).

4.1.4 Molecular characterization of bacterial isolates

4.1.4.1. BOX PCR, REP PCR and ARDRA based fingerprinting

After the biochemical characterization of bacterial isolates, genetic diversity of these calcifying bacteria was studied by PCR based molecular typing (BOX-PCR and REP-PCR). Amplification of the regions between highly conserved repetitive DNA sequences of the BOXA subunit of the BOX element (BOX-PCR) of isolate-specific DNA fingerprints as well as amplification of the regions between adjacent repetitive extragenic elements (REP-PCR) of isolate-specific DNA fingerprints was generated. These are dispersed throughout the prokaryote kingdom (Languerre *et al.*, 1996). BOX-PCR for all isolates yielded a genomic fingerprint consisting of 200 bp to >1kb amplicons of varying intensity while Rep-PCR for most of the bacterial isolates yielded genomic fingerprints consisting of ~10 Kbp to 100 bp amplicons of varying intensity (Fig 4.1.6a). Maximum number of amplicons was generated by SS13 in REP-PCR. Visual observation of the DNA fingerprints clearly showed that most of the isolates are genetically distinct. These results showed high degree of inter or intra specific genetic unrelatedness among the isolates (Fig 4.1.6 b).

As the sequence of 16S rRNA gene is widely used as phylogenetic marker now a days because extent of divergence in the sequence of this gene provides reliable estimate of phylogenetic distance between different species (Wakabayashi *et al.*, 1999), all the bacterial isolates were subjected to 16S rDNA amplification using universal primers, and about 1.5 Kb amplicon was observed in all isolates (Fig. 4.1.7).

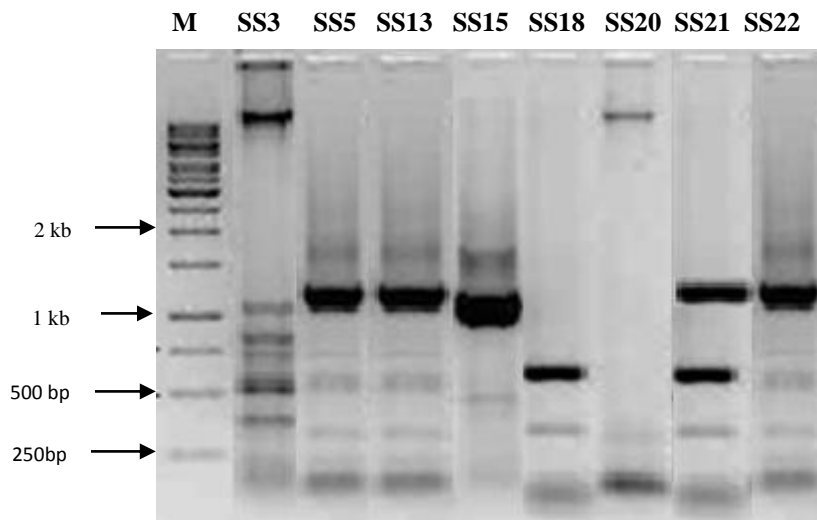
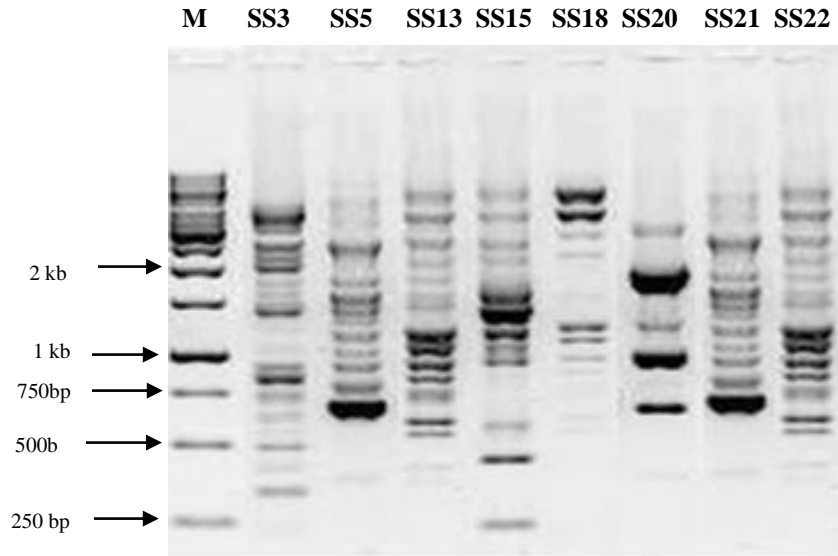


Fig. 4.1.6. Comparison of purified genomic DNA based fingerprints generated by a) BOX-PCR and b) REP PCR for different bacterial isolates. Lane M: 1 Kb marker (Fermentas, USA).

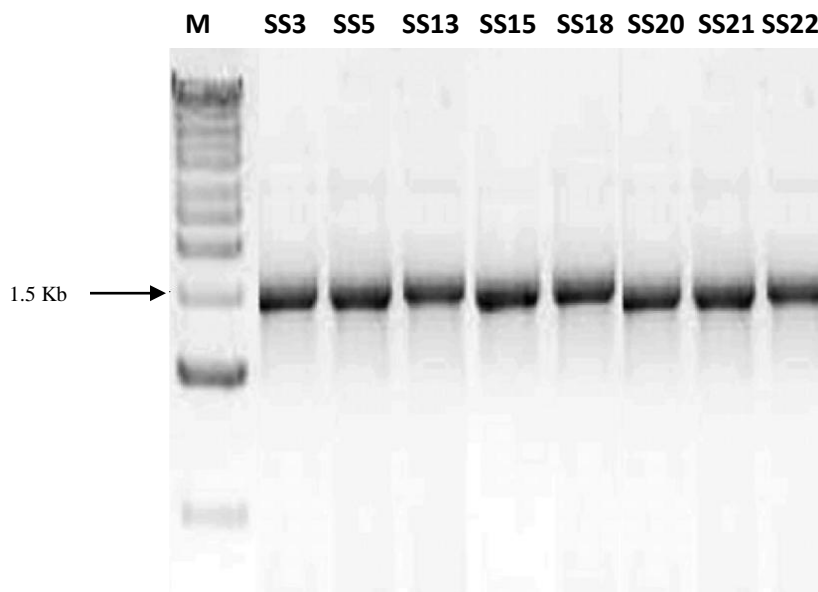


Fig. 4.1.7. 16S rDNA amplification of bacterial isolates. Lane M: 1 Kb marker (Fermentas)

The PCR products were then digested with different restriction enzymes: *Eco RI*, *Alu I* and *Taq I* (Fig. 4.1.8). Banding pattern of the amplified ribosomal DNA restriction analysis (ARDRA) also showed different banding pattern among most of the isolates.

Visual observation of the DNA fingerprints clearly differentiated similarity and dissimilarity among bacterial strains. These results showed complex banding patterns, which reflected a high degree of inter or intra specific genetic unrelatedness among isolates. In certain isolates, profiles showed >80% similarity indicating that these strains must be identical.

4.1.4.2. Identification of the bacterial isolates

16S rDNA PCR products were cloned into pTZ57R/T Vector (Fermentas, USA). The plasmid DNA was extracted from different clones and amplified with M13-F and M13-R primers. The 16S rDNA products from selected clones were then sequenced using Applied Biosystems automatic DNA sequencer (DNA sequencing facility, University of Delhi, South Campus, New Delhi). Sequencing reactions were performed with the primers M13-F and M13-R.

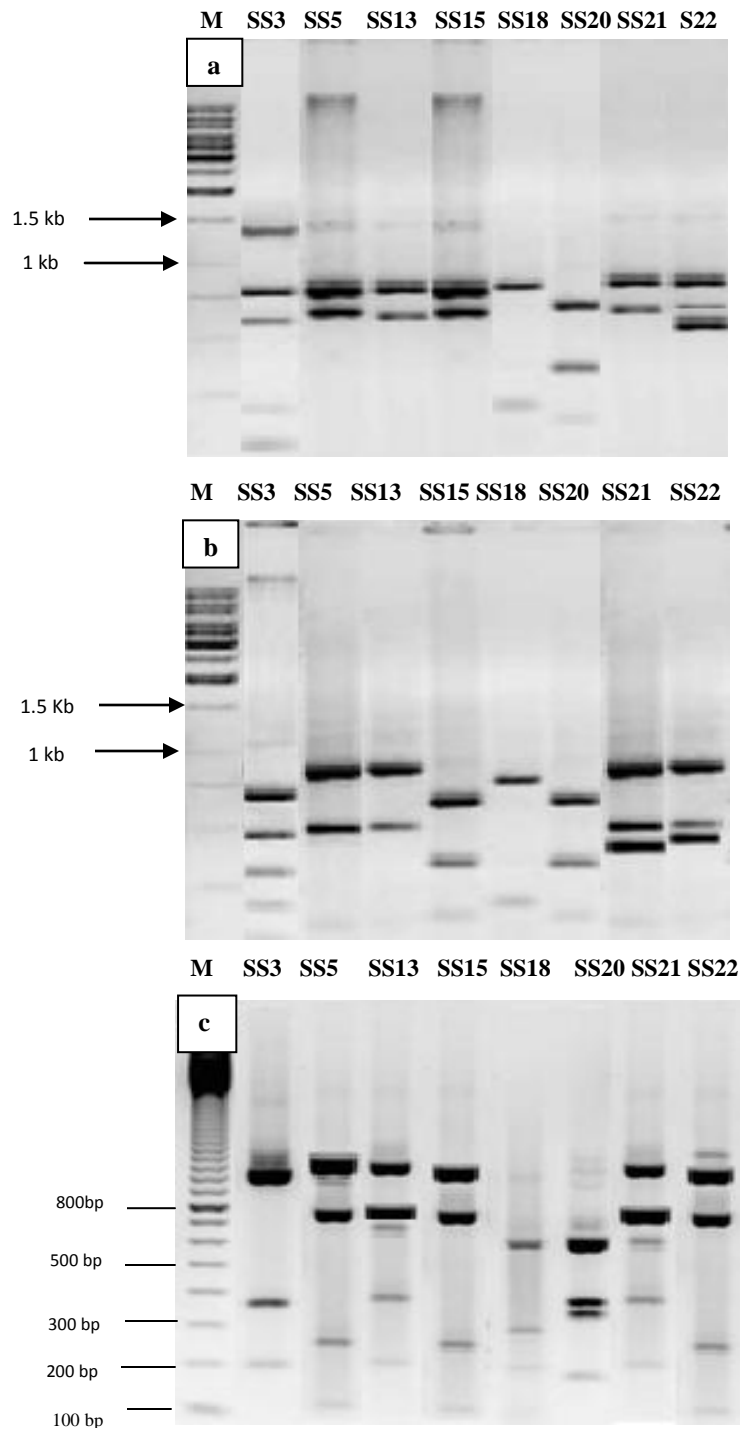


Fig. 4.8. Agarose gel electrophoresis of amplified 16S rDNA digested with restriction endonuclease a) *EcoRI* b) *AluI* and c) *TaqI* of different bacterial strains.

The sequences were analyzed by multiple sequence alignment to check the similarities among the isolates. The homologies among the sequences varied from 88 to 99% between isolates. Minimum of 88% similarity was found in SS13 with SS18 and maximum 99% similarity was found between SS5 and SS21 and SS5 and SS15 (Table 4.1.9). The sequences were further compared for the similarity in the GenBank DNA database using BlastN (NCBI) (Altschul *et al.*, 1997) (Table 4.1.10). The related sequences showing similarity in BLAST were retrieved from GenBank and RDPII and aligned using Clustal W (Thompson *et al.*, 1994). The resulting multiple alignments were optimized visually and evolutionary distances were calculated using Kimura 2 parameter. Phylogenetic tree was constructed using neighbour joining method of MEGA 5 package (Timura *et al.*, 2007). Gaps were treated as missing data. It has been reported that sequence identities of over 98% represent same species while the sequences that share an identity below 98% are usually considered to be part of the same genus (Sadowsky *et al.*, 1996). Blast results revealed that 16S rDNA of the bacterial isolates in present study had high similarity with the sequences of NCBI database (Fig. 4.1.9). SS3 had shown 99% similarity with *Bacillus megaterium* which is a known urease producing bacterium. SS5 had shown maximum similarity with *Bacillus cereus* (99%). SS13 showed 96% identity with *Bacillus subtilis* and *Bacillus amyloliquefaciens*. SS15 was 99% identical with *B. thuringiensis* while SS18 was 99% similar to *Lysinibacillus fusiformis*. SS20 has 99% similarity with 96% coverage to *Staphylococcus* sp. (new species) whereas SS21 showed 99% similarity with *Bacillus anthracis* along with SS22 which was 99% homologous with *Bacillus cereus* at 95% coverage (new species).

Table 4.1.9. Percentage similarity of 16S rDNA sequences of bacterial isolates using multiple sequence alignment (ClustalW)

Seq A	Name	Length	Seq B	Name	Length	Score
1	SS3	1456	2	SS5	1456	94
1	SS3	1456	3	SS13	1454	90
1	SS3	1456	4	SS15	1451	93
1	SS3	1456	5	SS18	1445	92
1	SS3	1456	6	SS20	1533	90
1	SS3	1456	7	SS21	1406	94
1	SS3	1456	8	SS22	1273	92
2	SS5	1456	3	SS13	1454	91
2	SS5	1456	4	SS15	1451	99
2	SS5	1456	5	SS18	1445	91
2	SS5	1456	6	SS20	1533	90
2	SS5	1456	7	SS21	1406	99
2	SS5	1456	8	SS22	1273	96
3	SS13	1454	4	SS15	1451	90
3	SS13	1454	5	SS18	1445	88
3	SS13	1454	6	SS20	1533	87
3	SS13	1454	7	SS21	1406	91
3	SS13	1454	8	SS22	1273	88
4	SS15	1451	5	SS18	1445	91
4	SS15	1451	6	SS20	1533	90
4	SS15	1451	7	SS21	1406	98
4	SS15	1451	8	SS22	1273	96
5	SS18	1445	6	SS20	1533	91
5	SS18	1445	7	SS21	1406	93
5	SS18	1445	8	SS22	1273	91
6	SS20	1533	7	SS21	1406	92
6	SS20	1533	8	SS22	1273	92
7	SS21	1406	8	SS22	1273	95

Table 4.1.10. Bacterial isolates and their closest relative species inferred from 16S rRNA gene sequences of NCBI database

Bacterial isolate	Nearest match	Phylum	Query coverage (%)	E value	% identity to closest related bacterial sp.
SS3	<i>Bacillus megaterium</i> (HM104232)	Firmicutes	100	0.0	99
SS5	<i>Bacillus cereus</i> (HM345997)	Firmicutes	100	0.0	99
SS13	<i>Bacillus subtilis</i> (EF 1544188) <i>Bacillus amyloliquefacians</i> (JX501686)	Firmicutes	100	0.0	96
SS15	<i>Bacillus thuringiensis</i> (GU120652)	Firmicutes	99	0.0	99
SS18	<i>Lysinibacillus fusiformis</i> (GQ245969)	Firmicutes	100	0.0	99
SS20	<i>Staphylococcus sp.</i> (EU373372)	Firmicutes	96	0.0	99
SS21	<i>Bacillus anthracis</i> (KF150341)	Firmicutes	99	0.0	99
SS22	<i>Bacillus cereus</i> (AB809566)	Firmicutes	95	0.0	99

Phylogenetic analysis revealed all the eight bacterial isolates were related to Phylum Firmicutes. Seven isolates were associated with the genera *Bacillus* while one was associated with *Staphylococcus* sp. (Fig. 4.1.9). The majority of bacterial isolates of the present study were found to be *Bacillus* genera. Numerous reports are already available that cite high amounts of urease production by soil *Bacillus* species (Mobley *et al.*, 1995; Ciurli *et al.*, 1996; Benini *et al.*, 1999; Bachmeier *et al.*, 2002). Rivadeneyra *et al.* (1993) also reported that most of the *Bacillus* spp. play major role in carbonate depositions in the natural habitats. As both SS5 and SS22 belonged to *Bacillus cereus*, SS5 was selected for further studies due to its higher urease activity. SS20 and SS21 are both known to be opportunistic

human pathogens, so they were also not taken for further studies (Spencer, 2003; Archer, 1998). The 16S rDNA gene sequences of the five selected calcifying bacterial isolates determined in this study were deposited in the GenBank of NCBI data library under the accession numbers KC121060, KC121061, KC121062, KC121063 and KC121064 for SS3, SS5, SS13, SS15 and SS18 respectively (Appendix II).

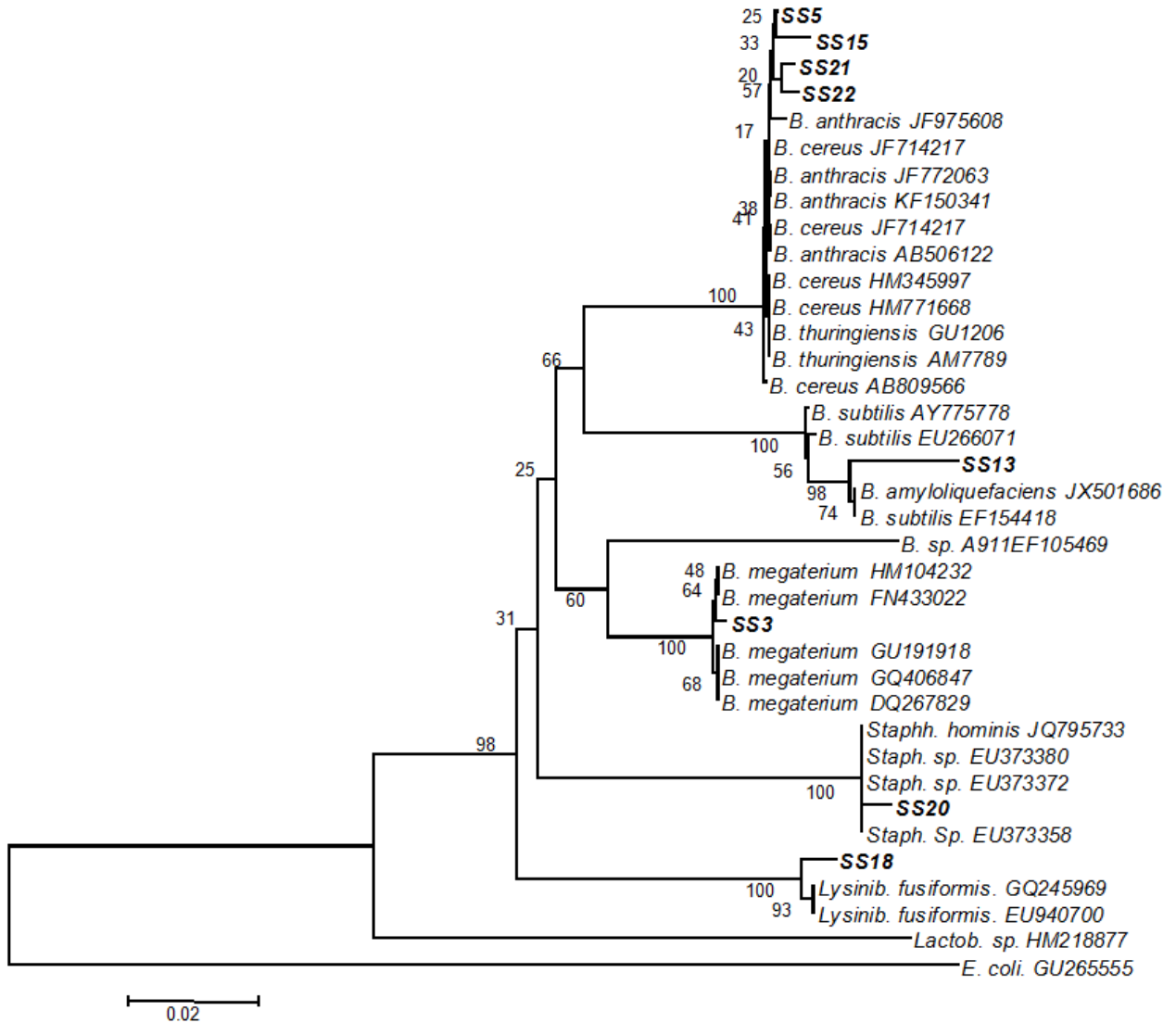


Fig. 4.1.9. Neighbor-joining tree based on bacterial 16S rRNA sequence data from different bacterial isolates of current study along with sequences available in GenBank database. Numerical values indicate bootstrap percentile from 1000 replicates. *Escherichia coli* was used outgroup taxa.

Conclusion and salient features

The aim of the present work was to explore various alkaline soils for indigenous ureolytic and calcifying bacterial isolates. The bacterial load of all alkaline soils varied from 0.003×10^3 to 3.6×10^3 per gm of soil. Though the presence of bacterial diversity in alkaline soils is not surprising, but their high number proved their adaption to any extreme environment. Though many neutrophilic bacterial isolates also harbour the enzyme urease but as most of the building materials including cement have high pH, the emphasis this time was to isolate the bacterial communities which are capable of growing and reproducing in alkalophilic soils. Urease producing bacteria were successfully isolated from alkaline soils of different regions. This could be due to sufficient nutrients in the soils which promote the growth of bacterial cells. The bacterial isolates which were capable of growing in presence of urea were screened for presence of urease qualitatively on urea agar media which contains phenol red indicator. These isolates were also tested for the precipitation of crystals on calcium carbonate precipitating agar plates. These carbonate crystals might be potential tools to act as binders in pores of building materials. Based on this, eight efficient ureolytic bacterial isolates were selected and characterized biochemically as well as on the basis of 16S rDNA sequence analysis. Eight highly efficient ureolytic and carbonate precipitating bacterial isolates belonging to phylum Firmicutes have been isolated. Out of eight, seven isolates were closely related to *Bacillus* species and one belonged to *Staphylococcus* sp. Sequence alignment of closely related ureolytic bacterial isolates showed that similarity varied from 96% to 99%, but none of the isolates had shown 100% sequence similarity with the bacteria of the existing database. Two new strains were successfully isolated for production of bacterial calcite (SS20, SS22).

4.2 Optimum conditions and role of enzymes in biomineralization of calcium carbonates

Before looking for biotechnological applications of microorganisms, it is prerequisite to look for parameters for maximal production of the specific microbial product. In the present work, it is therefore necessary to have knowledge of the effect of various parameters which contribute to successful production of the bacterial carbonates. In case of ureolytic calcium carbonate precipitation, the efficiency of the process is dependent fundamentally upon the optimal production of urease enzyme. Further, the basic parameters which affect the bacterial urease activity include media, substrate concentration, calcium source and concentration, addition of cofactors, pH and temperature. The concentration of substrate, pH and temperature are the prime factors upon which activity of every enzyme depends (Haltrich *et al.*, 1993). Recently growth media has also been found to have effect on bacterial enzyme activity. So, for optimizing the parameters for maximum production of urease, all the bacterial isolates (*B. megaterium* SS3, *B. cereus* SS5, *B. subtilis* SS13, *B. thuringiensis* SS15, *L. fusiformis* SS18 along with *Sporosarcina pasteurii* Sp P) were subjected to varying growth media, substrate concentration, calcium sources and concentrations, NiCl₂, pH and temperature.

4.2.1. Optimum conditions for Urease activity

4.2.1.1. Effect of different media

Culture medium plays an important role in supporting the growth and enzyme activity of bacterial isolates. Culture medium comprises of variety of nutrients as energy sources for bacterial cells and hence it is critical to provide proper and sufficient nutrients for growth and survival of ureolytic bacterial isolates. In the present study, all the bacterial isolates were grown in different nutritional media as Nutrient broth, Yeast extract, B4, Tryptic soy medium supplemented with 1 % urea labelled as NB-U, YE-U, B4-U, TS-U. It was recorded that maximum urease production occurred in NB – U medium followed by B4-U medium, TS-U medium and YE-U medium in all the isolates except SS13 which showed

marginally better production in B4-U medium (Table 4.2.1; Fig. 4.2.1). Nutrient broth proved to be better medium for all ureolytic *Bacillus* species. As the production of any enzyme is related to its biomass, which is under conditions of favorable growth, enzyme production is also favored during initial times. The amount of enzyme expressed by a specific microorganism is directly dependent on the nutrients available in the culture media. Though different research groups have used variety of media but 3g/L nutrient broth with minor variations and supplements has been found to be widely accepted for most of the ureolytic *Bacillus* species (Stocks - Fischer *et al.*, 1999). Wolfram *et al.* (2009) observed different urease activities in different culture media and reported that different culture conditions lead to varying results. Shirakawa *et al.* (2011) utilized two culture media for estimating their effect on carbonate deposition and found B4 medium to be better than 295 medium. Several researchers have utilized variety of different media for growth of bacterial isolates for carbonate precipitation studies as Growth medium, Nutrical, B4, M-3, M-3P, CC, SF, Growth medium DB and Biodeposition medium DB (De Muynck *et al.*, 2010 and references therein).

Table 4.2.1. Optimization of growth media for maximum urease (U/ml) production by different bacterial isolates.

Media	Sp P	SS3	SS5	SS13	SS15	SS18
NB-U	59.0 ± 1.5a	62.5 ± 1.9a	52.0 ± 1.1a	40.2 ± 1.9a	55.0 ± 1.2a	48.0 ± 2.1a
TS-U	48.5 ± 0.9c	51.5 ± 2.5c	43.5 ± 1.2c	30.5 ± 1.5c	47.0 ± 1.7c	41.0 ± 1.8c
YE-U	43.5 ± 2.1d	45.0 ± 2.2d	41.0 ± 1.8d	34.5 ± 2.0d	42.5 ± 2.3d	37.5 ± 2.4d
B4-U	52.1 ± 1.8b	57.6 ± 1.7b	48.1 ± 2.1b	43.5 ± 2.3a	51.1 ± 1.9b	42.1 ± 1.9b

Values bearing different letters in the same column are significant at $P < 0.05$. Values are mean ± SD (n = 3).

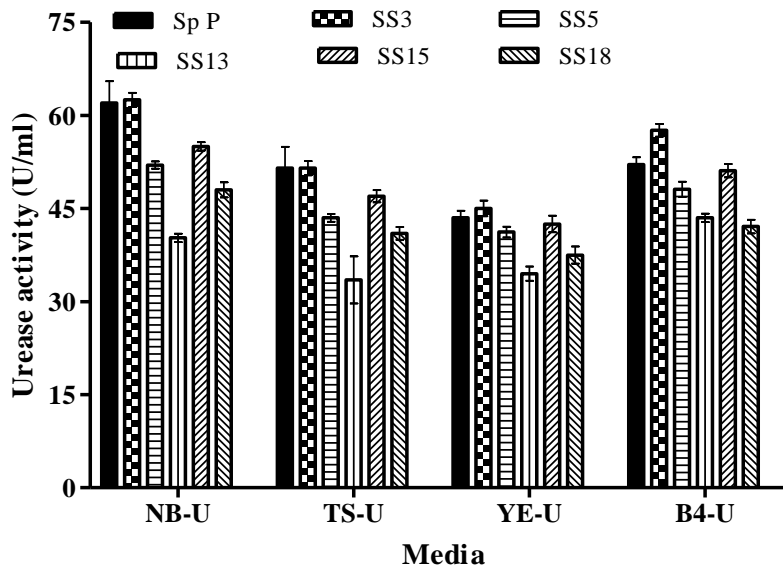


Fig. 4.2.1. Effect of different media on urease activity (U/ml) by bacterial isolates. Bars represent mean \pm SD (n =3)

4.2.1.2. Effect of varying concentrations of urea

Whiffin *et al.* (2004) reported that presence of substrate urea is pre - requisite and necessary for producing high levels of urease activity. In order to investigate this, all the bacterial isolates along with *S. pasteurii* were grown in Nutrient broth media with varying concentrations of urea. To envisage the effect of addition of urea to the bacterial culture medium, the concentrations of urea selected were in the range of 1 – 5%. The control medium was prepared without urea. It was found that urease activity as well as biomass increased significantly with the addition of urea in all the isolates (Table 4.2.2; Fig. 4.2.2). This might be due to coupling of urea hydrolysis and ATP generation as reported previously (Whiffin *et al.*, 2004). Very low amount of urease activity was observed in case of control. This further supplemented the previous studies that presence of urea/ ammonium is essential for high urease activity (Achal *et al.*, 2009; Stocks - Fischer *et al.*, 1999). It was observed that maximum urease activity occurred in presence of 2% urea whereas at concentrations higher than this, it declined. The urease activity increased more than two fold in the presence of 2% urea, compared to the lowest concentration of urea used (Table 4.4.2; Fig. 4.2.2).

Whiffin *et al.* (2004) reported significant increase in the specific activity of urease in presence of urea/ ammonium in case of *S. pasteurii*. The same group found that urease activity in *S. pasteurii* is not constitutive rather regulated. The activation of urease in the presence of urea might be attributed to higher diffusivity of urea into the cell, due to increased concentration gradient across cell membrane. So, if the concentration gradient is increased, and the enzyme is not saturated, urease activity will increase with increase in urea concentration (Whiffin *et al.*, 2004). It was also noticed in the present study that beyond a particular limit, the addition of high amounts of urea produces negative effects on the production of urease which could be due to accumulation of by products that either repress the bacterial growth or enzyme activity or both.

Table 4.2.2 Optimization of urea concentration for maximum urease (U/ml) production by different bacterial isolates.

Urea conc. (%)	Sp P	SS3	SS5	SS13	SS15	SS18
0	58.0 ± 2.5e	65.5 ± 7.9e	52.0 ± 3.1e	47.5 ± 4.3e	56.0 ± 3.8e	46.0 ± 3.1e
1	123.5 ± 5.9d	155.5 ± 9.5d	126.5 ± 9.2d	110.5 ± 9.2d	133.0 ± 5.5d	116.0 ± 6.0d
2	242.5 ± 7.2a	265.0 ± 15a	223.0 ± 13a	204.5 ± 12a	238.5 ± 10a	212.5 ± 13a
4	211.1 ± 6.3b	224.6 ± 10b	198.1 ± 11b	178.6 ± 14b	201.1 ± 11b	185.1 ± 12b
5	193 ± 7.8c	209 ± 11c	183.5 ± 9.5c	166 ± 11c	191 ± 12c	162.4 ± 7.5c

Values bearing different letters in the same column are significant at $P < 0.05$. Values are mean ± SD (n = 3).

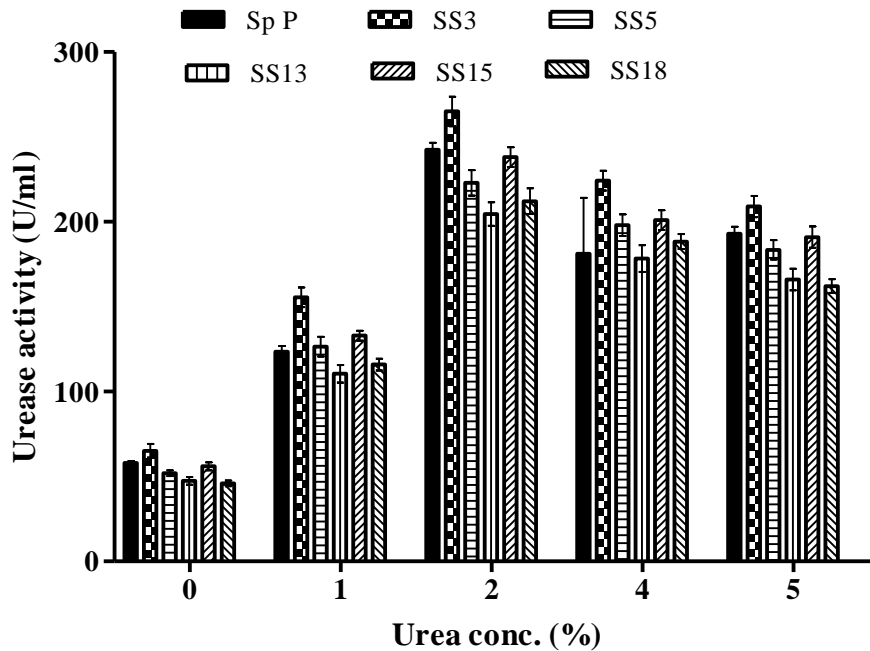


Fig. 4.2.2 Effect of different concentrations of urea on urease activity (U/ml) by bacterial isolates. Bars are mean \pm SD (n =3).

4.2.1.3. Effect of calcium sources and concentration on urease activity

Compared to urease, the role of calcium interaction and regulation in precipitation of carbonates received little attention and remained much of a black box till recent times. Calcium is not likely utilized by bacteria rather it is tightly regulated. Typical carbonate precipitation environment comprises high extracellular Ca^{2+} concentrations and low extracellular proton concentrations (Anderson *et al.*, 1992).

For production of calcium carbonate biocement, there is need to find the optimum source and concentration of calcium leading to maximum carbonate precipitation. In the present study, a range of calcium sources were investigated in order to determine their effect on production of urease activity. Different calcium sources tested were calcium chloride, calcium acetate, calcium sulphate, calcium nitrate and calcium lactate. All the calcium sources were added after filter sterilization only as they decompose after autoclaving.

It was observed that out of all the sources, calcium chloride was found to be the preferred source by all bacterial isolates except SS15 which showed better preference to calcium acetate (Fig. 4.2.3; Table 4.2.3). The variations in urease activity by varying calcium sources might be based on the availability of free calcium ions and also on the preference of calcium sources by bacteria. Previous studies have also reported that nitrate has an inhibitory effect on urease activity and inhibitory effect of these nitrate ions remains constant throughout the course of biocementation (Whiffin *et al.*, 2004). It was also noticed that presence of calcium along with urea further modulates the urease activity in almost all bacterial isolates. Hammes *et al.* (2003) reported 5-10 fold increase in the urease activity of few calcifying bacterial isolates upon addition of calcium source but in the present study, though there was enhanced urease upon addition of calcium source but it was not very high. Ca^{2+} ions in this case could be facilitating better transmembrane transport, or improving intracellular signalling process leading to higher urease production (Hammes *et al.*, 2003). Though previous reports have also established toxic effects of calcium on survival of bacteria but in the present study there was no such effect noticed as presence of all types of calcium sources positively affected the urease activity and had no deleterious effects on the growth of bacterial isolates. Alternative explanation for improved urease activity in presence of calcium might be a detoxification response of bacteria to calcium (McConnaughey and Whelan, 1997; Anderson *et al.*, 1992). Active calcium metabolism requires energy (ATP) and various microbes have been reported to produce ATP via urea hydrolysis (Burne and Chen, 2000; Mobley and Hausinger, 1989). So in the present bacterial isolates, urease might be utilised as a source of ATP.

After determining the suitable source of calcium as calcium chloride, the effect of varying concentrations of calcium on the urease activity of different bacterial isolates was also determined (10 - 100 mM). It was noticed that at initial stages, increase in Calcium concentration lead to increase in urease activity but at higher range, calcium ions had detrimental effect on urease production. The highest activity of urease was recorded at 25 mM concentration along with 2 % urea. So, 25 mM CaCl_2 was found to be suitable for significant urease activity (Fig. 4.2.4; Table 4.2.4).

Table 4.2.3 Optimization of calcium source for maximum urease (U/ml) production by different bacterial isolates

Calcium sources	Sp P	SS3	SS5	SS13	SS15	SS18
Calcium chloride	254 ± 8.4a	276 ± 6.2a	238 ± 7.2a	225 ± 4.7a	207 ± 4.8c	229 ± 6.9a
Calcium acetate	224 ± 7.2d	213 ± 5.4d	187 ± 3.8d	172 ± 5.8d	252 ± 6.3a	188 ± 7.4e
Calcium sulphate	210 ± 6.8e	193 ± 4.7e	171 ± 6.2e	163 ± 4.1e	217 ± 8.3c	211 ± 5.7c
Calcium nitrate	188 ± 10.0c	243 ± 8.3c	203 ± 4.8c	184 ± 5.9c	224 ± 7.2b	206 ± 7.3d
Calcium lactate	242 ± 7.9b	261 ± 3.6b	221 ± 5.1b	205 ± 9.2b	236 ± 8.9b	217 ± 4.1b

Values bearing different letters in the same column are significant at $P < 0.05$. Values are mean ± SD (n = 3).

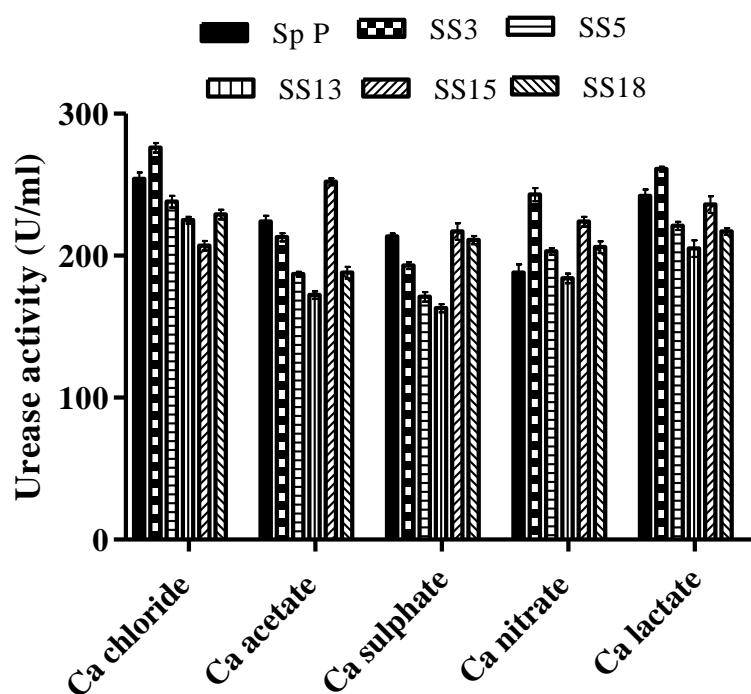


Fig. 4.2.3 Effect of different calcium sources on urease activity (U/ml) by bacterial isolates. Bars are mean ± SD (n = 3)

Table 4.2.4 Optimization of calcium concentration for maximum urease (U/ml) production by different bacterial isolates

CaCl ₂ conc. (mM)	Sp P	SS3	SS5	SS13	SS15	SS18
10	242 ± 7.2d	265 ± 15.0d	223 ± 13.0d	204.5 ± 12.0c	238 ± 10.0c	212 ± 13.0d
25	284 ± 7.2a	295 ± 5.4a	256 ± 3.8a	238 ± 5.8a	271 ± 6.3a	227 ± 7.4a
50	252 ± 6.8b	278 ± 4.7b	239 ± 6.2b	221 ± 4.1b	255 ± 8.3b	219 ± 5.7b
100	244 ± 10.0c	268 ± 8.3c	227 ± 4.8c	209 ± 5.9d	248 ± 7.2d	215 ± 7.3c

Values bearing different letters in the same column are significant at P<0.05. Values are mean ± SD (n =3).

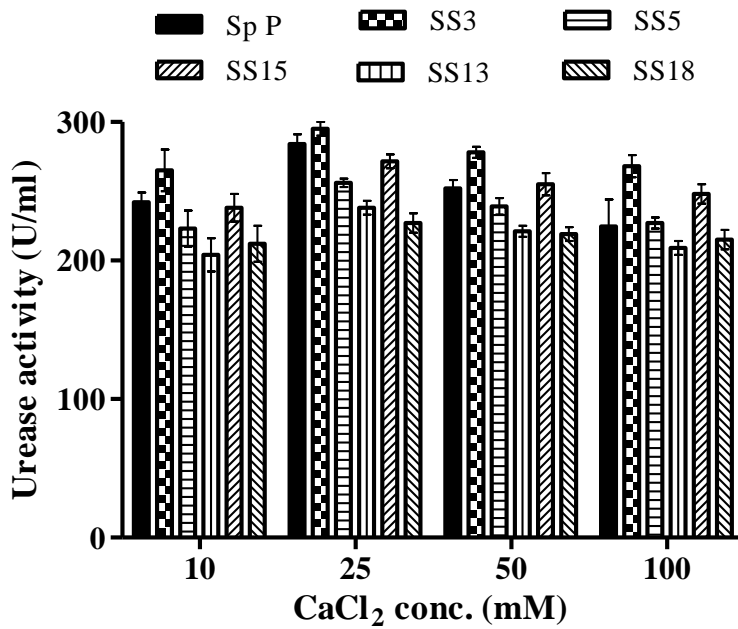


Fig. 4.2.4 Effect of different calcium sources on urease activity (U/ml) by bacterial isolates. Bars represent mean ± SD (n =3)

The decrease in urease activity at higher concentrations of calcium might be due to detrimental effect of biomineralization. Southman (2000) suggested that surface associated mineralization results in limitation of nutrient transport and eventual disruption of proton motive force, which leads to lowering of urease activity. Nemati and Voordouw (2003) also established that increasing urea and Ca^{2+} concentrations beyond 36 gL^{-1} and 90 gL^{-1} do not increase the amount of CaCO_3 precipitates. Recently, Okwadha and Li (2010) established 250 mM Ca^{2+} along with 666 mM urea as optimal concentration for carbonate precipitation. *Bacillus* cells utilize urea as energy source and produce ammonia along with carbonates and in the presence of Ca^{2+} ions under these alkaline conditions, CaCO_3 precipitates. Concentration of urea as well as calcium changes substantially during the process as concentrations of ions involved changes. The rate of reaction, shape and size of CaCO_3 precipitates do change over the course of time leading to desirable or non desirable precipitates. Varying the concentration of these two factors produces significant effect on urease activity and hence precipitation of carbonates. In order to achieve significant precipitation, the concentrations of urea and calcium must be proportionate otherwise it will only lower the enzyme activity as well as carbonate content. The concentration of both urea and calcium must be optimal for maintaining suitable urea hydrolysis rate. Disproportionate amounts of both these may lead to production of weak and very small sized crystals. It has also been reported that although ureolytic precipitation of carbonates in presence of urea and calcium lead to physical capturing of bacterial cells but this encrustation effect does not encompass the entire bacterial colony (Hammes, 2003). Younger cells continue to proliferate to ascertain the survival of these bacterial isolates.

4.2.1.4. Effect of Nickel on urease activity

Ureases are nickel containing metalloenzymes and presence of nickel in the active site of urease is essential for functional activity as well as integrity of the enzyme. In this study, varying concentrations of Nickel chloride ($0 - 100 \text{ }\mu\text{M}$) were added to Nutreint broth supplemented with urea and tested for their effect on urease activity in the ureolytic bacterial isolates (Fig. 4.2.5; Table 4.2.5). It was observed that there was minor increase in the urease production upon supplementation of $5 \text{ }\mu\text{M NiCl}_2$ in all bacterial isolates while increasing the

concentration of nickel beyond that led to inhibition of bacterial urease activity. It was also observed that beyond a concentration of 50 μM , there was noticeable decrease in the bacterial biomass. Higher concentrations of nickel ions might be repressible for growth of bacterial isolates leading to lowering of the enzyme activity. Bachmeier *et al.* (2002) in their study on effect of Nickel on urease production in *S. pasteurii* found insignificant change in the production of urease upon addition of low amounts of Ni^{2+} while at higher concentrations, Ni^{2+} ions led to lowering of urease production. As, supplementation of nickel did not affect the productivity of urease to much higher extent, so is not a pre - requisite for large scale cementations requiring ureolytic bacterial isolates.

Table 4.2.5 Optimization of Nickel concentration for maximum urease (U/ml) production by different bacterial isolates

NiCl ₂ (μM)	Sp P	SS3	SS5	SS13	SS15	SS18
0	242.5 \pm 7.2b	265.0 \pm 12b	223.0 \pm 13b	204.5 \pm 12b	238.5 \pm 10b	212.5 \pm 11b
5	253.5 \pm 10a	273.5 \pm 8.5a	234.5 \pm 9.2a	217.5 \pm 11a	249.0 \pm 9a	219.0 \pm 5.0a
25	217.5 \pm 7.1c	247.0 \pm 9c	201.0 \pm 13c	181.5 \pm 11c	211.5 \pm 11c	187.5 \pm 13c
100	196.1 \pm 6.2d	212.6 \pm 11d	183.1 \pm 12d	165.6 \pm 12d	188.1 \pm 10d	162.1 \pm 14d

Values bearing different letters in the same column are significant at $P < 0.05$. Values are mean \pm SD (n =3).

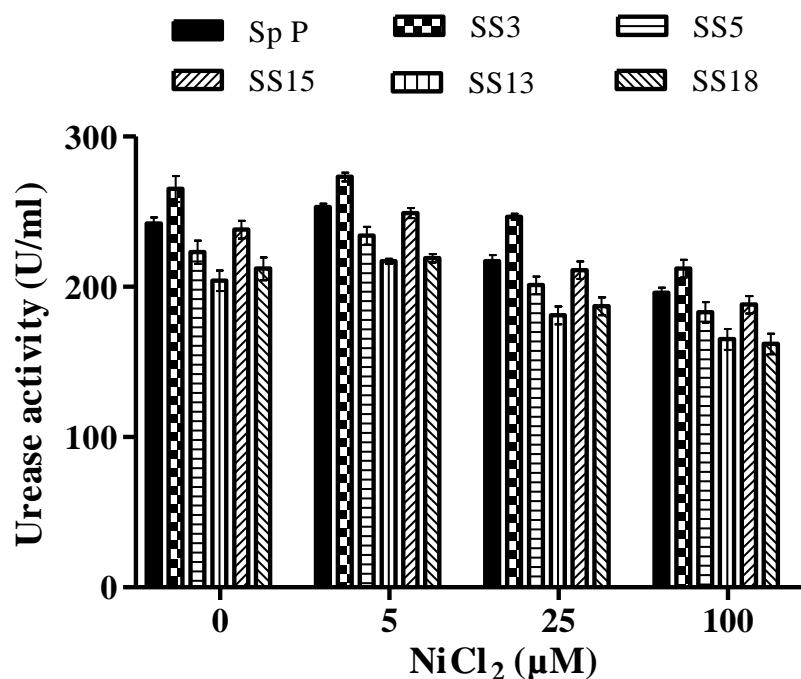


Fig. 4.2.5 Effect of different calcium concentrations on urease activity (U/ml) by bacterial isolates. Bars represent mean \pm SD (n =3)

4.2.1.5. Effect of pH on urease activity

pH plays a very important role in affecting the activity of an enzyme. Like all other enzymes, urease enzyme is only active at certain range of pH. In the present study, the activity of urease in all the bacterial isolates was tested at varying pH by using specific buffers (Fig. 4.2.6; Table 4.2.6). Urease activity was observed to increase from pH 6 to 9 in all the isolates except Sp P and SS5 which had higher activity at pH 8. Beyond pH 8 - 9, there was decline in the production of urease. This might be attributed to denaturation of the enzyme leaving it inefficient for its substrate as every enzyme operates at a specific pH only and change in the pH can directly alter the function of the enzyme by affecting the shape of the enzyme. As chemical makeup of the enzyme is changed, several bonds are made or broken which lead to alteration in the shape of the enzyme. This further makes the enzyme non specific for its substrate. The substrate molecule in these conditions becomes unable to

identify the enzyme and is no longer capable of attaching to it. Therefore, there would be no reaction. Sometimes the changed pH also brings change in the structure of the substrate so that the enzyme is unable to recognize it (no binding and thus, no reaction). So, minor deviations from the specific conditions of an enzyme affect its reactions significantly. Stocks - Fischer *et al.* (1999) stated optimum pH for urease enzyme in the range of 7.5 to 8.0 which was further supported by Evans *et al.* (1991) and Arunachalam *et al.* (2010).

Carbonate precipitation commences when urea hydrolysis occurs and pH increases, the species of carbonate forming bacterial isolates should adapt to this range of pH in order to perform well in producing urease enzyme for urea decomposition. In the present study, all the bacterial isolates had high urease activity at alkaline pH which makes them suitable for carbonate precipitation environments.

Table 4.2.6. Effect of pH on Urease activity (U/ml) of different bacterial isolates

pH	Sp P	SS3	SS5	SS13	SS15	SS18
6	184 ± 8.4e	196 ± 6.2e	148 ± 7.2e	125 ± 4.7e	177 ± 4.8e	143 ± 6.9e
7	224 ± 7.2d	223 ± 5.4d	187 ± 5.8d	172 ± 5.8d	207 ± 6.3d	188 ± 7.4d
8	241 ± 7.9b	260 ± 6.6b	249 ± 5.1a	207 ± 9.2b	238 ± 8.9b	219 ± 4.1b
9	265 ± 8.4a	287 ± 6.2a	222 ± 7.2b	236 ± 4.7a	263 ± 4.8a	240 ± 6.9a
10	231 ± 5.7c	228 ± 8.9c	194 ± 11.5c	183 ± 13.7c	213 ± 9.9c	197 ± 8.2c

Values bearing different letters in the same column are significant at P<0.05. Values are mean ± SD (n =3).

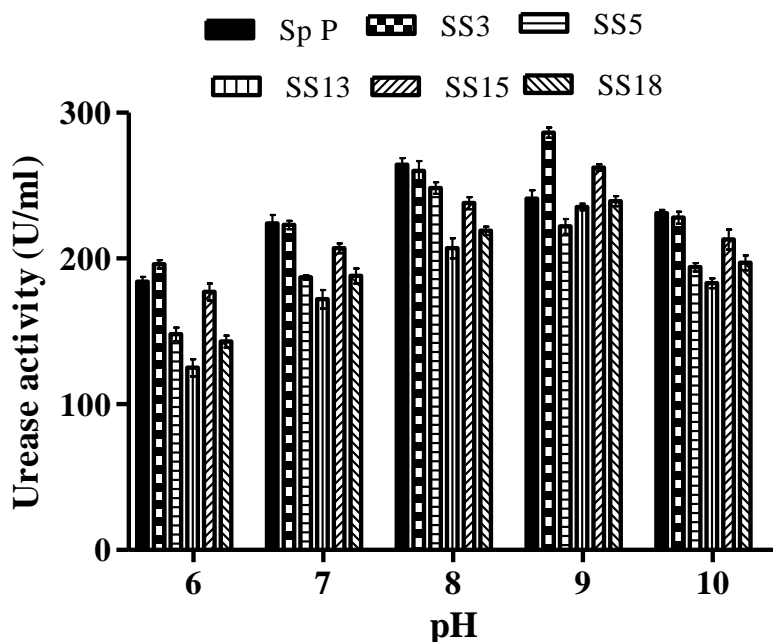


Fig. 4.2.6. Effect of varying pH on urease activity (U/ml) by bacterial isolates. Bars represent mean \pm SD (n =3)

4.2.1.6. Effect of temperature on urease activity

Temperature also plays a very important role in determining the activity of an enzyme. The effect of temperature on urease activity of all the bacterial isolates is shown in Table 4.2.7. It was noticed that urease activity was low at lower temperatures but increased later on from 35 – 45°C beyond which, it declined again. Maximum urease activity was recorded at 35°C in case of SS3, SS5 and SS18 while in case of Sp P, SS13 and SS15 maximum urease activity was recorded at 45°C although sufficient activity still remained upto 65 °C (Table 4.2.7; Fig. 4.2.7). Temperature affects the activity of an enzyme drastically as it alters the speed of molecules, the activation energy of the catalytic reaction and the thermal stability of the enzyme and substrate. The rate of reaction is slow at low temperatures as the molecules have low kinetic energy and collisions between them are less frequent and even if they do collide, the molecules do not possess the minimum activation energy required for the reaction to occur or they get deactivated. At higher temperatures, the molecules possess greater kinetic energy leading to increased activity. Generally, above 50°C there is decrease

in the activity of an enzyme because denaturation of proteins occurs at higher temperatures. It has also been reported that the microbial activity and growth are less sensitive to temperature within the range of 20°C to 30°C but rate of urea hydrolysis is higher in 30°C, as compared to 20°C (Ng *et al.*, 2012). In studies of Whiffin (2004) and van Paassen *et al.* (2009), urease activity of *S. pasteurii* (ATCC 11859) was found to increase up to a temperature of 60°C. In the studies of Sahrawat (1984) the urease activity of soil isolates was found to increase with increasing temperature from 10°C to 60°C, but the activity was completely inhibited at 100°C. The optimum temperature reported by Sahrawat (1984) is consistent with the findings from Liang *et al.* (2005) and Chen *et al.* (1996). As temperature of soils lies around 30°C, the bacterial isolates which can be utilised for technical applications should be able to sustain in such environments and harbour the ability of urea hydrolysis under such conditions. The bacterial isolates with higher temperatures for optimal urease activity are impractical to be applied for soil treatment either on site or in laboratory. All the isolates of present study are suitable for microbially induced calcium carbonate precipitation (MICCP) considering the optimum urease activity of these isolates around 35°C.

Table 4.2.7. Optimization of temperature for maximum urease (U/ml) production by different bacterial isolates

Temperature (°C)	Sp P	SS3	SS5	SS13	SS15	SS18
25	234 ± 8.4c	253 ± 6.2c	214 ± 7.2c	189 ± 4.7c	217 ± 4.8c	192 ± 6.9c
35	238 ± 7.2d	295 ± 5.4bc	257 ± 5.8bc	216 ± 5.8bc	241 ± 9bc	253 ± 7.4bc
45	273 ± 8.4a	261 ± 6.2a	242 ± 7.2a	249 ± 4.7b	275 ± 4.8a	224 ± 6.9a
55	260 ± 8.4b	242 ± 6.2b	214 ± 7.2b	218 ± 4.7a	251 ± 4.8b	219 ± 6.9b
65	211 ± 5.7e	221 ± 8.9d	192 ± 11.5d	162 ± 13.7d	197 ± 9.9d	174 ± 8.2d

Values bearing different letters in the same column are significant at P<0.05. Values are mean ± SD (n=3).

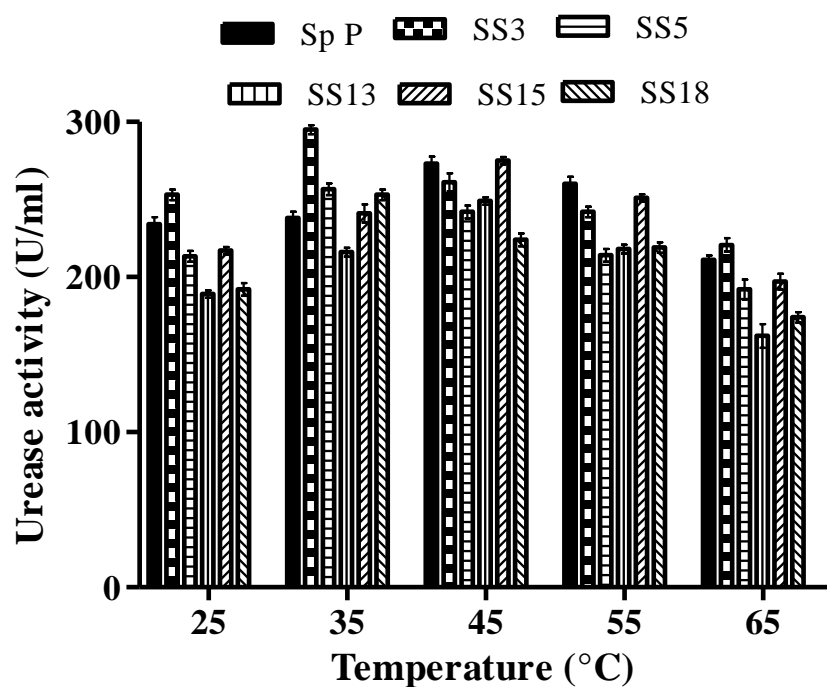


Fig. 4.2.7. Effect of different calcium sources on urease activity (U/ml) by bacterial isolates. Bars are mean \pm SD (n =3)

4.2.1.7. Growth Profile

The growth of all the bacterial isolates along with *S. pasteurii* was studied upto 30 hours in nutrient broth supplemented with 2% urea and 25 mM CaCl_2 (NBUC media) (Fig. 4.2.8). The growth pattern was similar in almost all the isolates except SS13 which showed slower growth in the initial hours. The cell growth was noticed to increase upto 30 hours. Cell concentration was determined from measurement of optical density in the media. The growth curve showed that all the cells started to grow around 2-3 hours followed by inoculation and log phase was continued till 13 hours. Longer generation time and shorter lag times were consistent with other *Bacillus* sp. (De Siano *et al.*, 2006). In the present study, the urea CaCl_2 medium supports microbial growth. NH_4^+ and Cl^- react with OH^- and H^+ and urea serves as energy source and facilitates the growth of bacteria. As no luxurious growth could be noticed in the absence of urea, it confirms the coupling of urea hydrolysis and ATP generation in all the bacterial isolates. CaCO_3

precipitation induced by microbes is far more complicated process than chemically - induced precipitation.

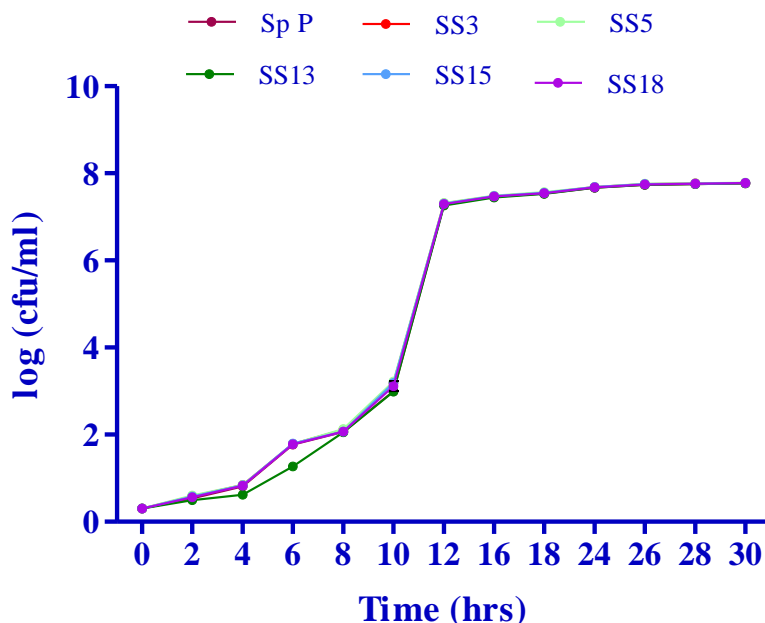


Fig. 4.2.8. Growth profiles of bacterial isolates in NBUC media. Lines are mean \pm SD (n =3).

From the above studies, it was noticed that both urea and calcium play most important role in determining the urease activity of ureolytic bacterial isolates. The production of urease is observed from early log phase; though its quite low in initial timings, but enhances significantly later on. In the present study also, all the bacterial isolates were seen to produce significant urease after 24 hours i.e. in the stationary phase. Other reports are also available on highest production of urease during late log phase as well as in the stationary phase (Ward, 1983; Durham, 1987; Manachini *et al.*, 1988; Altalo and Gashe, 1993; Purva *et al.*, 1998).

4.2.1.8. Effect of time on urease production from bacterial isolates

After understanding the basic parameters which affect urease activity, the next work was aimed at determining the time for maximum urease production by all the bacterial isolates.

The ability to produce urease by all the isolates has been already confirmed. All the bacterial isolates were then grown in NBUC media for 6 days and change in the urease production was recorded. It was noticed that urease activity of all the bacterial isolates increased with increase in time. The highest production in SS3 and SS15 was on 4th day while in case of SS5, SS13 and SS18 was on 5th day along with Sp P (Table 4.2.8; Fig.4.2.9). After 4th and 5th day, the production of urease started decreasing in all the isolates. The decline in enzyme production after its optimal level might reflect depletion of available nutrients and also due to high pH. Another reason could be accumulation of products as NH_4^+ , CO_3^{2-} or OH^- which repress the activity of urease. Bacteria are known to hydrolyze urea by urease for the purposes of: (1) increasing the ambient pH (Burne and Marquis, 2000), (2) utilizing it as a nitrogen source (Burne and Chen, 2001), and (3) using it as a source of energy (Mobley and Hausinger, 1989). Whiffin *et al.* (2004) suggested that in order to overcome the decrease in urease activity, the bacterial cells should be provided with fresh nutrient media so as to remove the repressive by products formed as a result of urea hydrolysis or the pH of the system should be maintained for optimizing the urease activity in case of *S. pasteurii*.

Table 4.2.8. Comparison of urease activity (U/ml) produced by the bacterial isolates at different time intervals

Isolates	Urease Activity (U/ml)					
	24 h	48 h	72 h	96 h	120 h	144 h
Sp P	245 ± 6.5b	388 ± 11b	467 ± 8.4d	595 ± 11b	637 ± 11a	523 ± 9.3a
SS3	270 ± 12a	425 ± 9a	583 ± 19a	690 ± 10a	598 ± 9.5a	476 ± 11b
SS5	228 ± 14c	347 ± 8.5c	475 ± 9.2c	514 ± 10b	587 ± 8.8b	503 ± 13a
SS13	209 ± 11d	326 ± 7.6d	411 ± 11	465 ± 13c	515 ± 6.3b	471 ± 9.7b
SS15	245 ± 9.8b	397 ± 5.9b	517 ± 14b	620 ± 15a	542 ± 5.4b	457 ± 13c
SS18	221 ± 13c	354 ± 9.2c	413 ± 17e	498 ± 13b	525 ± 8.1b	461 ± 11c

Values bearing different letters in the same column are significant at $P < 0.05$. Values are mean ± SD (n =3).

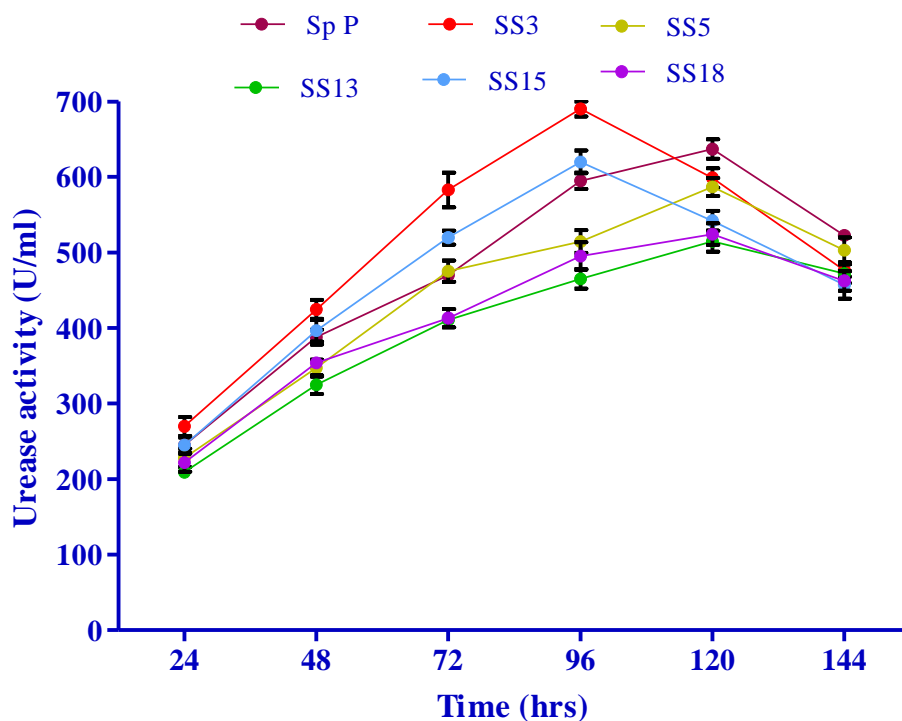


Fig. 4.2.9. Urease activity by all the bacterial isolates in NBUC media at various time intervals. Lines are mean \pm SD (n =3).

In biological systems, many calcareous organisms couple calcification to their metabolic assimilation processes to scavenge protons (McConnaughey and Whelan, 1997). The subsequent increase of pH in surrounding medium due to the presence of ammonia ions and the additional release of CO₂ from the enzymatic urea hydrolysis accelerates the rate of the urease induced calcium carbonate precipitation. Thus, an active participation of urease is of essence in carbonate precipitation. Earlier, Kantzas *et al.* (1992) reported that urease from *B. pasteurii* was detected in the culture medium and they concluded the urease produced was extracellular. Several reports have been available on production of high amounts of urease in the soil environments by *Bacillus* species (Mobley *et al.*, 1995; Ciurli *et al.*, 1996; Benini *et al.*, 1999; Bachmeier *et al.*, 2002). All the bacterial isolates in the present study successfully produced extracellular urease, which offers the advantage of being used solely for precipitation of carbonates where bacterial cell application is not requisite.

4.2.1.9. Specific activity of different bacterial isolates

The specific urease activity of all the isolates was also investigated at the time of their highest production from the total protein content. It was observed that maximum activity was shown by SS3 (Fig. 4.2.10; Table 4.2.9). The specific activity of the present bacterial isolates was also compared to that of literature and it was found to be within the limits of enzyme activities reported (Hammes, 2003b). All these studies showed that all the bacterial isolates have the potential for biocementation as they all harbour requisite ureases for carbonate precipitation but SS3 has been found to be the most efficient urease producer amongst all other isolates of the present study.

Table 4.2.9. Comparison of specific urease activity (U/ml) by different bacterial isolates

Bacterial isolates	Enzyme activity (U/ml) [mM urea hydrolyzed/min/ml]	Protein conc. (mg/ ml)	Specific activity (U/mg)
Sp P	0.63 ± 0.03a	0.28 ± 0.03c	2.25a
SS3	0.69 ± 0.04a	0.33 ± 0.06a	2.09b
SS5	0.58 ± 0.06ab	0.31 ± 0.04b	1.87c
SS13	0.51 ± 0.02b	0.33 ± 0.07a	1.54d
SS15	0.62 ± 0.07a	0.32 ± 0.02a	1.93c
SS18	0.52 ± 0.04b	0.34 ± 0.04a	1.52d

Values bearing different letters in the same column are significant at P<0.05. Values are mean ± SD (n =3)

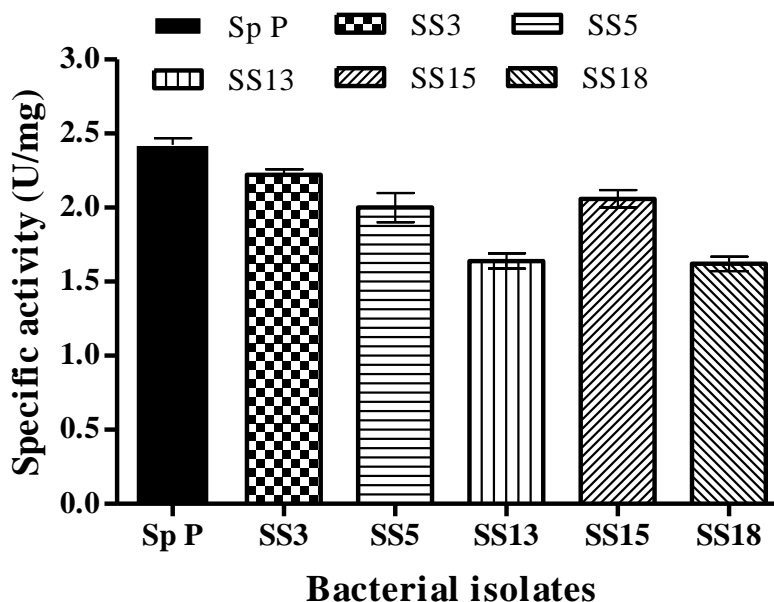


Fig. 4.2.10. Specific urease activity of all the bacterial isolates. Bars represent mean \pm SD (n =3)

4.2.1.10. Enzyme kinetics of urease from different bacterial isolates

After investigating the urease activity of all bacterial isolates in comparison to *S. pasteurii*, the next step was to investigate the kinetics of these ureases from different bacterial isolates. Optimal temperature and pH for crude enzyme extracts of all the isolates was investigated as before. The optimal temperature for SS3, SS5 and SS18 was found to be 35°C while in case of Sp P, SS13 and SS15, it was 45°C. pH 9 was found to be the most suitable for all bacterial isolates except SS5 which gave maximum enzyme activity at pH 8 along with Sp P. In general, the stability of urease increased from pH 7 to 8 reaching maximum at pH 9 and then declining but in case of SS5, the enzyme activity was seen to lower after pH 8. The Lineweaver – Burk plots were linear and indicated that hydrolysis of urea by the enzyme urease followed Michaelis–Menten kinetics in all crude enzyme extracts of all bacterial isolates. The graph gave two kinetic parameters, K_m and V_{max} , which indicate the substrate affinity of enzyme. The smaller K_m value indicates higher enzyme affinity to substrates while larger K_m value depicts lower enzyme affinity to its substrate. Distinct differences

among the isolates in terms of substrate affinity (K_m) and rate values (V_{max}) were observed. The K_m for Sp P, SS3, SS5, SS13, SS15 and SS18 were calculated as 27.2, 31.4, 35.8, 37.3, 43.2 and 39.6 mM whereas the V_{max} for Sp S, SS3, SS5, SS13, SS15 and SS18 was found to be 2.68, 2.45, 2.13, 1.98, 2.31 and 1.86 $\text{mmol min}^{-1} \text{mg}^{-1}$ (Table 4.2.10).

Table 4.2.10. Enzyme kinetics of Ureases from different bacterial isolates

Bacterial isolate	K_m (mM)	V_{max} ($\text{mmol min}^{-1} \text{mg}^{-1}$)
Sp P	27.2	2.68
SS3	31.4	2.45
SS5	35.8	2.13
SS13	37.3	1.98
SS15	43.2	2.31
SS18	39.6	1.86

Several ureolytic bacterial isolates have been characterized before, which includes *B. pasteurii*, *Pseudomonas* sp., *Variocorax* sp., *Leuconostoc mesenteroides*, *Klebsiella* sp., *Proteus* sp, *Lactobacillus* sp and *Streptococcus* sp. (Stocks - Fischer *et al.*, 1999; Ferris and Stehmeier, 1993; Fujita *et al.*, 2000; Hammes *et al.*, 2013b; Balan *et al.*, 2012). K_m value for ureases have been reported to be in the range of 0.1 to 100 mM urea (Mobley and Hausinger, 1989). Urease from crude extract of *B. pasteurii* exhibited a K_m of 26.2 mM at pH 7.7 and V_{max} of $1.72 \text{ mM min}^{-1} \text{mg}^{-1}$ (Stcoks Fischer *et al.*, 1999) while Bachmeier *et al.* (2001) reported a K_m of 17.3 mM and V_{max} of $1.57 \text{ mM min}^{-1} \text{mg}^{-1}$ for partially purified urease of *B. pasteurii*. The urease from *Proteus mirabilis* has been reported to have K_m of 13 mM while that of *Ureaplasma urealyticum* was 2.5 mM. The standard V_{max} values for purified ureases have been reported to be in the range of 1 – 5.5 $\text{mM min}^{-1} \text{mg}^{-1}$ protein while it was found to be 33 – 180 $\text{mM min}^{-1} \text{mg}^{-1}$ protein in case of *Ureaplasma urealyticum* (Mobley and Hausinger, 1989). In the present study, the isolates displayed moderate to high urea affinity with high specific rates. This might imply that the isolates are not scavengers of

urea, but respond well to high concentrations of urea available. The kinetics studies have further supported the ureolytic efficiency of all bacterial isolates for potential precipitation of carbonates.

4.2.1.11. SDS PAGE of bacterial isolates

Sodium dodecyl sulphate-polyacrylamide gel electrophoresis (SDS-PAGE) was carried out to investigate the protein profile in the supernatant from all bacterial isolates. After staining the gel with Coomassie Brilliant Blue R-250, multiple banding patterns were seen (Fig. 4.2.11). The protein bands showed similar pattern in almost all the isolates except SS5 and SS18. In case of SS3 and SS15, comparatively thick bands were observed. SDS PAGE depicted the presence of around 65 kDa, 15 Kda, 12 kDa proteins in all the isolates which might be that of urease as 11, 13 and 61 k Da bands were reported in the Urease from *B. pasteurii* by Mobley *et al.* (1995).

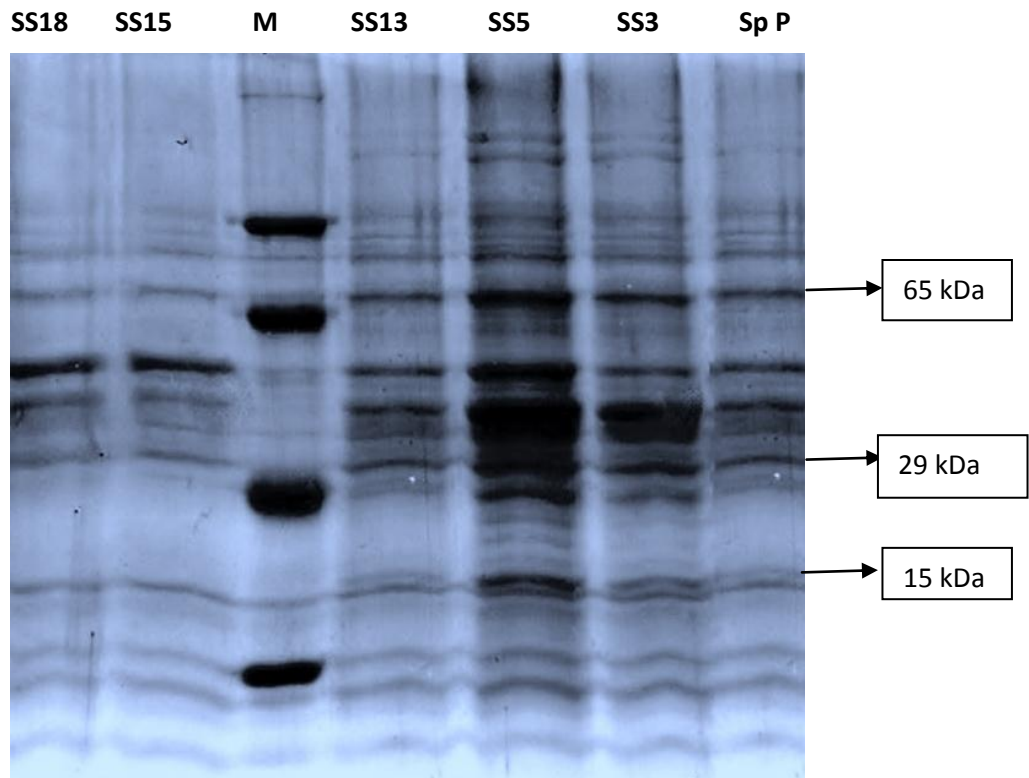


Fig. 4.2.11. SDS-PAGE bands obtained from supernatant of different isolates. M- Molecular Marker

4.2.1.12. Zymography of ureases from different bacterial isolates

Zymogram, or activity staining in non-denaturing polyacrylamide gel, is already an established method for identifying the presence of different catalytically active molecular species of urease (De Martin *et al.*, 1989). The current method is a very sensitive and inexpensive method to assay urease in polyacrylamide gels after separation on PAGE under native and non-denaturing conditions (Sharma *et al.*, 2008).

Zymogram analysis is very sensitive to detection of urease activity and successfully detects the presence of urease in all the bacterial isolates. After incubation of polyacrylamide gel with urea and β -mercaptoethanol – nitroprusside solution, purple colored bands developed corresponding to the site of urease activity. Transformation of the yellow colour of nitroprusside-thiol solution essentially requires alkaline pH to develop into the purple colour complex. The local alkalinity produced by ureolytic activity can theoretically be used to develop purple colour due to nitroprusside-thiol reaction. While developing the zymogram, β -mercaptoethanol was used as a thiol compound for colour development. The bands that developed due to urease activity were found to be at the same site in all the samples. Urease preparations from all the bacterial isolates demonstrated identical electrophoretic mobilities on a non-denaturing activity gel (Fig. 4.2.12). No colour change was observed in the rest of the gel, which leads to the clear visualization of urease activity bands. The colour formed after urease action was found to be stable for at least one hour. This method has also been used successfully by Bergdale *et al.* (2012) for studying the urease activity of *S. pasteurii* along with recombinant *P. aeruginosa* bacterial isolates. This method helps to understand the polymeric status of the enzyme under different environmental conditions of varying pH, ionic strength and storage conditions. In the present study, in gel activity staining indicated that all the bacterial isolates exhibited high urease activity. The mobility of all the enzymes was also found to be almost similar which might be due to similarity of ureases in different *Bacillus* sp.

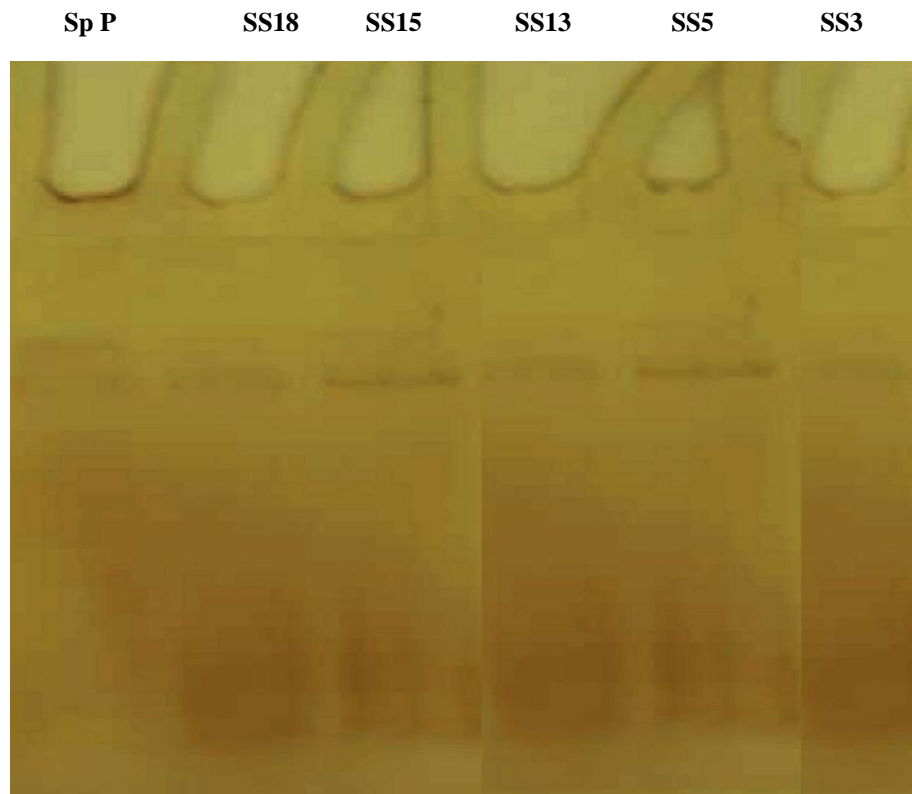


Fig. 4.2.12. Zymographic analysis of bacterial isolates.

4.2.2. Protease activity of different bacterial isolates with time

Extracellular protease activity of different bacterial isolates was also determined in the culture supernatant by method of Fukomoto *et al.* (1971) at different time intervals. It was noticed that the protease activity increases abruptly after 4 - 5 days in all the isolates (Table 4.2.11; Fig. 4.2.13). The production of protease was higher in SS5 as compared to other isolates. Protease production by Sp P, SS3, SS5, SS13, SS15 and SS18 was 38.3, 54.4, 63.7, 45.4, 38.4, 39.2 U/ml at the end of 144 hours.

The variance analysis pointed out that there was a significant difference in protease production among different isolates (Table 4.2.10). Production of proteases increased significantly ($P < 0.05$) with time in all the isolates. The high amount of proteases might be the responsible for breakdown of ureases and their accumulation in the culture media lowers the production of other enzymes. As urease from all bacterial isolates were found to degrade

with time after 4 - 5 days; for this, a complex system of proteins might be involved as proteins like urease are marked for destruction by the covalent attachment of chains of a protein or by selective hydrolysis (Berg *et al.*, 2002). This might be due to higher production of proteases with time which lead to breakdown of ureases and other enzymes.

Table 4.2.11. Comparison of protease activity (U/ml) produced by the bacterial isolates at different time intervals

Isolates	Protease Activity (U/ml)					
	24 h	48 h	72 h	96 h	120 h	144 h
Sp P	22.3±0.3d	23.73±0.2e	24.40±0.3ef	26.24±0.2de	27.87±0.1e	38.30±0.3e
SS3	26.1±0.5b	29.27±0.4b	33.9±0.3b	35.85±0.4b	38.27±1.0b	54.4±1.3b
SS5	31.7±0.4a	34.7±0.3a	37.73±0.4a	40.21±0.2a	43.89±0.4a	63.7±0.4a
SS13	21.75±0.4c	22.63±0.5c	24.13±0.9c	27.85±0.2c	31.51±0.5c	45.4±0.4c
SS15	19.49±0.6d	21.67±0.2e	23.00±0.3e	24.97±0.2d	27.63±0.1e	38.4±0.2e
SS18	21.26±0.4c	23.75±0.2d	24.84±0.2d	27.71±0.6c	30.33±0.6d	39.17±0.9d

Values bearing different letters in the same column are significant at $P < 0.05$. Values are mean \pm SD (n =3)

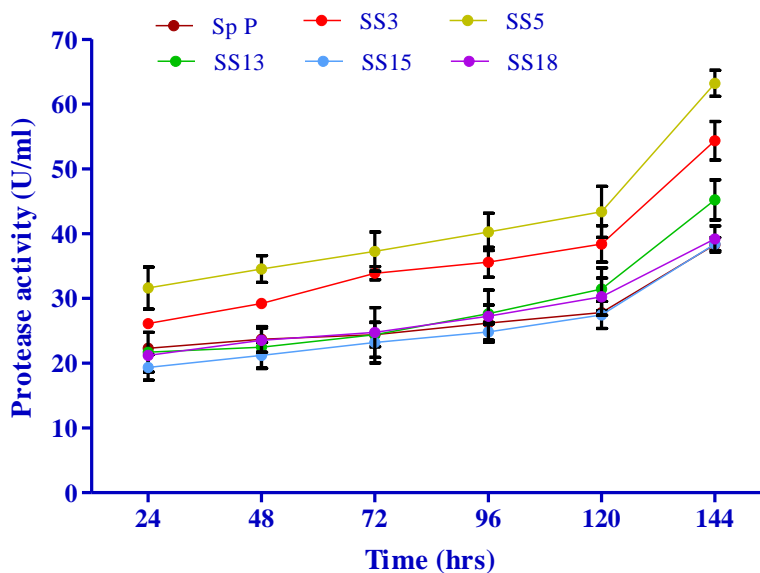


Fig. 4.2.13. Protease activity by all the bacterial isolates in nutrient media. Lines represent mean \pm SD (n =3)

4.2.3. Calcium carbonate precipitation via ureolytic pathway

Figure 4.2.14 represents the pattern of calcium carbonate precipitation, pH profile and urea hydrolysis by ureolytic bacterial isolates in Nutrient broth supplemented with 2% urea and 25 mM CaCl₂ (NBUC media) (Table 4.2.12).

In case of carbonate precipitation, it was observed that concentration of insoluble calcium started increasing in all the bacterial inoculated sets from early hours. Calcium carbonate precipitation was around 80% complete in all the bacterial sets within 12-16 hours but in case of control, insignificant precipitation of calcium carbonate was noticed.

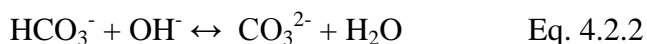
All the bacterial isolates efficiently hydrolyzed urea with time but in case of control, there was insignificant change in the amount of urea. The decrease in the concentration of urea with time correlated with precipitation of calcium carbonates and increase in pH in all the bacterial isolates.

The pH was observed to increase significantly with time and was > 9.2 in all the bacterial sets after 24 hours which was due to efficient hydrolysis of urea. But in case of control set,

not much change in the pH was noticed with time. The initial precipitation started after pH 8.4 ± 0.1 and was around 80% completed upto pH 9.5. Considerable hydrolysis of urea was observed from the initial hours. In case of control sets, there was very small change in the insoluble calcium concentration and insignificant change in amount of urea and pH even after 24 hours. Minor precipitation is due to chemically induced precipitation.

In the present study, all the ureolytic bacterial isolates exhibited their potential for efficient carbonate precipitation. Certain variations were clearly noticeable in the amount of carbonate precipitation among the isolates. Bacterial isolate SS18 was found to be least efficient in precipitating the carbonates compared to other isolates as it could precipitate only 80% till 24 hours. This could be due to poor diffusion of urea due to encrustation of bacterial cells in the carbonate crystals or accumulation of other inhibitory by - products which render the bacterial cells inaccessible to medium urea. SS3 and SS15 were found to be most efficient carbonate precipitating isolates whose precipitation efficacy was closely related to *S. pasteurii*.

In the medium, individual micro organisms produce ammonia as a result of enzymatic urea hydrolysis and create alkaline micro environment around the cell. The increase of pH due to the presence of ammonium ions and additional release of CO_2 from enzymatic urea hydrolysis accelerates the rate of urease induced carbonate precipitation. So, an active participation of bacterial urease is necessary for carbonate precipitation. Following equilibrium reactions are involved in production of carbonate ions:



Calcium carbonate precipitation in microbial systems typically occurs when the saturation index is above 1 (Rodriguez – Navarro *et al.* 2012). Once supersaturation is achieved, calcium carbonate formation by heterogeneous nucleation readily occurs on the bacterial cell walls and bacterial EPS or cell debris. Bacterial presence and activity are also found to be prerequisite for the precipitation of calcium carbonate as bacterial metabolic activity produces the necessary increase in supersaturation as to induce the heterogeneous crystallization of calcium carbonate on the surface of bacterial cells as well as on EPS (Rodriguez – Navarro *et al.* 2012).

Table 4.2.12. Calcium carbonate precipitation, pH profile and urea hydrolysis by ureolytic bacterial isolates at different time intervals

Insoluble Ca ²⁺ ions							
Time (Hrs)	Sp P	SS3	SS5	SS13	SS15	SS18	Control
0	0.52 ± 0.0a	0.52 ± 0.08a	0.52 ± 0.07a	0.52 ± 0.06a	0.52 ± 0.09a	0.52 ± 0.02a	0.53 ± 0.06a
2	8.6 ± 0.5a	8.3 ± 0.8a	6.9 ± 0.1bc	7.5 ± 0.2b	8.0 ± 0.8a	5.5 ± 0.4c	3.2 ± 0.08e
4	13.7 ± 0.7b	14.6 ± 1.4a	11.3 ± 0.9cd	12.6 ± 0.9c	13.5 ± 0.6b	8.3 ± 0.7f	4.3 ± 0.09i
6	17.4 ± 0.9b	18.2 ± 1.2a	14.7 ± 1.4c	17.3 ± 1.3b	17.3 ± 0.9b	12.3 ± 1.3d	4.9 ± 0.1hi
8	19.3 ± 1.7b	20.3 ± 1.9a	17.8 ± 1.3bc	18.9 ± 1.5bc	21.2 ± 1.3b	16.6 ± 0.9c	5.6 ± 0.2
10	21.2 ± 1.9b	22.9 ± 1.4a	20.1 ± 1.8c	21.7 ± 1.9b	22.3 ± 1.2b	19.9 ± 1.4cd	5.4 ± 0.4i
12	24.2 ± 1.2a	24.2 ± 1.2a	22.3 ± 1.1c	22.9 ± 1.3bc	23.1 ± 1.6b	21.2 ± 1.5c	5.7 ± 0.7i
18	24.4 ± 0.8a	24.4 ± 0.5a	23.1 ± 0.9b	22.6 ± 0.8c	23.4 ± 0.8b	21.9 ± 0.7c	5.9 ± 0.4i
24	24.6 ± 0.9a	24.6 ± 0.4a	23.5 ± 0.4b	22.7 ± 0.5c	23.5 ± 0.5b	22.4 ± 0.4c	5.4 ± 0.6i
pH							
0	8.12 ± 0.3a	8.12 ± 0.07a	8.12 ± 0.1a	8.12 ± 0.09a	8.12 ± 0.08a	8.12 ± 0.09a	8.04 ± 0.1b
2	8.32 ± 0.1b	8.43 ± 0.2a	8.32 ± 0.2b	8.4 ± 0.5a	8.38 ± 0.4a	8.28 ± 0.3bc	8.13 ± 0.3cd
4	8.53 ± 0.4c	8.67 ± 0.3b	8.46 ± 0.4cd	8.58 ± 0.9bc	8.76 ± 0.3a	8.54 ± 0.8c	8.28 ± 0.2de
6	8.87 ± 0.3b	8.88 ± 0.6b	8.59 ± 0.7c	8.76 ± 0.4bc	9.12 ± 0.7a	8.76 ± 0.9bc	8.36 ± 0.2d
8	9.10 ± 0.2b	9.23 ± 0.2ab	8.97 ± 0.4c	8.96 ± 0.5c	9.37 ± 0.4a	9.12 ± 0.4b	8.43 ± 0.7d
10	9.23 ± 0.1b	9.47 ± 0.5a	9.12 ± 0.8c	9.15 ± 0.2c	9.49 ± 0.9a	9.28 ± 0.9b	8.49 ± 0.4e
12	9.34 ± 0.4c	9.58 ± 0.4a	9.25 ± 0.7d	9.29 ± 0.6cd	9.58 ± 0.4a	9.44 ± 0.6b	8.46 ± 0.4f
18	9.57 ± 0.3b	9.77 ± 0.3a	9.44 ± 0.8c	9.36 ± 0.4cd	9.69 ± 0.7a	9.57 ± 0.4b	8.53 ± 0.5g
24	9.70 ± 0.2bc	10.1 ± 0.5a	9.67 ± 0.4bc	9.58 ± 0.7c	9.86 ± 0.6b	9.63 ± 0.7c	8.56 ± 0.6fg
Remaining Urea (mM)							
0	330 ± 5a	330 ± 3a	330 ± 4a	330 ± 3a	330 ± 4a	330 ± 4a	330 ± 3a
2	306 ± 10d	313 ± 9c	311 ± 9c	309 ± 7cd	308 ± 6cd	318 ± 7b	323 ± 9a
4	291 ± 7bc	298 ± 7b	298 ± 11b	297 ± 8b	295 ± 7b	299 ± 9b	319 ± 7a
6	266 ± 9c	276 ± 9bc	287 ± 14b	276 ± 8b	278 ± 9bc	280 ± 4bc	314 ± 8a
8	241 ± 12cd	254 ± 13c	266 ± 13c	256 ± 9c	256 ± 13c	243 ± 8cd	311 ± 10a
10	224 ± 10c	238 ± 11c	234 ± 11c	238 ± 11c	238 ± 11c	231 ± 7c	309 ± 7a
12	197 ± 13cd	212 ± 8c	223 ± 12c	221 ± 14c	219 ± 8c	212 ± 10c	308 ± 9a
18	179 ± 11cd	197 ± 9cd	215 ± 10c	218 ± 13bc	207 ± 13c	203 ± 11c	304 ± 11a
24	154 ± 9d	166 ± 12d	204 ± 9c	211 ± 11c	197 ± 11cd	189 ± 12cd	301 ± 13a

Values bearing different letters in the same column are significant at P<0.05. Values are mean ± SD (n=3)

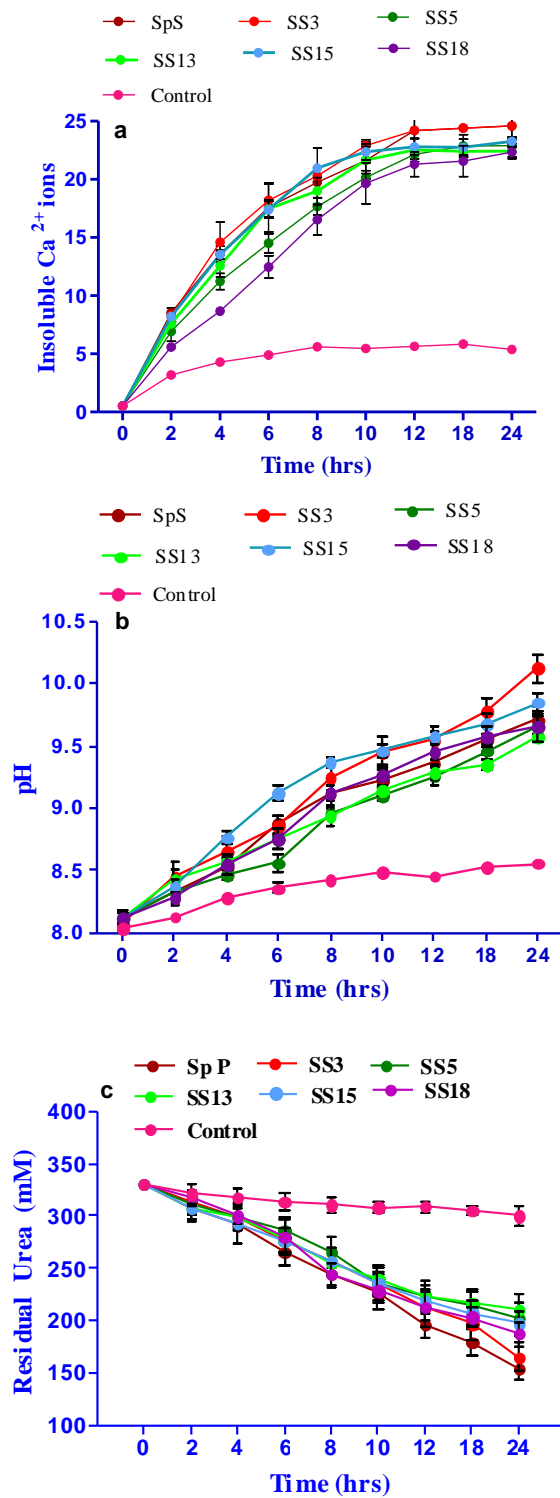
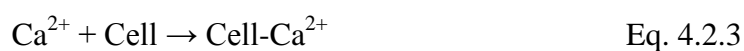


Fig. 4.2.14. Microbiologically induced CaCO_3 precipitation (a), pH (b) and urea hydrolysis (c) by different bacterial isolates in NBUC medium. Lines represent mean \pm SD (n =3)

Warren and Ferris (1998) demonstrated that the surfaces of bacteria can be particularly well-suited to act as mineral nucleation templates, providing a mechanism by which the activation energy required for precipitation to occur is lowered. As they demonstrate, under identical system conditions, authigenic precipitation can occur via nucleation and precipitation at the bacteria surface, yet no precipitation occur when no bacteria are present, presumably because the activation energy for bulk or homogeneous precipitation presents a greater barrier for the initiation of the precipitation process. The bacterial cell surface with a variety of ions non specifically induces mineral deposition by providing nucleation sites (Ferris *et al.*, 1986; 1987). Ca^{2+} is not likely utilized by microbial metabolic processes; rather it accumulates around the cell (Silver *et al.*, 1975). The biochemical reactions to precipitate CaCO_3 at the cell surface are:



Stocks - Fischer *et al.* (1999) hypothesized that when cell concentration is low, every cell is responsible for serving as nucleation site for CaCO_3 formation and produce ammonia to increase pH in the surroundings. Once the initial CaCO_3 precipitation occurs on the nucleation site, carbonate precipitates continue to grow due to presence of microbial activities: increase in pH, CO_2 production and Ca^{2+} binding to the cell surface (Morita, 1980).

4.2.4. Screening and characterization of carbonic anhydrase enzyme in different bacterial isolates

4.2.4.1. Carbonic anhydrase activity

Another enzyme which has been recently found to play role in bacterial calcium carbonate precipitation i.e. Carbonic anhydrase (CA) was also investigated in the present study. The production of CA in all the bacterial isolates was tested on nutrient agar plates supplemented with 1.0 mM p-NPA (para nitro phenyl acetate). Appearance of bright yellow colour on

pNPA plates indicated the production of carbonic anhydrase in all the isolates (Fig. 4.2.15). Ramanan *et al.* (2009) recently reported the p-NPA plate assay for detection of extracellular CA from bacterial isolates and successfully screened the CA activity from 102 bacterial isolates. This method has proved its potential in being convenient and reliable for detection of CA producing isolates. All the ureolytic bacterial isolates depicted the presence of carbonic anhydrase also.

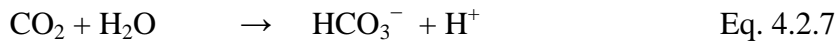


Fig. 4.2.15. Carbonic anhydrase production by bacterial isolate *B. megaterium* SS3 on p-NPA plate

CA catalyzes the inter-conversion of CO_2 and HCO_3^- , so that the rate of conversion to CO_2 may increase. Overall reactive equations by CA given by Li *et al.* (2010) are as follows: If HCO_3^- is the source of dissolved inorganic carbon (DIC), CA may catalyze its conversion into CO_2 , and the overall reactive equations are as follows:



If CO_2 is the source of DIC, CA may catalyze its conversion into HCO_3^- , and the overall reactive equations are as follows:



For quantitative analysis of the bacterial CA, the enzyme activity was compared to that of *Bacillus pumilis* (Bc P), a known carbonic anhydrase producing bacterium. The carbonic anhydrase activity of all bacterial isolates was found to be as given (table 5.13; Fig. 5.16).

Table 4.2.13. Comparison of carbonic anhydrase activity (U/ml) produced by different bacterial isolates

Bacterial isolate	CA (U/ml)
Bc P	28 ± 1.8a
SS3	24 ± 2.7 ab
SS5	21 ± 2.8ab
SS13	16 ± 1.2bc
SS15	19 ± 2.3b
SS18	15 ± 2.1c

Values bearing different letters in the same column are significant at $P < 0.05$. Values are mean ± SD (n = 3)

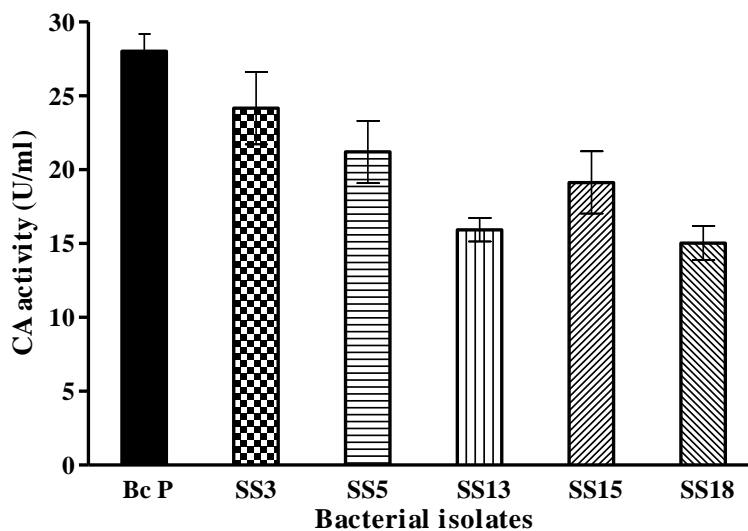


Fig. 4.2.16. Production of carbonic anhydrase by different bacterial isolates. Bars represent mean ± SD (n = 3)

It was found that SS3 and SS5 had comparative CA activity as that of *Bacillus pumilus* (Bc P) followed by SS15, SS13 and SS18. Though lot of work has been done on CA from

bovine erythrocytes and its applications in CO₂ hydration and carbonate precipitation, but not much had been explored from bacterial species till recent times. In case of bacterial system, carbonic anhydrase activity was first reported in *Neisseria sicca* by Veitch and Blankenship (1963) and this enzyme was the first carbonic anhydrase purified from a prokaryote (Silverman and Lindskog, 1988). After purification of CA from *Neisseria sicca*, many researchers made attempts to investigate this enzyme from other bacterial species (Alber and Ferry, 1994). It was found recently that CAs are widespread in metabolically diverse bacterial species. Buzolyova and Somov (1999) have reported the presence of CA in *Yersina pseudotuberculosis* and *Listeria monocytogenes*, the pathogens isolated from soil and water. Recently, CA from *Bacillus pumilis*, *Citrobacter freundii*, *Bacillus mucilaginosus*, *Methanobacterium thermoautotrophicum*, *Enterobacter gergoviae*, *Enterobacter taylorae*, *Aeromonas hydrophila*, *Aeromonas caviae*, *Pseudomonas fragii*, *Helicobacter pylori*, *Pseudomonas aeruginosa*, *Salmonella typhimurium*, *Vibrio Fischeri*, *Proteus vulgaris* and *Bacillus subtilis* have also been reported (Brauss Stromeyer *et al.*, 1997; Smith *et al.*, 1999; Sharma *et al.*, 2008; Ramanan *et al.*, 2009; Zhang *et al.*, 2011; Wanjari *et al.*, 2011; Prabhu *et al.*, 2011; Yadav *et al.*, 2011). In the present study also, all the bacterial isolates were found to exhibit comparative CA activity to *Bacillus pumilis* (Bc P).

Before investigating the effect of bacterial CA in carbonate precipitation studies, its prerequisite to investigate the conditions for sufficient enzyme activity of these bacterial isolates. As CA is a zinc containing enzyme that dramatically catalyzes the reversible hydration of CO₂ ($\text{CO}_2 + \text{H}_2\text{O} \leftrightarrow \text{HCO}_3^- + \text{H}^+$), addition of zinc may have pronounced effect on the production / activity of this enzyme. For investigating the effect of addition of zinc on CA production and activity, all the bacterial cultures were subjected to varying concentrations of ZnSO₄ (Table 4.2.14; Fig 4.2.17).

It was found that addition zinc enhances the activity of CA in all bacterial isolates at a concentration of 10 µM which assuages the fact that zinc activates the activity of CA. Ramanan *et al.* (2009) in their study on *Citrobacter freundii* SW3 isolate from environmental wastes found significant enhancement in the CA activity upon supplementation of zinc.

Table 4.2.14. Optimization of Zinc for maximum CA activity (U/ml) by different bacterial isolates.

ZnSO ₄ (μM)	Bc P	SS3	SS5	SS13	SS15	SS18
0	29.0 ± 1.5c	23.5 ± 1.9c	27.6 ± 1.1c	17.5 ± 2.3c	20.0 ± 1.2bc	16.0 ± 2.1c
10	39.0 ± 1.5a	35 ± 1.5a	31 ± 2.2a	27 ± 2.7a	28 ± 1.4a	24 ± 1.7a
25	33.5 ± 2.1b	27.0 ± 2.2b	23.0 ± 1.8b	22.5 ± 2.0b	23.5 ± 2.3b	21.5 ± 2.4b
50	22.1 ± 1.8d	19.6 ± 1.7d	18.1 ± 2.1d	17.6 ± 1.2c	17.1 ± 1.9c	18.1 ± 1.9c

Values bearing different letters in the same column are significant at P<0.05. Values are mean ± SD (n=3).

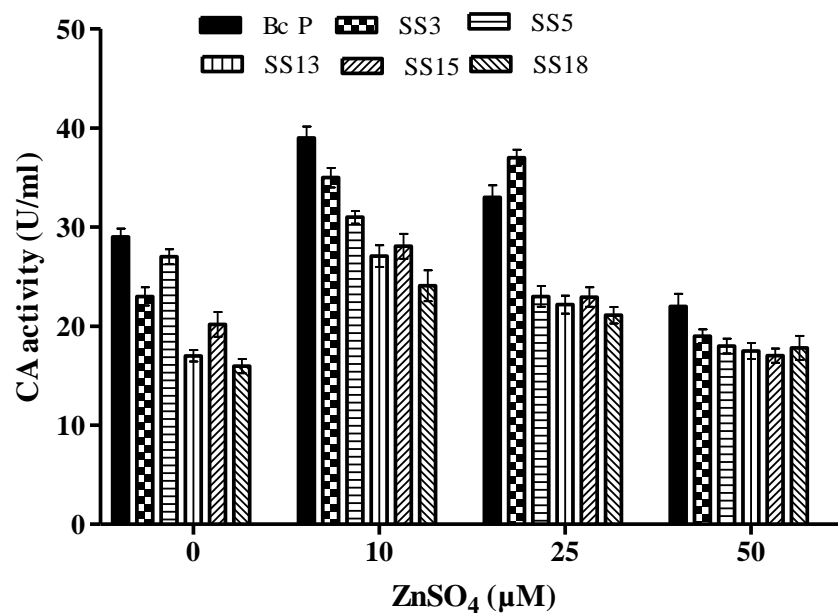


Fig. 4.2.17. Effect of different concentrations of ZnSO₄ on CA activity (U/ml) by different bacterial isolates. Bars are mean ± SD (n=3)

Smith and Ferry (2000) also emphasized the positive effect of zinc ions in CA activity in bacteria. Zinc's role in carbonic anhydrase is to facilitate the water to create a proton H^+ and a nucleophilic hydroxide ion. The nucleophilic water molecules attack the carbonyl group of carbon dioxide to convert it into bicarbonate. This is obtained through the +2 charge that the zinc ion has, which attracts the oxygen of water, deprotonates water, thus converting it into a better nucleophile so that the newly converted hydroxyl ion can attack the carbon dioxide (Berg, 2002). In the present study it was observed that higher concentrations of zinc had a repressible effect on the activity of CA in all the bacterial isolates. High concentrations of zinc might be causing inhibitory effect on the growth of bacterial cells which further leads to lower enzyme activity.

In order to investigate optimum pH and temperature for crude CA enzyme extract of various bacterial isolates, the enzyme extracts were incubated at varying pH buffers (described in Appendix I) and temperatures. It was noticed that the activity of CA from different bacterial isolates was highest at pH 8 except in SS13 where it was maximum at pH 9 (Table 4.2.15; Fig. 4.2.18). In case of temperature, all the extracellular CAs showed maximum activity at temperature of 35°C for all bacterial isolates except SS5 and SS18 which had maximum activity at 45°C (Table 4.2.16; Fig. 4.2.19). Sharma *et al.* (2008) noticed pH 8.0 to be optimum for CA activity of *Enterobacter gergoviae* and *Enterobacter taylorae* while pH 8.5 for *Aeromonas hydrophila* and *Aeromonas caviae*. In case of temperature, *Enterobacter gergoviae*, *Aeromonas hydrophila* and *Aeromonas caviae* depicted maximum enzyme production at 40°C while in case of *Enterobacter taylorae*, maximum enzyme activity was observed at 45°C. So, the CA activity results of present bacterial isolates at varying pH and temperatures were in agreement with the previous works.

Table 4.2.15. Effect of pH on carbonic anhydrase activity (U/ml) of different bacterial isolates

pH	Bc P	SS3	SS5	SS13	SS15	SS18
6	33 ± 1.8b	28 ± 1.3c	22 ± 1.1c	18 ± 1.5c	19 ± 1.2c	16 ± 1.6bc
7	37 ± 1.6b	31 ± 1.7b	26 ± 1.4b	22 ± 1.9ab	22 ± 1.8b	19 ± 0.9b
8	40 ± 2.2a	36 ± 1.9a	30 ± 1.8a	24 ± 1.2a	25 ± 1.4b	22 ± 1.4a
9	34 ± 1.2b	32 ± 2.1b	25 ± 1.3b	21 ± 1.4b	27 ± 1.1a	18 ± 1.9b
10	26 ± 1.9d	28 ± 1.2c	21 ± 1.1c	17 ± 1.9c	21 ± 1.9b	15 ± 1.2c

Values bearing different letters in the same column are significant at P<0.05. Values are mean ± SD (n=3).

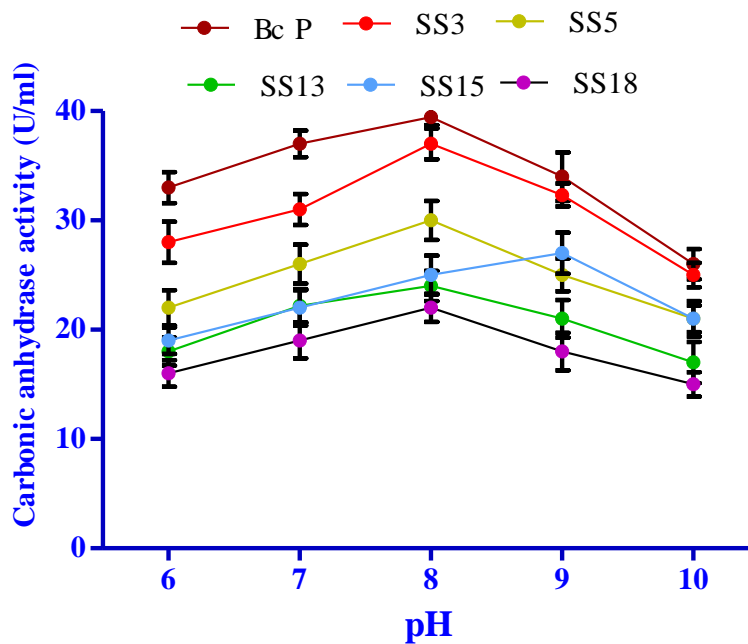


Fig. 4.2.18. Effect of varying pH on carbonic anhydrase activity (U/ml) of different bacterial isolates. Lines represent mean ± SD (n=3)

Table 4.2.16. Effect of temperature on carbonic anhydrase activity (U/ml) of different bacterial isolates

Temp (°C)	Bc P	SS3	SS5	SS13	SS15	SS18
25	23 ± 1.8c	20 ± 1.3c	14 ± 1.1d	13 ± 1.5c	14 ± 1.2d	11 ± 1.6c
35	34 ± 1.6b	29 ± 1.7b	23 ± 1.4b	18 ± 1.9b	18 ± 1.8c	16 ± 0.9b
45	40 ± 2.2a	36 ± 1.9a	30 ± 1.8a	24 ± 1.2a	23 ± 1.4b	22 ± 1.4a
55	31 ± 1.2b	26 ± 2.1b	24 ± 1.3b	17 ± 1.4b	27 ± 1.1a	15 ± 1.9b
65	22 ± 1.9c	21 ± 1.2c	19 ± 1.1c	12 ± 1.9c	21 ± 1.9b	12 ± 1.2c

Values bearing different letters in the same column are significant at $P < 0.05$. Values are mean \pm SD (n = 3).

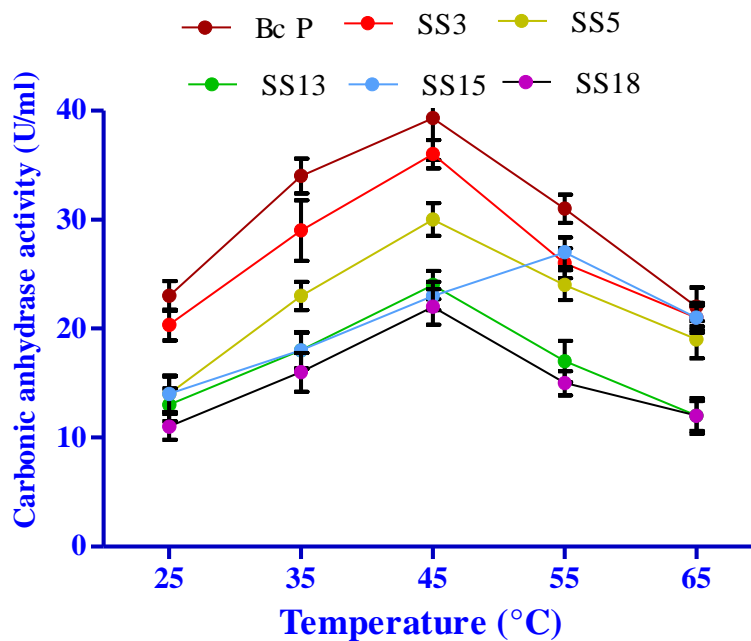


Fig. 4.2.19. Effect of varying temperature on carbonic anhydrase activity (U/ml) of different bacterial isolates. Lines represent mean \pm SD (n = 3)

4.2.4.2. Effect of time on CA activity of different bacterial isolates

After investigating the parameters for CA production by all bacterial isolates, the bacterial isolates were then tested for their efficacy to produce CA at different time intervals (Table 4.2.17; Fig. 4.2.20). It was observed that CA activity of all the bacterial isolates increased with increase in time as was the case of urease (section 4.2.1.8). The highest production of CA was seen in case of SS3 followed by SS5 on 4th day while in case of SS15, SS13 and SS18 the activity was maximum on 5th day. After 4th and 5th day, the production of CA started decreasing in all the isolates. It was noticed that the CA activity in all bacterial isolates correlated with that of urease activity suggesting some link between the two. Botre and Botre (1989) hypothesized that UA and CA might have a synergic pattern in enzyme catalyzed reactions and work together to regulate CaCO₃ formation. Achal and Pan (2011) recently reported the precipitation of CaCO₃ by UA and CA in *Bacillus* species but their study do not reveal the role of these enzymes and their relation in bacterially induced calcium carbonate precipitation.

Table 4.2.17. Comparison of carbonic anhydrase activity (U/ml) produced by the bacterial isolates at different time intervals

Time (hrs)	Carbonic Anhydrase activity (U/ml)					
	24	48	72	96	120	144
Bc P	43 ± 2.5a	54 ± 1.6a	88 ± 3.2a	124 ± 3.8a	99 ± 4.2a	88 ± 3.3a
SS3	35 ± 1.7b	48 ± 1.6b	77 ± 2.1b	115 ± 3.6b	87 ± 2.7b	74 ± 2.4b
SS5	28 ± 1.3c	41 ± 2.1c	69 ± 2.3c	90 ± 3.1c	62 ± 2.4d	51 ± 2.7e
SS13	31 ± 1.6b	44 ± 1.3b	58 ± 2.4d	62 ± 2.7e	70 ± 3.1c	56 ± 1.3d
SS15	25 ± 1.6d	42 ± 1.3c	65 ± 1.7c	72 ± 2.4d	85 ± 2.8b	67 ± 2.1c
SS18	28 ± 1.8c	37 ± 1.5d	42 ± 2.4f	52 ± 2.8f	58 ± 1.7e	48 ± 1.8f

Values bearing different letters in the same column are significant at P<0.05. Values are mean ± SD (n=3).

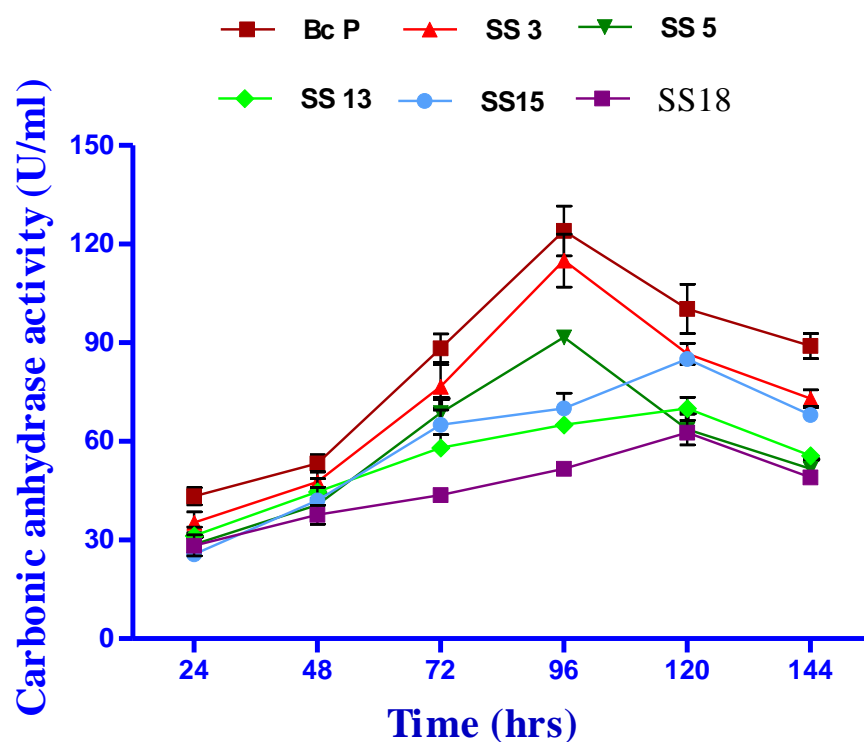


Fig. 4.2.20. Carbonic anhydrase activity by bacterial isolates at various time intervals. Lines represent mean \pm SD (n =3).

4.2.4.3. Enzyme kinetics of CA from different bacterial isolates

The enzyme kinetics of crude enzyme extracts of CAs from all the isolates were also determined and compared with *Bacillus pumilus* (Bc P), which is a known CA producing bacterial isolate. The kinetic parameters - maximum reaction velocity (V_{max}) and apparent Michaelis constant (K_M) for all the isolates were determined at varying substrate p-NPA concentrations (1 – 5 mM). Distinct differences among all the isolates in terms of substrate affinity (K_m) and rate values (V_{max}) were noticed. The K_m for Bc P, SS3, SS5, SS13, SS15 and SS18 were found to be 1.73, 1.88, 1.97, 2.19, 2.06 and 2.31 mM whereas the V_{max} for Bc P, SS3, SS5, SS13, SS15 and SS18 was found to be 0.98, 0.73, 0.67, 0.58, 0.62 and 0.53 $\mu\text{mol}/\text{min}$ respectively (Table 4.2.18).

Table 4.2.18. Enzyme kinetics of crude carbonic anhydrases from different bacterial isolates

Bacterial isolate	K_m (mM)	V_{max} ($\mu\text{mol}/\text{min}$)
Bc P	1.73	0.98
SS3	1.88	0.73
SS5	1.97	0.67
SS13	2.19	0.58
SS15	2.06	0.62
SS18	2.31	0.53

Yadav *et al.* (2012) reported the K_m and V_{max} for purified CA from *B. pumilus* as 1.594 mM and 1.307 $\mu\text{mol min}^{-1}$ while in case of immobilized CA, it was reported as 1.727 mM and 1.189 $\mu\text{mol min}^{-1}$. Both these enzymes showed reasonably good CO_2 sequestration capability leading to precipitation of CaCO_3 . As all the isolates of the present study were having sufficient CA activity which responds well to pNPA, so, the kinetics study has paved the way for investigation of CA in bacterially induced calcium carbonate precipitation from ureolytic bacterial species.

4.2.4.4. Activity staining of carbonic anhydrase from different bacterial isolates

Activity staining of bacterial CAs within the gel by electrophoresis has been recently introduced for investigating these enzymes based upon color change of bromothymol blue in presence of CA (Ramanan *et al.*, 2009). Hou *et al.* (2000) exhibited the presence of yellowish bands in blue background of bromothymol blue in case of CA from dioscorins, i.e. storage proteins of yam tubers. In the present study, carbonic anhydrase activity staining of

crude enzyme extracts was performed in 15% SDS–PAGE gels followed by color change with bromothymol blue stain. CA activity revealed yellow bands against the blue background of bromothymol blue in all the enzyme extracts (Fig 4.2.21) confirming visually the presence of CAs. The size of the enzymes ranged between 24 – 28 kDa.

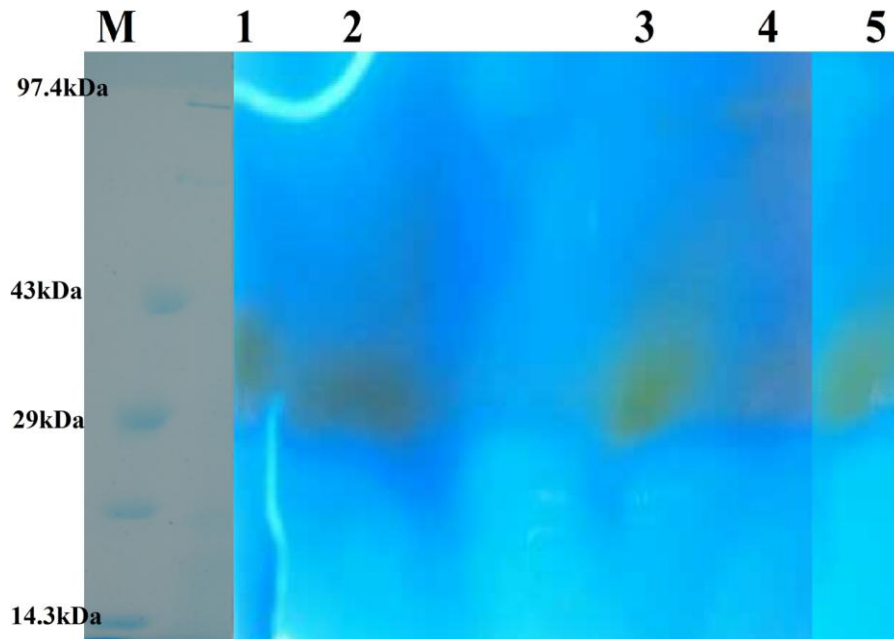


Fig. 4.2.21. Carbonic anhydrase activity staining of different bacterial isolates

Ramanan *et al.* (2009) reported positive yellow bands in CAs of *Proteus vulgaris* RS7; *Citrobacter freundii* SW3; *Bacillus subtilis* SA3; *Enterobacter sp.*, RS1. Sharma *et al.* (2010) isolated CA from *Enterobacter taylorae*, *Aeromonas hydrophila*, *Aeromonas caviae*, *Pseudomonas fragii* which was reported to be 29 around kDa. Similar results have been reported for α -CA in *Helicobacter pylori*, *Rhodopseudomonas palustris* and *Chlamydomonas reinhardtii* (Chirica *et al.*, 2002; Pushkas *et al.*, 2000; Rawat & Moroney, 1995). On the basis of molecular weight in the region of ~29 kDa, it can be predicted that the CA from the isolates of present study belong to α - class.

Present investigation revealed that *B. megaterium* SS3 is the most potent strain for production of both urease and carbonic anhydrase and should be investigated further to

study the influence of both these enzymes in CaCO₃ precipitation. This might help in finding a beneficial microbial calcite producing isolate for long-term goal of development of an efficient bioreactor for production of microbially induced carbonates.

4.2.5. Influence of UA and CA in calcium carbonate precipitation

In order to understand the detailed role of urease and carbonic anhydrase in bacterially induced CaCO₃ precipitation, most efficient urease and carbonic anhydrase producing bacterial isolate SS3 was selected to investigate the role of these enzymes.

4.2.5.1. Effect of inhibitors on UA and CA enzyme activity

In order to investigate the effect of both urease and carbonic anhydrase enzymes on CaCO₃ precipitation, it is pre-requisite to inhibit these enzymes and check the level of reduction of calcium carbonate. For inhibition of urease enzyme, *B. megaterium* SS3 cells were treated with Acetohydroxamic acid (AHA) i.e. potent inhibitor of urease while CA inhibition was done by Acetazolamide (ACZ), which is sulfonamide and a known inhibitor of CA (Bachmeier *et al.*, 2001; Li *et al.*, 2011). Bacterial cells were treated with both the inhibitors individually as well as in combination in order to inhibit these enzymes singly as well as together. Inoculums were taken at different time intervals and both the activities were estimated.

Fig. 4.2.22 a,b demonstrates that in case of untreated bacterial cells, urease (UA) activity of *B. megaterium* SS3 increased significantly with increase of incubation time along with pH and the maximum activity was observed at 96 hrs as discussed earlier (Table 4.2.18). But in case of AHA treated cells, more than 80% of the urease activity was successfully inhibited. This compound chelates the nickel atoms at the active site of the enzyme. pH of the culture filtrate in this case did not increase with increase in time due to inhibition of urease activity. It clearly showed that urease enzyme is involved in maintaining pH in the alkaline range. Acetohydroxamic acid has also been reported to inhibit urease of *B. pasteurii* (Bachmeier *et al.*, 2001).

In case of untreated *B. megaterium* SS3 cells, there was rising trend in carbonic anhydrase activity with increase of incubation time and maximum activity was recorded at 96 hrs as discussed earlier (Fig. 4.2.22 c; Table 4.2.18). The pH of the culture did not change much in the later hours though initially there were minor changes. In case of ACZ treated cells, there was significant fall in the enzyme activity (Fig. 5.22 d). pH was slightly increased during initial 6 hours from 8.3 at 2 hrs to 8.6 after 6 hrs but later remained constant. As CA plays a role in acid production, inhibition of CA hindered this and caused increase in pH during the initial time periods. But later on, due to some compensatory mechanism or up regulation of urease, net effect of CA inhibition was suppressed (Pedrozo *et al.*, 1997).

Supplementation of both enzyme inhibitors (AHA + ACZ) in the culture medium inhibited both UA and CA activity almost completely (Fig.4.2.22 e-f). Urease activity was found to be inhibited to a higher extent compared to addition of only Acetohydroxamic acid (AHA) while the pH pattern was almost similar to that of urease inhibition alone. The increase in pH due to CA inhibition seems to be suppressed by urease inhibition. This seems to be attributed to the dominant role of urease in pH maintenance.

In order to determine the rate of urea hydrolysis in urease induced as well as inhibited sets, the amount of urea remaining at different time intervals was also determined (Table 4.2.19; Fig. 4.2.23). In case of urease induced set, the rate of urea hydrolysis was quite high during first 24 hours showing around 30 % hydrolysis. In case of urease inhibited set, amount of urea hydrolysis was insignificant. This further proved the role of urease in maintaining alkaline pH due to hydrolysis of urea.

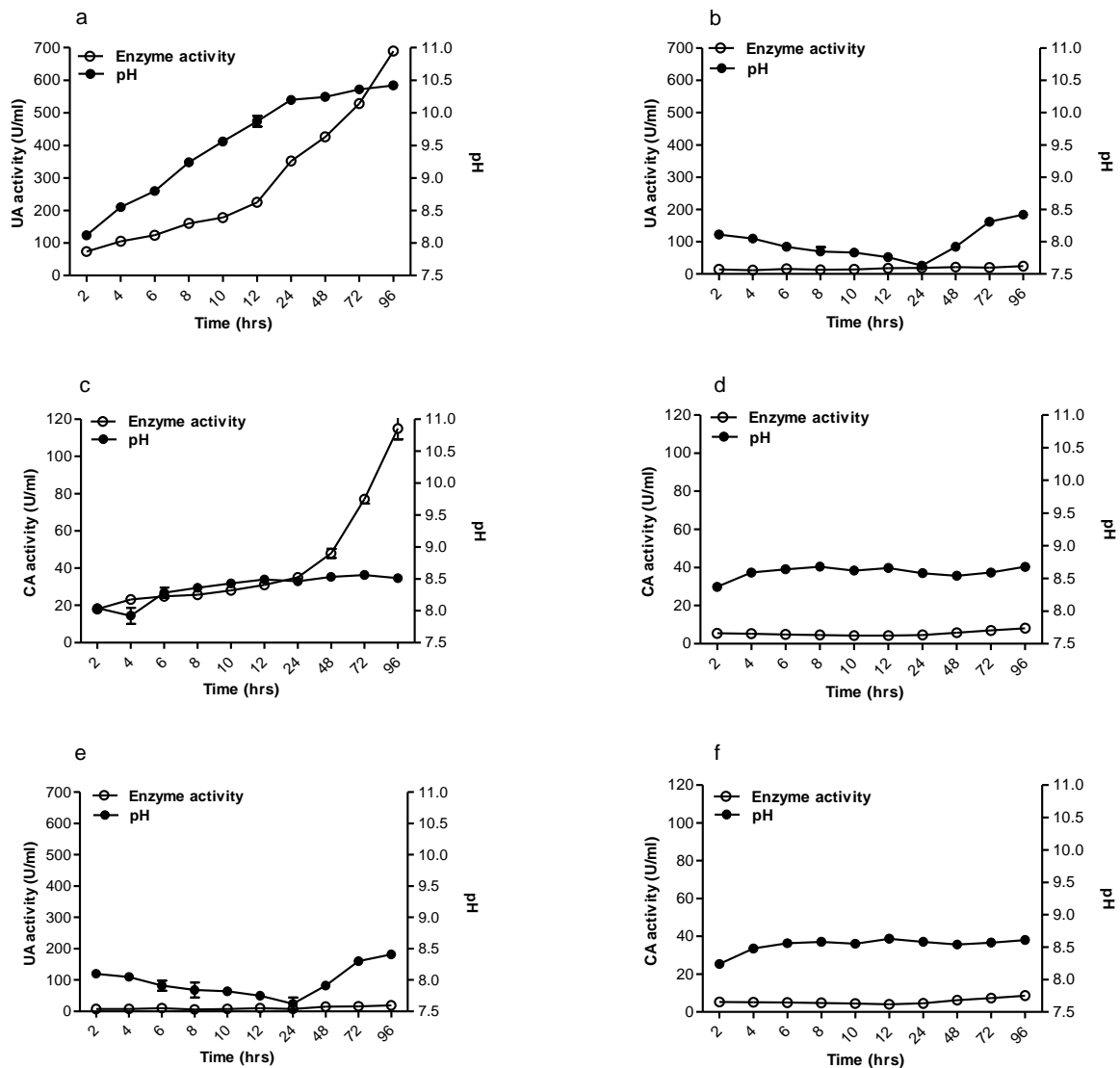


Fig. 4.2.22. Urease activity (UA), Carbonic anhydrase activity (CA) and pH profile of *B. megaterium* SS3.

- (a) UA activity and pH profile of bacterial culture group
- (b) UA activity and pH profile in presence of acetohydroxamic acid (AHA)
- (c) CA activity and pH profile of bacterial culture group
- (d) CA activity and pH profile in presence of acetazolamide (ACZ)
- (e) UA activity and pH profile in presence of both AHA and ACZ
- (f) CA activity and pH profile in presence of both AHA and ACZ.

Table 4.2.19. Urea hydrolysis in case of bacterial culture and urease inhibited bacterial culture

Time (Hrs)	mM remaining urea (Bacterial culture)	mM remaining urea (Bacterial culture + AHA)
0	330 ± 5a	330 ± 7a
12	243 ± 12c	323 ± 8a
24	198 ± 14d	319 ± 4a
36	113 ± 9e	314 ± 6a
48	94 ± 6f	311 ± 7a
60	74 ± 4g	309 ± 4a
72	52 ± 7h	308 ± 8a
84	44 ± 5i	304 ± 5a
96	38 ± 4i	301 ± 9a

Values bearing different letters in the same column are significant at $P < 0.05$. Values are mean \pm SD (n=3).

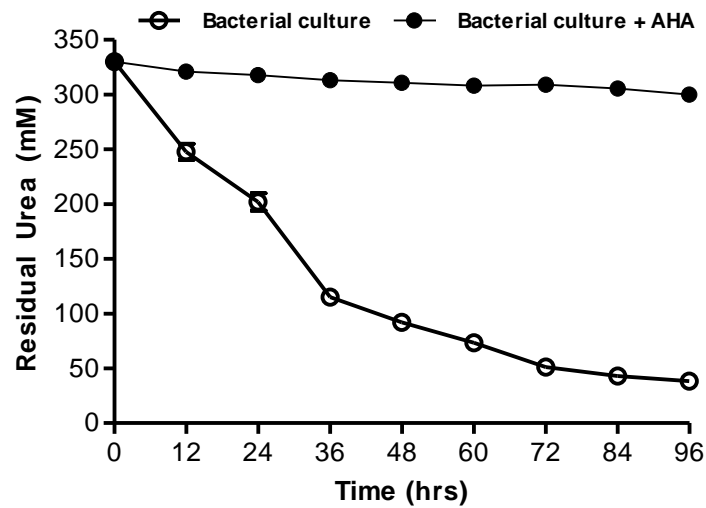


Fig. 4.2.23. Estimation of urea hydrolysis in urease induced and urease inhibited (+ AHA) bacterial culture. Lines represent mean \pm SD (n=3).

4.2.5.2. Effect of UA and CA inhibition on CaCO₃ precipitation in vitro

The descending trend in the concentration of Ca²⁺ was observed in all the test sets of experimental systems (Fig. 4.2.24). The concentration of Ca²⁺ decreased sharply during first 4 hrs of experiment and then decreased gradually and approached equilibrium. In general, the concentration of Ca²⁺ in the test groups with bacteria decreased more rapidly than without bacteria in both UA and CA systems. Immediate precipitation of CaCO₃ was observed in urease induced bacterial culture as well as crude enzyme set during first 2 hours (Fig. 4.2.24a). The Ca²⁺ concentration in UA induced bacterial culture reduced significantly up to 6 hrs and attained equilibrium after 6 hrs whereas in crude enzyme solution Ca²⁺ level decreased up to 12 hrs and reached equilibrium thereafter. The Ca²⁺ level reduction is higher in case of bacterial culture than crude urease enzyme solution. At the end of 24 hrs, Ca²⁺ that remained in the solution was 4.4 mM and 7.5 mM in bacterial culture and urease enzyme solution, respectively. In presence of UA inhibitor, Ca²⁺ levels reduced up to 4 hrs and approached equilibrium thereafter. In case of bacterial culture UA inhibitor case, Ca²⁺ concentration left in the bacterial solution was 17.3 mM while in case of UA inhibitor enzyme solution, the Ca²⁺ concentration was found to be 17.8 mM after 24 hrs.

The Ca²⁺ concentration in CA induced bacterial culture drastically reduced in first 2 - 4 hrs which showed that CA enhances the rate of reaction, while it decreased gradually thereafter and attained equilibrium after 12 hrs (Fig. 4.2.24 b). In case of crude enzyme solution, Ca²⁺ level decreased gradually up to 24 hrs. The Ca²⁺ level reduction is higher in case of bacterial culture than crude enzyme solution. The amount and rate of Ca²⁺ precipitation was higher in case of CA induced set compared to urease induced set during the initial 4 hours. After 4 hrs, the level of Ca²⁺ concentration in case of bacterial culture was 8.9 mM while it was 13.6 mM in case of CA enzyme solution. At the end of 24 hrs, Ca²⁺ remained in the solution was 5.2 mM and 8.5 mM in bacterial culture and enzyme solution, respectively. In presence of CA inhibitor, Ca²⁺ levels reduced up to 10 hrs and approached equilibrium thereafter. After 4 hrs, the level of Ca²⁺ concentration in case of bacterial culture with CA inhibitor was 18.1 mM while in case of enzyme solution inhibitor set, it was 18.5 mM. After 24 hrs, Ca²⁺

remained in the culture group was 9.4 mM while 12.0 mM remained in enzyme solution group.

In case of both UA and CA induced bacterial set, soluble Ca^{2+} found at the end of 24 hrs was found to be 3.4 mM and 6.2 mM in case of crude enzymes which was much lower compared to individual enzymes (Fig. 4.2.24 c). This proved maximum precipitation when both the enzymes are induced and depicted their synergism in CaCO_3 precipitation. When both UA and CA inhibitors were supplemented in the bacterial medium, the soluble Ca^{2+} concentration present in the solution was found to be 20.1 mM after 24 hours and 20.6 mM in case of inhibited crude enzyme solutions which was again higher compared to individual inhibitors.

The overall inhibition of calcium carbonate deposition is much higher in presence of UA inhibitor compared to CA inhibitor but during earlier hours, the rate of carbonate precipitation was found to be much higher in case of CA induced system. These results suggest that in case of *B. megaterium* SS3, most of the Ca^{2+} deposition during early hours is mediated by both urease and CA enzyme but later on, urease seems to be the primary component as the effect of CA inhibition on calcium carbonate precipitation was quite low in the later hours. The inhibition of urease reduced the amount of CaCO_3 precipitation as well as pH signifying the role of urease in CaCO_3 precipitation. Bang and Ramakrishnan (2001) reported that urease is the main component that initiates CaCO_3 precipitation.

Though application of CA in CO_2 sequestration had been successfully proved by many but till now, the effect of bacterial CA on CaCO_3 precipitation had not been elucidated in depth (Wanjari *et al.*, 2011; Ramanan *et al.*, 2008; Yadav *et al.*, 2011). Li *et al* (2011; 2012) reported that bacterial CA can promote CaCO_3 as an activator. Botre and Botre (1989) also reported that in enzyme catalysed reactions, increase in the rate of removal of CO_2 from solution facilitated by CA increases the rate of production of NH_3 consequent from urea dissociation. But in the present study, we have deduced the effect of CA inhibition on CaCO_3 precipitation in depth.

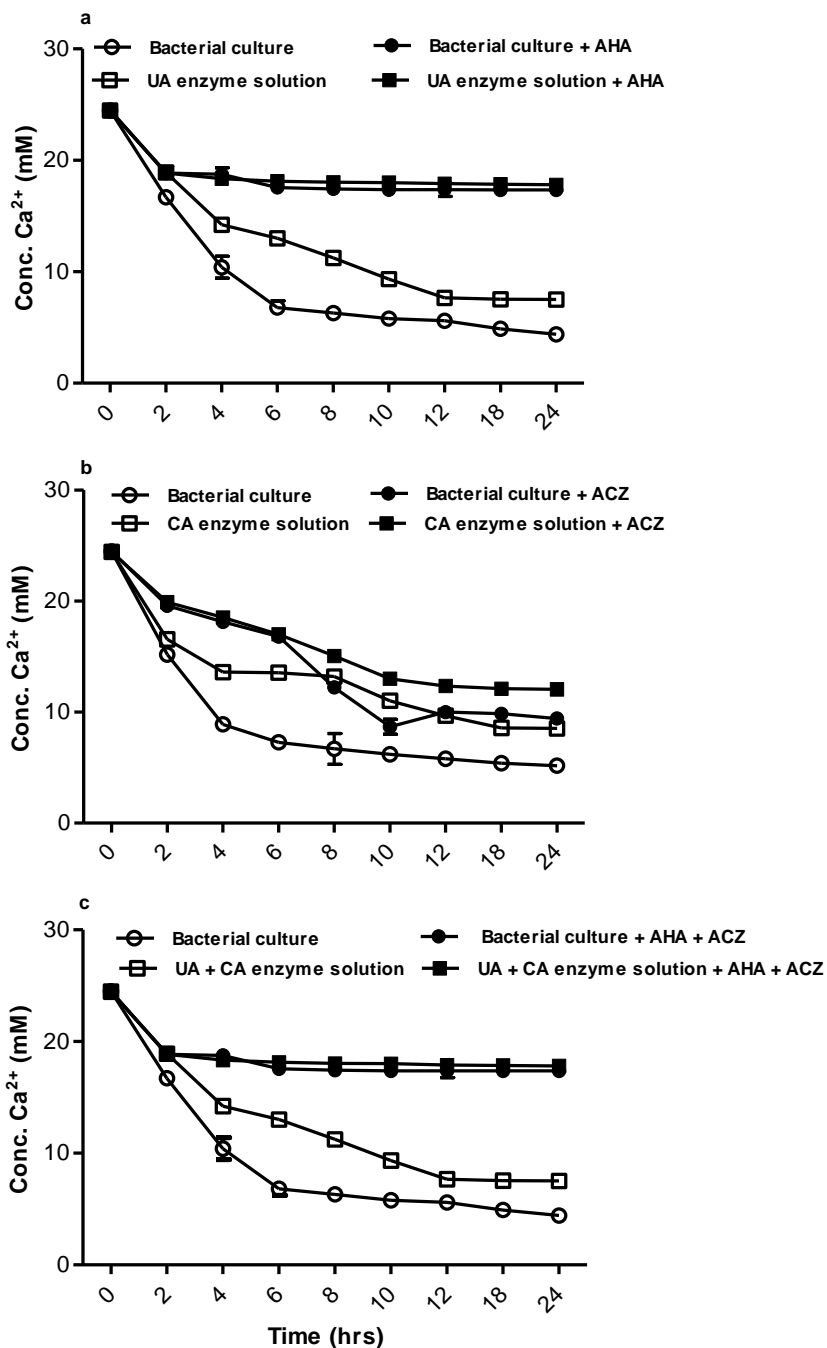
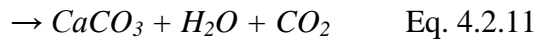
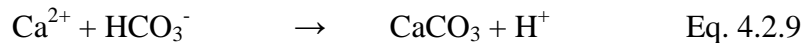


Fig. 4.2.24. Change of Ca^{2+} concentration of *Bacillus megaterium* SS3 with time under different treatments. (a) UA culture, UA culture + AHA, UA enzyme solution, UA enzyme solution + AHA (b) CA culture, CA culture + ACZ, CA enzyme solution, CA enzyme solution + ACZ (c) UA + CA culture, UA + CA culture + AHA + ACZ, UA + CA enzyme solution, UA + CA enzyme solution + AHA + ACZ.

Hydrolysis of urea results in accumulation of both bicarbonate and ammonia in the cell, which favors the physiological and regulatory links between urea and bicarbonate metabolism (Stahler *et al.*, 2005). The incorporation of nickel into the active site of urease is dependent on CO₂/ HCO₃⁻ metabolism which is in turn regulated by carbonic anhydrase (Park and Hausinger, 1995). Following reactions involving UA and CA might be taking place during CaCO₃ precipitation (Li *et al.*, 2011):



In the above results, the rate of Ca²⁺ precipitation was significantly faster with bacterial system compared to only enzyme solutions and some precipitation of Ca²⁺ occurred even in the presence of inhibitors, this showed the involvement of other bacterial cell components in calcium deposition. Li *et al.* (2011) also suggested that bacterial culture and culture filtrate might have other metabolites produced or secreted by bacteria during the growth and metabolic processes, as well as residual medium ingredients, which have some effects on CaCO₃ precipitation. Watanabe *et al.* (2003) reported the possible role of matrix proteins in formation of calcified hard tissues in invertebrates and pointed those matrix proteins may promote nucleation of calcium crystals.

The present results were in agreement with Pedrozo *et al.* (1997) where it was concluded that ammonia, produced by urease-mediated hydrolysis of urea, acts as a proton acceptor, which promotes carbonate formation from HCO₃⁻, ultimately promoting CaCO₃ precipitation. Rodriguez - Navarro *et al.* (2012) recently found that once supersaturation of calcium ions is achieved in the surrounding of bacterial cells and within bacterial biofilms, CaCO₃ formation by heterogenous nucleation occurs readily on bacterial cell walls as well on EPS.

The saturation index, SI ($SI = \log \Omega = \log IAP/Ks$; where Ω is the saturation state of the system, IAP is the ion activity product and Ks is the thermodynamic solubility product of the relevant phase) of the present medium with respect to $CaCO_3$ phases was also calculated by Visual Minteq software (Visual MINTEQ, version 2.01b; KTH, Stockholm, Sweden). It was found that the bacterial medium was saturated with all the three phases of calcium carbonate ($SI_{\text{calcite}} = 3.47$, $SI_{\text{aragonite}} = 3.34$ and $SI_{\text{vaterite}} = 2.94$). It has already been reported that $CaCO_3$ precipitation in microbial systems typically occurs when the saturation index is above 1.0 (Rodriguez Navarro *et al.*, 2012). However, lesser precipitation was observed for bacterial enzyme inhibited sets as in those cases, there is no increase in the supersaturation which is necessary to induce heterogenous crystallization of $CaCO_3$ on the surface of bacterial cells as well as on EPS (Rodriguez Navarro *et al.*, 2012).

4.2.5.3. Effect of UA and CA inhibition on carbonate precipitation in sand plugs

The $CaCO_3$ content (weight %) in sand columns prepared with UA and CA induced and inhibited bacterial cultures were tested. The $CaCO_3$ content of the sand column without any inhibitor was about 32%. In case of UA inhibition alone, the $CaCO_3$ precipitated was 19% while in case of CA inhibition, it was 27%. When both the inhibitors were added, the $CaCO_3$ content determined was 15% which showed about 50% reduction compared to bacterial treatment (Table 4.2.20; Fig. 4.2.25). This further confirmed that both UA and CA inhibition reduces $CaCO_3$ precipitation suggesting the synergistic role of these enzymes in $CaCO_3$ precipitation.

4.2.5.4. Effect of UA and CA inhibition on morphology and constituents of $CaCO_3$ crystals

SEM analysis clearly indicated the presence of calcite and vaterite crystals in bacterial treated samples (Fig. 4.2.26 A-D). The crystals had rough surfaces and spherical as well as rhombohedral shapes (Fig. 4.2.26 A-B). There was not much difference in the morphology of crystals in all the sets with bacterial inoculations with or without inhibitors. Rod shaped bacterial cells in close contact with the crystals were clearly observed (Fig. 4.2.26 C-D). The presence of crystals associated with bacteria proves that bacteria served as nucleation sites

during the mineralization process which has been reported earlier by other researchers (Ferris *et al.*, 1987; Li *et al.*, 2011). Lian *et al.* (2006) demonstrated that the process of carbonate crystal formation by SS3 involved the nucleation of calcite on the bacterial cell walls.

Table 4.2.20. Amount of calcite precipitation in sand plugs treated with bacterial culture and bacterial culture supplemented with UA and CA inhibitors

Treatment	Calcite content (%)
Bacterial culture	33 ± 4.0a
Bacterial culture + AHA	19 ± 2.8c
Bacterial culture + ACZ	27 ± 3.6b
Bacterial culture + AHA + ACZ	13 ± 2.8cd

Values bearing different letters in the same column are significant at $P < 0.05$. Values are mean ± SD (n = 3).

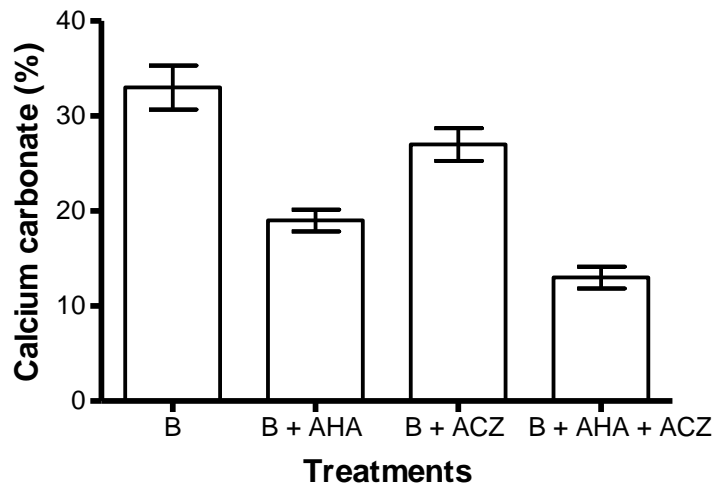


Fig. 4.2.25. Effect of UA inhibition (B + AHA), CA inhibition (B + ACZ) and simultaneous inhibition of UA and CA (B + AHA + ACZ) along with UA and CA induced bacterial culture (B) on calcium carbonate precipitation of *B. megaterium* SS3 in sand plugs.

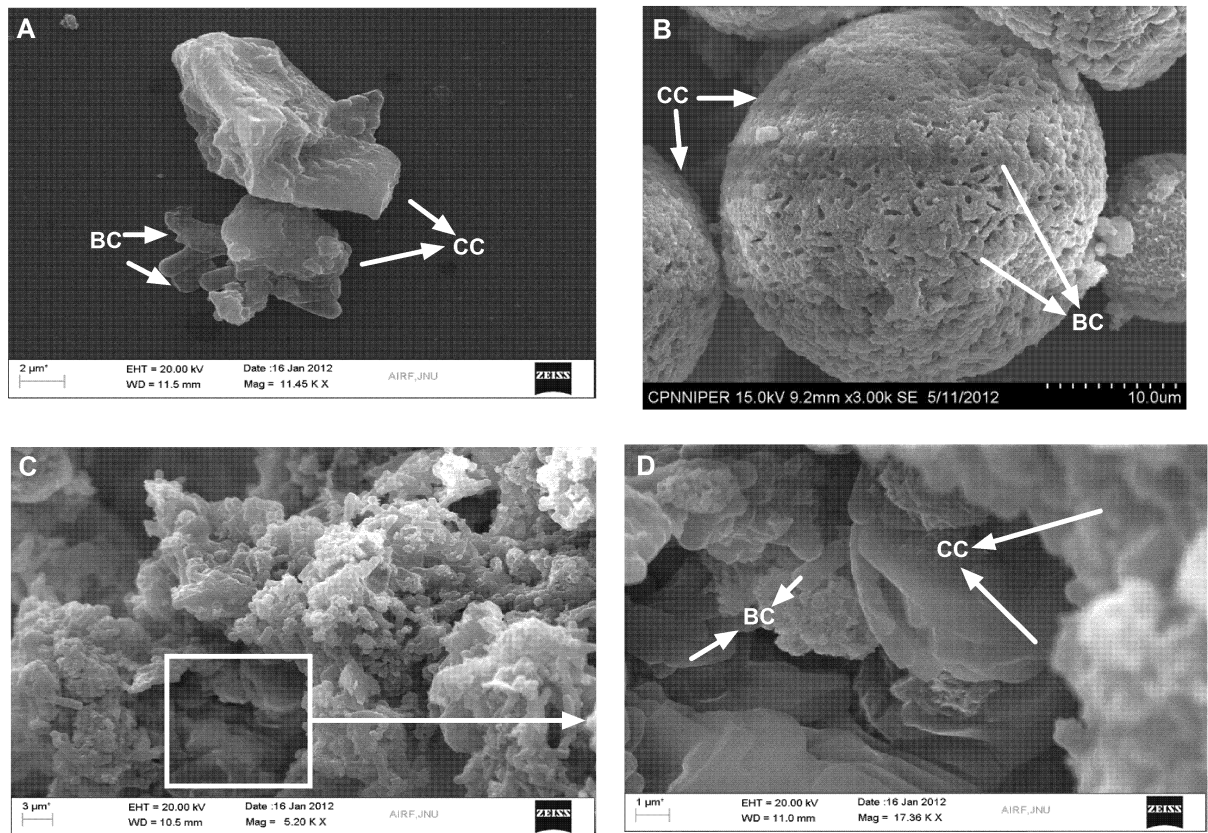


Fig. 4.2.26. SEM images of calcium carbonate crystals (CC) associated with bacterial cells (BC)

XRD analyses of pure carbonate crystals showed that majority of the carbonate deposits were calcite and vaterite (Fig. 4.2.27a). In case of bacterial sand columns also, calcite and vaterite were the major forms while in case of untreated sand column, no calcium carbonate peak was recorded (Fig. 4.2.27 b-d). EDX analysis further revealed the mineral constituents of sand columns. High amount of calcium was seen in case of bacteria treated sand column while very low calcium content was recorded in control sand column (Fig. 4.2.28).

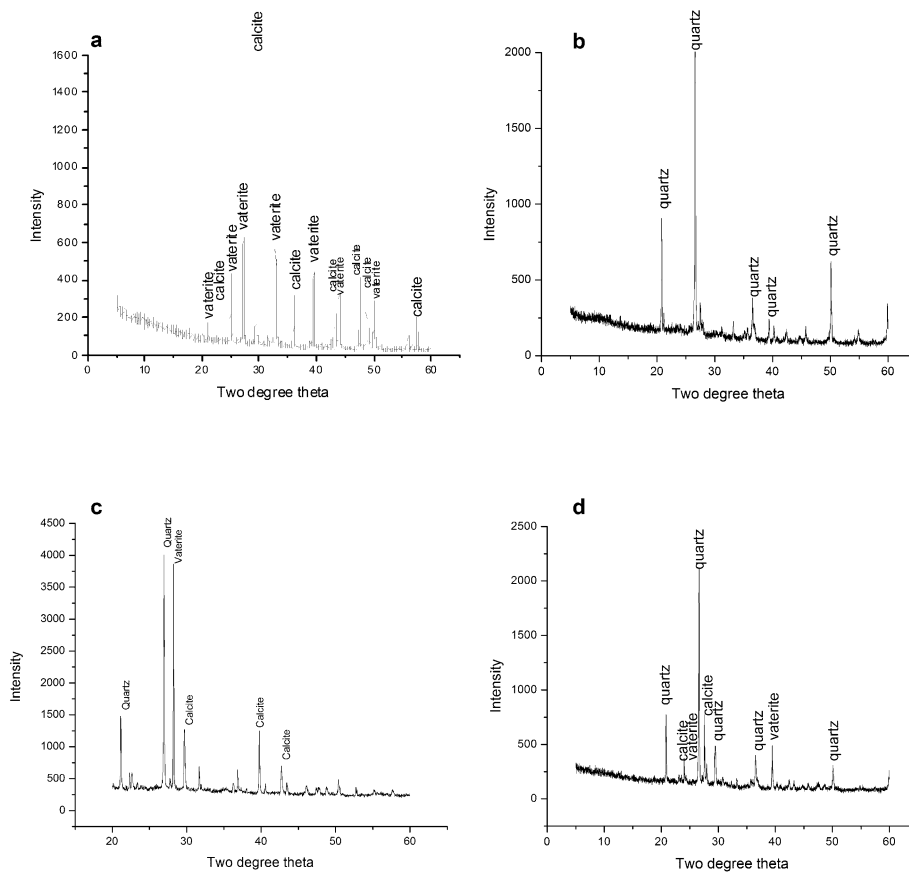


Fig. 4.2.27. XRD analysis of different carbonate crystals (a) Pure calcium carbonate crystal (b) Untreated sand column (c) Bacterial treated sand column (d) Both UA and CA inhibited sand column.

The data presented in this investigation demonstrate that both urease and carbonic anhydrase play important role in bacterially induced calcite precipitation. Observing the decreased calcification upon inhibition of any of the two enzymes, we can undoubtedly say that efficient calcification is dependent upon the activity of both the enzymes. We have hereby elucidated the role of bacterial urease and CA as well as their synergistic effect in calcification by *B. megaterium*. The main role of CA seems to be in production of CO₂ and bicarbonate ions and that of urease is in maintaining the pH.

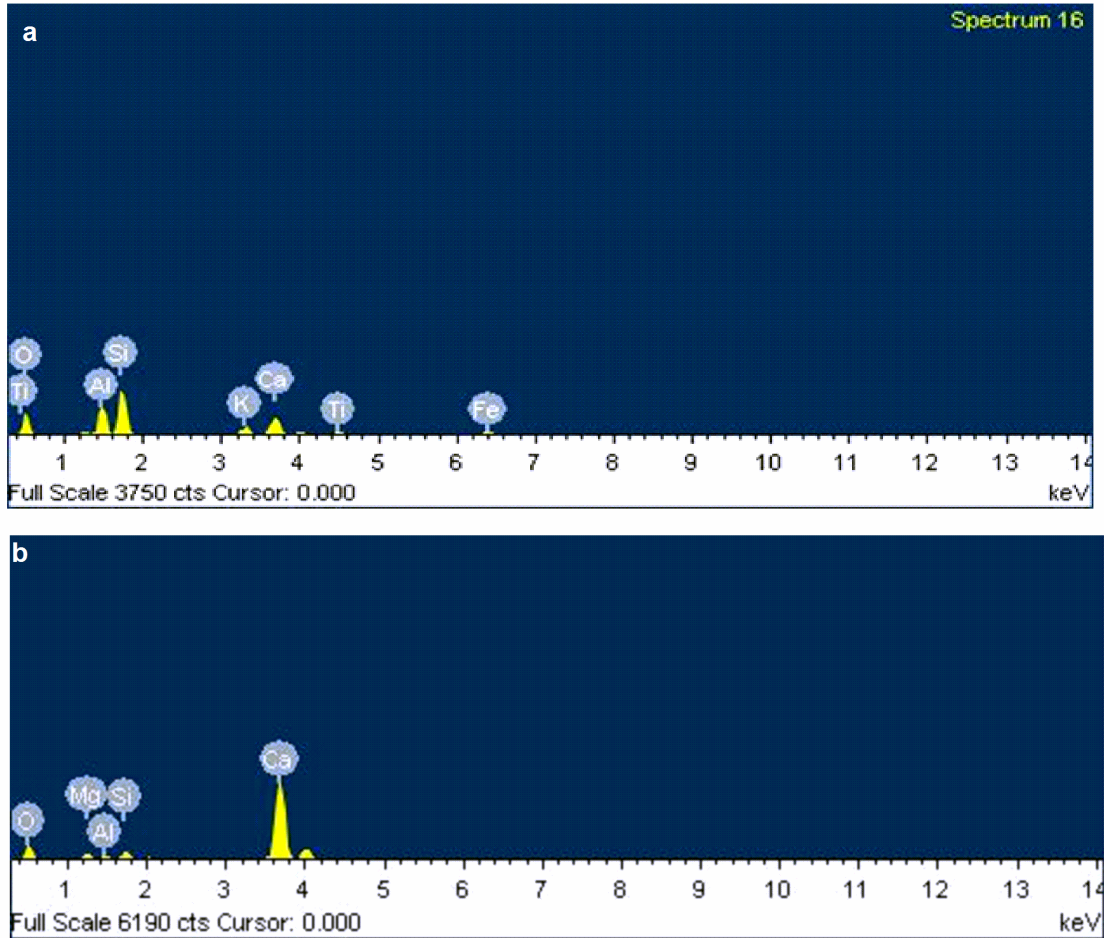


Fig. 4.2.28. Amount of Ca in a) UA and CA inhibited sand column b) bacterial treated sand column

4.2.6. Calcium carbonate precipitation via CA in different bacterial isolates

After investigating the effect of CA from SS3 in CaCO_3 precipitation, an attempt was made to study the precipitation of CaCO_3 via CA in all other bacterial isolates (Fig. 4.2.29; Table 4.2.21). It was noticed that the concentration of insoluble Ca^{2+} showed ascending trend in bacterial CA induced sets while there was minor change in the concentration of Ca^{2+} in the control group during initial 4 hours. The concentration of Ca^{2+} increased sharply in all bacterial CA induced sets during the first 8 hours. Though calcium carbonate precipitation occurred successfully in all CA sets, but it was less efficient as compared to ureolytic carbonate precipitation.

Table 4.2.21. Amount of insoluble Ca^{2+} precipitated by different bacterial isolates over different intervals of time via CA pathway

Insoluble Ca^{2+} ions							
Time (Hrs)	Bc P	SS3	SS5	SS13	SS15	SS18	Control
0	$0.52 \pm 0.0a$	$0.52 \pm 0.0a$	$0.52 \pm 0.0a$	$0.52 \pm 0.0a$	0.52 ± 0.0	$0.52 \pm 0.0a$	$0.53 \pm 0.0a$
2	$8.0 \pm 0.5a$	$7.9 \pm 0.8a$	$6.5 \pm 0.1b$	$7.2 \pm 0.2ab$	$7.5 \pm 0.8a$	$7.1 \pm 0.4ab$	$3.7 \pm 0.0e$
4	$12.8 \pm 0.7a$	$11.8 \pm 1.4a$	$9.5 \pm 0.9b$	$9.9 \pm 0.9b$	$11.6 \pm 0.6a$	$10.4 \pm 0.7ab$	$4.6 \pm 0.1e$
6	$14.7 \pm 0.9a$	$13.6 \pm 1.2ab$	$12.1 \pm 1.4b$	$12.6 \pm 1.3b$	$14.7 \pm 0.9a$	$13.3 \pm 1.3ab$	$5.9 \pm 0.1d$
8	$17.9 \pm 1.7a$	$16.5 \pm 1.9a$	$14.2 \pm 1.3b$	$15.8 \pm 1.5a$	$15.9 \pm 1.3a$	$17.7 \pm 0.9a$	$5.8 \pm 0.2d$
10	$19.7 \pm 1.9b$	$18.4 \pm 1.4b$	$18.1 \pm 1.8b$	$17.5 \pm 1.9ab$	$17.9 \pm 1.2ab$	$21.8 \pm 1.4a$	$6.2 \pm 0.4d$
12	$21.3 \pm 1.2a$	$20.3 \pm 1.2a$	$20.3 \pm 1.1a$	$19.2 \pm 1.3a$	$21.2 \pm 1.6a$	$21.7 \pm 1.5a$	$5.8 \pm 0.7d$
18	$22.1 \pm 0.8a$	$21.9 \pm 0.5a$	$19.1 \pm 0.9a$	$20.6 \pm 0.8a$	$22.1 \pm 0.8a$	$22.1 \pm 0.7a$	$6.1 \pm 0.4d$
24	$22.7 \pm 0.9a$	$22.2 \pm 0.4a$	$20.5 \pm 0.4a$	$22.8 \pm 0.5a$	$22.5 \pm 0.5a$	$22.4 \pm 0.4a$	$5.9 \pm 0.6d$

Values bearing different letters in the same column are significant at $P < 0.05$. Values are mean \pm SD (n=3).

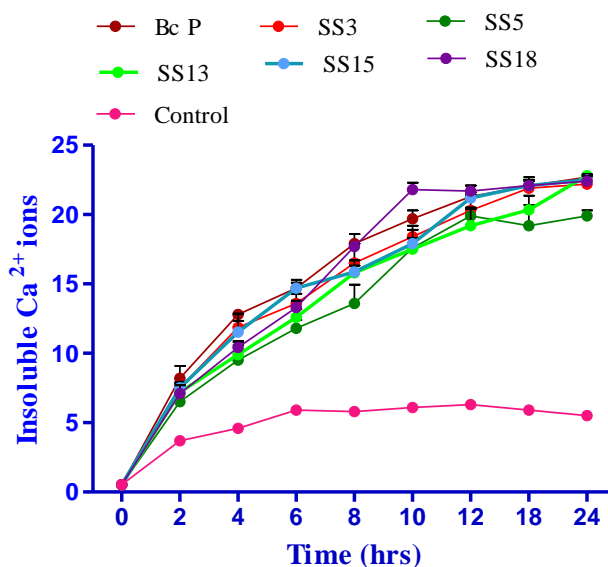


Fig. 4.2.29. Precipitation pattern of CaCO_3 by different CA producing bacterial isolates. Values are mean \pm SD (n=3).

This work further proved that precipitation of calcium carbonates via ureolytic pathway, in which bacterial urease promotes pH increase and leads to precipitation of carbonates is much more efficient and less time consuming. Though CA also plays an active role in precipitation of carbonates, and catalyzes the process at a very fast pace in the initial hours but compared to urease, much more needs to be investigated in order to promote the process of calcification via CA. Though CA might be acting synergistically with urease for bacterial calcium carbonate precipitation, but individually it is less efficient than the enzyme urease for inducing precipitation of carbonates.

Conclusion and salient features

In the present study, different parameters affecting the activity of ureases were studied. These included both chemical (media, substrate, calcium, nickel) as well as physical (pH and temperature) parameters. It was observed that urease activity varies significantly with change in any of the above cited parameters and therefore, they need to be optimized. pH 9 and 35°C was found to be more optimum physical conditions for almost all bacterial isolates which matched well with conditions of carbonate precipitation in soils. In case of chemical factors, it was seen that urea and calcium concentration play significant role in bacterial urease production. Compared to varying calcium concentration, varying concentration of urea produces greater control on urease activity. Around 2 fold increase was noticed in urease activity at 2% urea concentration. Results from the present study indicated that both urea & calcium activates urease till a particular concentration but beyond that there is decline in the urease activity which might be due to inhibitory effects of the by products formed. As urea and calcium concentration presents a means to control the level of urease activity, alteration in the concentration of both of these can generate known effect on the urease activity. The ureases from all the bacterial isolates were found to be quite stable over long time courses but after 5-6 days, urease activity declines. This might be due to depletion of nutrients, high pH or production of other proteases. To facilitate the recycling of degraded urease proteins, a complex system for controlled turnover of proteins might be involved. Damaged proteins like ureases are marked for destruction after certain time by covalent attachment of chains of proteins or by selective hydrolysis (Berg *et al.*, 2002). Rate of urea hydrolysis is quite high in

the initial times but not much change occurs after 5-6 days. All the bacterial isolates were found to produce significant amounts of ureases. The urease production profile was examined in complex nutrient medium and it was seen that all the isolates produced significant amounts of urease from early exponential phase to stationary phase. Enzyme kinetics as well as zymogram analysis also revealed the potential ureases in all bacterial isolates. In case of carbonate precipitation studies, all the bacterial isolates successfully induced the formation of carbonates though there were few differences in the rate and amounts of precipitation. It was observed that amongst all the bacterial isolates, *Bacillus megaterium* SS3 served as most potent isolate with maximum urease production and high amount of calcium carbonate precipitation.

Along with urease, carbonic anhydrase was also investigated for its role in MICCP. The results from the current study suggest that all the ureolytic bacterial isolates also harbour significant CA activity. Though ureases form the primary component but it was seen that CA also play synergistic role along with urease to induce carbonate precipitation. This work presented the first study on relation of bacterial ureases and CA as well as their role in MICCP by enzyme inhibition studies. Compared to ureolytic pathway for precipitation of carbonates, CA pathway was seen to be less efficient and effective.

These bacterial isolates provide well matched surface to seed calcium carbonate precipitation and promote supersaturation conditions paving way for their applications in production of carbonate binders for building materials.

4.3 Characterization of CaCO₃ precipitates

4.3.1. Isolation of CaCO₃ crystals

Calcium carbonate precipitation has been found to occur in all bacterial isolates. Though the process of carbonate mineralization by ureolytic bacterial isolates has been found to occur in wide range of environments including soils, lakes, caves and laboratory but there has been great variation in the phases of different carbonates (Baskar *et al.*, 2005; Novitsky, 1981; Rivadeneyra *et al.*, 2004). Characterization of the CaCO₃ phase forms the pre - requisite before application of these biominerals for various technical purposes. In the present study, all the bacterial carbonates were isolated, quantified and characterized by several microscopic and chemical analyses.

Precipitation of calcium carbonate crystals was observed in all the bacterial isolates with small variations. The carbonate crystals were found precipitated at the bottom of all bacterial inoculated flasks as well as along the sides of the walls. Differences in the amounts of carbonate crystal precipitates were noticeable visually (Fig. 4.3.1). The amount of precipitates increased with time in all the bacterial flasks. Insignificant precipitation was observed in the control sets without bacterial inoculation. All the isolates were capable of producing the crystals at temperature range from 30°C to 40°C. The formation of carbonate crystals by all the ureolytic bacterial isolates depicted their potential for biotechnological applications.

After a period of 3 weeks, all the carbonate crystals were isolated by filtration and quantified (Table 4.3.1). It was seen that carbonate crystal precipitation was highest in case of *B. megaterium* SS3 which produced 187 mg/100 ml precipitates followed by *B. subtilis* SS13 (178 mg/100 ml), *B. thuringiensis* SS15 (167 mg/100 ml), *B. cereus* SS5 (156 mg/100 ml) and *L. fusiformis* SS18 (152 mg/100 ml) (Fig. 4.3.2). Similar studies were also conducted by Zamarreno *et al.* (2009) who also found increase in the quantity of carbonate crystals by bacterial isolates from fresh waters.

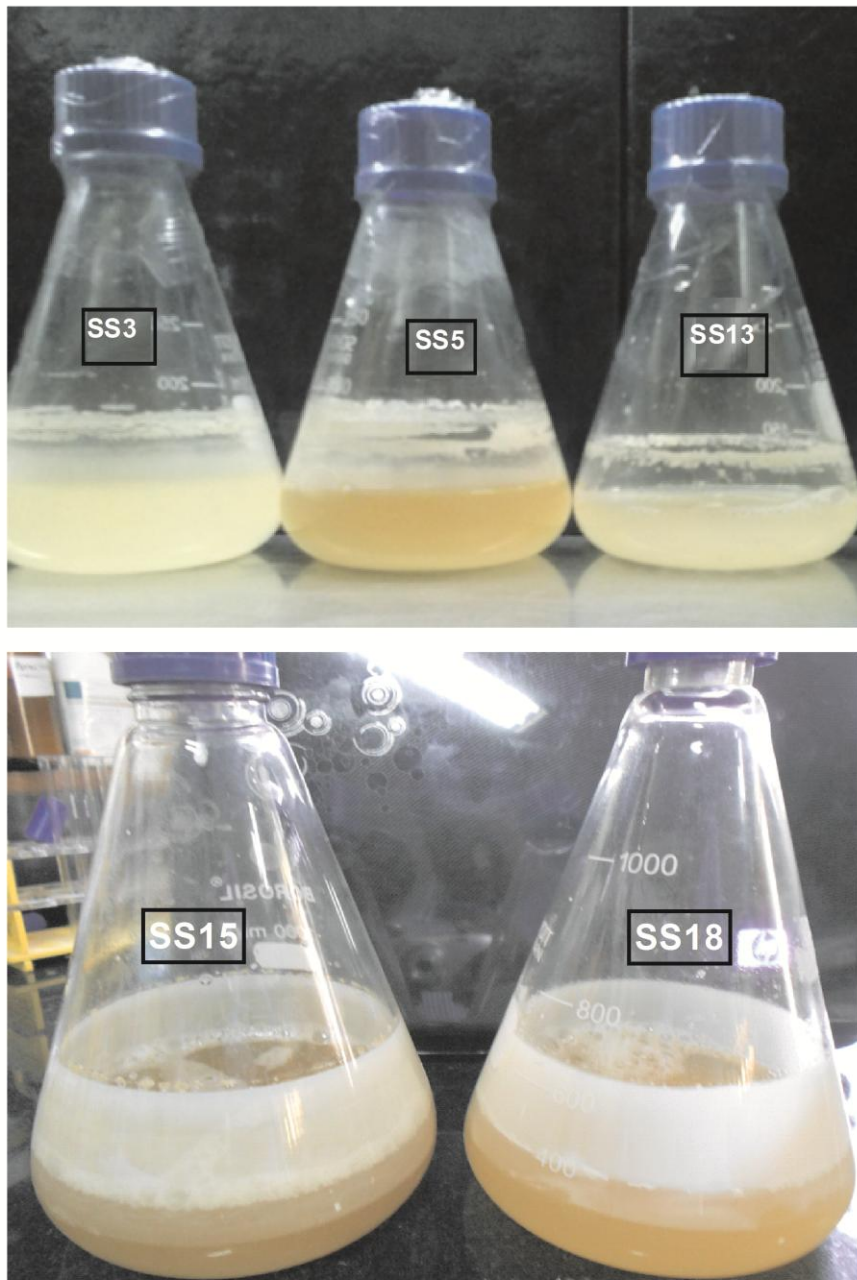


Fig. 4.3.1. Precipitates of CaCO_3 crystals along the walls as well as at bottom of culture flasks inoculated with *B. megaterium* SS3, *B. cereus* SS5, *B. subtilis* SS13, *B. thuringiensis* SS15 and *L. fusiformis* SS18.

Table 4.3.1. Calcium carbonate crystals precipitated by different bacterial isolates after 3 weeks.

Bacterial isolate	Carbonate crystals precipitated (mg/100ml)
<i>B. megaterium</i> SS3	187 ± 16a
<i>B. cereus</i> SS5	156 ± 15d
<i>B. subtilis</i> SS13	178 ± 11b
<i>B. thuringiensis</i> SS15	167 ± 17c
<i>L. fusiformis</i> SS18	152 ± 13d

Values bearing different letters in the same column are significant at $P < 0.05$. Values are mean ± SD.

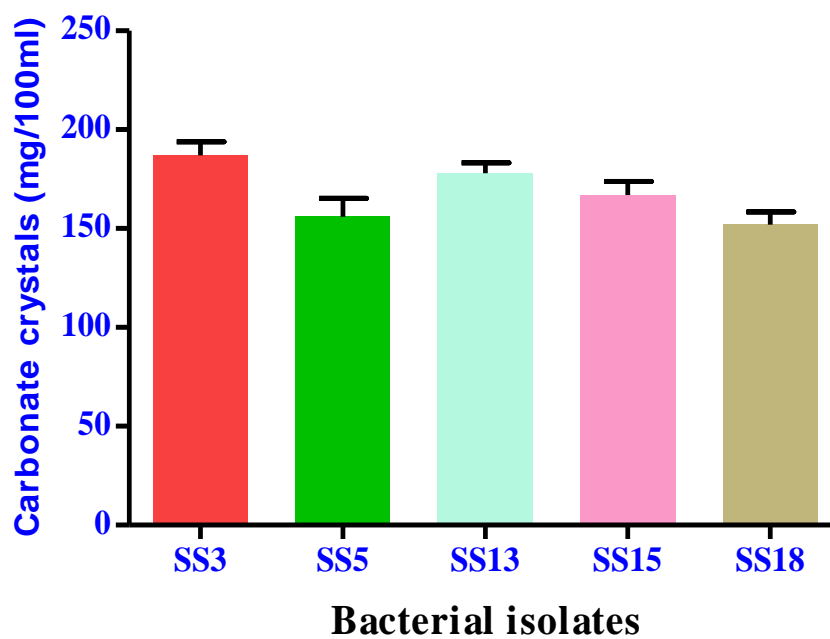


Fig. 4.3.2. Calcium carbonate crystals precipitated by different bacterial isolates after 3 weeks. Bars represent mean ± SD.

4.3.2. Characterization of CaCO₃ crystals

4.3.2.1. Methylene blue and PAS Staining of carbonate crystals

The isolated carbonate crystals were stained by Loeffler's methylene blue stain and observed with white light by the use of 1,000 x magnification. Different crystals displayed different shapes and sizes. Figure 4.3.3 depicts the morphology of all the crystals precipitated by different ureolytic bacterial isolates. *B. megaterium* SS3, *B. cereus* SS5 and *B. subtilis* SS13 formed comparatively bigger crystals compared to *B. thuringiensis* SS15 and *L. fusiformis* SS18. Crystals formed by *B. megaterium* SS3 were spherical, rhombohedral as well as few oval. *B. cereus* SS5 formed crystals with pointed edges but most of them were rhombohedral. In case of *B. subtilis* SS13 and *B. thuringiensis* SS15, the crystals were mostly spherical while in case of *L. fusiformis* SS18, they were again mixed spherical and rhombohedral. Few bacterial cells were also found to be associated to the crystals.

The polysaccharides associated with all the bacterial isolates were detected using alcian blue periodic acid Schiff stain (Fig. 4.3.4). Sections of crystals showed that bacteria were embedded inside as well as distributed on the outer surface of the carbonate crystals in all the cases. Acidic (blue) as well as neutral polysaccharides (pink) were clearly seen located in different areas of the carbonate crystals. Rod shaped bacterial cells were also visible in the centre as well as along the outer surface of the carbonate crystals. Methylene blue and alcian blue staining of carbonate crystals has also been reported by Zamarreno *et al.* (2009) and they found different polysaccharides in which bacteria were embedded inside the crystal structures.

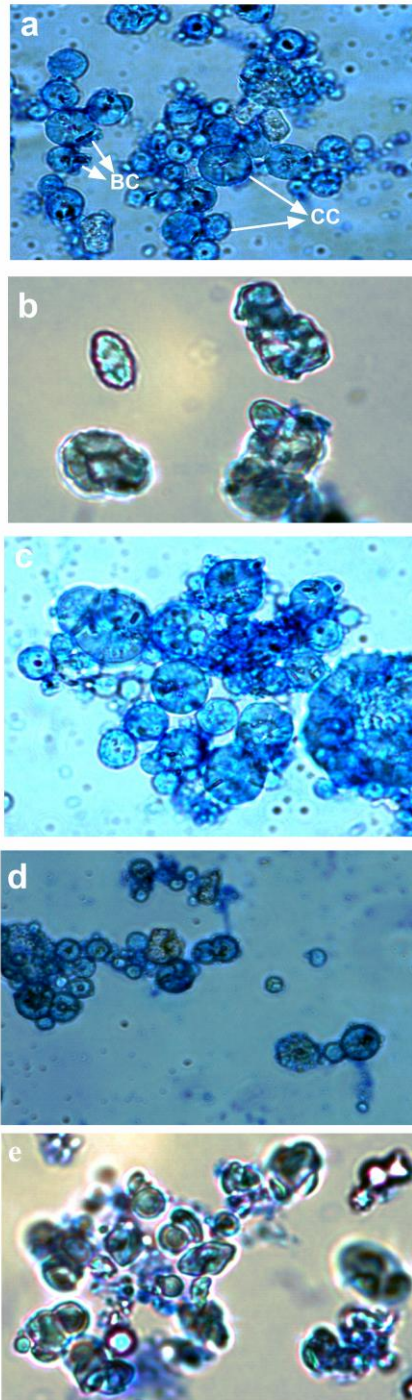


Fig. 4.3.3. CaCO₃ crystals of different bacterial isolates stained by Loeffler methylene blue staining (a: *B. megaterium* SS3, b: *B. cereus* SS5, c: *B. subtilis* SS 13, d: *B. thuringiensis* SS15 and e: *L. fusiformis* SS18) CC: carbonate crystals; BC: bacterial cells

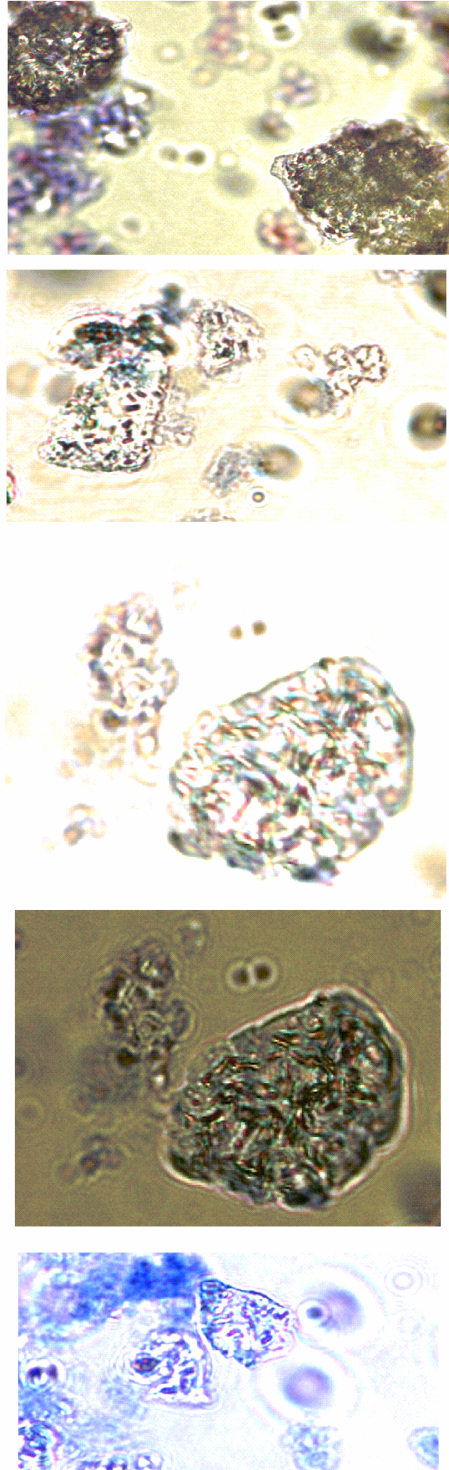


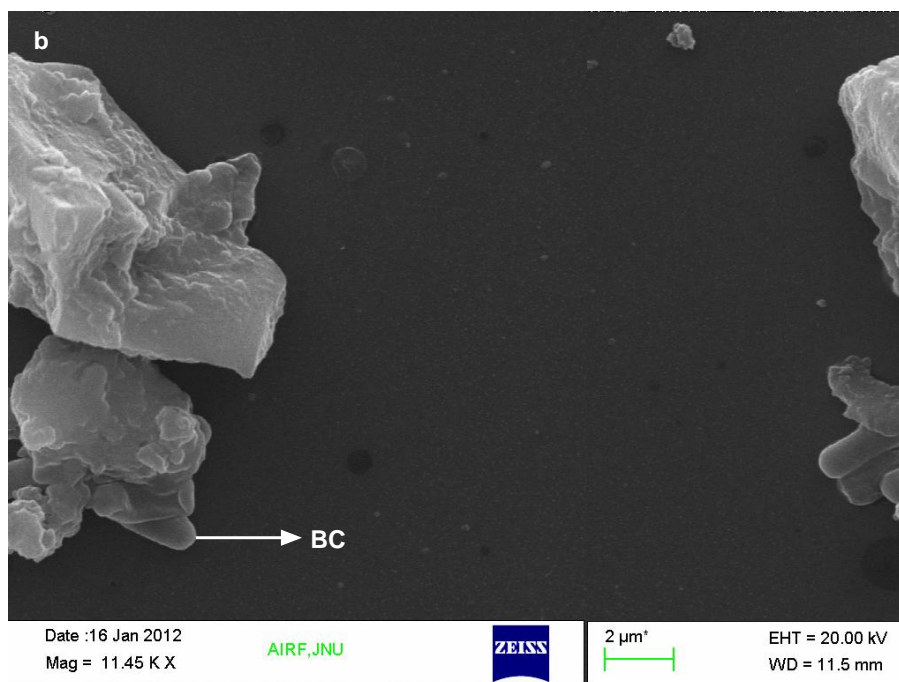
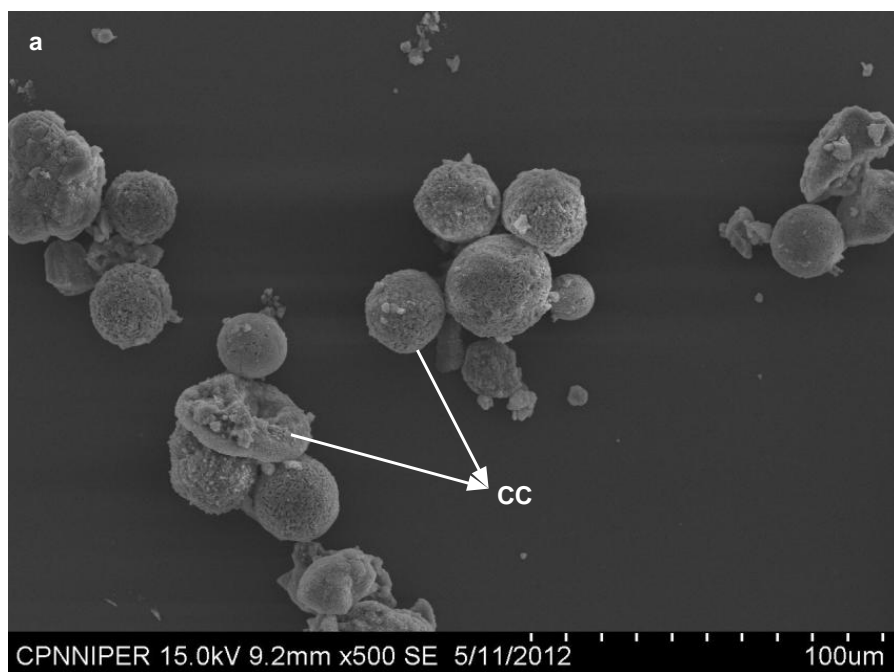
Fig. 4.3.4. CaCO₃ crystals of different bacterial isolates stained by Alcian blue PAS staining (a: *B. megaterium* SS3, b: *B. cereus* SS5, c: *B. subtilis* SS 13, d: *B. thuringiensis* SS15 and e: *L. fusiformis* SS18).

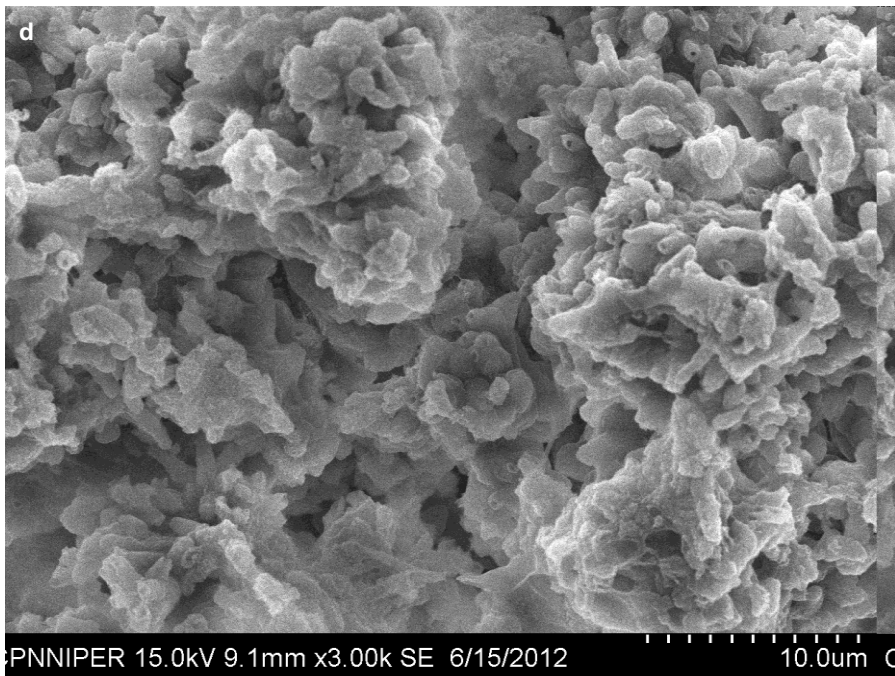
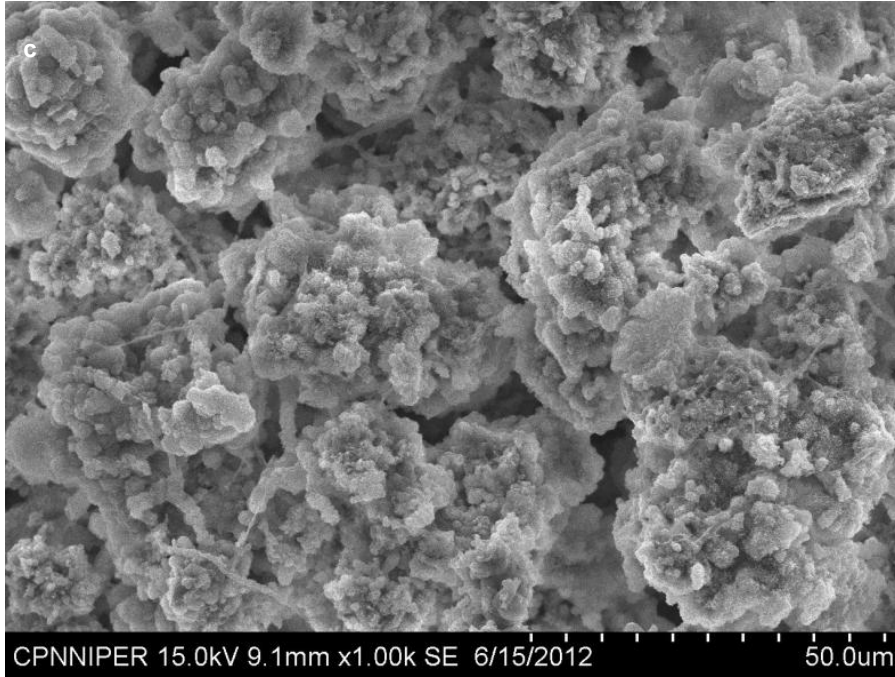
4.3.2.2. Scanning electron microscopic (SEM) and Confocal laser scanning microscopic (CLSM) analysis of carbonate crystals

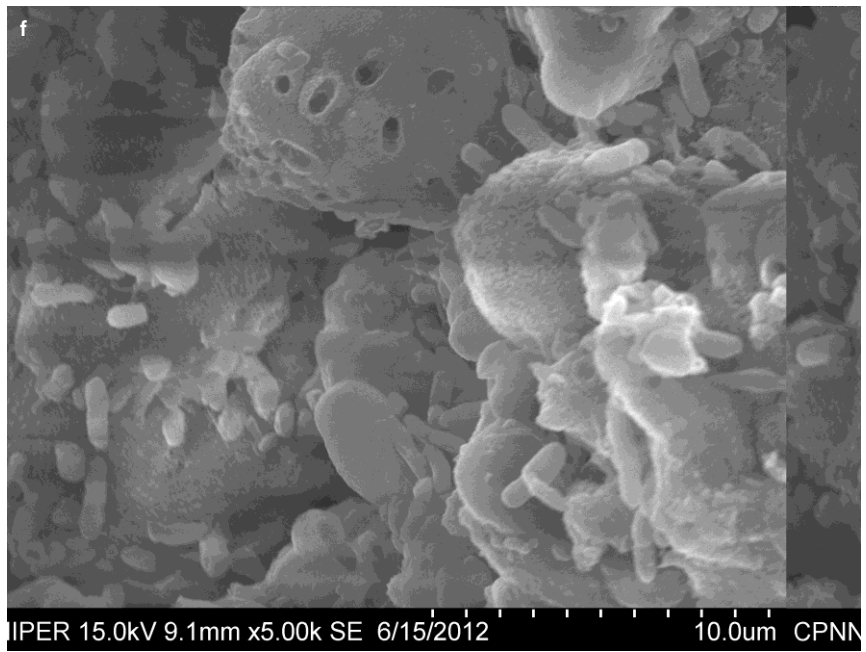
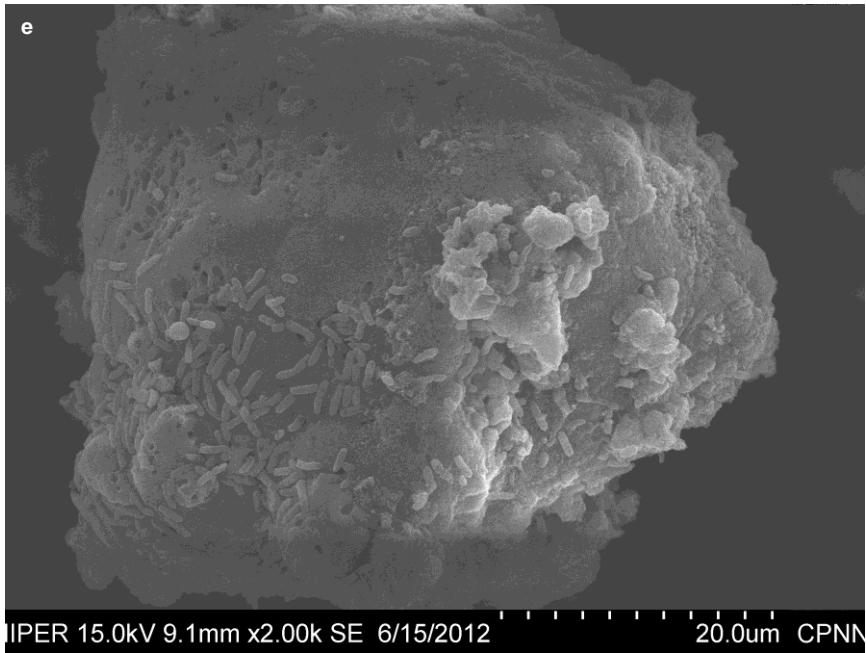
Scanning electron microscopic study depicted detailed analysis of various crystals formed by different bacterial isolates and showed obvious differences in size and shape (Fig. 4.3.5). Distinct carbonate crystals embedded with bacterial cells were clearly seen in case of all bacterial isolates. The size of all the crystals was seen to increase with time. Size of crystals varied from 2 - 50 μm . The carbonate crystals formed by *B. megaterium* SS3 were 30 - 50 μm in diameter whereas the size varied from 15 - 40 μm in *B. cereus* SS5, 10 - 50 μm in *B. subtilis* SS13, 2 - 15 μm in *B. thuringiensis* SS15, 2 - 10 μm in *L. fusiformis* SS18. SEM pictures clearly showed the association of carbonate crystals with bacterial cells. Crystals formed by SS3 were spherical, oval, rhombohedral as well as triangular in shape with smooth and rough surfaces. Number of crystals with smooth surfaces was relatively more abundant than with rough surfaces. Rod shaped imprints of about 1 μm of bacterial cells were clearly observed on the surface of crystals. SEM observation also showed formation of mucous matrix over the calcified bacterial cells. The crystals formed by SS5 were needle like and layer flake structures. The crystals were quite irregular and approximately of square morphology. In case of SS13, very smooth spherical and ellipsoidal crystals along with embedded bacterial cells were observed. The magnified SEM photograph of these crystals indicated that they were packed closely and regularly. Few bacterial cells were also seen on the surface of crystals. The crystals formed by SS15 were small, round, circular ring and rectangular in morphology. In case of SS18, the crystals had very rough surface with flaky needle like mesh formed around.

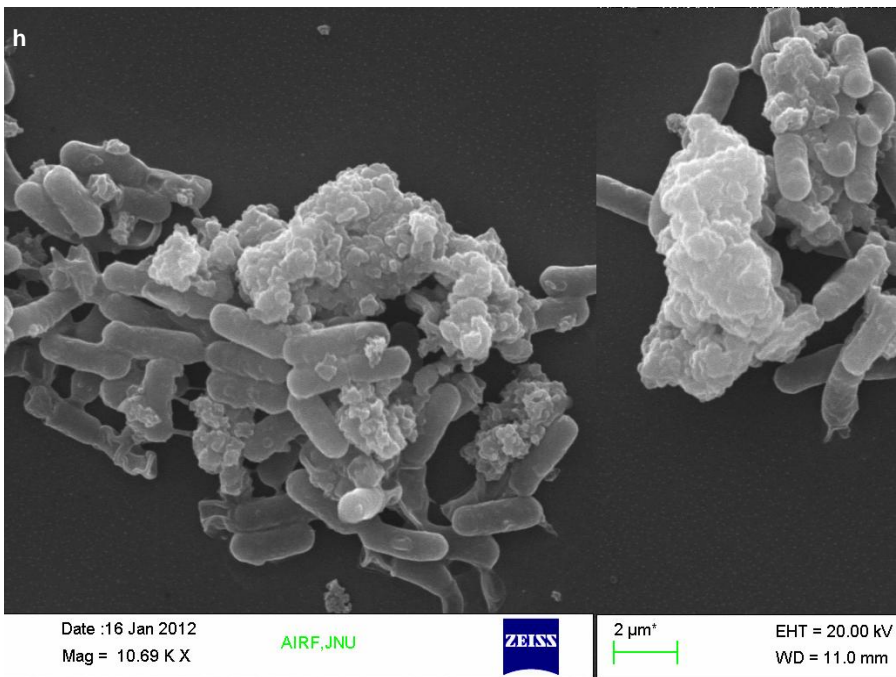
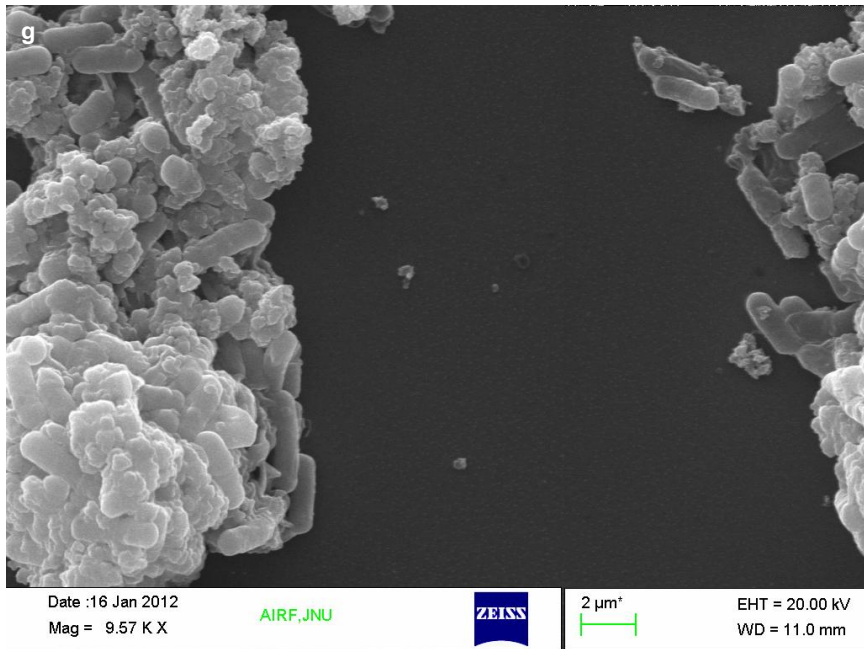
In certain cases, the surface of crystals was very rough which was due to the deposition of new carbonates. Some slimy extra polymeric substances (EPS) layers were also clearly seen in these crystals. The EPS seemed to facilitate crystal to crystal association along with forming mucous layer over them. These findings are in agreement with previous research by Geesey and Jang (1990), Buczynski and Chafetz (1991) and Van Lith *et al.* (2003), whose results showed that EPS play an important role in the formation of carbonate crystals not only by providing nucleation sites but also by attaching small crystals to each other to

increase the size of the bioliths. In summary, different morphologies of carbonate crystals were formed by different bacterial isolates.









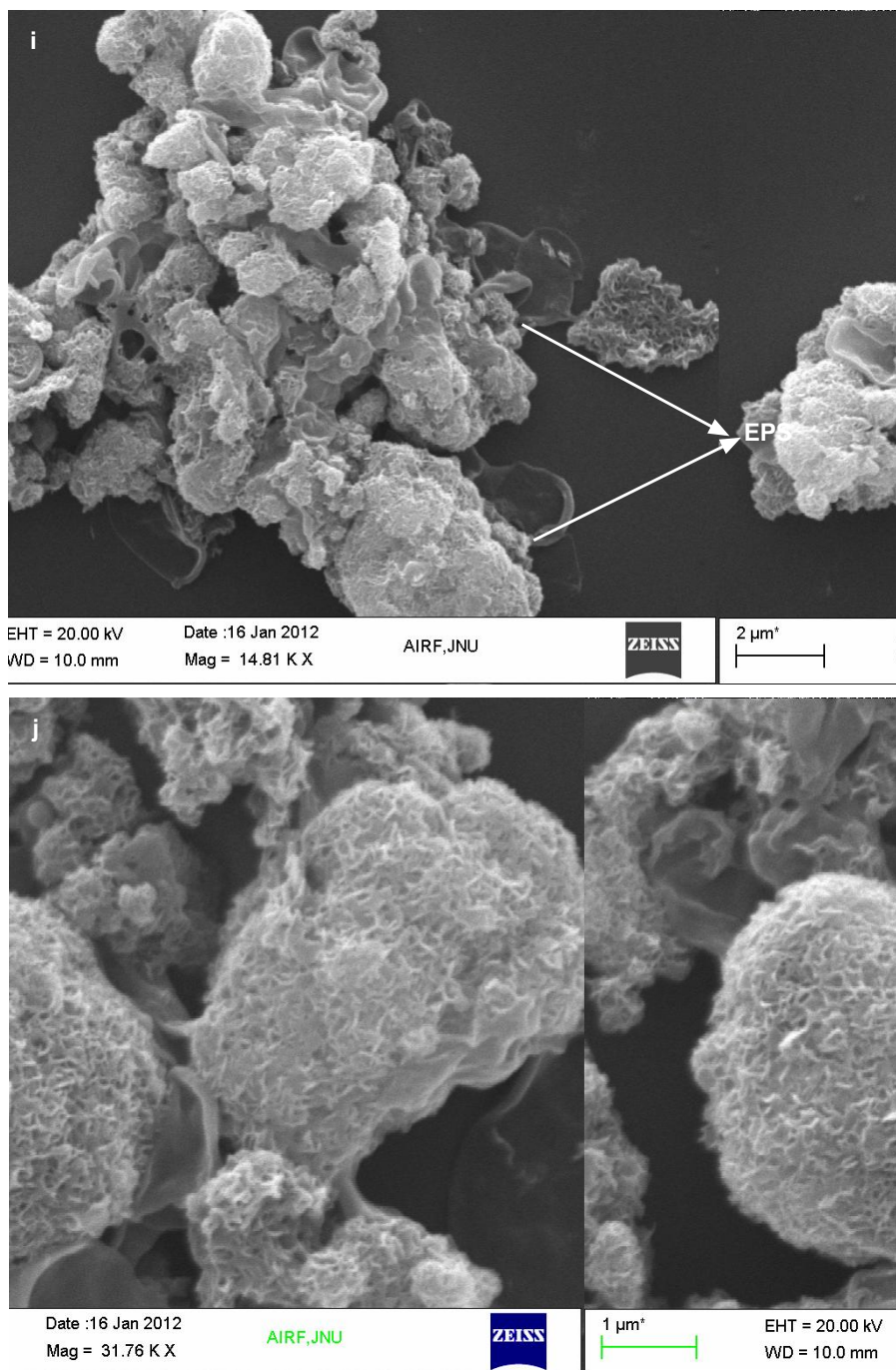


Fig. 4.3.5. Scanning electron microscopic images of carbonate crystals precipitated by (a, b) *B. megaterium* SS3, (c, d) *B. cereus* SS5, (e, f) *B. subtilis* SS13, (g, h), *B. thuringiensis* SS15 and (i, j) *L. fusiformis* SS18. CC: carbonate crystals; BC: bacterial cells; EPS: Extra polymeric substances

Confocal laser scanning microscopic analysis was also done to analyze the crystals (Fig. 4.3.6). It was seen that all the crystals produced strong fluorescence at 453 nm. Some of the bacterial cells were also clearly seen associated to the surface of carbonate crystals while few were seen independently. Fluorescence was more intense with rhombohedral and spherical crystals as compared to others. The CLSM images showed polycrystals formed by *B. megaterium* SS3. The crystals produced by all other isolates appeared as separated and mixture of spherical, ellipsoidal and rectangular with few bacterial cells associated with them.

SEM and CLSM analysis indicated different morphologies of CaCO_3 crystals induced by different bacteria. There were many bacterial imprints on the surface of carbonate crystals which suggested that bacteria might serve as nucleation sites for carbonate precipitation, which is in agreement with earlier research works (Stocks - Fischer *et al.*, 1999; Hammes and Verstraete, 2002). The bacterial cell surface with various ions could non specifically induce mineral deposition by providing nucleation sites. Lian *et al.* (2006) demonstrated that the process of carbonate crystal formation by *Bacillus megaterium* involved the nucleation of calcite on the bacterial cell walls. In the bacterial culture medium, Ca^{2+} is not likely utilized by bacterial metabolic processes; it just accumulates outside the cell. As a result of enzymatic reversible hydration of CO_2 , CO_2 or HCO_3^- is produced and the dissolved CO_2 transforms to CO_2^{3-} or HCO_3^- around the cell, commencing the growth of CaCO_3 crystals around the cell.

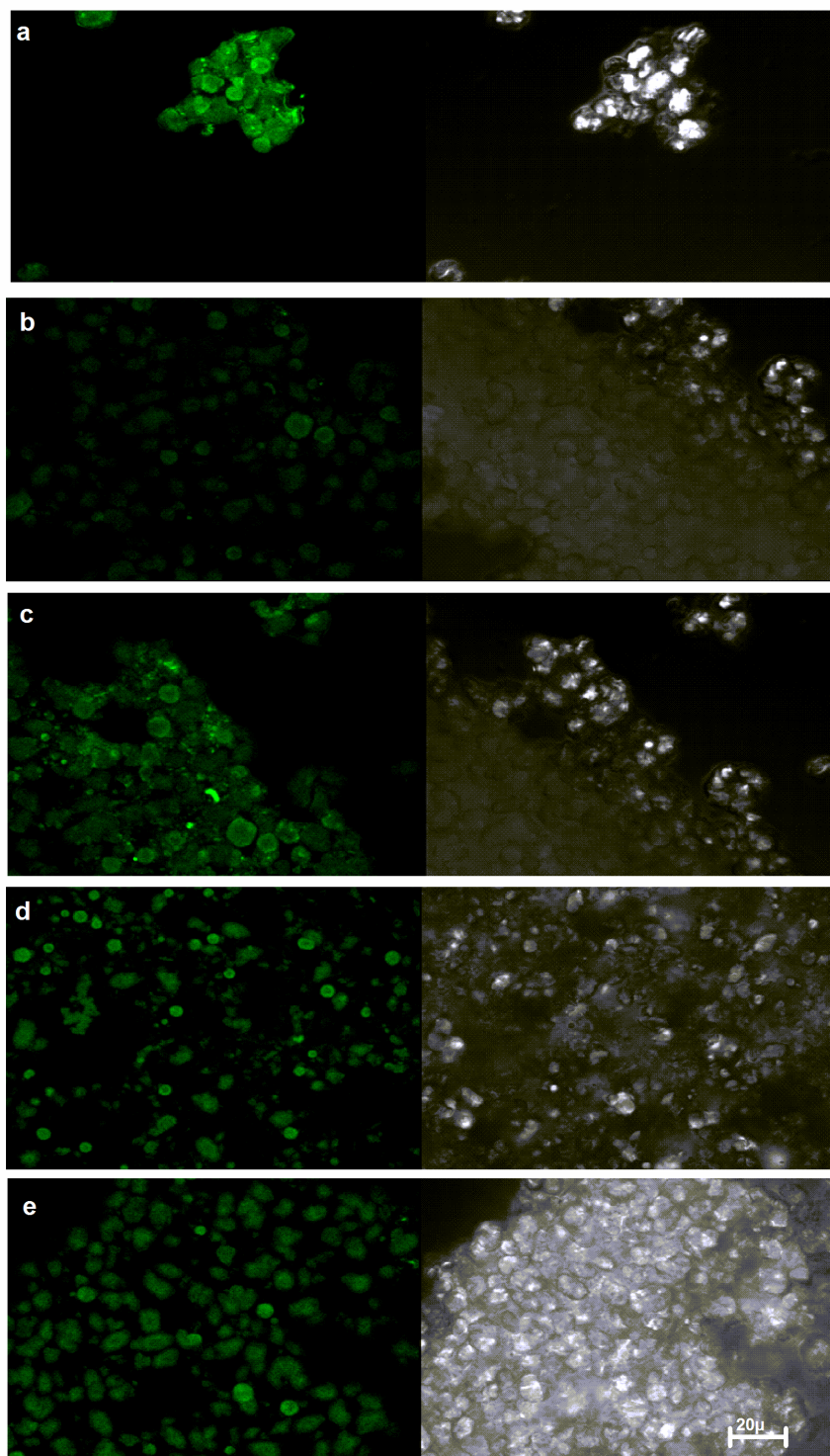


Fig. 4.3.6. Confocal laser scanning microscopic images of carbonate crystals precipitated by (a) *B. megaterium* SS3, (b) *B. cereus* SS5, (c) *B. subtilis* SS13, (d), *B. thuringiensis* SS15 and (e) *L. fusiformis* SS18.

4.3.2.3. Energy dispersive X ray, X ray diffraction and Fourier transmission Infra red spectroscopic analysis of carbonate crystals

In order to elucidate the chemical constituents of all the crystals, they were analyzed by EDX, XRD and FTIR analysis. EDX analysis of the crystals showed large amounts of calcium along with small amounts of silica, magnesium, aluminium, potassium, iron and titanium in case of all crystals (4.3.7). The amount of calcium varied from different carbonate crystals. It was maximum in case of *B. megaterium* SS3 followed by *B. thuringiensis* SS15, *B. subtilis* SS13, *B. cereus* SS5 and *L. fusiformis* SS18.

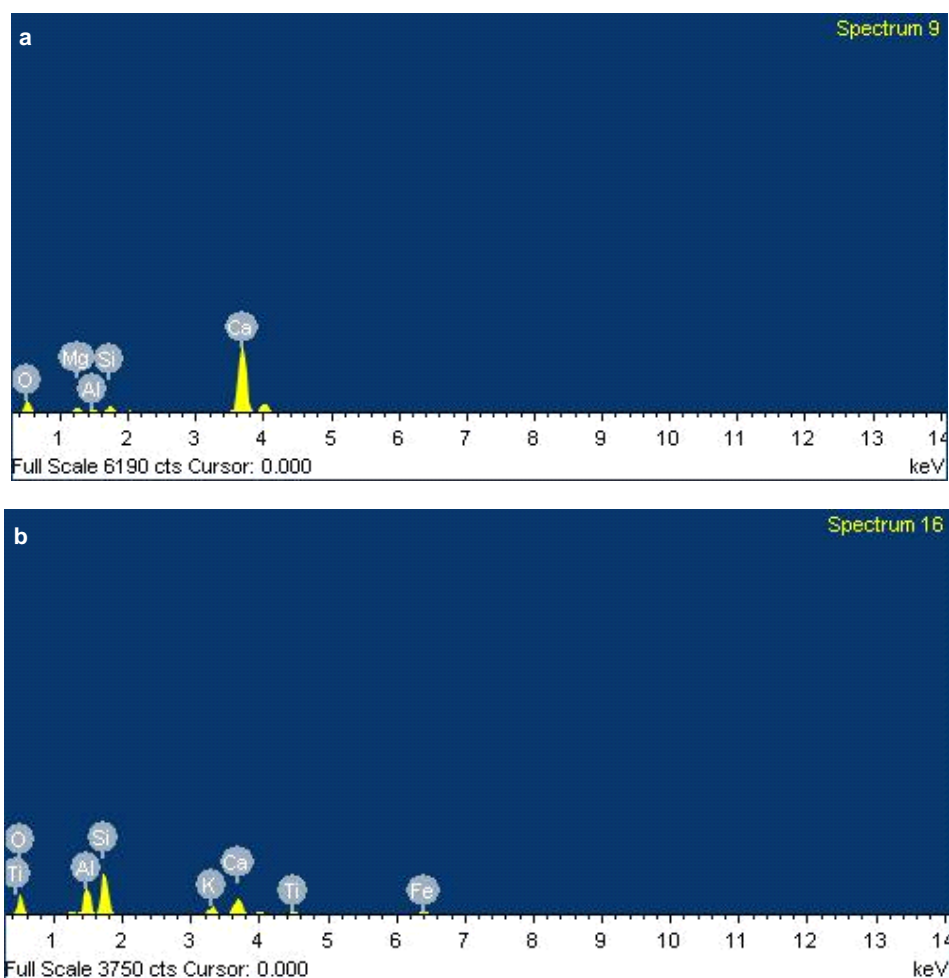


Fig. 4.3.7. Energy dispersive X ray spectra of carbonate crystals precipitated by (a) *B. megaterium* SS3, (b) *L. fusiformis* SS18

X ray diffraction analysis showed that in all cases, calcite and/or vaterites were formed (Fig. 4.3.8). XRD analysis of crystals precipitated by *B. megaterium* SS3 showed that calcite phase formed the major form of crystals along with few vaterites (Fig. 4.3.8 a). In case of *B. cereus* SS5 and *B. subtilis* SS13, the major phase was again found to be calcite along with very few calcite peaks. XRD analysis of *B. thuringiensis* SS15 and *L. fusiformis* SS18 revealed that in this case, vaterite formed the major form of crystals along with few calcite peaks in *B. thuringiensis* SS15 (Fig. 4.3.6 b). X ray analysis of pure bacterial carbonate crystals has been recently determined by Rodriguez - Navarro *et al.* (2012) who investigated the effect of substrate on calcium carbonate polymorph.

Fourier transmission infra red (FT - IR) spectra of all the crystals were also determined. The spectra of crystals formed by *B. megaterium* SS3, *B. cereus* SS5 and *B. subtilis* SS13 isolates showed strong absorption peak at $\lambda = 713 \text{ cm}^{-1}$ which corresponds to calcite while in case of isolates *B. thuringiensis* SS15 and *L. fusiformis* SS18, the absorption peak at 750 cm^{-1} depicted vaterite formation (Fig.4.3.9). This further confirmed XRD results. The morphological differences of different carbonate crystals were further found to be different as per XRD and FTIR analysis (Fig. 4.3.8, 4.3.9). XRD and FTIR studies showed the presence of calcite as main polymorph in three isolates while two isolates had vaterite as the main phase.

All the samples produced very similar XRD results, while clear morphological differences were evident. This suggests that these differences were a result of variations in crystal growth rates along different planes of the crystal structure. This could have been a result of the colony growth rate and/or actual urease activity, which thus influenced the rate of supply of chemical species required for precipitation (Sondi and Matijevic, 2001). Alternatively, crystal growth can be inhibited or altered by the adsorption of proteins, organic matter, or inorganic components to specific crystallographic planes of the growing crystal (Kawaguchi and Decho, 2002; Rivadeneyra *et al.*, 1998).

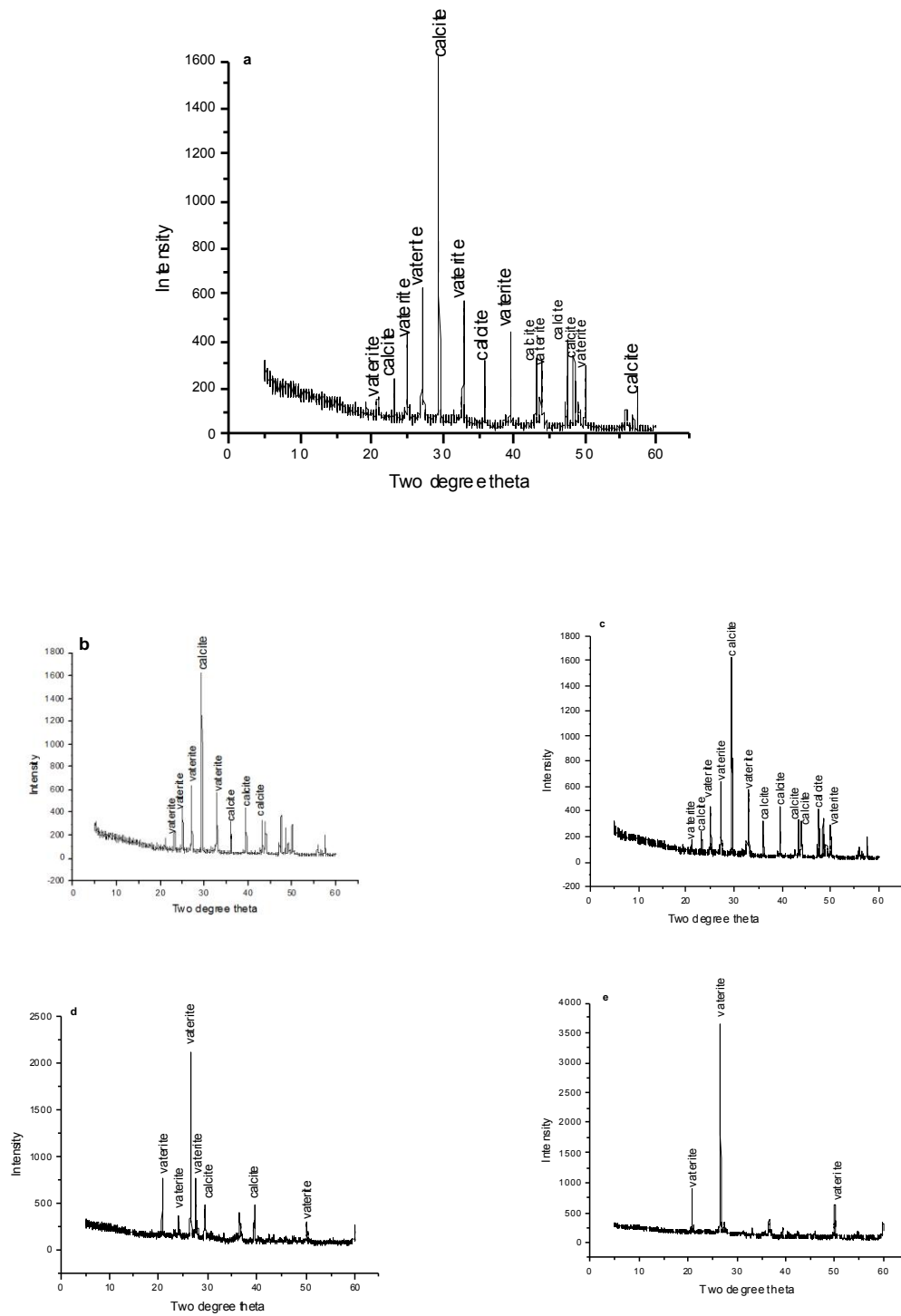


Fig. 4.3.8. X ray diffraction analysis of carbonate crystals precipitated by (a) *B. megaterium* SS3, (b) *B. cereus* SS5, (c) *B. subtilis* SS13, (d), *B. thuringiensis* SS15 and (e) *L. fusiformis* SS18.

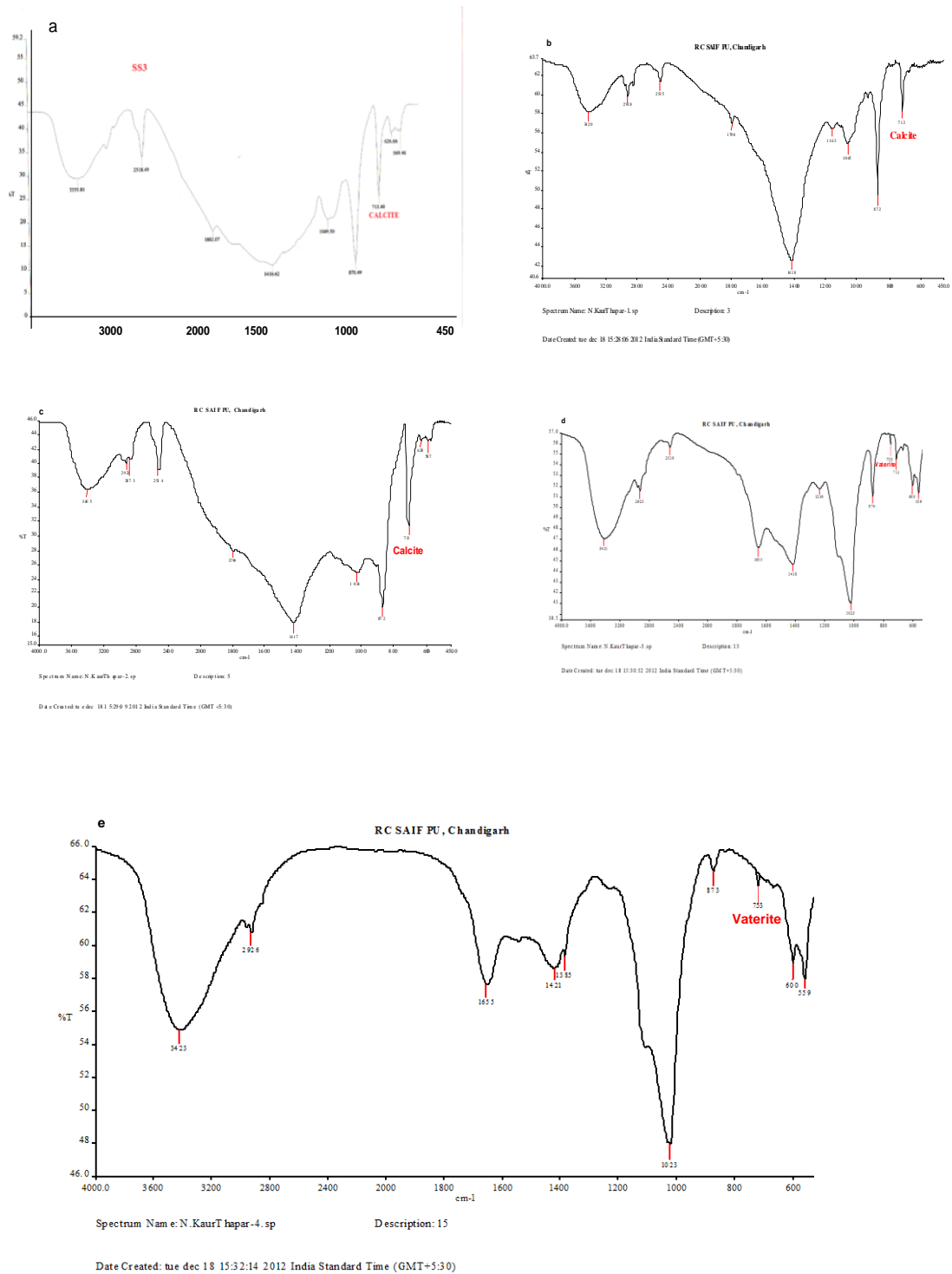


Fig. 4.3.9. Fourier transmission Infra red spectroscopic analysis of carbonate crystals precipitated by (a) *B. megaterium* SS3, (b) *B. cereus* SS5, (c) *B. subtilis* SS13, (d), *B. thuringiensis* SS15 and (e) *L. fusiformis* SS18.

All tested bacteria induce the precipitation of a significant amount of calcium carbonate in the present study which is not unexpected. The formation of calcium carbonate has been reported for many bacterial species. Studies performed since the beginning of the XX century demonstrate that numerous heterotrophic bacteria induce the precipitation of calcium carbonate in a range of natural environments and laboratory culturing conditions (Gonzalez *et al.*, 2011; Rodriguez *et al.*, 2003). Many studies have emphasized the fact that bacterial carbonatogenesis is a common and widespread phenomenon, which can take place in a range of environments. There is uncertainty about what causes bacteria to precipitate different carbonate polymorphs. Although the composition of the growth medium has been seen to have some effect on the type of carbonate precipitated (Rivadeneira *et al.*, 1998), particular bacterial species also have an important influence on carbonate polymorph precipitated, as found for *Halomonas eurihalina* (Rivadeneira *et al.*, 1996) and *Nesterenkonia halobia* (Rivadeneira *et al.*, 2000). Cacchio *et al.* (2004) demonstrated that, with respect to carbonate precipitation on B4 agar by *Kocuria*, *Acinetobacter*, *Bacillus*, and *Renibacterium* spp., only *Kocuria* spp. were able to precipitate vaterite. However, work on bioconsolidation of stone by *Myxococcus xanthus* (Rivadeneira *et al.*, 2003) and on bioconsolidation of cement by *B. sphaericus* (De Muynck *et al.*, 2008) showed that both bacterial species were able to precipitate calcite and vaterite.

It has also been reported that the formation of different polymorphs of carbonate by bacteria is dependent on various factors like the composition of growth medium, type of substrate, temperature, pH, saturation index, $[Ca^{2+}] / [CO_3^{2-}]$ ratio and bacterial species (Rivadeneira *et al.*, 1998; Rodriguez *et al.*, 2012). As per the type of substrate concerned, calcitic substrates favor bacterial attachment and promote the formation of abundant calcite while under the same culture conditions, vaterite spheres are formed on silicate substrates. Vaterite is metastable at normal temperature and atmospheric pressure, and it has been suggested that metastable polymorphs form initially and subsequently convert to stable polymorph, i.e. calcite. It was also reported that specific proteins present in biological cellular polymeric substances cause the formation of different $CaCO_3$ polymorphs (Kawaguchi and Decho, 2002; Ercole *et al.*, 2012; Chen *et al.*, 2009). Briassant *et al.* (2009) have associated polymorph selection (vaterite vs. calcite) during bacterial carbonatogenesis with the

characteristics of EPS. Rodriguez *et al.* (2012) also reported that the final bacterial calcium carbonate polymorph that appears in a particular situation strongly depends on the amount of dissolved organic carbon (DOC) from bacterial activity which hinders the vaterite to calcite phase transition. Little DOC favors the final formation of calcite, while high DOC promotes the kinetic stabilization of vaterite. These observations imply that carbonate precipitating bacterial isolates exert a higher degree of control on biomineralization as morphology and polymorph selection are characteristics of bacterially controlled mineralization in higher order organisms (Mann, 2001).

As CaCO₃ crystals have advantages in special structures and excellent material properties for their use in various industries like paper, paint, plastics, and medicines, along with bioremediation of building materials, calcium carbonate polymorph selection can have important technical implications (Warren *et al.*, 2001; Wang *et al.*, 2008; Li *et al.*, 2010). In conclusion, in the present study successful characterization of various calcium carbonate crystals has been done and based on the type of polymorph precipitated, the technology of MICCP can be applied for various purposes.

Conclusion and salient features

The aim of the present work was to investigate CaCO₃ precipitating ability of the different bacterial isolates from calcareous soils and to characterize the various CaCO₃ polymorphs produced by such bacteria. Characterization of carbonates play an important role for various technical applications involving these biominerals. Recent advances in microscopy as well as various chemical constituent analysis techniques have made the study of different mineral constituents very easy and convenient. In the present work, all the bacterial isolates successfully precipitated calcium carbonate crystals. These crystals have been characterized morphologically as well as chemically. Different carbonates elucidated different features under similar conditions. SEM, EDX, XRD and FTIR analysis indicated clear differences among the different carbonate polymorphs formed by different bacterial isolates. *B. megaterium* SS3, *B. cereus* SS5 and *B. subtilis* SS13 have been found to be calcite

precipitating bacterial isolates while in case of *B. thuringiensis* SS15 and *L. fusiformis* SS18 vaterite formed the dominant phase of CaCO₃ polymorph. Though various reasons have been hypothesized by several researchers for development of different carbonate polymorphs by different bacterial isolates under similar conditions, but there has not been one common line of thought about what causes different bacteria to precipitate different polymorphs. In our study also, all the carbonate polymorphs varied morphologically as well as chemically. As different technical applications based on CaCO₃ biominerals require different polymorphs (as calcite in remediation of buildings), our work has led to isolation of varying carbonate polymorph precipitating bacterial isolates which can be utilized for various technical applications.

4.4. Application of calcifying bacteria in different building materials

The previous chapters indicated successful production of biomineralized carbonates by several ureolytic bacteria. It has been established that for remediation and restoration of building materials, production of coherent and durable calcium carbonate polymorph calcite is required. Calcifying bacterial isolates have paved the way for applying these biomineralized carbonate binders for improving the qualities of the building materials. Though this innovative technology can be applied successfully by several ureolytic bacterial isolates but ideal strain will have the capability to produce high level of urease and carbonates. Many bacterial species isolated in the present study depicted the capability of urease and CaCO_3 production, hence, the performance of these bacterially produced biominerals in building materials was investigated. *Bacillus megaterium* SS3 was used for this study as it was capable of producing high amount of urease, Carbonic anhydrase, EPS, biofilm and carbonates. The application of this bacterial isolate on durability parameters of various building materials was assessed.

4.4.1. Evaluation of bacterial calcite in varying grain sizes and densities sand columns

As grain size of sand forms one of the most fundamental property for determining its porosity, permeability and hence strength, it is thus imperative to evaluate the effect of bacterial biomineral precipitation on properties of these sand grains. Finding the optimum grain size where maximum carbonate precipitation occurs leading to significant improvement in its properties is pre - requisite for various applications of sand consolidation. Though applications of these ureolytic bacterial isolates have been proved in many cementitious materials, but in case of varying grain sizes sand columns, these bacterial carbonates need to be investigated. The sand columns of varying grain sizes were prepared as per Achal *et al.* (2009) by mixing sand with bacterial cells grown in nutrient broth media supplemented with 2% urea and 25 mM CaCl_2 (NBUC media) and casted in plastic columns. The assembled plugs have been shown in Fig. 4.4.1.



Fig. 4.4.1. Assembly of microbial sand columns

4.4.1.1. Effect of microbial calcium carbonate precipitation on flow rate, pH, electrical conductivity and urea hydrolysis of varying grain sizes sand columns

In order to investigate the effect of biocalcification on various grain sized sand columns, bacterial isolate *B. megaterium* SS3 was mixed with all the columns and NBUC media was fed till 10 days. The flow rate was measured by measuring the volume of media that came out of columns per minute. The flow rates of bacterial as well as control sand columns were monitored and were found to change over time in bacterial columns as bacterial calcification and plugging progressed in the columns containing bacterial cells (Table 4.4.1). Continuous decrease in the flow rate of bacterial columns was observed with time. The flow rate of bacterial column (0.5 mm grain size) was recorded to be 13.2 ml/min on day 1 while it reduced to 6.2 ml/min after 6 days. On 10th day, there was complete plugging of the column. In case of control columns, the flow rate was found to change from 14.3 ml/min to 12.6 ml/min after 10 days. The decrease in flow rate of media in bacterial columns is primarily due to entrapped biomass, deposition of carbonates leading to clogging in the bacterial treated columns while in case of control sand columns, no significant change of flow rate

was noticed. The bacterial biomass increases along with increase in CaCO_3 precipitates in presence of urea, calcium and nucleation sites. These carbonate biominerals reduce the pore spaces in between sand columns and affect the flow rate. In this case, maximum change in the flow rate of 0.5 mm grain sized columns was noticed which suggested maximum clogging in this case.

Bacillus species are known to produce a large amount of urease in soil environments (Mobley *et al.*, 1995; Ciurli *et al.*, 1996; Benini *et al.*, 1999; Bachmeier *et al.*, 2002). The growth related microbiological urea degradation is the main source of inorganic carbon dioxide in calcium and carbonate oversaturated medium and the cause of calcium carbonate precipitation (Merz-Preiss and Riding, 1999; Yates and Robbins, 1999, Warren *et al.*, 2001). The carbonate layer formed as a result of biological ureolytic activity, clogs the pores of sand to decrease the void spaces amongst sand columns leading to decreased flow rate.

The effluent that came out of the column was also investigated for change in pH and electrical conductivity after regular intervals. Both pH and EC were recorded after a regular interval of 24 hours to investigate if urea hydrolysis is occurring successfully. The pH of the effluent in case of all bacterial columns was found to be quite high as compared to control columns where there was negligible change in the pH (Table 4.4.2; Fig. 4.4.3). Though the pH increased in all the bacterial sand columns, but after 7th - 8th day, it was noticed that there was comparatively lesser rise in the pH. Initially higher pH was seen in case of 0.2 mm grain sized columns while in the later times, higher pH was recorded in 0.5 mm columns.

Table 4.4.1. Flow rate (mL/min) of media from varying grain sizes bacterial treated and control sand columns

Flow rate (mL/min)								
Time	Bacterial treated (0.2 mm)	Control (0.2 mm)	Bacterial treated (0.5 mm)	Control (0.5 mm)	Bacterial treated (1 mm)	Control (1mm)	Bacterial treated (1.5 mm)	Control (1.5 mm)
Day 1	11.2 ± 0.4a	12.1 ± 0.3a	13.2 ± 0.4a	14.3 ± 0.3a	16.3 ± 0.3a	17.8 ± 0.3a	18.4 ± 0.3a	19.8 ± 0.4a
Day 2	9.1 ± 0.4b	11.8 ± 0.3a	9.3 ± 0.3c	13.8 ± 0.4b	13.3 ± 0.2b	17.3 ± 0.2a	16.8 ± 0.3ab	19.2 ± 03a
Day 4	8.2 ± 0.1bc	11.3 ± 0.4ab	7.1 ± 0.2cd	13.4 ± 0.4b	10.4 ± 0.2c	16.3 ± 0.3b	13.3 ± 0.2b	18.4 ± 0.3b
Day 6	7.3 ± 0.1c	11.1 ± 0.3b	6.2 ± 0.0d	13.6 ± 0.2b	8.8 ± 0.1cd	16.6 ± 0.1ab	9.8 ± 0.2c	17.7 ± 0.2b
Day 8	6.7 ± 0.2cd	10.7 ± 0.2b	5.1 ± 0.0e	12.9 ± 0.2bc	7.9 ± 0.1d	16.1 ± 0.2b	9.1 ± 0.1c	17.9 ± 0.2b
Day 10	6.1 ± 0.3d	10.5 ± 0.3bc	2.4 ± 0.0fg	12.6 ± 0.3c	7.2 ± 0.1d	15.8 ± 0.2bc	8.4 ± 0.1c	17.2 ± 0.1bc

Bacterial treated: Sand columns treated with *B. megaterium* SS3; Control: Untreated sand columns. Values bearing different letters in the same column are significant at P<0.05. Values are mean ± SD (n = 3).

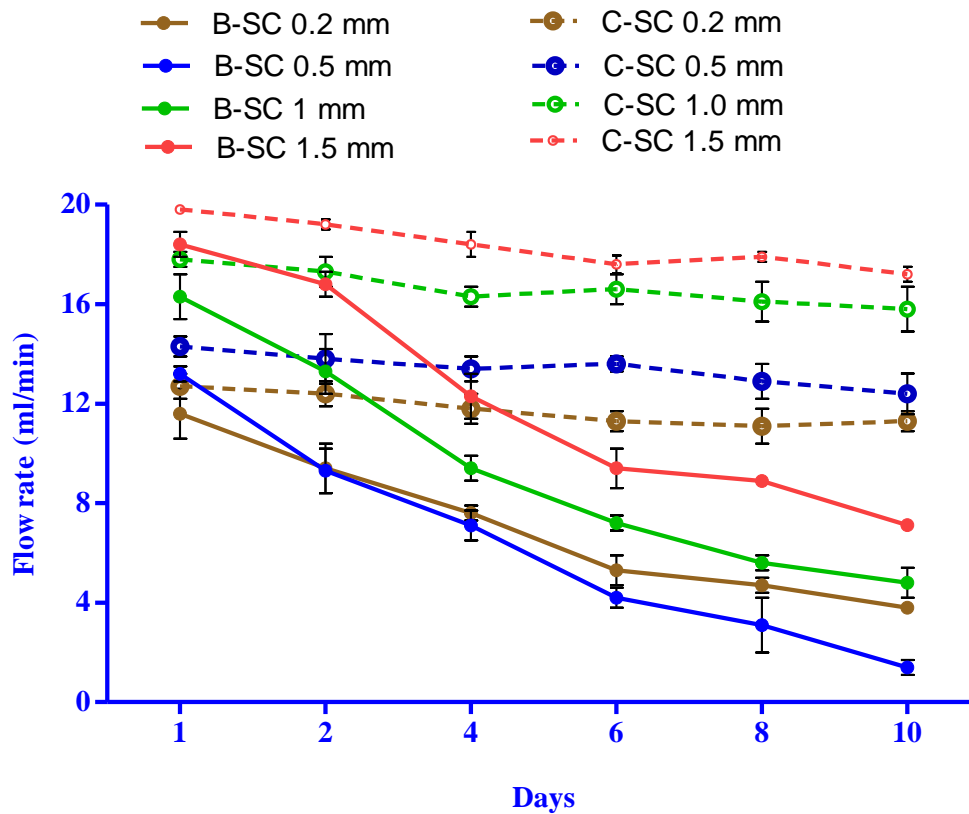


Fig. 4.4.2. Estimation of flow rate (mL/min) in different grain sized sand columns. Bacterial sand columns (B-SC) treated with *B. megaterium* SS3 and control sand columns (C-SC). Lines represent mean \pm SD (n = 3).

De Jong *et al.* (2012) reported that the pH of the effluent reaches between 8.5 – 9.3 within the sand column after 20 hrs upon treatment by ureolytic bacterial isolates for biomediated improvement of the soils. Okwadha and Li (2010) also reported the rise in pH upon urea hydrolysis and found that higher the bacterial cell concentration, higher is the urea hydrolysis as well as pH.

Table 4.4.2. pH of the effluent from varying grain sizes bacterial treated and control sand columns

pH								
Time (Days)	Bacterial treated (0.2 mm)	Control (0.2 mm)	Bacterial treated (0.5 mm)	Control (0.5 mm)	Bacterial treated (1 mm)	Control (1 mm)	Bacterial treated (1.5 mm)	Control (1.5 mm)
1	8.69 ± 0.5a	8.12 ± 0.8a	8.63 ± 1.2ab	8.07 ± 0.6b	8.59 ± 0.7a	8.14 ± 0.7ab	8.47 ± 0.5a	8.07 ± 0.6a
2	8.88 ± 0.8a	8.09 ± 0.9ab	8.72 ± 0.8a	8.12 ± 0.7ab	8.63 ± 1.2ab	8.17 ± 0.4a	8.53 ± 0.7ab	8.13 ± 0.9a
4	8.74 ± 0.7a	8.14 ± 0.5a	8.81 ± 0.7a	8.17 ± 1.1a	8.68 ± 0.9a	8.19 ± 0.8a	8.59 ± 0.6ab	8.18 ± 0.6a
6	8.67 ± 0.9a	8.17 ± 0.5a	8.63 ± 0.9ab	8.19 ± 0.9a	8.64 ± 0.7a	8.13 ± 0.9ab	8.62 ± 0.8a	8.14 ± 0.7a
8	8.62 ± 1.1a	8.13 ± 0.6a	8.61 ± 0.7ab	8.16 ± 0.4a	8.73 ± 0.6a	8.19 ± 0.7a	8.72 ± 0.9a	8.12 ± 0.9ab
10	8.54 ± 0.4ab	8.11 ± 0.8ab	8.58 ± 0.6b	8.18 ± 0.8a	8.66 ± 0.5a	8.17 ± 0.4a	8.64 ± 1.1a	8.14 ± 0.7a

Bacterial treated: Sand columns treated with *B. megaterium* SS3; Control: Untreated sand columns. Values bearing different letters in the same column are significant at P<0.05. Values are mean ± SD (n = 3).

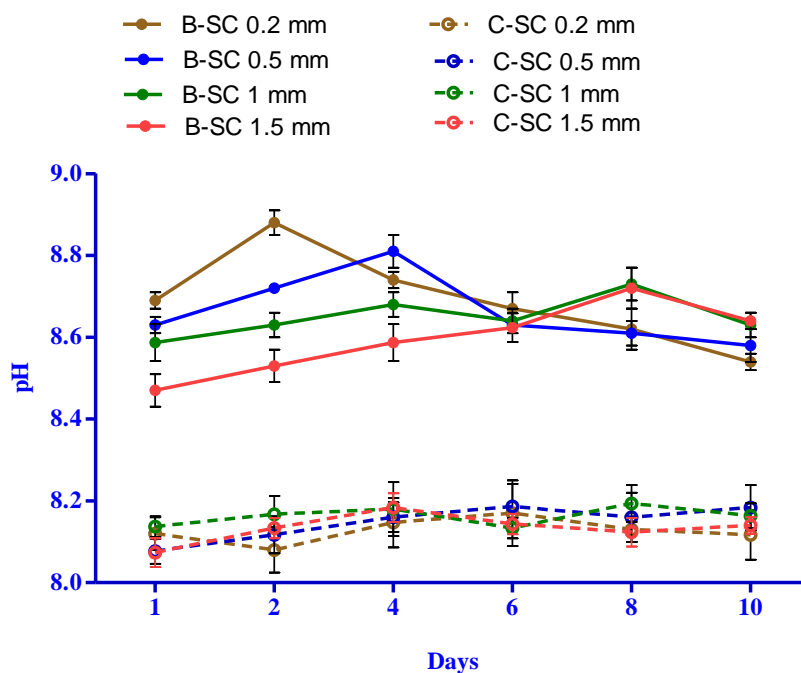


Fig. 4.4.3. Change in pH of the effluent from varying grain sized sand columns. Bacterial sand columns (B-SC) treated with *B. megaterium* SS3 and Control sand columns (C-SC). Lines represent mean \pm SD (n = 3).

In case of conductivity tests also, the effluent showed continuous increase in all bacterial columns compared to the control specimens after 24 hrs (Table 4.4.3). The increase in the measured electrical conductivity correlates with the hydrolysis of urea inside the column. The increase in conductivity depicts the generation of ionic products of NH_4^+ and CO_3^{2-} from non-ionic substrate, urea (Whiffin, 2004). Though the EC was all time higher in case of bacterial columns, but, at times there were minor fluctuations also. The high correlation between conductivity increase and urea hydrolysis has also been reported in several previous studies (Chin and Kroontje, 1962; Whiffin, 2004; Al-Thawadi, 2008; van Paassen *et al.*, 2010; Hammad *et al.*, 2013).

Table 4.4.3. Electrical conductivity (mS/cm) of the effluent from varying grain sizes bacterial treated and control sand columns.

EC (mS/cm)								
Time (Days)	Bacterial treated (0.2 mm)	Control (0.2 mm)	Bacterial treated (0.5 mm)	Control (0.5 mm)	Bacterial treated (1 mm)	Control (1 mm)	Bacterial treated (1.5 mm)	Control (1.5 mm)
1	2.29 ± 0.07cd	1.61 ± 0.1b	2.46 ± 0.3a	1.69 ± 0.4ab	2.19 ± 0.4b	1.59 ± 0.3b	2.19 ± 0.4b	1.69 ± 0.2ab
2	3.38 ± 0.1a	1.65 ± 0.2b	3.79 ± 0.4a	1.73 ± 0.3a	2.26 ± 0.4b	1.64 ± 0.4ab	2.26 ± 0.3b	1.72 ± 0.2a
4	3.34 ± 0.3a	1.67 ± 0.2ab	3.89 ± 0.1a	1.66 ± 0.4b	2.38 ± 0.3ab	1.63 ± 0.3ab	2.98 ± 0.3a	1.76 ± 0.4a
6	3.53 ± 0.3a	1.63 ± 0.3b	3.18 ± 0.2ab	1.73 ± 0.4a	2.67 ± 0.4a	1.69 ± 0.4a	2.67 ± 0.4ab	1.70 ± 0.4ab
8	3.15 ± 0.3ab	1.72 ± 0.2a	3.11 ± 0.3ab	1.78 ± 0.2a	2.74 ± 0.3a	1.74 ± 0.3a	2.74 ± 0.4a	1.73 ± 0.3a
10	3.11 ± 0.4ab	1.76 ± 0.4a	3.04 ± 0.3ab	1.76 ± 0.3a	2.79 ± 0.4a	1.71 ± 0.3a	2.79 ± 0.3a	1.78 ± 0.4a

Bacterial treated: Sand columns treated with *B. megaterium* SS3; Control: Untreated sand columns. Values bearing different letters in the same column are significant at P<0.05. Values are mean ± SD (n = 3).

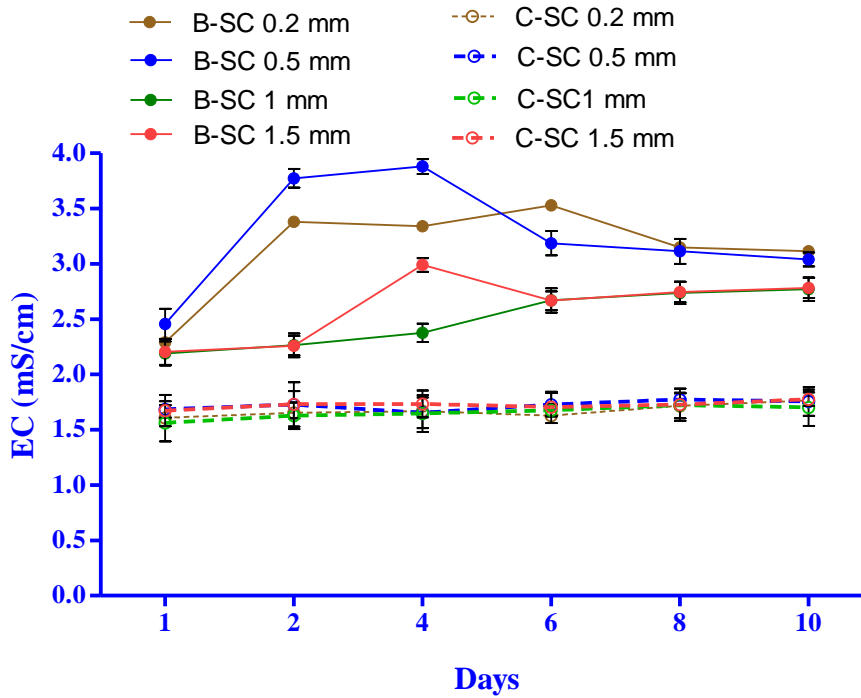


Fig. 4.4.4. Electrical conductivity of the effluent from varying grain sized sand columns treated with *B. megaterium* SS3 (B - SC) and control sand columns (C - SC). Lines represent mean \pm SD (n = 3).

After investigating the pH and EC of the effluents, the next step was to estimate the hydrolyzed urea within each sand column (Table 4.4.4; Fig. 4.4.5). The effluents of all columns were analyzed for remaining urea by the method of Knorst *et al.* (1997). It was observed that the amount of urea in effluent of all bacterial columns declined significantly while there were minor variations in control sand columns. The hydrolysis of urea in sand columns with grain size higher than 0.5 mm was more compared to low grain sized sand columns. After 7-8 days, there was comparatively lower urea hydrolysis in all bacterial columns which was in agreement with the previous results of pH and EC.

Table 4.4.4. Estimation of urea hydrolysis in the effluent from varying grain sizes bacterial treated and control sand columns.

Remaining urea (mM)								
Time (Days)	Bacterial treated (0.2 mm)	Control (0.2 mm)	Bacterial treated (0.5 mm)	Control (0.5 mm)	Bacterial treated (1 mm)	Control (1 mm)	Bacterial treated (1.5 mm)	Control (1.5 mm)
Day 1	214 ± 9a	321 ± 6.8a	173 ± 5.6a	319 ± 5.7a	235 ± 3.6a	321 ± 5.4a	263 ± 3.4a	313 ± 6.2ab
Day 2	229 ± 8.3a	327 ± 8.9a	144 ± 3.7b	323 ± 4.3a	213 ± 5.1a	317 ± 5.8b	251 ± 4.3a	324 ± 3.2a
Day 4	198 ± 5.6b	319 ± 5.7ab	123 ± 7.2c	311 ± 4.2ab	183 ± 4.3c	310 ± 4.9b	217 ± 4.1b	316 ± 7.1ab
Day 6	159 ± 6.9cd	315 ± 7.3ab	112 ± 4.5cd	325 ± 7.8a	198 ± 6.2b	317 ± 3.5b	179 ± 3.7cd	321 ± 6.2a
Day 8	173 ± 8.5c	325 ± 4.5a	163 ± 3.7a	323 ± 5.9a	179 ± 5.5cd	322 ± 5.1a	195 ± 4.2c	315 ± 5.8a
Day 10	194 ± 3.9b	322 ± 6.3a	179 ± 6.3a	316 ± 4.7a	194 ± 3.5b	312 ± 4.3b	211 ± 6.6b	320 ± 5.5a

Bacterial treated: Sand columns treated with *B. megaterium* SS3; Control: Untreated sand columns. Values bearing different letters in the same column are significant at P<0.05. Values are mean ± SD (n = 3).

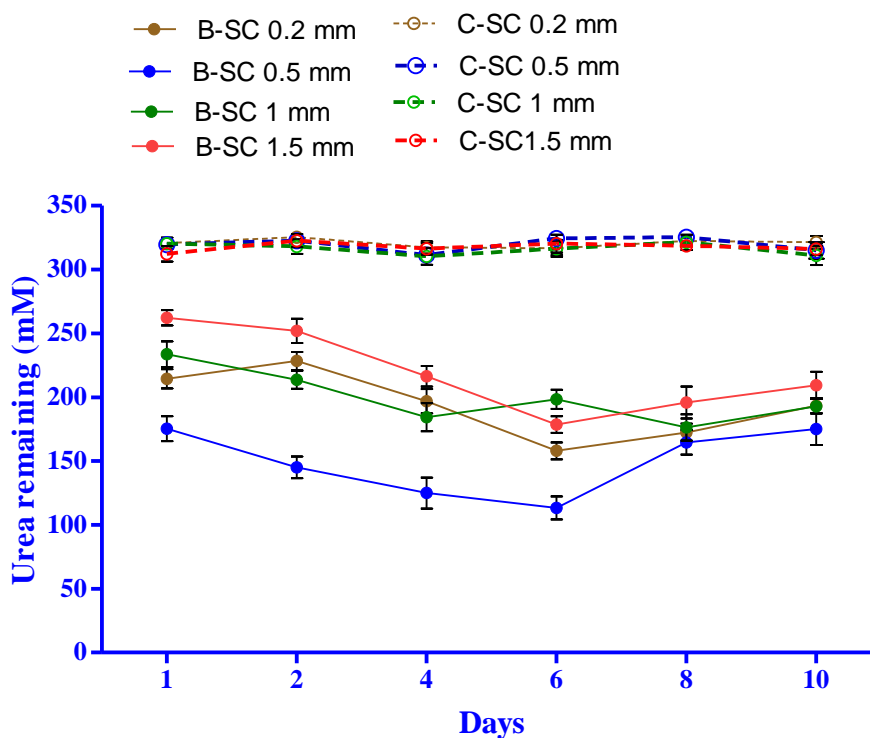


Fig.4.4.5. Estimation of remaining urea (mM) in the effluent from varying grain sized bacterial treated and control sand columns. Lines represent mean \pm SD (n = 3).

The decrease in pH, EC and urease activity after 7-8 days could be due to decline in bacterial activity which could have been due to restraining of bacteria (i.e., encapsulation of bacteria as a result of precipitation or being trapped inside pores) and interruption of chemical transport in the pore spaces after precipitation (which would prevent nutrients required for growth and chemicals required for further precipitation from reaching the bacteria). Both these reasons (cells encapsulation and starvation) have also been reported by van Paassen (2009). Thick calcite matrices are formed due to precipitation of carbonates which give rise to faster decline in bacterial activity as the urea becomes less available to the microbial cells. Rebata-Landa (2007) reported the bacterial activity drop to start between 16 and 32 days. van Paassen *et al.* (2009) also cited that bacterial activity dropped below 5 mM urea/hr after 20 days. Another explanation for this could also be the limitation of space in case of saturation of the pore fluid (Mitchell and Santamarina, 2005). Although Stocks -

Fisher *et al.* (1999) reported that urease is still active in degrading urea even during the stationary phase of cell growth, these reasons in addition to possible accumulation of metabolic wastes also result in the decrease of bacterial urease activity, which directly reduces its affinity for carbonate precipitation. In the present study also, there was minor decrease in the bacterial activity after 7-8 days. Stocks - Fischer *et al.* (1999) reported that the availability of microbial cells and extracellular urease enzyme produced around these cells have a significant impact on the rate of ammonia production and, consequently, precipitation. Van Paassen (2009) reported that reaction (hydrolysis) and diffusion rates also have a large impact on crystal properties at different stages of precipitation and should be taken into account when discussing distribution of solutes (urea molecules) with respect to crystals, because they could affect the supply of carbonate ions toward the crystal surface.

Few bacterial cells were also found to be present in the effluent (Fig. 4.4.6). The viability of bacterial cells was investigated by CTC dye. The formation of red colour upon reduction of CTC proved the viability of bacterial cells within the effluent. CTC has long been used to investigate the viability of bacterial cells by many researchers (Zamarreno *et al.* 2009; Sherr *et al.*, 1999; Flood *et al.*, 1999; Karner and Fuhrman, 1997; Nielsen *et al.*, 2003). In the present study also distinct red cells were visible which proved the presence of live bacterial cells. The presence of bacterial cells in the effluent of coarse soils further supports the fact that retention has not been fully successful due to loose consolidation and high pore sizes. Previous works have also reported that the retention of bacterial cells depends upon different factors including grain size distribution (Scholl *et al.*, 1990; Foppen and Schijven, 2006). Coarse grained materials require higher amounts of bacteria as well as regents as flushing with the media at regular intervals leads to limited adsorbed bacteria. This can be overcome by addition of fixation medias (Harkes *et al.*, 2010). So from the above studies, it has been envisaged that size of grain do plays a very important role in affecting calcification.

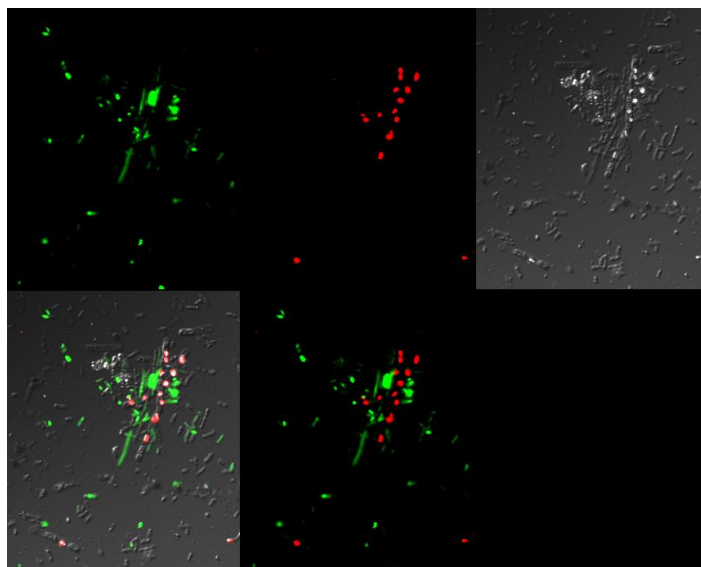


Fig. 4.4.6. Live viable cells in the effluent (red) of bacterial treated sand column

4.4.1.2. Effect of bacterial calcite on physico - chemical properties of sand columns

Biodeposition of carbonates in all the bacterial treated columns was clearly visible on the surface after 10 days. All the specimens (bacterial treated as well as control of each grain size) were taken (out of the plastic case) and dried in oven at 50°C for overnight. Control columns in most cases collapsed and lost the form (Fig. 4.4.7). All the sand columns were divided into three layers, namely, upper, middle and lower layer (Table 4.4.5; Fig. 4.4.8). The calcite content in each layer was estimated by EDTA method (section 3.2.3). It was noticed that all bacterial columns had significantly higher calcite content compared to their control. The maximum amount of calcite was deposited in the upper layer of all bacterial sand columns followed by middle and lower layer which is attributed to the fact that facultatively anaerobic cells grows at a higher rate in the presence of oxygen leading to higher precipitation of CaCO_3 around the surface (Stocks-Fischer *et al.*, 1999). Amongst all the layers, calcite content was found to be higher in case of upper layer of 0.5 mm grain sized column. It again followed the principle that very fine and very coarse soils have lower biocementation as compared to moderately grain sized soils. The calcite content in all control columns varied from 4 – 6 %.

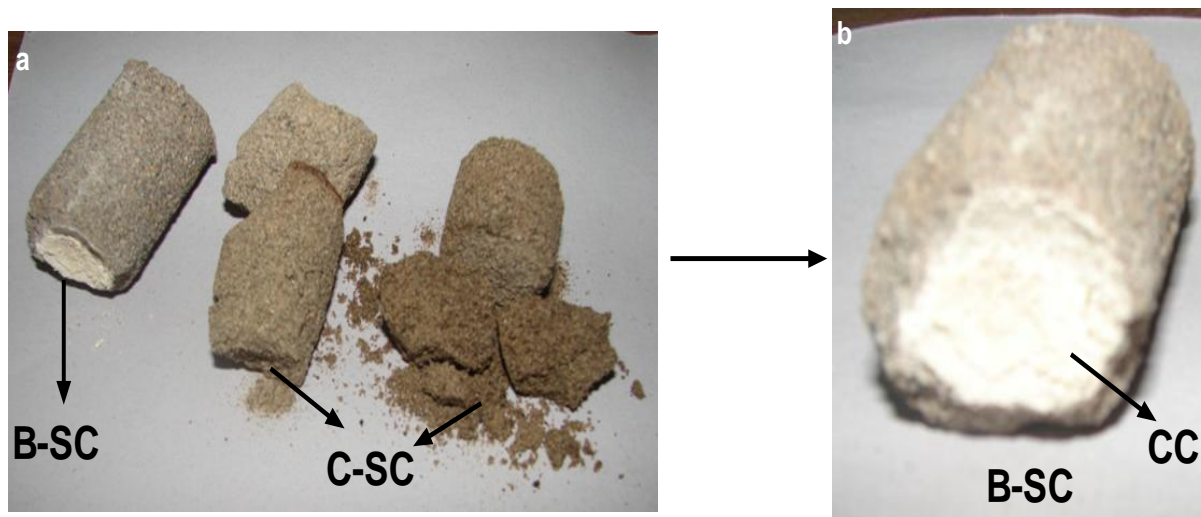


Fig. 4.4.7. Layer of carbonate crystals (CC) on the surface of bacterial sand column (B-SC) treated with *B. megaterium* SS3 along with collapsed control sand column (C-SC)

Table 4.4.5. Calcite content (%) in different layers of bacterial treated varying grain sized sand columns

Calcite content (%)					
Layer	Bacterial treated (0.2 mm)	Bacterial treated (0.5 mm)	Bacterial treated (1 mm)	Bacterial treated (1.5 mm)	Control
Upper	26 ± 3.5bc	31 ± 2.8a	27 ± 2.4b	24 ± 2.6c	5 ± 0.4gh
Middle	12 ± 1.4c	17 ± 1.6a	14 ± 1.1b	11 ± 1.3c	6 ± 0.6fg
Lower	5 ± 0.6b	8 ± 0.7a	6 ± 0.5b	7 ± 0.8a	5 ± 0.7b

Bacterial treated: Sand columns treated with *B. megaterium* SS3; Control: Untreated sand columns. Values bearing different letters in the same column are significant at $P < 0.05$. Values are mean ± SD (n = 3).

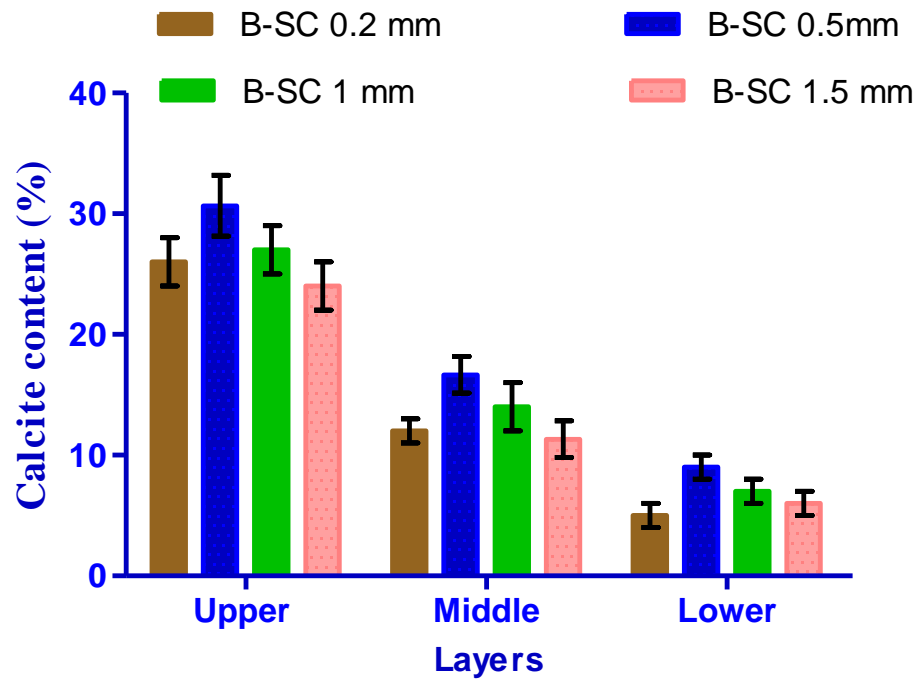


Fig. 4.4.8. Calcite content in the different layers of bacterial sand columns (B-SC) of varying grain sizes. Bars represent mean \pm SD (n = 3).

From all these results, it was clear that sand grains with 0.5 mm grain size are best suited for bioconsolidation compared to lower or higher grain sizes. The ability for microbially induced calcite precipitation (MICP) to be effective is dependent on the permeability of the soil being sufficient to allow injected chemicals to flow to the bacteria and the number of particle contacts available within the matrix (Mitchell and Santamarina, 2005). The increase in strength and stiffness due to the calcium carbonate precipitation is most effective at the particle contacts i.e. the more particle contacts within the matrix, the larger the effect of the precipitation. Another factor might be that very fine soils don't provide sufficient space for bacterial activity and coarse soils need much higher dose of nutrients and bacterial cells for compactness. So, moderate sands have faster rate of precipitation than finer and more poorly graded soils (Mortenesen *et al.*, 2011). Rebata-Landa (2007) also supported that lesser consolidation occurs for the soils with more extreme soil particle sizes.

In order to further determine the presence of carbonate crystals within sand grains, bioconsolidated columns along with controls were subjected to SEM, EDX and XRD. SEM analysis clearly depicted the formation of carbonate crystals within the sand grains. The carbonate crystals sealed the gaps within the pore spaces of the sand columns and involvement of bacterial cells was also clearly visible (Fig. 4.4.9). Bacterial cells were shown embedded within the carbonate crystals at few regions while at other regions they were seen in close proximity of the crystals. The presence of carbonate crystals associated with bacteria depicts that bacteria served as nucleation sites during the mineralization process.

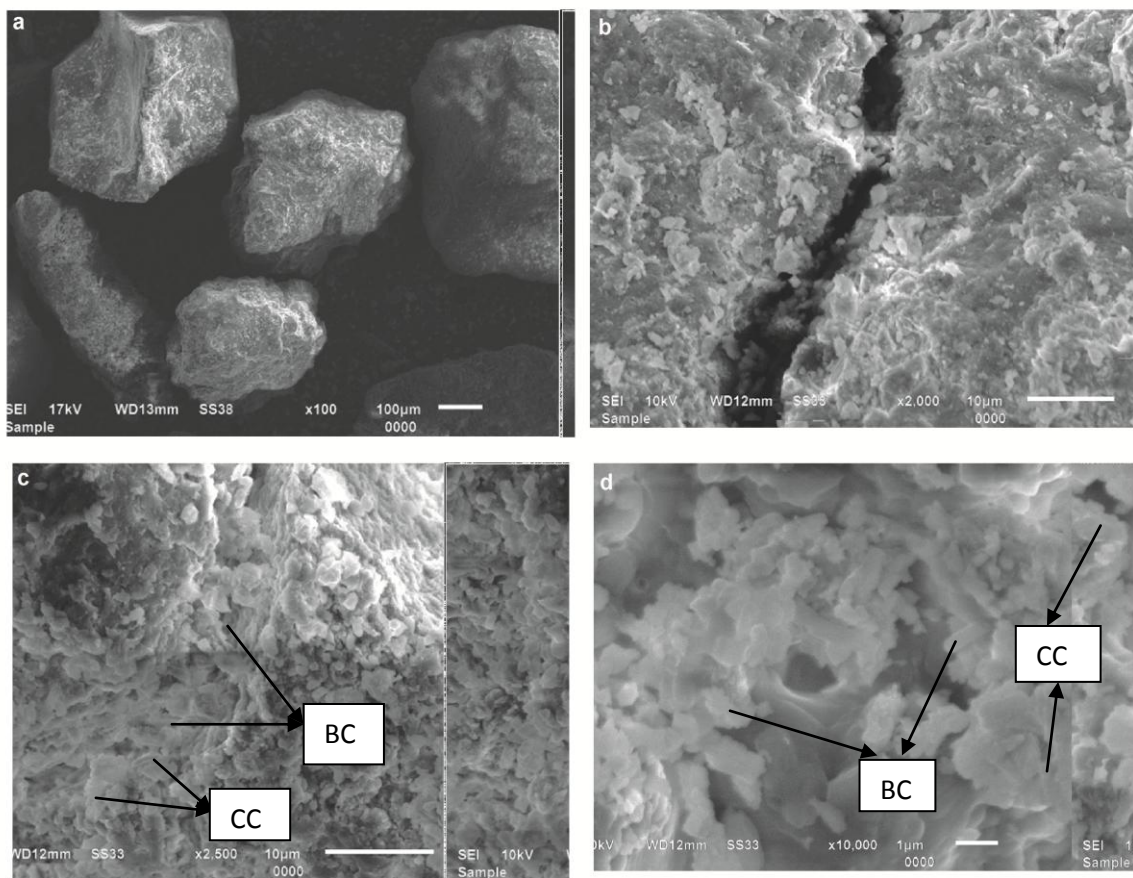


Fig. 4.4.9. Scanning electron microscopic analysis of sand columns a,b) control sand column (C-SC) c,d) bacterial sand column (B-SC) depicting the formation of carbonate crystals (CC) and bacterial cells (BC)

The mineral constituents of both bacterial treated as well as control sand columns were then investigated by Energy dispersive X ray analysis. High amount of calcium was observed in all the bacterial treated sand columns along with other components of sand while in case of control columns, insignificant amount of calcium was recorded (Fig. 4.4.10). This further proved the formation of calcium carbonates in case of bacterial treated sand columns.

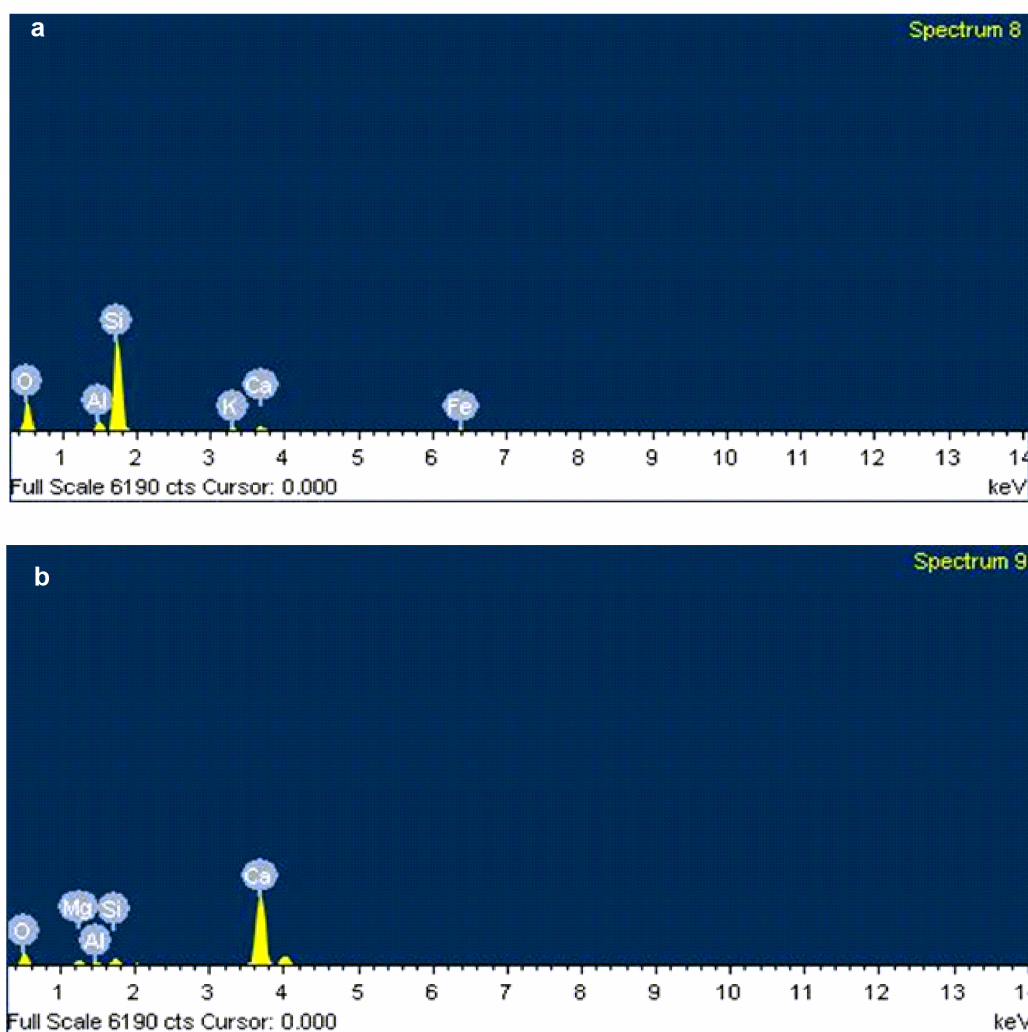


Fig. 4.4.10. Energy dispersive X ray spectra of a) control sand column b) bacterial treated sand column with abundant amount of Calcium seen

X ray diffraction analysis of upper layers of both bacterial treated as well as control columns was carried to analyze the constituents. It was depicted that majority of carbonate crystals

formed in bacterial columns were calcite along with few vaterites though quartz formed the main component of sand while there was no carbonates in control sand columns (Fig. 4.4.11). High amount of calcium and high number of calcite peaks in bacterial columns suggests that EDX and XRD analysis results are complimentary to each other.

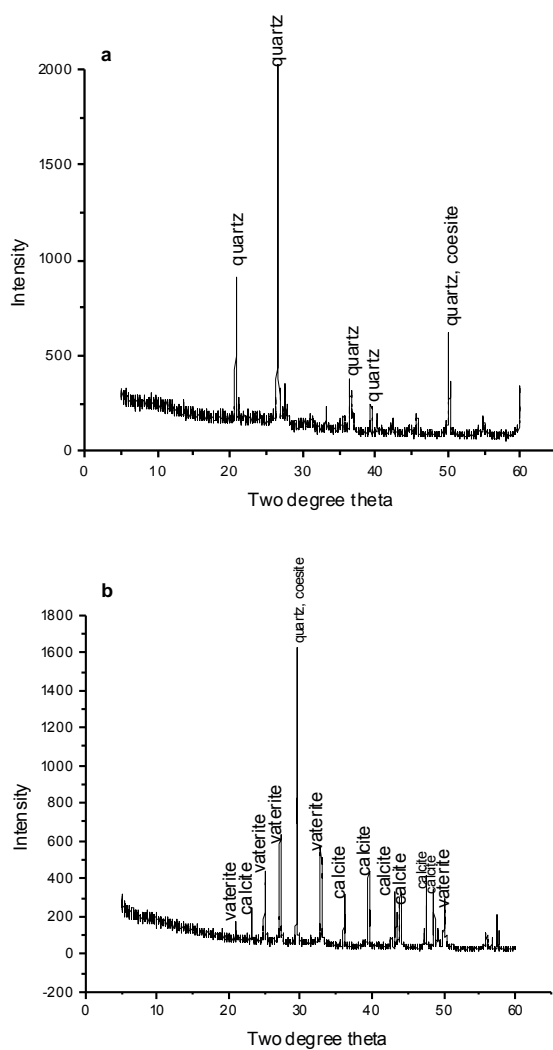


Fig. 4.4.11. X ray diffraction spectra of a) control sand column b) microbial sand column representing the presence of calcite as well as vaterite peaks

XRD analysis of pure calcium carbonate crystals had shown that calcite form was the dominant phase but in case of sand columns, both vaterite and calcite were formed. It might be due to different substrates in these cases. Rodriguez Navarro *et al.* (2012) recently pointed that carbonate polymorph formation is dependent on the type of substrate present for bacterial attachment. They demonstrated that calcitic substrates favor bacterial attachment and promote the formation of abundant calcite while under the same culture conditions, vaterite spheres are formed on silicate substrates. Rodriguez *et al.* (2012) also reported that the final bacterial calcium carbonate polymorph that appears in a particular situation strongly depends on the amount of dissolved organic carbon (DOC) from bacterial activity which hinders the vaterite to calcite phase transition. Little DOC favors the final formation of calcite, while high DOC promotes the kinetic stabilization of vaterite.

So, results of all these studies confirmed the successful formation of calcium carbonate crystals by ureolytic bacteria within varying grain sized sand columns. Better bioconsolidation leading to improved physical and chemical characteristics of sand grains has been found in sand columns with 0.5 mm grain sizes compared to much finer or coarser particles.

4.4.1.3. Effect of MICCP on varying density sand columns

For estimating the effect of bacterial calcification on varying density sand columns (1.65, 1.70, 1.75 g/cc), different sand columns were prepared as depicted in figure 7.12 by fixing their densities. The sand columns were prepared by block making machine and in this case, the biodeposition treatment was applied as a surface treatment where all the columns were subjected to spraying of 30 ml nutrient broth supplemented with 2% urea and 25 mM CaCl₂ (NBUC media) daily on their surface for 10 days. The biodeposition treatment in this case resulted in precipitation of carbonates on the overall surface of the columns (Fig. 4.4.13).



Fig. 4.4.13. Preparation of varying density sand columns by block making machine

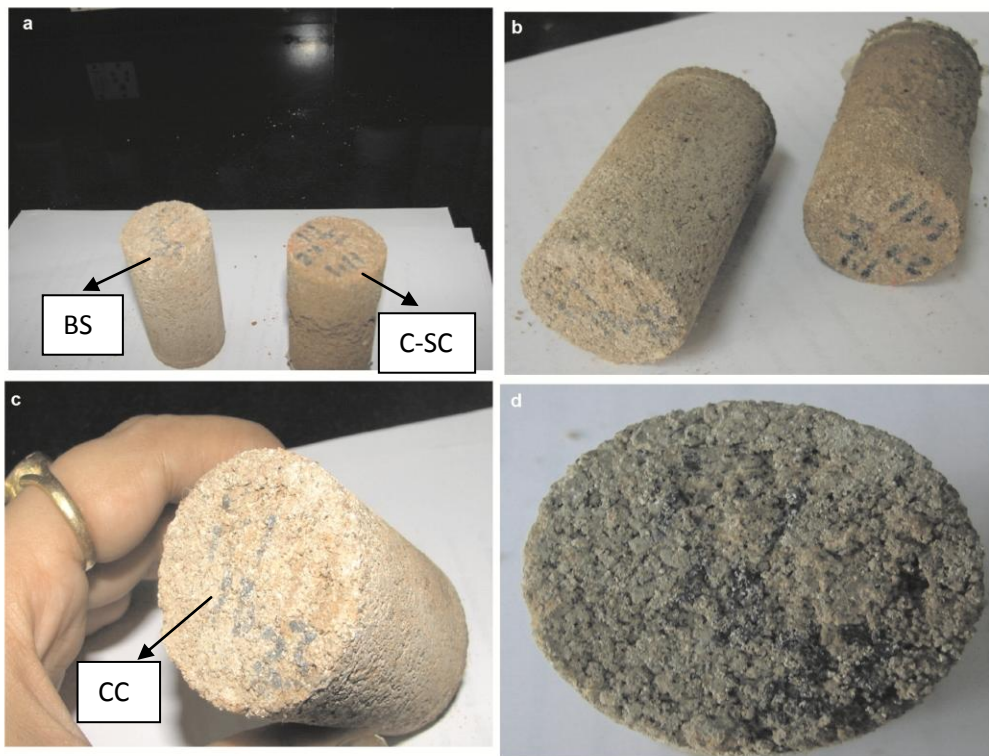


Fig. 4.4.12. Effect of carbonate crystal (CC) precipitation on the surface of bacterial sand column (B-SC) treated with *B. megaterium* SS3 compared to control sand column (C-SC).

4.4.1.3.1. Water absorption test

Water absorption test was carried out as per IS 3495 for different density sand columns. The decreased permeability in case of bacterial treated sand columns compared to control columns was clearly noticed (Table 4.4.6). Fig.7.14 shows the influence of carbonate precipitation on water absorption of various sand columns. The percentage of water absorption by 1.75 g/cc sand column was 7.6 % while in case of control sand column, it was observed to be 9.4 % which showed 23.6% reduction. In case of 1.70 g/cc sand column, it was 7.8% while the control displayed 10.1%; i.e. 29.4% reduction. Finally, in case of 1.65 g/cc sand column, it was found to be 9.3% while in case of control it was 11.3% i.e. 21.5% reduction.

Table 4.4.6. Effect of microbial calcite precipitation on water absorption of varying density (1.65 g/cc, 1.70 g/cc and 1.75 g/cc) sand columns

	Water absorption (%)	Reduction (%)
Control (1.65 g/cc)	11.3 ± 2.1a	--
Bacterial treated (1.65 g/cc)	9.3 ± 0.7c	21.5%
Control (1.70 g/cc)	10.1 ± 0.9b	--
Bacterial treated (1.70 g/cc)	7.8 ± 0.5d	29.4%
Control (1.75g/cc)	9.4 ± 0.6c	--
Bacterial treated (1.75 g/cc)	7.6 ± 0.3d	23.6%

Bacterial treated: Sand columns treated with *B. megaterium* SS3; Control: Untreated sand columns. Values bearing different letters in the same column are significant at P<0.05. Values are mean ± SD (n = 3).

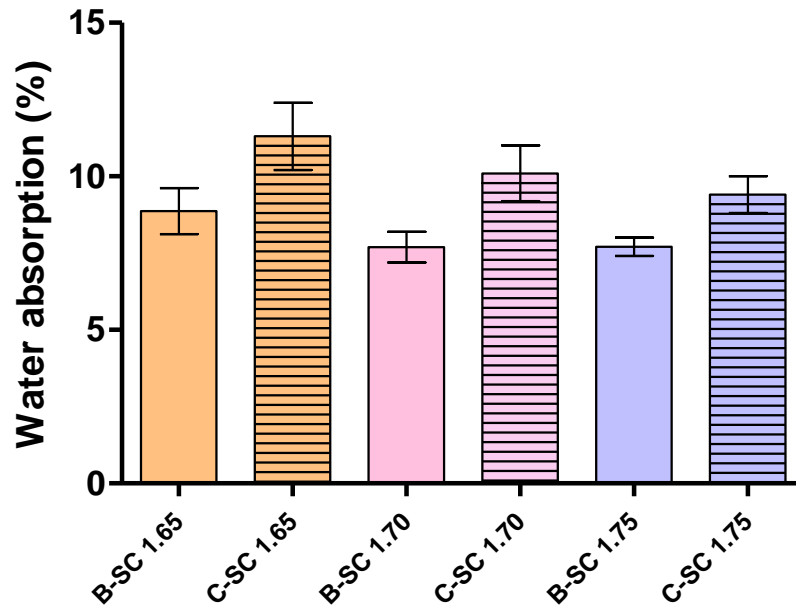


Fig. 4.4.14. Influence of the bacterial treatment on water absorption of varying density sand columns. Bars represent mean \pm SD (n = 3).

It was seen that all the bacterial columns showed significant reduction in the absorption of water which is attributed to the formation of carbonate binders on the overall surface of all sand columns as discussed previously. Amongst all sand columns, the columns with 1.75g/cc density absorbed minimum amount of water but maximum reduction was observed in columns with 1.70 g/cc. This might be providing optimal space for growth of bacteria leading to maximum carbonate precipitation as discussed earlier. The deposition of layer of carbonate crystals on the surface of the columns resulted in decreased permeability and water absorption.

4.4.1.3.2. Compressive strength

Compressive strength is considered as an index to assess the quality of a building material and is one of the most important characteristic of it. The compressive strength of varying densities sand columns was investigated to check the effect of biocementation on these sand

columns. The experimental set up for determining the strength of sand columns has been demonstrated in figure 7.15.



Fig. 4.4.15. Machine showing set up for measurement of Compressive strength

Formation of bacterial carbonate binders showed 19.6% improvement in the strength of sand columns with 1.70g/cc density followed by 17.5% improved performance in 1.65 g/cc and 11% improvement in strength of sand columns with 1.75 g/cc (Fig. 4.4.16; Table 4.4.7). In this case also, the carbonate deposition lead to improved strength in all the columns irrespective of their density. But maximum improvement was seen in columns with 1.70 g/cc density. So, this can be considered as the optimum density for maximum efficacy of bacterial carbonate deposition.

Microbial cells obtain good nourishment from nutrient broth along with urea and calcium, grow actively and upon cell growth, calcite precipitates on the cell surface as well as within the matrix. This might be due to variety of ions present in the media. As the pores in the matrix are plugged, the compressive strength improves. This increase in the strength results in lesser mean expansion (Ramakrishnan *et al.*, 1998). Thus, it was concluded that the improvement in compressive strengths of all bacterial columns is mainly due to consolidation of the pores inside the matrix with microbiologically induced calcium carbonate precipitation.

Table 4.4.7. Effect of microbial calcium carbonate precipitation on compressive strength of varying density sand columns (1.65 g/cc, 1.70 g/cc and 1.75 g/cc)

Treatment	Compressive strength (MPa)	Improvement (%)
Control (1.65 g/cc)	1.20 ± 0.5f	--
Bacterial treated (1.65 g/cc)	1.41 ± 0.6de	17.5%
Control (1.70 g/cc)	1.58 ± 0.3d	--
Bacterial treated (1.70 g/cc)	1.89 ± 0.4c	19.6%
Control (1.75g/cc)	2.08 ± 0.4b	--
Bacterial treated (1.75 g/cc)	2.31 ± 0.6a	11%

Bacterial treated: Sand columns treated with *B. megaterium* SS3; Control: Untreated sand columns. Values bearing different letters in the same column are significant at P<0.05. Values are mean ± SD (n = 3).

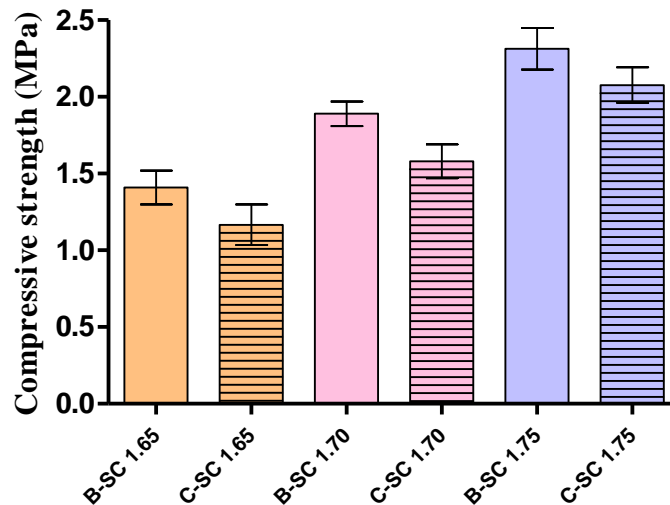


Fig. 4.4.16. Influence of the bacterial treatment on water absorption of varying density sand columns. Bars represent mean ± SD (n = 3).

The applicability of microbial concrete to affect the compressive strength of mortar and concrete has also been reported by several studies (Bang *et al.*, 2001; Ramachandran *et al.*, 2001; Ghosh *et al.*, 2005; De Muyneck *et al.*, 2008 a,b; Jonkers *et al.*, 2010; Achal *et al.*, 2011a,b) where different microorganisms have been applied in the concrete mixture. Ramchandran *et al.* (2001) observed the increase in compressive strength of cement mortar cubes at 7 and 28 days by using various concentrations of *Bacillus pasteurii*. They found that increase of strength resulted from the presence of adequate amount of organic substances in the matrix due to microbial biomass. Ghosh *et al.* (2005) studied the positive potential of *Shewanella* on compressive strength of mortar specimens and found that the greatest improvement was at cell concentration of 10^5 cells/ ml for 3, 7, 14 and 28 days interval. They reported an increase of 17% and 25% after 7 and 28 days. But no noticeable increase was recorded in case of specimens treated with *Escherichia coli* (low urease producing). It was concluded that choice of microorganism plays the prime role in improvement of strength characteristics. Jonkers and Schlangen (2007) studied the addition of bacterial spores ($10^8/\text{cm}^3$) of *Bacillus pseudofirmus* and *Bacillus cohnii* to concrete specimens and reported an increase of 10% in the compressive strength. Achal *et al.* (2009a) treated mortar cubes with *Sporosarcina pasteurii* and observed 17% improvement in compressive strength. Park *et al.* (2010) observed 22% increase in the strength of mortar cubes treated by *Arthrobacter crystallopoietes* which was higher compared to *Sporosarcina soli*, *Bacillus massiliensis* and *Lysinibacillus fusiformis* used along with. Upon addition of *Bacillus* sp. CT-5 to cement mortar specimens, the same group reported 36% increase in the compressive strength (Achal *et al.*, 2011a). Microbial calcite might have precipitated on the surface of cells and eventually within the pores leading to their plugging. So, in the present study also, the improvement in strength upon treatment with ureolytic calcifying bacteria was within the range of previous reports.

4.4.1.3.3. Porosimetry analysis

Reduction in permeability of sand columns upon treatment with bacterial carbonate binders was assessed by Mercury intrusion porosimetry (Table 4.4.8, 4.4.9). Mercury intrusion porosimetry data of bacterial and control specimens reflected the effect of microbial calcite

precipitation on reduction of total porosity. Sand columns with density 1.70 g/cc were found to be most efficiently bioconsolidated compared to others as the total porosity of control specimens in this case was found to be 23.5% while upon calcification; it was estimated to be 17.1% which showed 27.2% reduction. Fig. 4.4.17 represents typical pore size distribution curve of bacterial and control specimens. The porosity of the samples was calculated using cumulative intrusion volume and relevant mass measurements.

The reduction in porosity is attributed to filling of the voids and clogging of pores due to calcite binders. Calcium carbonate forms an impervious layer on the surface. Entrapped bacterial biomass and sometimes gas bubble formation also leads to decreased porosity. Whiffin *et al.* (2004) observed 90% decrease in porosity of sand column upon bacterial calcite formation. Both porosity and permeability are related to each other. If porosity is high and pores are well connected, permeability is high. If porosity is low or pores are badly connected, permeability is low. In this case, precipitation of calcium carbonate in the pore spaces on the surface of specimens resulted in reduction of pore space volume, lowering of permeability as well as porosity.

In the studies of Zamarreno *et al.* (2009), treatment of the limestone slides with biocalcifying bacteria to reduced the area of open pore space by at least 20% more than the application of isolate medium alone. Rodriguez-Navarro *et al.* (2003) also used mercury intrusion porosimetry (MIP) to study changes in pore size due to biocalcification by *Myxococcus xanthus*; however, the MIP method was not sensitive enough to detect the small changes produced by bacterially precipitated calcium carbonates. They also stated that the information from MIP is important in assessing the depth of penetration of bacteria, but these methods do not necessarily provide information on the relationship between open pore spaces and bacteria on the surface of the sample. They do not provide information on the spatial extent of the relationship between open pore space and bacterial growth.

Table 4.4.8 a) Mercury intrusion porosimetry of Control sand column (density 1.70 g/cc)

Pressure (psia)	Pore diameter (μm)	Cumulative pore volume (mL/g)	Incremental pore volume (mL/g)
0.54	337.9243	0	0
1.03	176.3791	0.0056	0.0056
2.02	89.7196	0.0105	0.0049
3	60.2712	0.013	0.0025
4.01	45.121	0.0153	0.0023
5	36.1568	0.0173	0.002
6	30.148	0.019	0.0017
7.5	24.12	0.0211	0.0021
8.5	21.2842	0.0222	0.0011
10.5	17.2292	0.0239	0.0016
13	13.917	0.0261	0.0022
15.99	11.3076	0.0287	0.0026
19.99	9.0461	0.0307	0.002
24.99	7.2365	0.0329	0.0022
29.99	6.0313	0.0348	0.0019
37.07	4.8783	0.0372	0.0023
46.27	3.9091	0.0398	0.0027
56.8	3.1845	0.0424	0.0025
71.54	2.5282	0.0456	0.0033
86.62	2.088	0.0483	0.0027
110.86	1.6314	0.0525	0.0042
136.99	1.3203	0.0561	0.0037
171.55	1.0543	0.0602	0.004
215.94	0.8376	0.0643	0.0041
266.82	0.6779	0.068	0.0037
326.79	0.5535	0.0715	0.0035
416.51	0.4342	0.0756	0.0041
516.76	0.35	0.0791	0.0035
636.76	0.284	0.0825	0.0033
796.98	0.2269	0.086	0.0036
987.37	0.1832	0.0894	0.0034
1196.76	0.1511	0.0926	0.0031
1496.1	0.1209	0.0964	0.0039
1896.44	0.0954	0.1009	0.0044

2346.01	0.0771	0.1053	0.0044
2895.17	0.0625	0.1098	0.0046
3593.62	0.0503	0.1146	0.0048
4487.2	0.0403	0.1199	0.0053
5581.24	0.0324	0.1254	0.0055
6877.63	0.0263	0.1312	0.0058
8574.81	0.0211	0.1372	0.006
10567.7	0.0171	0.1422	0.005
13153.31	0.0138	0.1465	0.0042
14755.82	0.0123	0.1483	0.0019
16362.12	0.0111	0.1499	0.0016
19951.89	0.0091	0.1523	0.0024
24984.66	0.0072	0.1546	0.0022
29985.88	0.006	0.1561	0.0015
27290.93	0.0066	0.1557	-0.0004
21017.19	0.0086	0.1552	-0.0005
16019.81	0.0113	0.1549	-0.0002
12426.28	0.0146	0.1547	-0.0002
9626.97	0.0188	0.1543	-0.0005
7315.51	0.0247	0.1534	-0.0009
5719.54	0.0316	0.1519	-0.0014
4307.53	0.042	0.1493	-0.0026
3303	0.0548	0.1459	-0.0034
2602.09	0.0695	0.1423	-0.0035
2002.68	0.0903	0.1384	-0.004
1502.75	0.1204	0.1341	-0.0043
1202.05	0.1505	0.1305	-0.0036
902.03	0.2005	0.1256	-0.0048
701.83	0.2577	0.1212	-0.0044
502.56	0.3599	0.116	-0.0052
403.97	0.4477	0.1129	-0.0031
302.14	0.5986	0.1095	-0.0035
242.59	0.7455	0.1071	-0.0024
192.58	0.9391	0.1047	-0.0024
148.2	1.2204	0.102	-0.0027
113.32	1.596	0.0994	-0.0026
88.23	2.05	0.097	-0.0024
68.1	2.6559	0.0944	-0.0026
54.12	3.3421	0.0922	-0.0022

Table 4.4.8 b) Mercury intrusion porosimetry of bacterial sand column (density 1.70 g/cc)

Pressue (psia)	Pore diameter (μm)	Cumulative pore volume (mL/g)	Incremental pore volume (mL/g)
0.54	337.9243	0	0
1.03	176.3791	0.0051	0.0051
2.02	89.7196	0.0118	0.0067
3	60.2712	0.0158	0.004
4.01	45.121	0.0192	0.0034
5	36.1568	0.0228	0.0036
6	30.148	0.0246	0.0019
7.5	24.12	0.0268	0.0021
8.5	21.2842	0.0281	0.0013
10.5	17.2292	0.0303	0.0023
13	13.917	0.0323	0.002
15.99	11.3076	0.034	0.0017
19.99	9.0461	0.0357	0.0017
24.99	7.2365	0.0374	0.0016
29.99	6.0313	0.0386	0.0012
37.16	4.8676	0.0395	0.001
47.42	3.8142	0.0408	0.0013
56	3.2295	0.0416	0.0008
72.68	2.4884	0.0429	0.0012
86.9	2.0813	0.0437	0.0009
110.66	1.6344	0.0449	0.0012
136.96	1.3206	0.0459	0.0009
171.65	1.0537	0.0469	0.0011
217.51	0.8315	0.0481	0.0011
267.06	0.6772	0.0492	0.0011
326.39	0.5541	0.0504	0.0013
416.06	0.4347	0.0521	0.0017
516.78	0.35	0.0536	0.0015
636.59	0.2841	0.0551	0.0015
797.23	0.2269	0.0569	0.0018
987.37	0.1832	0.0587	0.0018
1196.78	0.1511	0.0604	0.0017
1497.15	0.1208	0.0623	0.002
1896.81	0.0954	0.0645	0.0022

2345.4	0.0771	0.0666	0.0021
2894.38	0.0625	0.0686	0.002
3592.87	0.0503	0.0709	0.0023
4486.24	0.0403	0.0734	0.0025
5582.67	0.0324	0.0758	0.0024
6873.9	0.0263	0.0781	0.0023
8574.42	0.0211	0.0804	0.0024
10566.89	0.0171	0.0826	0.0021
13157.69	0.0137	0.0847	0.0021
14759.72	0.0123	0.0859	0.0011
16355.3	0.0111	0.087	0.0011
19948.59	0.0091	0.0889	0.0019
24983.99	0.0072	0.091	0.0021
29973.83	0.006	0.0923	0.0014
27282.34	0.0066	0.092	-0.0003
21018.65	0.0086	0.0916	-0.0004
16022.37	0.0113	0.0916	-0.0001
12424.23	0.0146	0.0915	0
9628.29	0.0188	0.0915	0
7316.98	0.0247	0.0914	-0.0001
5717.56	0.0316	0.0911	-0.0003
4307.51	0.042	0.0906	-0.0005
3304.42	0.0547	0.09	-0.0006
2603.79	0.0695	0.0894	-0.0006
2001.81	0.0903	0.0886	-0.0008
1499.13	0.1206	0.0877	-0.0009
1200.92	0.1506	0.0869	-0.0008
902.49	0.2004	0.086	-0.001
702.24	0.2576	0.0851	-0.0009
502.39	0.36	0.0841	-0.0011
402.76	0.4491	0.0833	-0.0008
302.52	0.5979	0.0825	-0.0008
242.48	0.7459	0.0817	-0.0007
192.06	0.9417	0.0811	-0.0007
148.13	1.221	0.0804	-0.0007
112.33	1.61	0.0797	-0.0007
89.37	2.0237	0.0792	-0.0005
68.22	2.6513	0.0786	-0.0006
53.15	3.4032	0.0781	-0.0005

Table.4.4.9. Mercury intrusion porosimetry analysis of control and bacteria treated blocks with 1.70g/cc density.

Parameter	Control sand column	Bacterial sand column
Total Intrusion Volume (mL/g)	0.15 ± 0.00a	0.09 ± 0.00b
Total Pore Area (m²/g)	10.60 ± 0.5a	6.20 ± 0.3c
Median Pore Diameter (µm Volume)	0.37 ± 0.01a	0.30 ± 0.06b
Median Pore Diameter (µm Area)	0.01 ± 0.00a	0.01 ± 0.00a
Average Pore Diameter (µm 4V/A)	0.05 ± 0.00a	0.04 ± 0.00b
Bulk Density at 0.60 psia (g/mL)	1.82 ± 0.06b	1.90 ± 0.07a
Apparent (skeletal) Density (g/mL)	2.17 ± 0.11b	2.30 ± 0.13a
Porosity (%)	23.50 ± 1.2a	17.10 ± 0.7b

MIP data (Mean ± SD) of control and bacterial specimens. These results are average of three replicates.

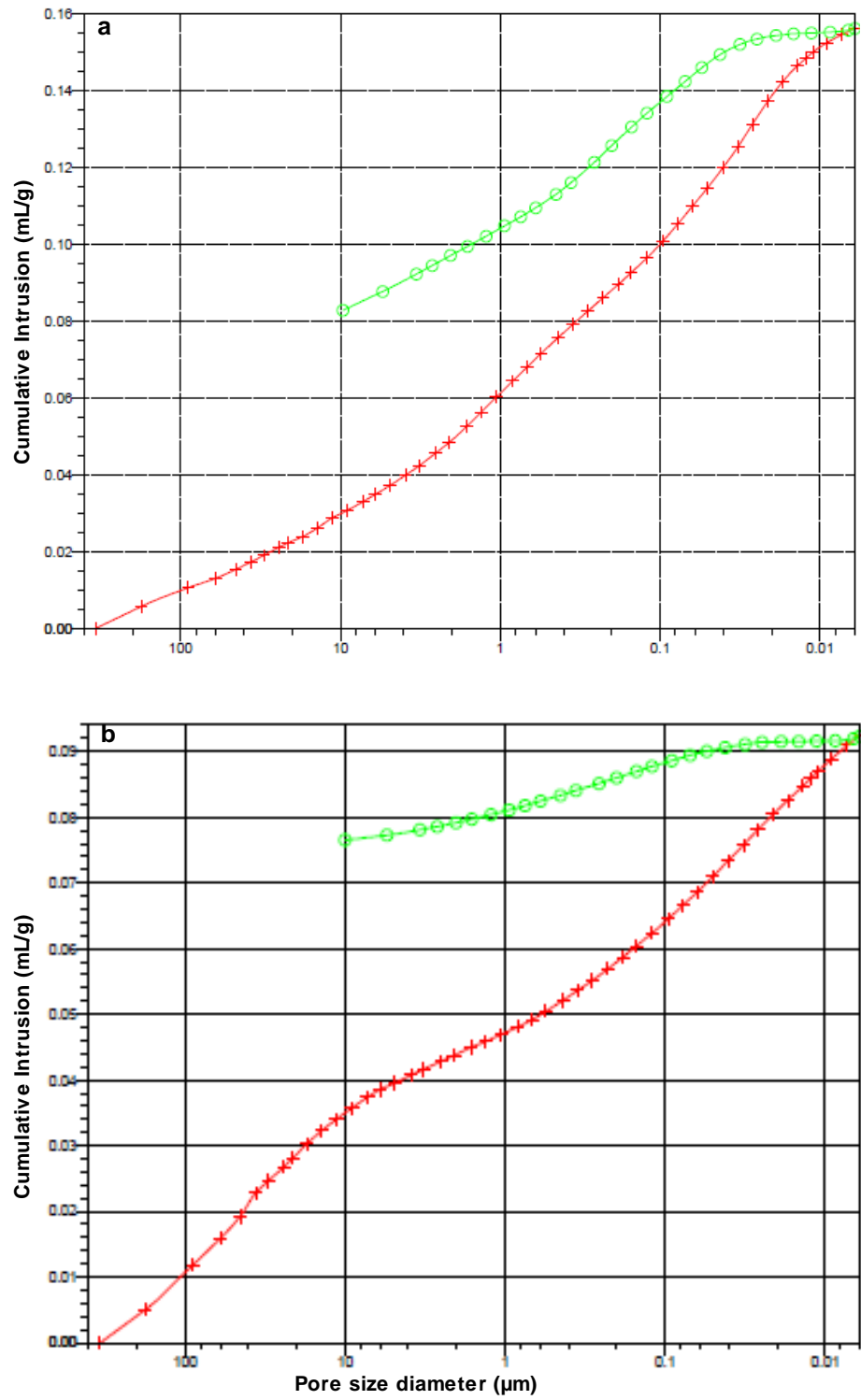


Fig. 4.4.17. Pore size distribution curve of bacterial and control specimens

To further determine whether the decrease in permeability and increase in strength in case of bacterial treated sand columns is due to the formation of bacterial carbonate crystals only, the surface of the bacterial as well as control columns was subjected to EDX and XRD analysis. Highest amount of calcium peak was found in the sand column with 1.70 g/cc density which further supported the previous results (Fig. 4.4.18). XRD analysis also depicted calcite and vaterite peaks along with quartz (Fig. 4.4.19).

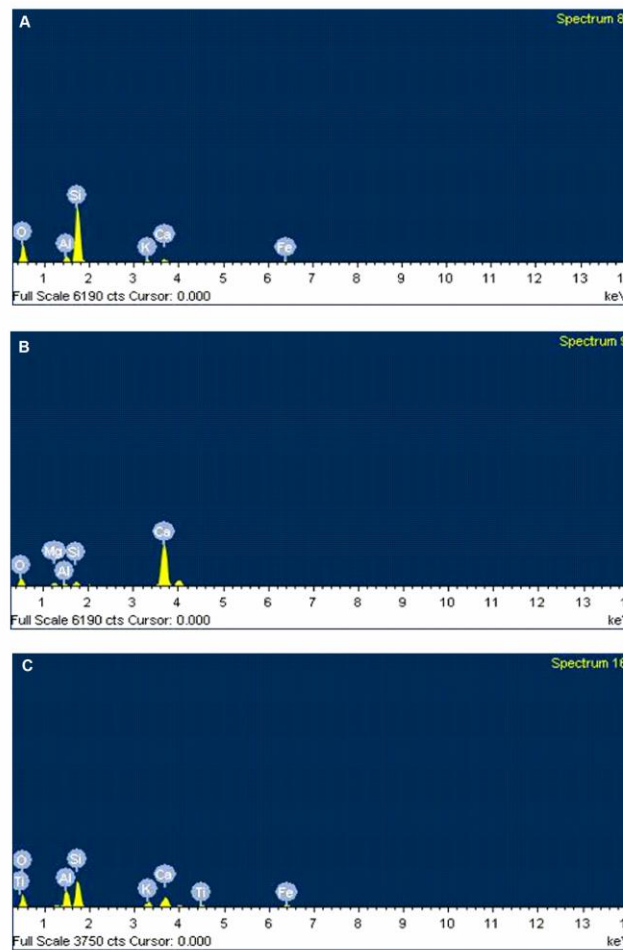


Fig. 4.4.18. Energy dispersive X ray spectrum of varying density sizes bacterial columns (a: 1.65g/cc; b: 1.70g/cc; c: 1.75g/cc)

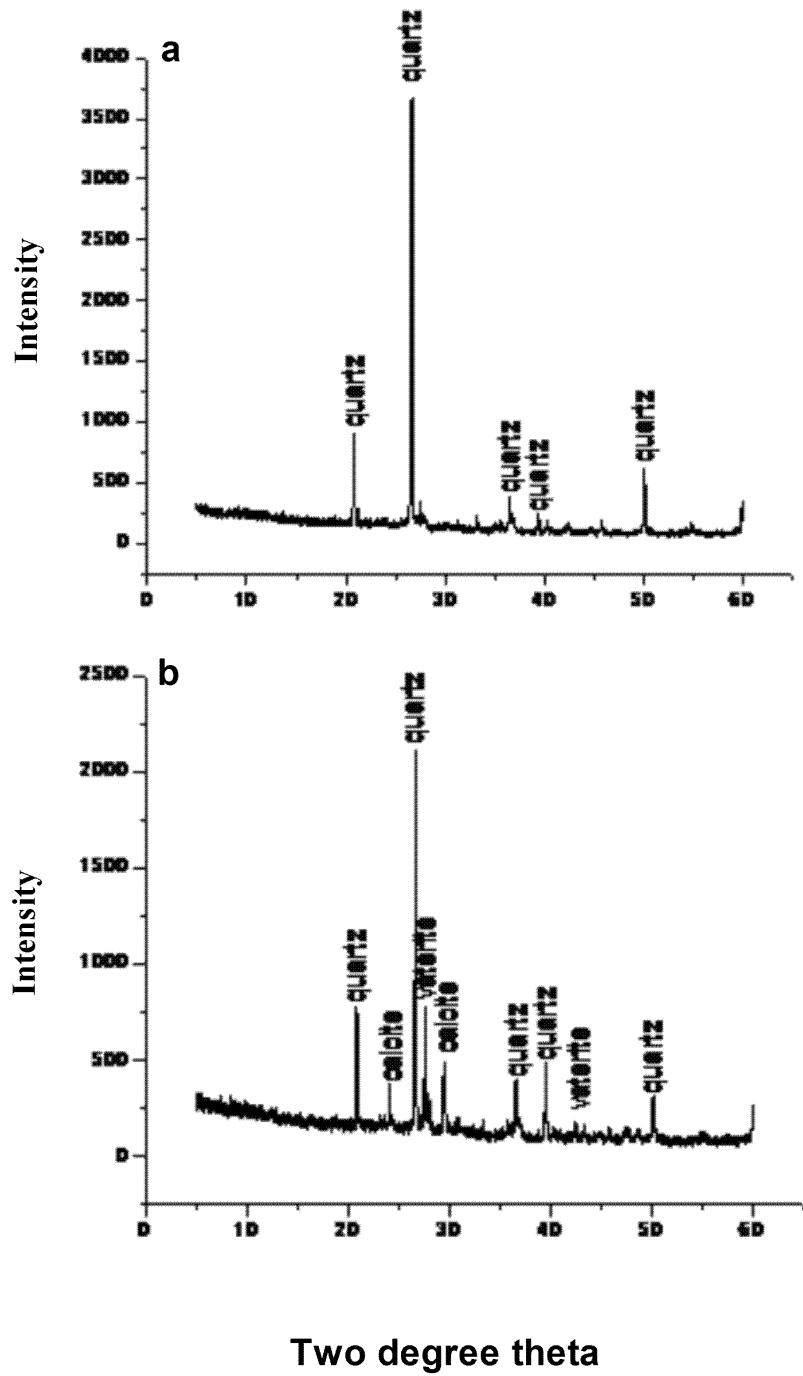


Fig. 4.4.19. X ray diffraction analysis of a) 1.70 g/cc density control sand column b) 1.70 g/cc density bacterial sand column

4.4.2. Effect of microbially induced calcium carbonate precipitation on durability of Soil cement Blocks

Soil cement blocks have been found to be the most energy efficient building materials. These blocks consume merely 23.5% energy of burnt clay bricks with energy content of 2.75 – 3.75 MJ per block with size 230 mm x 190 mm x 100 mm. But due to certain issues of durability and moisture absorption leading to expansions and structural weakening, they are not much in use. The aim of the present work was to investigate the influence of bacterial carbonates in improving the durability of these low energy building materials which will pave way for highly energy efficient and green buildings that are the need of time. The manufacturing of these low energy building materials has been shown in figure 4.4.20. Upon treatment of these low energy building materials to bacterial cells along with NBUC media for 28 days as discussed in section 3.4.2, various parameters were studied to assess the effect of bacterial carbonates on durability of low energy building materials as follows.



Fig. 4.4.20. Set up for making soil cement blocks (Reddy and Jagadish, 2003)

4.4.2.1. Absorption characteristics of Bacterial Blocks

Influence of bacterial mineralization on the absorption characteristics of soil cement blocks was examined by measuring rate of water absorption and saturated water content (Table 4.4.10 a, b). Both bacterial treated as well as control blocks when soaked in water absorbed water rapidly during first few minutes as shown in figure 7.21a. But later it became apparent that rate of water absorption was significantly reduced upon bacterial treatment. The saturated water content of bacterial treated blocks was also determined and it was found to be 6.6 % while in case of untreated blocks, it was found to be 9.93% which showed 33.6 % reduction (Fig. 4.4.21b). The presence of bacterial biomass as well as biominerals contributed to a large extent in the overall decrease of the water permeability in bacterial treated specimens. Significant decrease in water absorption is attributed to the physical obstruction of pores. Studies on the effect of microbial calcite on cementitious structures and limestone have been conducted by various researchers. De Muynck *et al.* (2008b) studied the effect of biodeposition of calcite on permeability characteristics of mortar by *B. sphaericus*. Significant differences in carbonation depth between treated and untreated specimens were noticeable after 2 weeks of accelerated carbonation in treated mortar specimens. Achal *et al.* (2010a) reported the decreased water permeability of bioremediated cement mortar cubes treated by *Sporosarcina pasteurii*. The lower permeability of the bioremediated cubes compared with that of the control cubes was probably due to a denser interfacial zone formed because of calcite precipitation between the aggregate and the concrete matrix. This demonstrated the profound effect of microbial calcite on the permeability of concrete. Six times reduction in absorption of water was reported upon treatment of mortar cubes with *Bacillus* sp. CT-5 as compared to untreated specimens (Achal *et al.*, 2011b). Tiano *et al.* (1999) studied the effect of microbial calcite crystals on Pietra di Lecce bioclastic limestone by use of *Micrococcus* spp. and *Bacillus subtilis*. Dick *et al.* (2006) reported 50% reduction in water absorption by treating limestone cubes with two strains of *B. sphaericus*. Zamarreno *et al.* (2009) investigated the application of calcite crystals precipitated by fresh water bacteria on limestone and found significant reduction in pore sizes of the bacterial treated substrate stone specimens as compared to the untreated ones.

Table 4.4.10 a. Effect of bacterial treatment on the rate of water absorption by Soil cement blocks at different time intervals

Time (mins)	Control blocks	Bacterial treated blocks
0.5	2.81 ± 0.1a	1.62 ± 0.2b
1	4.24 ± 0.1a	2.14 ± 0.2b
1.5	5.21 ± 0.2a	2.99 ± 0.1b
2	5.79 ± 0.1a	3.68 ± 0.1b
2.5	6.36 ± 0.3a	4.47 ± 0.1 b
3	6.88 ± 0.2a	4.87 ± 0.2b
4	7.28 ± 0.1a	4.93 ± 0.2b
5	7.51 ± 0.2a	5.1 ± 0.1b
6	7.74 ± 0.1a	5.39 ± 0.3b
7	7.79 ± 0.3a	5.73 ± 0.3b
8	7.97 ± 0.2a	5.96 ± 0.2b
9	8.02 ± 0.3a	6.07 ± 0.3b
10	8.19 ± 0.1a	6.3 ± 0.2b
15	8.19 ± 0.1a	6.47 ± 0.1b
20	8.31 ± 0.2a	6.53 ± 0.1b
30	8.71 ± 0.3a	6.81 ± 0.09b
40	8.77 ± 0.2a	6.98 ± 0.05b
50	8.77 ± 0.3a	7.15 ± 0.07b
60	8.83 ± 0.3a	7.21 ± 0.1b
80	8.83 ± 0.2a	7.27 ± 0.08b
100	8.83 ± 0.2a	7.32 ± 0.1b

120	8.83 ± 0.1a	7.32 ± 0.06b
140	8.83 ± 0.2a	7.32 ± 0.07b
160	8.83 ± 0.1a	7.38 ± 0.09b
180	8.83 ± 0.1a	7.38 ± 0.1b
210	8.83 ± 0.1a	7.38 ± 0.1b
240	8.83 ± 0.1a	7.38 ± 0.07b
300	8.83 ± 0.1a	7.44 ± 0.05b
360	8.83 ± 0.05a	7.44 ± 0.06b
480	8.83 ± 0.09a	7.44 ± 0.08b
720	8.83 ± 0.07a	7.5 ± 0.04b
960	8.83 ± 0.1a	7.5 ± 0.1b
1440	8.88 ± 0.1a	7.5 ± 0.06b

Values bearing different letters in the same column are significant at $P < 0.05$. Values are mean \pm SD (n = 3).

Table 4.4.10 b. Effect of bacterial treatment on saturated water content of soil cement blocks

Samples	% saturated water content	% decrease in saturated water content
Control	9.93 ± 0.8a	--
Bac treated	6.6 ± 0.3b	33.6%

Values bearing different letters in the same column are significant at $P < 0.05$. Values are mean \pm SD (n = 3).

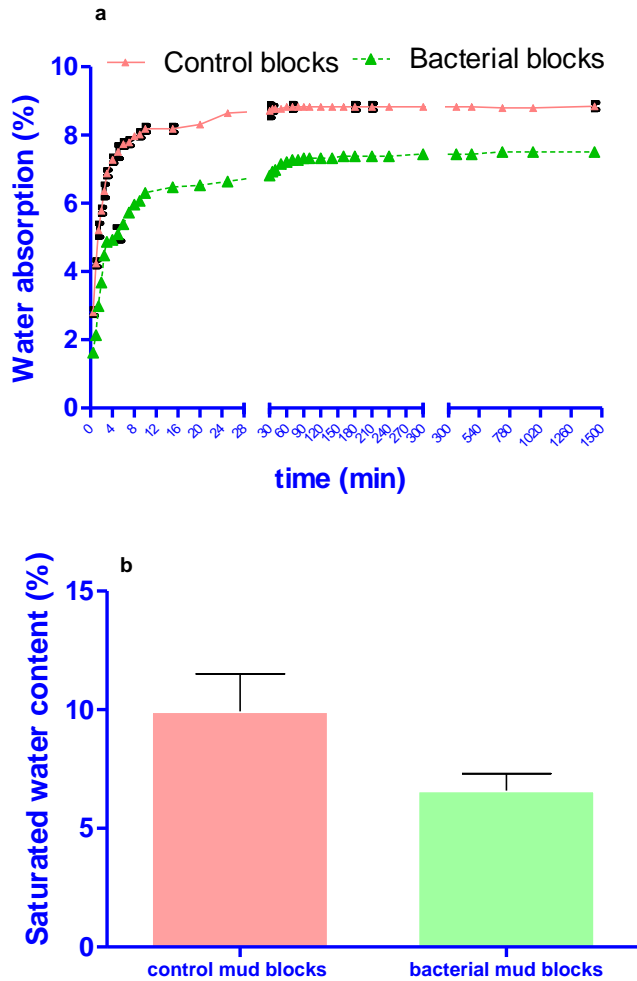


Fig. 4.4.21. Effect of MICP on a) rate of water absorption b) saturated water content in soil cement blocks. Lines and bars are mean \pm SD (n = 3).

4.4.2.2. Wet Compressive strength and linear expansion of soil cement blocks

Wet compressive strength test and linear expansion on saturation indicates the stability and performance of a building material. The set up for both these tests has been demonstrated in figure 4.4.22. In this case, both the wet strength (as per IS 3495) and the linear expansion (Reddy and Jagadish, 2003) displayed significant improvement of bacterial treatment on efficiency of the soil cement blocks (Table 4.4.11; Fig. 4.4.23). The compressive strength in

case of bacterial soil cement blocks was found to be 5.9 MPa while that of control blocks was 4.8 MPa which showed 23% improvement (Fig. 1c). Linear expansion on saturation of <math><0.10\%</math> generally leads to stable long term performance (Reddy, 2002). Linear expansion in case of bacterial blocks was found out to be 0.05% while in case of untreated blocks it came out to be 0.09%. Measurable increase in compressive strength of cement mortar cubes and limestone by application of *S. pasteurii* has been reported previously (Ramachandran *et al.*, 2001; Achal *et al.*, 2011a,b, Le Metayer-Levrel *et al.*, 1999).

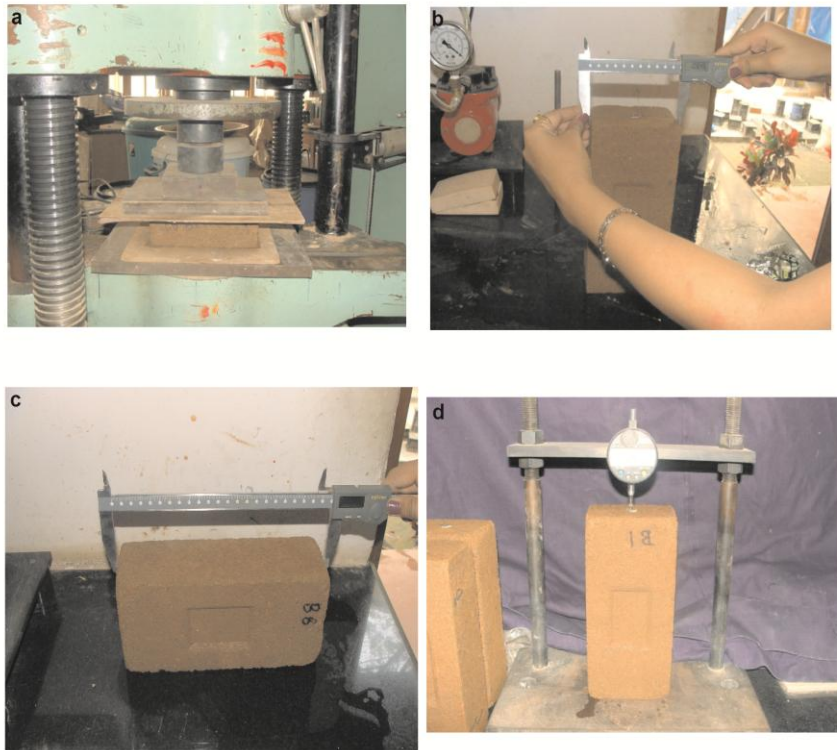


Fig. 4.4.22. Set up for a) compressive strength b,c,d) Linear expansion test

Table 4.4.11. Effect of microbial calcite precipitation on Compressive strength and linear expansion of soil cement blocks

Parameter	Control	Bacterial treated	Improvement
% compressive strength	4.8 ± 0.06b	5.9 ± 0.07a	23%
% Linear expansion	0.09 ± 0.0a	0.05 ± 0.0b	44%

Values bearing different letters in the same column are significant at $P < 0.05$. Values are mean ± SD (n = 3).

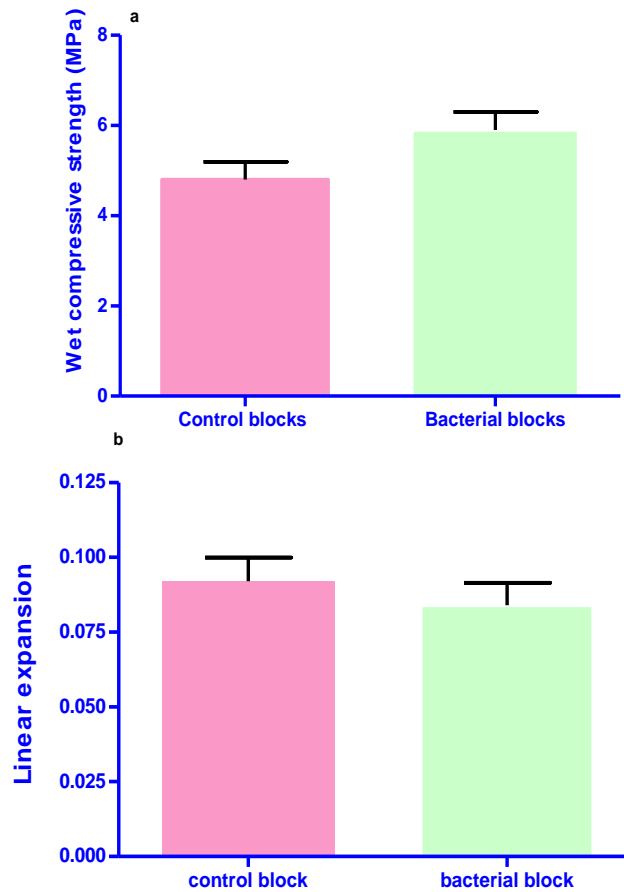


Fig. 4.4.23. Effect of MICP on a) Compressive strength b) Linear expansion of soil cement blocks. Bars are mean ± SD (n = 3).

4.4.2.3. Mercury intrusion porosimetry test

Mercury intrusion porosimetry test in this case depicted that the average porosity decreased from 25.3% to 17.5 % upon bacterial treatment. Mercury intrusion porosimetry analysis further supported the earlier data which proved the potential of bacterial calcite in reducing the porosity of building material and enhancing the durability and strength characteristics.

Table 4.4.12. Effect of MICP on porosity of soil cement blocks by Mercury intrusion porosimetry analysis

Parameter	Control Block	Bacterial Block
Total Intrusion Volume (mL/g)	0.15 ± 0.00a	0.09 ± 0.00c
Total Pore Area (m²/g)	10.60 ± 0.5a	6.20 ± 0.3c
Median Pore Diameter (µm Volume)	0.37 ± 0.01d	1.20 ± 0.06a
Median Pore Diameter (µm Area)	0.01 ± 0.00a	0.01 ± 0.00a
Average Pore Diameter (µm 4V/A)	0.04 ± 0.00a	0.05 ± 0.00a
Bulk Density at 0.60 psia (g/mL)	1.82 ± 0.06a	1.90 ± 0.07 a
Apparent (skeletal) Density (g/mL)	2.17 ± 0.11b	2.30 ± 0.13a
Porosity (%)	25.30 ± 1.7a	17.50 ± 0.92b

MIP data (Mean ± SD) of control and bacterial blocks. These results are average of three replicates

4.4.2.4. Freeze thaw resistance test and weight loss test

Two other tests that depict the durability of building structures are freeze thaw resistance test and weight loss test (Table 4.4.13; Fig 7.24). Freeze thaw test was conducted as per ASTM C67. In this case also, it was noticed that there was again considerable improvement in strength which was found to be 18% higher than control blocks.

The bacterial treated and control blocks were subjected to 8 hrs wetting and 16 hrs drying as per IS3495. 2 - 3% weight loss was noticed in case of bacterial specimens while in case of untreated specimens the weight loss was found to be 4 - 5% which was again considerable improvement. These results further proved the high physiochemical resistance of bacterial

cement. Rodriguez - Navarro *et al.* (2012) also stated that bacterial cement is highly coherent and ensures high physicochemical resistance. Bacterially induced calcite crystals are more resistant to dissolution since it has been experimentally demonstrated that biomineralized calcite is less soluble than inorganically precipitated calcite.

Table 4.4.13. Effect of MICP on freeze thaw strength test and weight loss durability test of soil cement blocks.

Test	Control	Bacterial treated	Improvement
Freeze thaw resistance (MPa)	4.1 ± 0.4c	4.8 ± 0.3a	17%
Weight loss (%)	4.5 ± 0.2a	2.5 ± 0.1d	44%

Values bearing different letters in the same column are significant at P<0.05. Values are mean ± SD (n = 3).

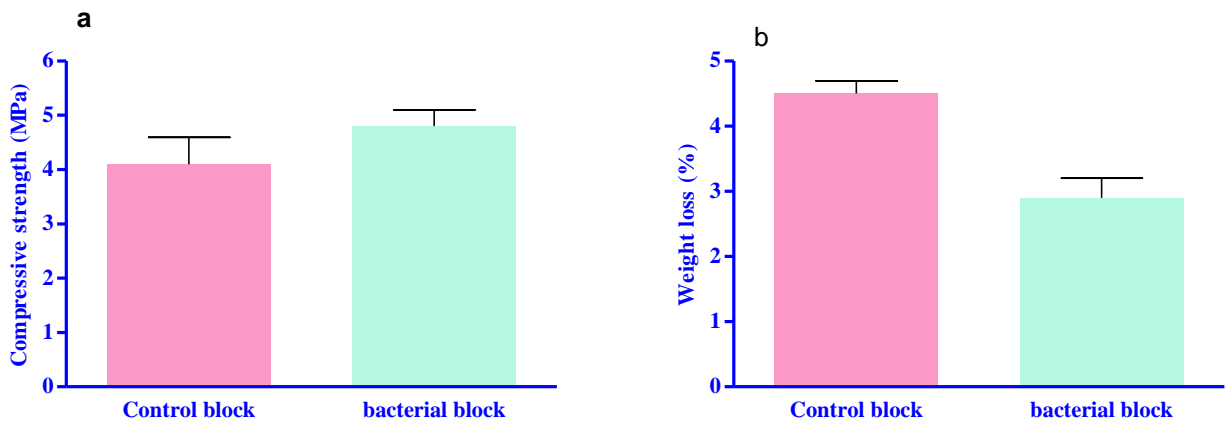


Fig. 4.4.24. Effect of MICP on a) freeze thaw strength test b) weight loss test of soil cement blocks. Values are mean ± SD (n = 3).

4.4.2.5. SEM, EDX and XRD investigations

SEM, EDX and XRD results revealed the involvement of bacteria and bacterial carbonates as discussed above (Fig. 4.4.25).

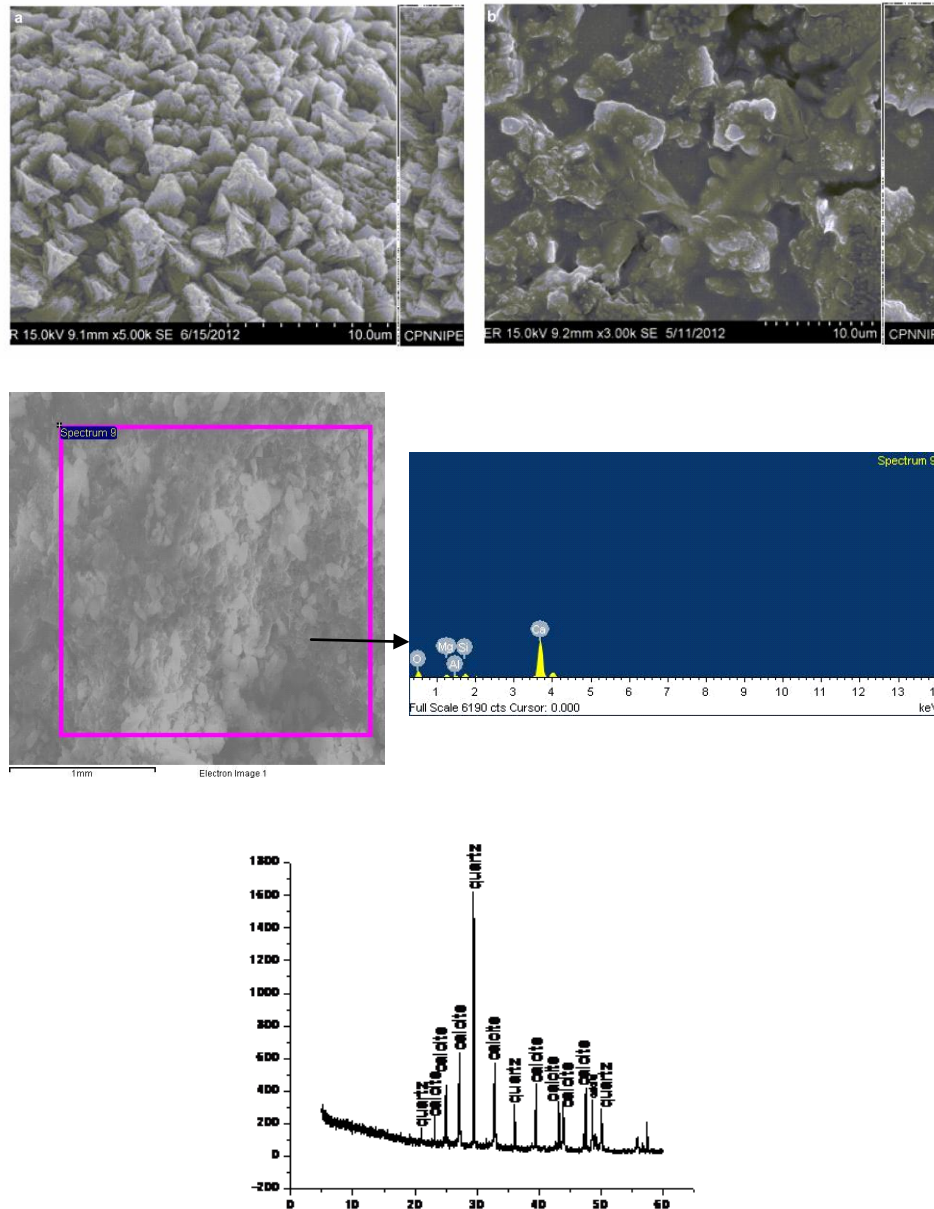


Fig. 4.4.25. a,b) Scanning electron microscopic images c,d) Energy dispersive X ray spectrum e) X ray diffraction analysis of bacterial treated soil cement blocks.

The reduction in porosity is attributed to filling of the voids and clogging of pores due to calcite binders. Bacterial calcite forms an impervious layer on the surface of soil cement blocks. Entrapped bacterial biomass and sometimes gas bubble formation also leads to decreased porosity. Whiffin *et al.* (2007) observed 90% decrease in porosity of sand column upon bacterial calcite formation. Both porosity and permeability are related to each other. If

porosity is high and pores are well connected, permeability is high. If porosity is low or pores are badly connected, permeability is low. In this case, precipitation of calcium carbonate in the pore spaces on the surface of specimens resulted in reduction of pore space volume, lowering of permeability, porosity and enhancement of performance.

Application of MICCP technology has significantly increased the durability properties of low embodied energy soil cement blocks which are great requirement of the current times. As these blocks are highly energy efficient (consuming only one fourth of the energy of burnt clay bricks and 45% reduced embodied energy), the use of MICP technology in soil cement blocks seems to bring a new revolution in construction industry. This is the first study elucidating the application of microbial calcite in improving the durability of low energy building materials. The present work will inspire a new perspective to investigate the application of biomineralization paving way for eco friendly, novel, low cost, durable and greener building materials.

4.4.3. Effect of Microbial calcite on properties of Ash bricks

As bricks are commonly used building blocks for many civil structures, the utilization of industrial by - products like fly ash and rice husk ash as partial replacement of clay in bricks can serve important economical, environmental and technical benefits. However, problems associated with ash bricks are low strength, higher water adsorption, low resistance to abrasion, low fire resistance and high porosity. In the present investigation, an attempt was also made to check the effect of MICCP on properties of ash bricks.

Both types of bricks were subjected to *B. megaterium* SS3 cells (OD 1.0) grown in nutrient broth media with urea and calcium chloride as in case of soil cement blocks for 4 weeks. In case of bricks also, deposition of carbonate precipitation was clearly observed on the surface upon bacterial treatment while there was no such deposition on control bricks which is due to microbial metabolic activities contributing to selective cementation and producing relatively insoluble organic and inorganic compounds (Fig. 4.4.26).

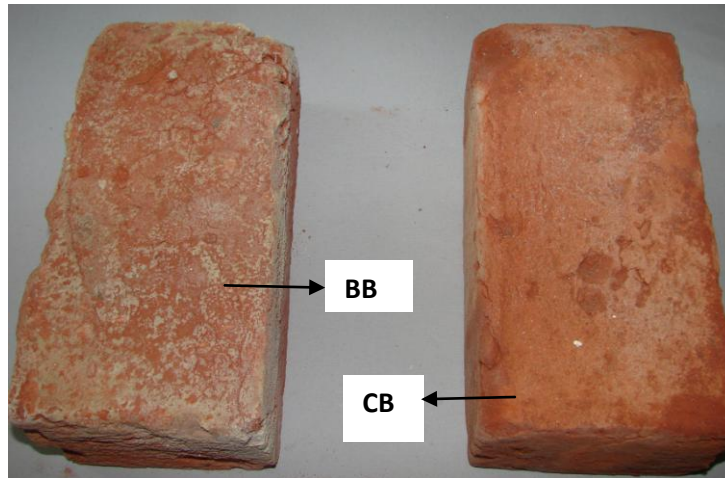


Fig. 4.4.26. Deposition of CaCO_3 on the surface of Bacterial treated brick (BB) of fly ash along with untreated control brick (CB)

All the brick samples were analyzed for their water absorption capacity as well as compressive strength, and the results are depicted below.

4.4.3.1. Water absorption test

Table 4.4.15 shows the influence of microbiologically induced calcium carbonate precipitation on water absorption in case of bacterial treated and control bricks. The percentage of water absorption by bacterial treated rice husk ash bricks (B-RHAB) was found to be 8% compared to 15% in case of untreated rice husk ash bricks (U-RHAB) which is about 46% reduction compared to control. In case of bacterial treated fly ash bricks (B – FAB), percentage of water absorption was 7.5% while that of untreated fly ash bricks (U - FAB) was 13.5% (44% reduction compared to control) (Fig. 4.4.26). The initial rate of absorption (IRA) of B-RHAB was 12 g/min/30 in² while that of U- RHAB was 27 g/min/30 in². In case of B-FAB, IRA was 10 g/min/30 in² whereas in case of U- FAB it was about 21 g/min/30 in² (Fig 7.26b).

Table 4.4.15. Effect of MICP on water absorption and Initial rate of absorption in case of rice husk ash (RHAB) and fly ash bricks (FAB)

Test	B-RHAB	U-RHAB	Improvement (%)	B-FAB	U-FAB	Improvement (%)
Water absorption (%)	8 ± 0.3d	15 ± 0.7a	46	7.5 ± 0.2d	13.5 ± 0.6a	44
Initial rate of absorption (g/min/30 in ²)	12 ± 0.8d	27 ± 1.1a	55	10 ± 0.9d	21 ± 1.8a	52

Values bearing different letters in the same column are significant at P<0.05. Values are mean ± SD (n = 3).

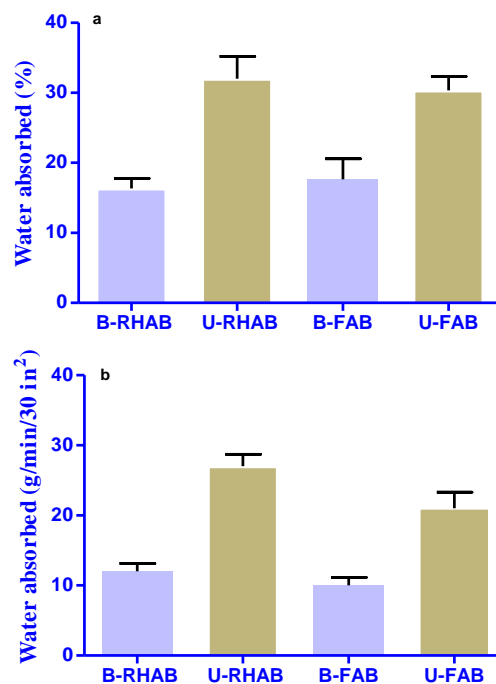


Fig. 4.4.26. Effect of MICCP on a) water absorption b) Initial rate of water absorption in ash bricks [B-RHAB: Bacterial treated rice husk ash bricks, U-RHAB: untreated rice husk ash bricks, B-FAB: Bacterial treated fly ash bricks, U-FAB: untreated fly ash bricks]. Bars represent mean ± SD (n = 3).

Significant reduction in the extent of water absorption was seen in both the cases which clearly indicated that due to bacterial calcification carbonate crystals were deposited and the pores have been reduced within the bricks. The deposition of a layer of calcium carbonate crystals on the surface resulted in a decrease of the permeation properties. As large amount of pores are plugged due to precipitation, the pore connectivity and water accessible porosity is decreased (De Muynck *et al.*, 2009). Because micro - organisms are mainly retained in the pores that are two to five times larger than cells (Samonin and Elikova, 2004), precipitation therefore, will initially occur in pores with diameter ranging from 2- 20 μm . However, as a result of the alkalinisation of the environment, heterogenous precipitation can also occur on the surface of the pores. This could result in the plugging of smaller pores (De Muynck *et al.*, 2009). Nemati and Voordouw (2003) also noticed a decrease of the permeability of sandstone cores after injecting CaCO_3 forming reactants. De Muynck *et al* (2008 a, b) observed significant decrease in water absorption rate in cement mortar cubes upon treatment with bacteria as compared to control.

4.4.3.2. Compressive strength of bricks

Compressive strength test of bricks was done after an interval of 3, 7, 14 and 28 days to check the extent of improvement upon treatment with bacterial calcite produced by *B. megaterium* SS3 (Table 4.4.16) as per IS3495. The compressive strength of bacterial ash bricks increased significantly compared to control bricks. In case of B - RHAB, the compressive strength was 12.8 MPa after 28 days while the strength of U- RHAB was 9.7 MPa which showed 24.2% improvement. In case of B- FAB, the compressive was 14.94 MPa while that of the U- FAB was 11.68 MPa which showed 21.8% improvement with respect to the control specimen (Fig. 4.4.27 a).

After the freeze thaw test, compressive strength of B- RHAB was found out to be 11.23 MPa while that of U- RHAB specimen was 8.62 MPa . In case of B- FAB, compressive strength after freeze thaw test was 12.63 MPa but in case of U- FAB specimens it was 9.21 MPa. The compressive strength of red bricks after freeze thaw test came out to be 10.93 MPa (Fig. 4.4.27 b).

Table 4.4.16. Effect of MICP on compressive strength (after 28 days) and freeze thaw resistance test of rice husk ash (RHAB) and fly ash bricks (FAB)

Test	B-RHAB	U-RHAB	Improvement (%)	B-FAB	U-FAB	Improvement (%)
Compressive strength (MPa)	12.8 ± 0.7b	9.7 ± 0.4d	24.2	14.94 ± 0.4a	11.68 ± 0.3b	21.8
Freeze thaw resistance test (MPa)	11.23 ± 0.9ab	8.62 ± 0.8d	23.2	12.63 ± 0.9a	9.21 ± 0.7cd	27.0

Values bearing different letters in the same column are significant at P<0.05. Values are mean ± SD (n = 3).

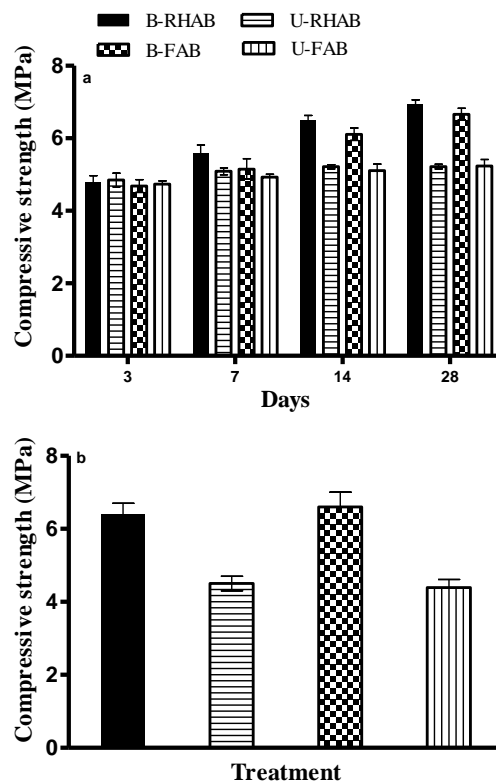


Fig. 4.4.27. Effect of MICCP on a) Compressive strength after 3,7,14 and 28 days b) Freeze thaw resistance strength in ash bricks [B-RHAB: Bacterial treated rice husk ash bricks, U-RHAB: untreated rice husk ash bricks, B-FAB: Bacterial treated fly ash bricks, U-FAB: untreated fly ash bricks] Bars represent Mean ± SD (n = 3).

In this case also SEM, XRD investigations and chemical constituents of all types of bricks by EDX depicted the involvement of bacteria and bacterial calcite for improving the durability of ash bricks (Fig. 4.4.28, 7.29, Table 4.4.16).

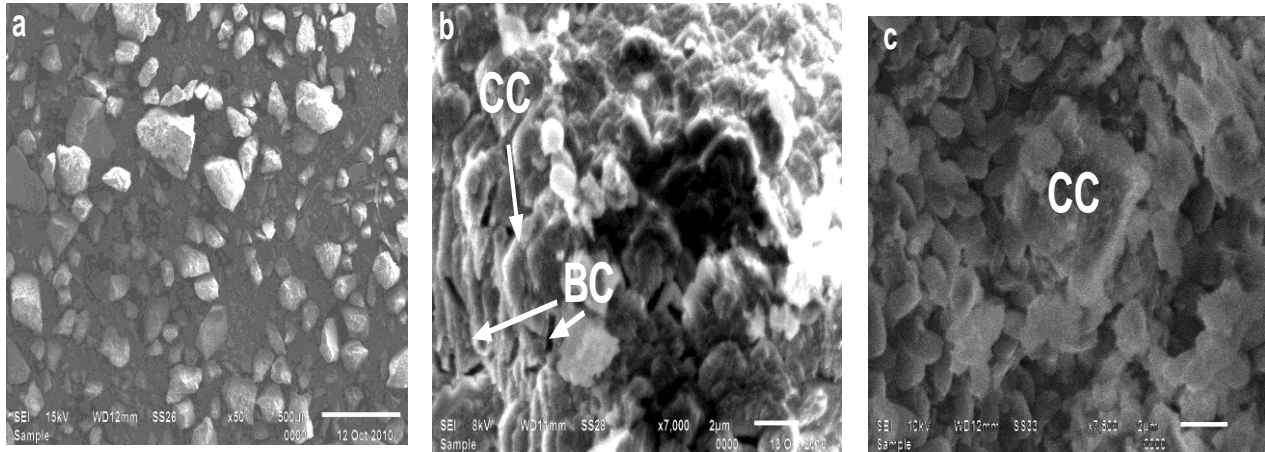


Fig. 4.4.28. Scanning electron micrograph of a) control brick sample b, c) bacterially treated fly ash bricks depicting the presence of carbonate crystals (CC) and bacterial cells (BC).

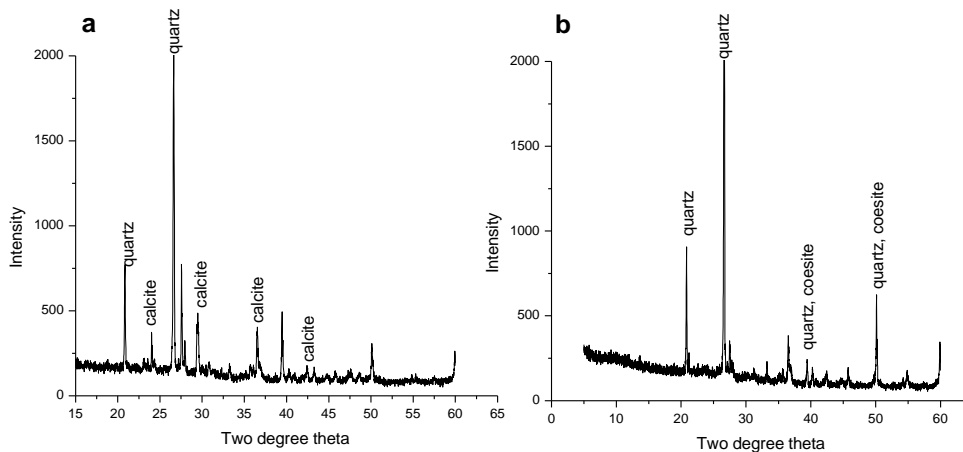


Fig. 4.4.29. XRD analysis of a) crystals precipitated on rice husk ash bricks (collected after 4 weeks) by application of *B. megaterium* SS3 (b) control rice husk ash brick. No calcite peaks were seen.

Table 4.4.16. EDX analysis of bacterial treated (B-RHAB) and untreated (U-RHAB) rice husk ash bricks and bacterial treated (B-FAB) and untreated (U-FAB) fly ash bricks.

Element	Weight (%)		Atomic (%)		Compound (%)		Formula
	B- RHAB	U-RHAB	B-RHAB	U-RHAB	B- RHAB	U-RHAB	
C	5.42	1.24	6.18	2.11	6.49	4.53	CO ₂
Na	1.53	---	1.77	---	2.07	---	Na ₂ O
Al	13.30	2.72	13.09	2.07	25.13	5.15	Al ₂ O ₃
Si	24.18	37.09	22.86	27.12	51.72	79.34	SiO ₂
K	5.32	1.50	3.61	0.79	6.40	1.80	K ₂ O
Ca	13.45	3.01	8.91	1.54	18.82	4.21	CaO
Ti	3.25	---	1.80	---	5.42	---	TiO ₂
Fe	7.26	3.86	3.45	1.42	9.34	4.97	FeO
Zn	3.70	---	1.50	---	4.60	---	ZnO
O	34.43	50.58	57.17	64.94	---	---	

The improvement in properties of ash bricks is attributed to consolidation by calcium carbonates precipitated by *B. megaterium* SS3 on the surface of treated bricks. In the present study, the strength of ash bricks reached nearby to that of conventional red bricks by the application of bacterial calcite. The improvement in compressive strength and decrease of water absorption capacity is due to deposition of calcium carbonates on bacterial cell surfaces and hence within the pores which leads to decrease in porosity and permeability. Thus it was concluded that the increase in strength is mainly due to consolidation of the pores inside the bricks with microbiologically induced calcium carbonate precipitation. So, it can be concluded that microbiologically induced calcium carbonate precipitation by *Bacillus megaterium* SS3 has the potential to enhance the durability of ash bricks by reducing the water absorption and improving the compressive strength of ash bricks. This is

the first study where successful application of bacterial calcite has been proved in low energy buildings as well as building materials from industrial by products.

Conclusion and salient features

The aim of this experimental study was to investigate the effect of bacterial carbonates on enhancement of the durability of varying grain sized and density sand columns, low energy building materials and building materials produced from industrial by - products. The efficacy of biomineralization is based on the ability of bacteria to promote the precipitation of carbonates. *Bacillus megaterium* SS3 strain isolated from calcareous soils was found to be capable of precipitating high amounts of calcium carbonate, high urease, CA, EPS as well as biofilms and was therefore selected to study its effect on various building materials. All types of the materials were treated with bacterial cells either for complete consolidation or as surface treatment. The supplementation of calcifying bacterial cells revealed positive effect on strength, porosity, permeability and durability of sand columns, low energy building materials as well as in industrial by - products building materials. Mercury intrusion porosimetry analysis clearly revealed the decrease in porosity of bacterial specimens compared to control samples. SEM examination also revealed the growth of carbonate crystals embedded with bacterial cells within the pores of building materials upon bacterial treatment. XRD and EDX analysis also proved the formation of calcite crystals formed by calcifying bacterial cells. The formation of impervious calcite layer on the surface of building materials acts as a natural skin over them. The formation of carbonate crystals within the pores and voids of the materials leads to clogging of these pores at the surface and decreases their ability to absorb water. The degradation of urea by these ureolytic bacteria is the main source of inorganic carbon dioxide in calcium and carbonate oversaturated medium and the cause of calcium carbonate precipitation (Merz-Preiss and Riding, 1999; Yates and Robbins, 1999, Warren *et al.*, 2001). Treatment of sand columns with bacteria demonstrated a significant improvement in their porosity. It was also established that microbially induced calcite precipitation (MICP) effectively impedes percolation of water in soil cement blocks as well as ash bricks. Experiments also showed

that MICP successfully improves the strength of different building materials by acting as a coherent superficial layer on the surface. From the durability results of low energy building materials, it was observed that biological calcite is highly coherent. Presence of biofilms and EPS was also confirmed by SEM analysis in certain portions which further play a major role towards reduction of permeability and enhancement of compressive strength.

In conclusion, the current study first time reported the positive potential of MICCP on enhancing the properties of low energy building materials as well as bricks from industrial by - products. The coherent and impervious nature of biological carbonates has been confirmed from the current results. The presence of a layer of calcium carbonate due to microbially induced precipitation resulted in decrease of the permeation properties as well as porosity of various types of building materials leading to improving their strength and durability.

4.5 Efficacy of fly ash as carrier for calcifying bacterial cells

In the previous studies we demonstrated the potential of different ureolytic bacterial isolates for precipitation of carbonates. Though the application of fresh bacterial cells has been proved for successful production of different biominerals but as such preparations are not applicable for commercial purposes. An attempt was made to prepare formulations of such isolates for long term storage and simplified usage for commercial purposes. The formulations of bacterial cells in industrial by - product fly ash were prepared at varying temperature and moisture contents and the viability of the calcifying bacterial cells was evaluated over different intervals of time.

4.5.1. Viability of calcifying bacterial cells within fly ash formulations at varying moisture and temperature till one year

4.5.1.1. Viability testing of bacterial formulations by plate count method

The physicochemical characterization of the fly ash used in present study showed that it had optimum pH and other mineral constituents (Table. 4.5.1). The organic carbon content was found to be 0.58 % while other mineral constituents were also present.

Three efficient calcifying bacterial isolates *Bacillus megaterium* SS3, *Bacillus cereus* SS5 and *Lysinibacillus fusiformis* SS18 grown in nutrient media were mixed in fly ash at three different moistures (30%, 40% and 50%) to prepare formulations with initial cfu of 5×10^8 cells/g and incubated at 4, 25 and 37 °C for 1 year. The inoculums were taken at regular intervals of time to estimate the viability of bacterial cells. It was observed that the survival of these bacterial isolates at various temperatures and moisture contents within fly ash formulations over a period of one year had similar trend. The cfu count of all bacterial formulations showed somewhat upward trend during the first month in case of 25°C and 37°C at all moisture contents which indicated the optimum environment and nutrients in the formulation supported bacterial multiplication (Fig. 4.5.1). The multiplication rate of bacterial cells was higher at 37°C compared to 25°C while there was no increase in the bacterial population at 4°C. But after 2nd month, microbial load declined sharply in samples

stored at 37°C and 25°C (all moisture conditions). The increase in the bacterial population at initial stages might be due to the presence of some of the mineral nutrients along with low levels of organic carbon in fly ash.

Table. 4.5.1. Physico chemical characteristics of fly ash

Parameter	Units
pH	7.4
EC (mS/cm)	0.32
Organic C (%)	0.58
P (mg/kg)	2.30
N (mg/kg)	85.0
Constituent	Percentage
SiO ₂	53.8
Al ₂ O ₃	31.3
CaO	6.4
MgO	0.52
Fe ₂ O ₃	5.8
MnO	0.13
TiO ₂	0.96
Na ₂ O	0.12
K ₂ O	0.21

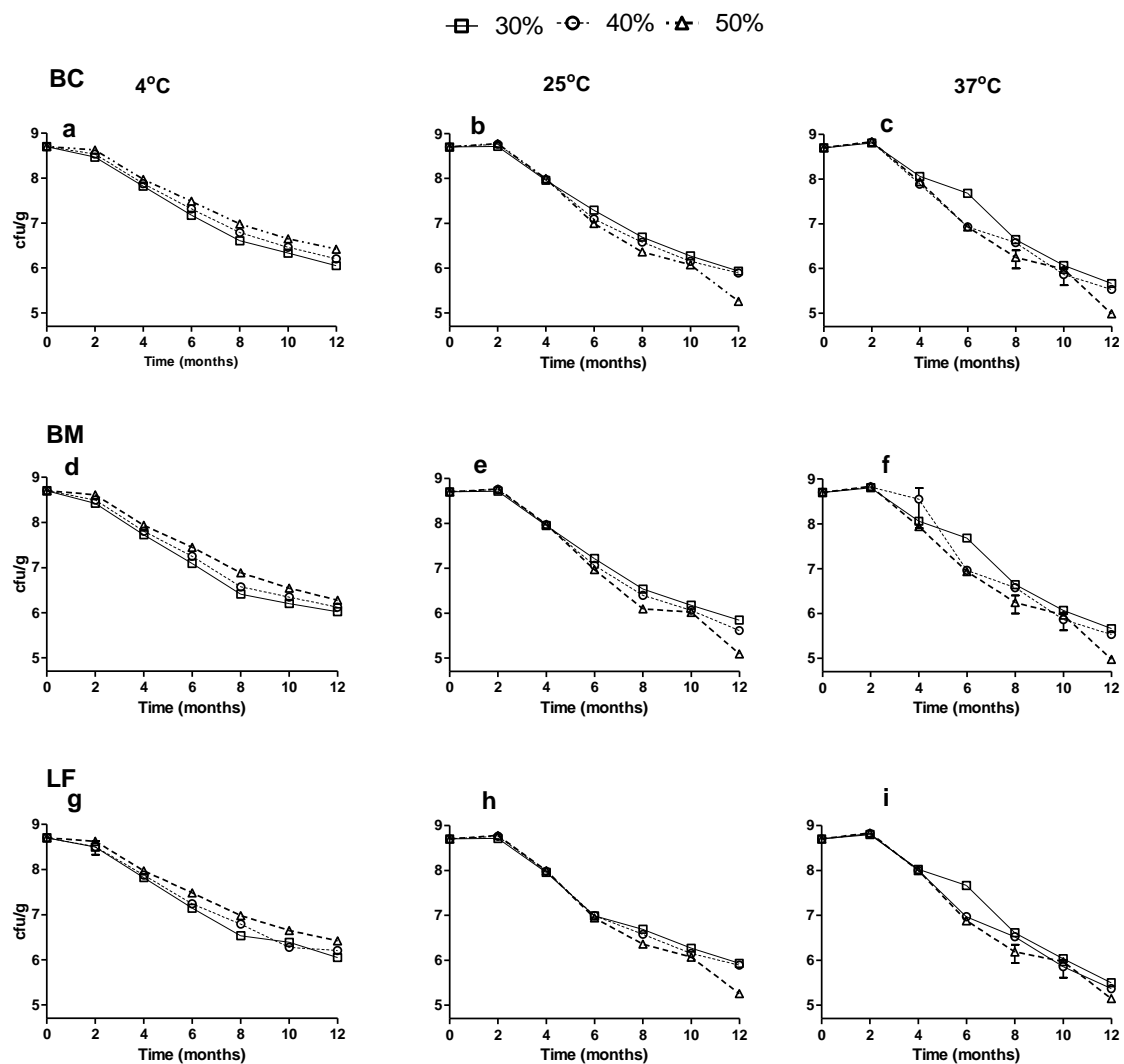


Fig. 4.5.1. Viability of various inoculum formulations at varying temperatures (4°C, 25°C and 37°C) and moisture contents (30%, 40%, 50%) over a period of 1 year. a, b, c) *Bacillus cereus* SS5 (BC), d, e, f) *Bacillus megaterium* SS3 (BM), g, h, i) *Lysinibacillus fusiformis* SS18 (LF)

4.5.1.2. Viability testing of fly ash formulations via fluorescent dye 5-cyano-2,3-ditolyl tetrazolium chloride

Viability of different bacterial cells within in the fly ash formulations was also tested by CTC dye. The results showed presence of both viable (red) and dead (green) cells in the formulations (Fig. 4.5.2). Both live and dead cells exhibited green florescence but

intracellular accumulation of CTC in viable cells produced strong red fluorescence as visible by confocal laser scanning microscopy. As healthy cells respiring via the electron transport chain absorb and reduce CTC into an insoluble, red fluorescent formazan product while cells not respiring do not reduce CTC and are counterstained by SYTO[®] 24 green - fluorescent nucleic acid stain.

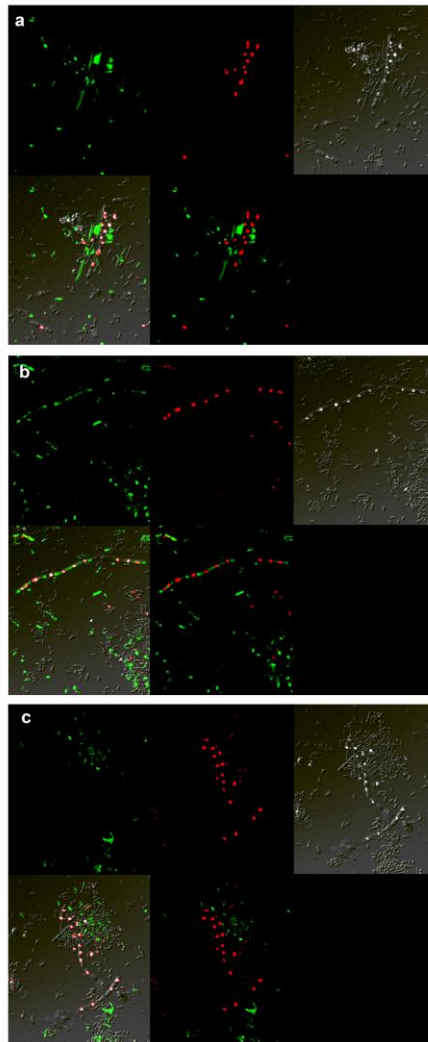


Fig. 4.5.2. Confocal laser scanning microscopy of bacterial formulations after staining with CTC and SYTO green where red colour indicates CTC reduction and green colour indicates total count. Different panels depict different spectra (green channel, red channel and superimposed green & red channels) a) *B. cereus* SS5, b) *B. megaterium* SS3, c) *L. fusiformis* SS18.

Theoretically, viable cells could appear yellow because of an overlap of the green and red channels, but in our study no yellow cells were observed. The advantage of using fluorescent dyes over plate count is that, at times certain bacterial cells not capable of forming colonies actively reduce these dyes and give fluorescence (Sherr *et al.*, 1999). CTC has been successfully used to determine respiratory activity of many complex microbial systems (Nielsen *et al.*, 2003). The present work has first time proved the easy and reliable usage of fluorescent dye CTC in case of inoculum formulations.

4.5.2. Effect of time on metabolic activity of bacterial isolates, pH and moisture content of the formulations

The metabolic activity of all bacterial isolates was investigated by determining the urease activity of bacterial formulations and comparing them with initial urease activity. It was found that the urease activity of bacterial formulations at the beginning of the experiment was in the range of $74.3 \pm 2.5 \mu\text{M/g/h}$ while after 1 year, the urease activity declined to $53.6 \pm 2.9 \mu\text{M/g/h}$. Though the urease activity declined with time but still considerable amount of activity was noticed. The moisture content in all the formulations was also investigated after a year and it was found that the moisture loss varied between 4.5 to 5.6%. In case of pH, the drop varied from 0.18 - 0.23 at 4°C, 0.34 – 0.41 in case of 25°C formulations and 0.56 - 0.63 in case of formulations stored at 37°C.

4.5.3. Scanning electron microscopic analysis of fly ash formulations

Scanning electron microscopy of formulations containing *B. megaterium* SS3, *B. cereus* SS5 and *L. fusiformis* SS18 revealed various sizes of the particles after one year (Fig. 4.5.3). Smooth, rugged and porous surfaces were seen (4.5.3 c, d, e, f, g, h). Particles of bacterial formulations containing *B. megaterium* SS3 were larger compared to others (4.5.3 e, f). At higher magnifications, bacterial cells were clearly detected on the rugged areas. Though carbogel has also been devised as effective carrier material for application of bacterial cells in biodeposition of limestone because of its higher retention of viable bacteria by Cappitelli *et al.* (2007) in Biobrush consortium but it adds heavily to the cost of biodeposition treatment. For the formation of a gel, 10 g/L of Carbogel is required. Considering thickness

of the gel of about 1 cm, this brings the cost per m² to about 2.8 € per m² which is further added by using Japanese paper as it is used along with carbogel bringing an extra cost of about 12.3 € m⁻². High density polyethylene sheets used on external wall assemblies also amount to about 2.3 € m⁻². Hence, these factors favour the use of fly ash as a carrier material for calcifying bacterial inoculum formulations in biodeposition studies. Though the composition of fly ash do vary to some extent from one source to another but most of them are good source of mineral nutrients, have optimum pH and good water holding capacity. These properties favour the application of fly ash as economical carrier for bacterial formulations.

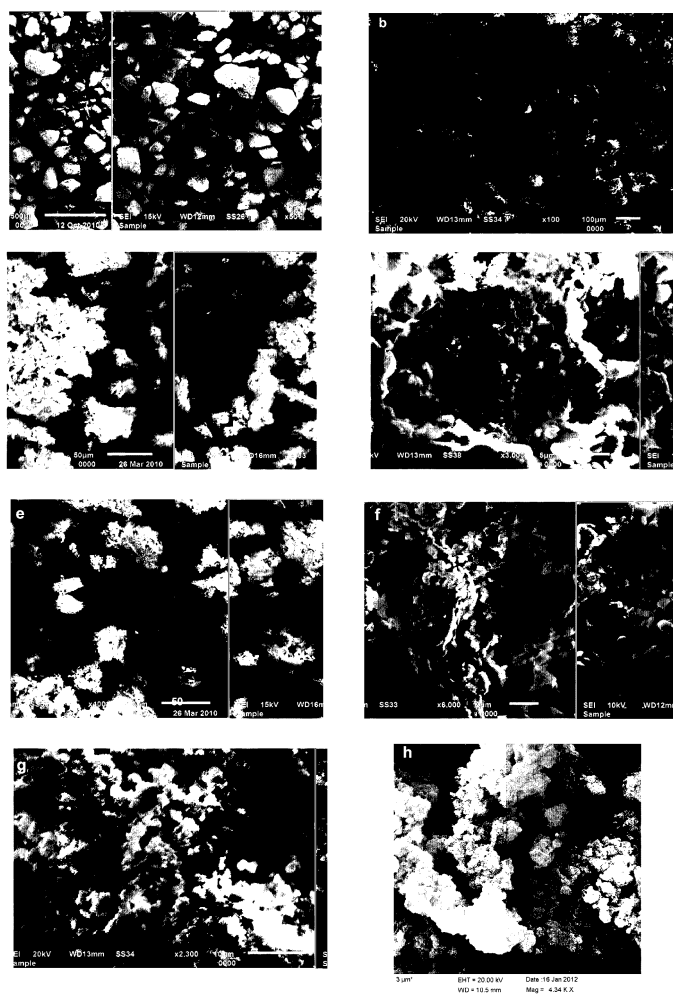


Fig. 4.5.3. Scanning electron micrography of different inoculum formulations. a, b) Fly ash, c, d) *B. cereus* SS5 formulation, e, f) *B. megaterium* SS3 formulation, g, h) *L. fusiformis* SS18 formulation.

4.5.4. Calcium carbonate precipitating efficacy of formulated bacterial cells

4.5.4.1. Efficacy of formulated bacterial cells for carbonate precipitation *in vitro*

Figure 4.5.4 represents the pattern of insoluble Ca^{2+} in formulated cells, fresh bacterial cells and control NBU media. Though addition of urea adds to the total cost of the media, but it has been found to be most efficient and simple mechanism for precipitation of carbonates by bacterial cells (De Muynck *et al.*, 2010). It was seen that calcium carbonate precipitation was about 75% completed in 12 hrs in case of formulated cells while it was 90 % completed in case of fresh bacterial cells in same amount of time. In case of control, there was very small change in the concentration of Ca^{2+} which proves the involvement of bacteria in carbonate precipitation. CaCO_3 precipitation is dependent on the concentration of Ca^{2+} and CO_3^{2-} in solution. Hydrolysis of urea by bacterial urease is the major player in creating alkaline conditions in the surrounding medium due to production of ammonium ions and additional release of CO_2 (Stocks-Fischer *et al.*, 1999; Bachmeier *et al.*, 2002). An increase in CO_3^{2-} concentration occurs under alkaline conditions abundant of calcium (Ca^{2+}) and carbonate (CO_3^{2-}) ions (Qian *et al.*, 2010). Bacterial presence and activity are prerequisite for the precipitation of calcium carbonate as bacterial metabolic activity produces the necessary increase in supersaturation to induce the heterogeneous crystallization of calcium carbonate on the surface of bacterial cells (Rodriguez Navarro *et al.*, 2012). The reduction in efficiency of carbonate precipitation in case of formulated cells compared to fresh bacterial cells is observed which might be due to poor accessibility of bacterial cells due to entrapment in fly ash particles or due to decreased metabolic activity which leads to lesser precipitation. It is also possible that the cells within the formulations which had a larger particle size are entrapped inside the particles of fly ash and are therefore not effective in precipitation process. Though the precipitation of carbonates decreased in comparison to fresh cells but still formulated cells showed promising precipitation capability which offered the possibility of using them for commercial applications but more research is needed to work on the characteristics of fly ash, its particle size etc.

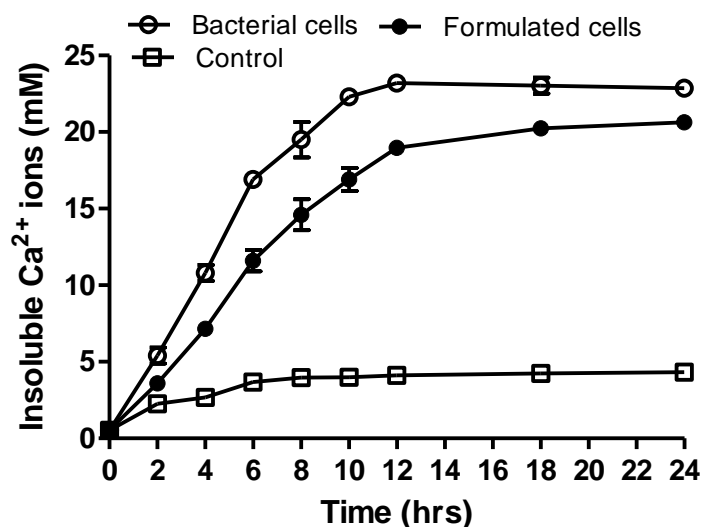


Fig. 4.5.4. Amount of insoluble Ca^{2+} concentration in fresh bacterial cells, formulated bacterial cells and control solution at different time intervals.

4.5.4.2. Calcification efficacy of bacterial formulations within in sand plugs

4.5.4.2.1. CaCO_3 content in sand columns with formulated and control formulations

The application of formulated cells and fresh bacterial cells on the surface of sand columns brought interesting results. The calcified layer on the surface of the columns was checked for amount of carbonate precipitation. In case of formulations, the amount of precipitated calcium carbonate was found to be 24% compared to 32% in case of fresh bacterial cells where as in case of control, the carbonate content was merely 6% (Fig. 4.5.5). The higher amount of precipitates in case of formulated cells as well as fresh cells depicts active bacterial carbonate precipitation. Inoculation of bacterial formulations consolidated the surface of sand columns due to formation of CaCO_3 precipitates efficiently. The success of biodeposition treatment also depends upon the pore structure of the material used (Achal *et al.*, 2011a). Precipitation of CaCO_3 was predominantly observed on the surface of the columns compared to inside the column. This may be due the facultatively anaerobic nature of *Bacillus* spp. that grow at a higher rate in the presence of oxygen and consequently induce

active precipitation of CaCO_3 around the surface area (Achal *et al.*, 2010; Stocks-Fischer *et al.*, 1999).

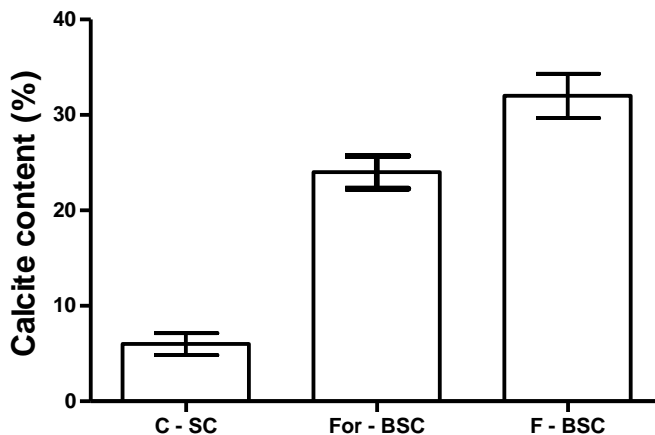


Fig. 4.5.5. CaCO_3 content in control sand column (C - SC), formulated bacterial cells sand column (For - BSC) and fresh bacterial cells sand column (F - BSC).

4.5.4.2.2. XRD analysis of formulated sand columns

XRD analysis of the three types of columns revealed that carbonate deposits were present as calcite and vaterite in case of F – BSC as well as For – BSC while in case of control sand column, no calcium carbonate peak was noticeable (Fig. 4.5.6 a - c). The formation of coherent durable calcite in our study has ensured high physicochemical resistance because of its high chemical and mechanical stability. Though extensive studies on bacterial carbonatogenesis have been carried out, little is known on what are the causes of polymorph selection during bacterial calcium carbonate mineralization (Rivadeneira *et al.*, 1998; Rodriguez-Navarro *et al.*, 2012). EDX analysis further revealed the mineral constituents of sand columns. High amount of calcium was seen in case of fresh as well as inoculum treated sand columns while control sand column was seen to have very low calcium content.

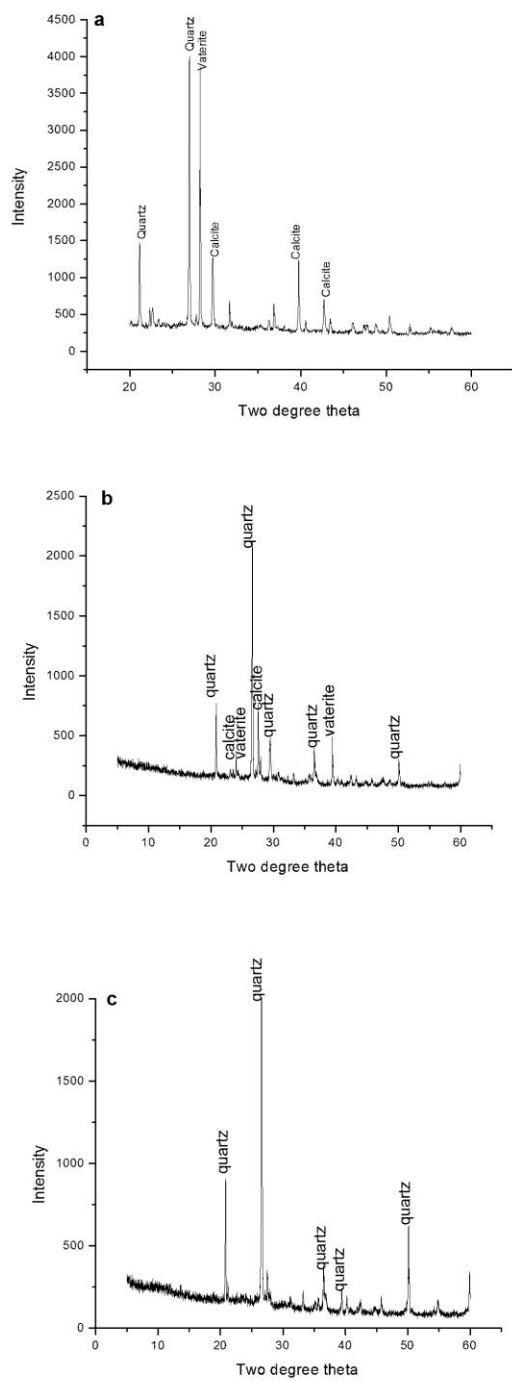


Fig. 4.5.6. X ray diffraction pattern of carbonate crystals precipitated in fresh bacterial cells sand column (F - BSC), formulated bacterial cell sand column (For - BSC) and control sand column (C - SC).

4.5.4.2.3. Effect of bacterial formulations on properties of sand columns

The percentage of water absorption by formulated bacterial cell columns was found to be 8.84% while in case of fresh bacterial cell treated columns, it was 7.35% (Fig. 4.5.7). Water absorption in case of control specimens was 12.15%. This showed that formulated cells reduced the absorption level to significantly low level. Achal *et al.* (2011) and De Muynck *et al.* (2008) also reported significant decrease in water absorption in cement mortar cubes upon treatment with bacteria as compared to control. Lowering of water absorption is attributed to the deposition of biogenic carbonate crystals leading to reduction of pores on the surface of bacterial cylinders. This leads to decreased permeation due to plugging of pores and hence the porosity decreases.

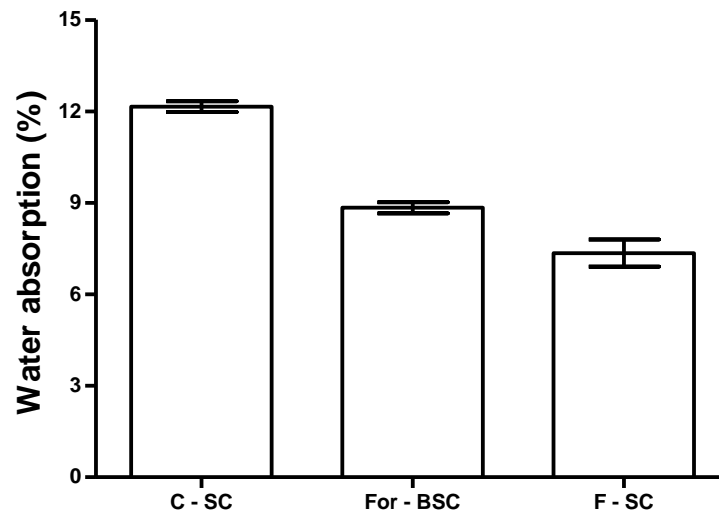


Fig. 4.5.7. Influence of microbial calcite deposition on water absorption in control sand columns (C - SC), formulated bacterial sand columns (For - BSC) and fresh bacterial sand columns (F - BSC).

Mercury intrusion porosimetry data (Table 4.5.2) of formulated bacterial cells, fresh bacterial cells and control specimens also reflected sufficient efficacy of formulated bacterial cells on reduction of total porosity. The total porosity of control specimens was found to be 25.3% while upon calcification by formulated cells; it was estimated to be 19.2% which showed 24% reduction. In case of fresh bacterial cells application, the porosity

was found to be 17.4% which was 31% reduction. The porosity of the samples was calculated using cumulative intrusion volume and relevant mass measurements.

Table. 4.5.2. Mercury intrusion porosimetry analysis of control sand columns (C - SC), formulated bacterial sand columns (For - BSC) and fresh bacterial sand columns (F - BSC).

Parameter	C – SC	For – BSC	F – BSC
Total Intrusion Volume (mL/g)	0.14 ± 0.00a	0.11 ± 0.01b	0.10 ± 0.00b
Total Pore Area (m ² /g)	10.12 ± 0.55a	8.41 ± 0.50b	5.89 ± 0.29c
Median Pore Diameter (µm Volume)	0.31 ± 0.01a	0.29 ± 0.01ab	0.27 ± 0.06b
Median Pore Diameter (µm Area)	0.01 ± 0.00a	0.01 ± 0.00a	0.01 ± 0.00a
Average Pore Diameter (µm 4V/A)	0.06 ± 0.00a	0.05 ± 0.00a	0.05 ± 0.00a
Bulk Density at 0.60 psia (g/mL)	1.61 ± 0.06b	1.81 ± 0.06a	1.80 ± 0.07a
Apparent (skeletal) Density (g/mL)	2.19 ± 0.11b	2.24 ± 0.14a	2.30 ± 0.13a
Porosity (%)	23.30 ± 1.72a	19.23 ± 1.31b	16.20 ± 0.92c

Values bearing different letters in the same column are significant at P <0.05. Values are mean ± SD (n =3).

Whiffin *et al.* (2007) also observed 90% decrease in porosity of sand column upon bacterial calcite formation. The reduction in porosity is attributed to the filling of the voids and clogging of pores due to precipitated carbonate crystals. Entrapped bacterial biomass and extrapolymeric substances also leads to reduction in porosity (Dhami *et al.*, 2012). Though there was again some reduction in the extent of carbonate precipitation by formulated cells compared to bacterial cells but still, application of formulated cells successfully reduced the porosity of sand columns to a good extent and hence proved its efficacy. Zamarreno *et al.* (2009) also reported that biodeposition treatment resulted in a decrease in pore size of about 50% in limestone.

Conclusion and salient features

Development of stable formulations for application of MICCP in commercial purposes is of great importance as this technology offers eco friendly, novel and convenient solution to various problems of building materials. Use of fly ash as carrier in these formulations is an effective way of utilization of problematic fly ash waste in a useful manner and in the present study, an attempt was made to investigate the potential of fly ash as a carrier material for calcifying bacterial cell formulations. As both moisture and temperature play important role in long term survival of any formulation, in the present work optimum moisture and temperature were sorted for maximum survival of the bacterial cells. Though the bacterial count decreased with time within the formulations, but still considerable viability was retained at different temperatures and moistures. Among all the conditions of storage, maximum viability was seen at 4°C and 50% moisture. Fluorescent dye CTC has been firstly reported for investigating the viability of bacterial cells within the formulations. The results of the present study have proved the potential of fly ash as a carrier for calcifying bacterial isolates to sustain their viability and efficacy for 1 year.

4.6. Response Surface Methodology for enhanced urease and carbonate production

As it was envisaged that ureolytic pathway is very efficient and economical way for generating large amounts of carbonate precipitates in short periods of time, an attempt was made to enhance the production of urease for enhancing the production of carbonates by optimizing the media components through Response Surface Methodology.

4.6.1. Selection of constituents of growth media

The constituents of the growth media and process variables play a significant role in production of various enzymes. Among these, the major players are: Carbon source, nitrogen source, temperature, time of incubation, concentration of urea, CaCl_2 , size of inoculum, trace salts, supplements etc. As many of these factors have already been investigated in earlier work, in the present study physicochemical parameters that were studied by one factor at a time (OFAT) were carbon source, nitrogen source and inoculum density. The various carbon sources tested were: glucose, sucrose, fructose, lactose, starch and mannitol while different nitrogen sources tested were beef extract, peptone, casein, ammonium sulphate and sodium nitrate. The initial inoculums were investigated from range of 5×10^6 cells/ml to 5×10^9 cells/ml (Fig.4.6.1a,b,c).

Glucose (2%) was found to be the best carbon source compared to sucrose, fructose, lactose and starch. In case of nitrogen sources, peptone (1%) was found to be better source of nitrogen compared to beef extract, casein, soyabean meal and sodium nitrate while 5×10^8 cells/ml was found to be the optimal cell concentration for high urease production on 4th day. This was followed by Placket Burman experiment to investigate the most significant parameters for urease production in the media constituents at two levels in total of 12 experiments. The variables and their selected levels are given in table 4.6.1. The data was analyzed to find the significant factors by F test. The results of Placket burman experiment indicated that there was a wide variation in total urease production yield in the different trials (450 U/ml to 725U/ml Table 4.6.1). Significant rise in the amount of urease production was seen with different combinations of the factors studied.

These variations reflected the importance of media optimization for higher urease production. The ANOVA table of different factors involved in urease production demonstrated that the model was significant (Table 4.6.2).

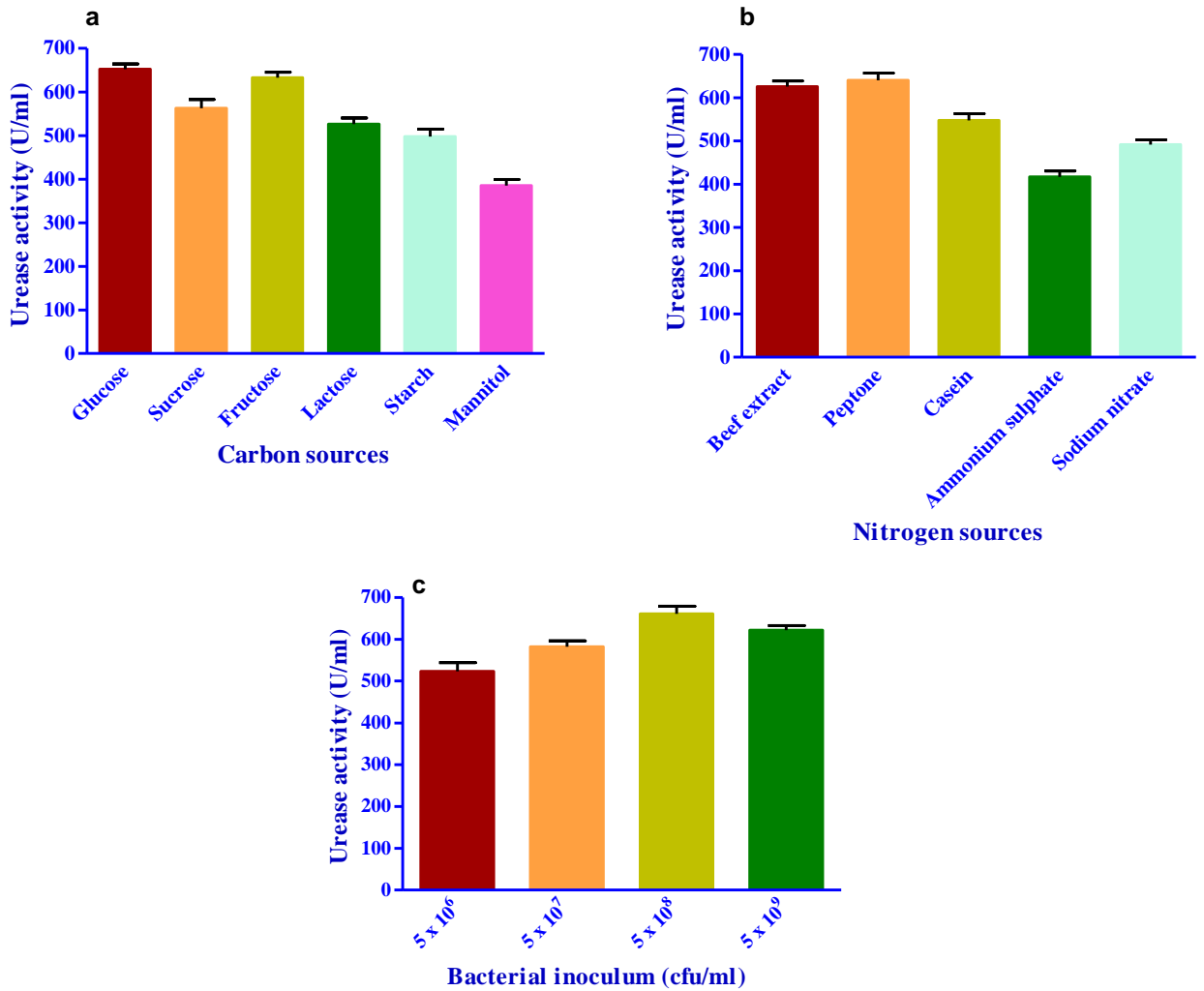


Fig. 4.6.1.a) Effect of different carbon sources **b)** nitrogen sources and **c)** bacterial inoculums concentration on urease production in *B. megaterium* SS3

The medium components with a p value < 0.05 at 5% level were considered to have greater impact on the enzyme activity. The data of regression analysis for Plackett Burman design demonstrated that out of the eight variables studied, 3 variables had significant influence on enzyme activity as evidenced by their p value and were found to be concentration of glucose, urea and NaHCO₃.

Table 4.6.1. Plackett Burman design matrix for screening the variables influencing Urease activity.

Std	Run	Factor 1 Urea	Factor 2 Glucose	Factor 3 NaHCO ₃	Factor 4 Peptone	Factor 5 NH ₄ Cl	Factor 6 MgSO ₄ ·7H ₂ O	Factor 7 CaCl ₂	Factor 8 KH ₂ PO ₄	Response Urease activity (U/ml)
4	1	1	3	0.1	1.5	1.5	0.002	0.3	0.6	493
9	2	3	3	0.3	0.5	0.5	0.002	0.3	0.2	725
3	3	3	1	0.3	1.5	0.5	0.006	0.3	0.6	598
12	4	1	1	0.1	0.5	0.5	0.002	0.1	0.2	450
5	5	1	1	0.3	0.5	1.5	0.006	0.1	0.6	485
2	6	1	3	0.3	0.5	1.5	0.006	0.3	0.2	562
1	7	3	3	0.1	1.5	1.5	0.006	0.1	0.2	646
7	8	3	1	0.1	0.5	1.5	0.002	0.3	0.6	528
6	9	1	1	0.1	1.5	0.5	0.006	0.3	0.2	478
8	10	3	3	0.1	0.5	0.5	0.006	0.1	0.6	687
10	11	1	3	0.3	1.5	0.5	0.002	0.1	0.6	553
11	12	3	1	0.3	1.5	1.5	0.002	0.1	0.2	581

Table 4.6.2. Analysis of variance for urease activity by different factors using Plackett Burman design.

Source	Sum of Squares	Df	Mean Square	F Value	p-value Prob > F
Model	81075	8	10134.4	25.09	0.0114
A-Urea	46128	1	46128	114.18	0.0018
B-Glucose	24843	1	24843	61.49	0.0043
C-NaHCO₃	4107	1	4107	10.17	0.0498
D-Peptone	645.33	1	645.33	1.6	0.2956
E-NH₄Cl	3201.33	1	3201.33	7.92	0.067
F-MgSO₄.7H₂O	1323	1	1323	3.27	0.1681
G-CaCl₂	27	1	27	0.067	0.8127
H-KH₂PO₄	800.33	1	800.33	1.98	0.254
Residual	1212	3	404		
Cor Total	82287	11			

$R^2 = 0.9853$; $Adj R^2 = 0.9460$; $Pred R^2 = 0.7643$; Adeq Precision = 14.30

Statistical designs serve as effective tools for determining main as well as interactive influences of different parameters on production of different enzymes. Response surface methodology (RSM) is a collection of certain statistical techniques for designing the experiments, building models, evaluating effect of factors and searching for optimal conditions for desirable responses (Myers and Montgomery, 2002). Various important extracellular enzymes have been evaluated for their enhanced production by RSM by

various researchers (Saxena and Saxena, 2004; Senthilkumar *et al.*, 2005; Deepak *et al.*, 2008; Himabindu *et al.*, 2006; Vohra and Satayanayarana, 2002).

In the present study, Central composite design (CCD) for three independent variables was used to obtain the combination of values for optimizing the response within the region of three dimensional observation spaces. CCD provides the information regarding optimum level of each variable along with their interactions with other variables and effect on enzyme activity. To examine the effect of these independent variables on urease production, central composite factorial design of $2^3 = 8$ plus 6 centre points and $(2 \times 3 = 6)$ star points leading to total of 20 experiments were performed (Table 4.6.3).

The relationship between independent variables and response was calculated by second order polynomial equation. The corresponding ANOVA is presented in table 4.6.4.

The ANOVA of the model indicated that the model is significant. The calculated F value of 1156 in the present study implied that the model is highly significant. P values are the tool to investigate the significance of each of the coefficients, which further help to determine the pattern of mutual interactions between the test variables. Values of $P < 0.0001$ indicate the model terms to be significant. At the same time, a relatively lower value of the coefficient of variation (=11.12%) indicated better precision and reliability of the experiments conducted (Myers and Montgomery, 1995; Khuri and Cornell, 1987).

The predicted R squared of 0.9936 is in reasonable agreement with the Adj R squared of 0.9982. As ratio greater than 4 is desirable and in the present study ratio of 102 indicates adequate signal. The coefficient of regression R^2 which determines the fit of the model was found to be 0.9990 indicating 99% of the variability in the response is explained by the model. In the present study, test variables A, B, C, AB, AC, BC, A^2 , B^2 , C^2 are significant model terms. Values greater than 0.1000 indicate the model terms are not significant.

Table 4.6.3. Experimental Design and results of CCD of response surface methodology.

Std	Run	Factor 1 Urea (g/100 ml)	Factor 2 Glucose (g/100 ml)	Factor 3 NaHCO ₃ (g/100 ml)	Actual urease activity (U/ml)	Predicted urease activity (U/ml)
18	1	2	2	0.2	862	862.1
17	2	2	2	0.2	858	862.1
12	3	2	2.87	0.2	640	640.9
16	4	2	2	0.2	865	862.1
5	5	1.5	1.5	0.25	519	519.2
19	6	2	2	0.2	864	862.1
7	7	1.5	2.5	0.25	600	604.9
9	8	1.13	2	0.2	550	542.1
13	9	2	2	0.11	660	655.6
6	10	2.5	1.5	0.25	562	563.3
8	11	2.5	2.5	0.25	808	800.5
15	12	2	2	0.2	867	862.1
2	13	2.5	1.5	0.15	508	505.1
11	14	2	1.13	0.2	415	411.2
10	15	2.87	2	0.2	655	660.0
1	16	1.5	1.5	0.15	555	564.5
14	17	2	2	0.29	715	716.5
4	18	2.5	2.5	0.15	683	684.8
20	19	2	2	0.2	857	862.1
3	20	1.5	2.5	0.15	592	592.7

Table 4.6.4. ANOVA for Urease activity using CCD of response surface methodology.

Source	Sum of squares	df	Mean Squares	F Value	p-value Prob > F
Model	4.05E+05	9	45033.6	1156.63	< 0.0001
A-Glucose	16242.9	1	16242.9	417.18	< 0.0001
B-Urea	61607.49	1	61607.49	1582.31	< 0.0001
C-NaHCO₃	4331.81	1	4331.81	111.26	< 0.0001
AB	11476.13	1	11476.13	294.75	< 0.0001
AC	5356.13	1	5356.13	137.57	< 0.0001
BC	1653.13	1	1653.13	42.46	< 0.0001
A²	1.19E+05	1	1.19E+05	3063.48	< 0.0001
B²	1.98E+05	1	1.98E+05	5076.45	< 0.0001
C²	54252.01	1	54252.01	1393.4	< 0.0001
Residual	389.35	10	38.94		
Lack of Fit	310.52	5	62.1	3.94	0.0794
Pure Error	78.83	5	15.77		
Cor Total	4.06E+05	19			

$$R^2 = 0.9990; \text{Adj } R^2 = 0.9982; \text{Pred } R^2 = 0.9936; \text{Adeq Precision} = 102.677$$

By applying multiple regression analysis of the experimental data, the experimental results of the central composite design (CCD) were fitted with a second-order full polynomial equation. The empirical relationship between urease production and the three test variables is obtained by equation:

$$\text{Urease activity} = +862.17 + 34.06*A + 66.34*B + 17.59*C + 37.88*A*B + 25.88*A*C + 14.38*B*C - 87.02*A^2 - 112.02*B^2 - 58.69*C^2$$

The three dimensional response surface plots and contour plots were employed to demonstrate the interaction among various factors (Fig. 4.6.2, 4.6.3). Each graph represents an infinite number of combinations of all the test variables with each other.

Highest urease production was seen in with concentration of glucose = 2.17g, urea = 2.11 g and $\text{NaHCO}_3 = 0.19$ g per 100 ml. RSM design yielded a maximum urease activity of 866 U/ml which was also experimentally verified. So, in comparison with the pre optimized media where the activity was 680 U/ml, optimized media had enhanced urease production.

So, the optimal conditions for production of urease contained urea = 21.1 g, glucose = 21.7g, $\text{NaHCO}_3 = 1.9$ g, peptone = 10 g, $\text{NH}_4\text{Cl} = 10$ g, $\text{MgSO}_4 \cdot 7\text{H}_2\text{O} = 0.05$ g, $\text{CaCl}_2 = 2.8$ g, $\text{KH}_2\text{PO}_4 = 5$ g per litre at pH 8.0 and temperature of 35°C for incubation of 4 days. So, it was verified that optimized media led to 1.2 times fold increase in the activity of urease. The optimized media was also checked for the amount of carbonate precipitates. The carbonate precipitates in this case were found to be 92 mg/100 compared to 54 mg/100 ml in case of unoptimized media, which is 1.7 times increase. So, it has been undoubtedly proved that with the application of RSM, the enzyme production and hence the carbonate precipitation can be enhanced significantly.

Design-Expert® Software

Factor Coding: Actual

Urease activity

● Design points above predicted value

○ Design points below predicted value

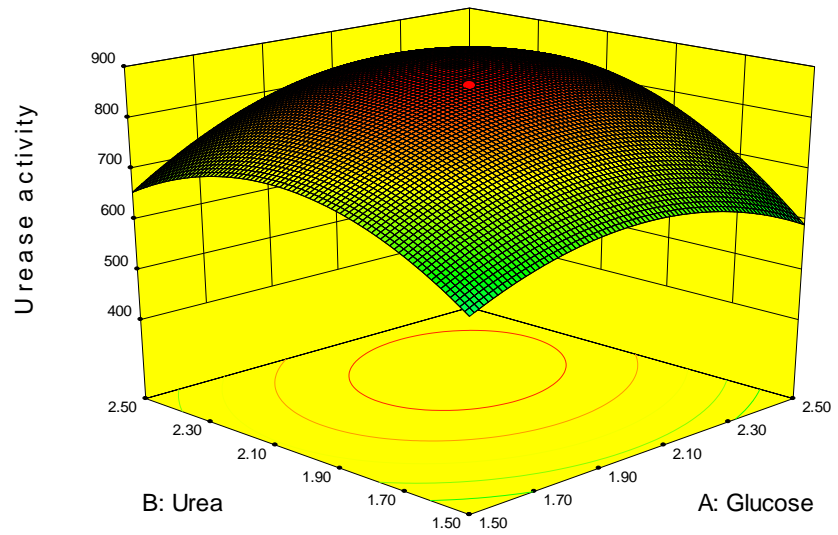


X1 = A: Glucose

X2 = B: Urea

Actual Factor

C: NaHCO₃ = 0.20



Design-Expert® Software

Factor Coding: Actual

Urease activity

● Design points above predicted value

○ Design points below predicted value

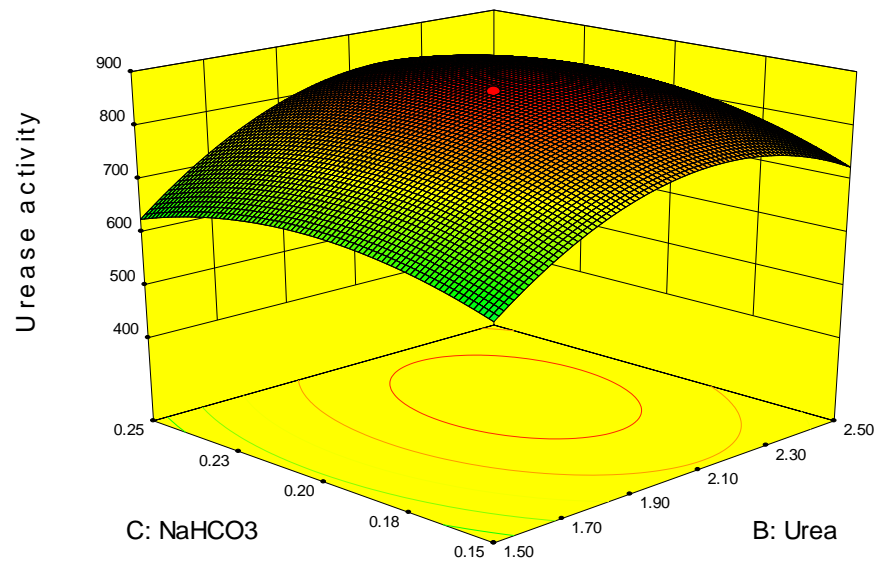


X1 = B: Urea

X2 = C: NaHCO₃

Actual Factor

A: Glucose = 2.00



Design-Expert® Software
Factor Coding: Actual
Urease activity

- Design points above predicted value
- Design points below predicted value



X1 = A: Glucose
X2 = C: NaHCO₃

Actual Factor
B: Urea = 2.00

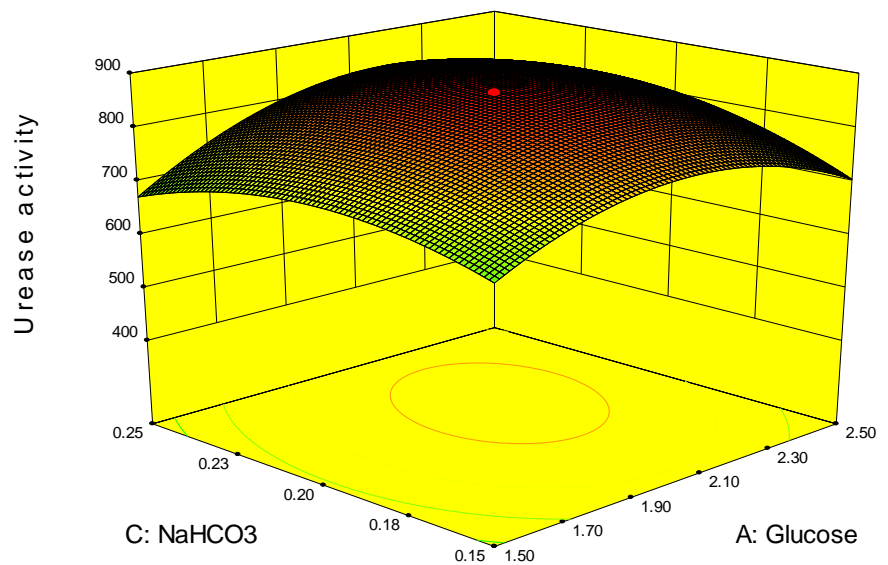


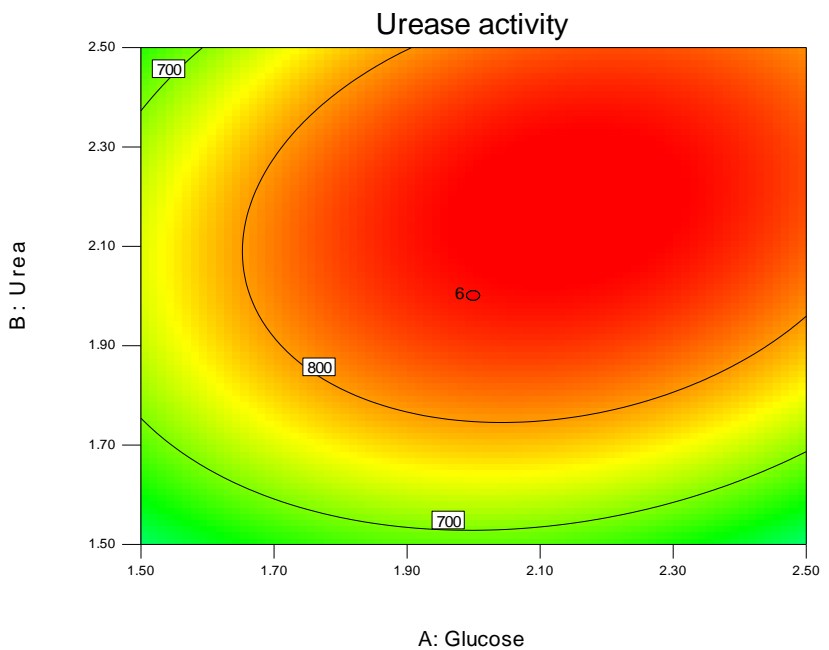
Fig. 4.6.2 a). Surface plot showing the effect of Urea and glucose on urease production b) Surface plot showing the effect of Urea and NaHCO₃ on urease production c) Surface plot showing the effect of NaHCO₃ and glucose on urease production

Design-Expert® Software
Factor Coding: Actual
Urease activity

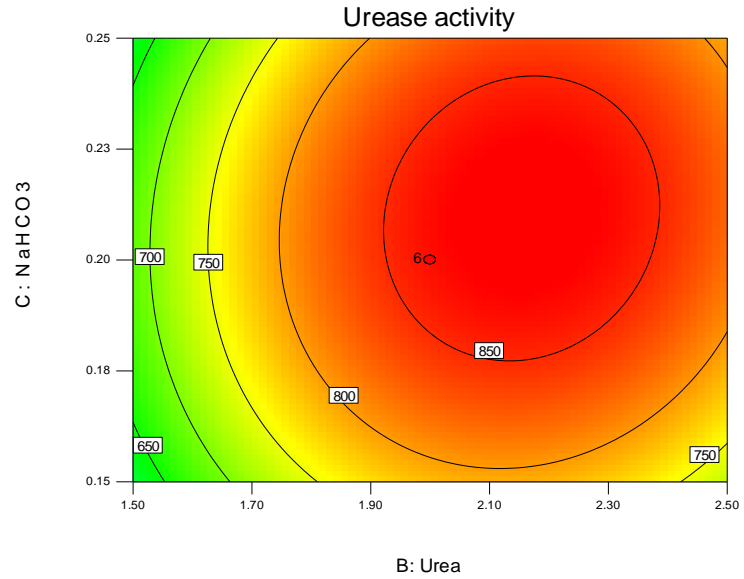
- Design Points

X1 = A: Glucose
X2 = B: Urea

Actual Factor
C: NaHCO₃ = 0.20



Design-Expert® Software
 Factor Coding: Actual
 Urease activity
 • Design Points
 867
 415
 X1 = B: Urea
 X2 = C: NaHCO₃
 Actual Factor
 A: Glucose = 2.00



Design-Expert® Software
 Factor Coding: Actual
 Urease activity
 • Design Points
 867
 415
 X1 = A: Glucose
 X2 = C: NaHCO₃
 Actual Factor
 B: Urea = 2.00

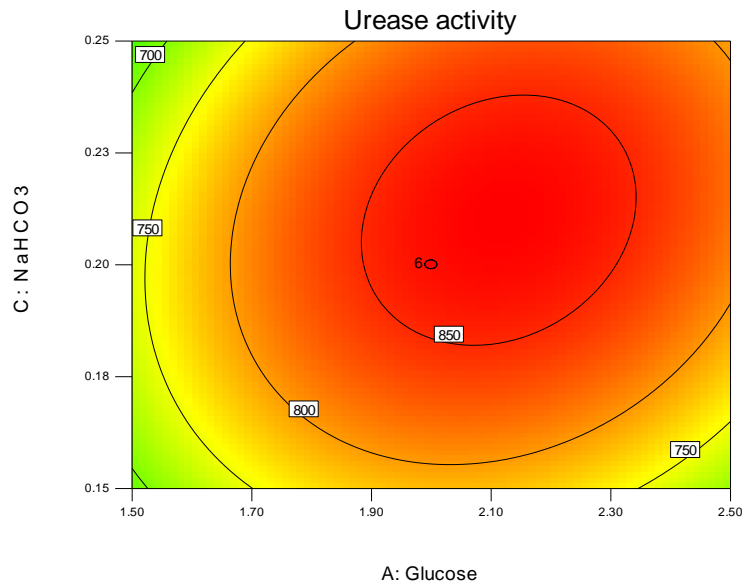


Fig.4.6.3 a) Contour plot between effect of Urea and glucose on urease production b) Contour plot between effect of Urea and NaHCO₃ on urease production c) Contour plot between effect of NaHCO₃ and glucose on urease production.

This work has highlighted the application of Response surface methodology by shedding light on fact that this process allows rapid screening of most important factors for production of enzymes and reduces the number of experiments significantly. Combination of placket burman and central composite design proved as an effective and reliable tool to study statistically significant factors and evaluating their optimal concentration within the medium for highest urease and thereby calcium carbonates.

Conclusion and salient features

The present work has culminated in production of higher urease and carbonate precipitates by the application of Response surface methodology. The physical and chemical factors which affect the production of urease in *Bacillus megaterium* SS3 were firstly varied one at a time and after that, placket burman design was demonstrated to screen multiple variables which affect the production of urease. Concentration of urea, glucose and NaHCO_3 were found to be most significant factors for the enzyme production. Based on results of central composite design, the optimized media and conditions for maximum urease production comprised urea = 21.1 g, glucose = 21.7g, NaHCO_3 = 1.9g, peptone = 10g, NH_4Cl = 10g, $\text{MgSO}_4 \cdot 7\text{H}_2\text{O}$ = 0.05, CaCl_2 = 2.8 g, KH_2PO_4 = 5g per litre at pH 8.0 and temperature of 35°C for incubation of 4 days which resulted in 1.2 folds increase in the activity of urease and 1.7 folds increase in the production of carbonates in the optimized media. Based on the promising results of this study, other more efficient ureolytic bacterial isolates can also be investigated for higher production of carbonates.

Summary

The production of carbonate biominerals via microbial cells has long been seen in natural environments as formation of rocks, shells, corals, limestone caves, ant hills etc. through various mechanisms. Apart from the fact that biological mineral precipitation is a natural phenomenon that occurs through ages, possibility of inducing precipitation of these carbonates in very short times within the lab represents a promising approach for various applications.

Natural processes, such as weathering, earthquakes, human activities etc., deteriorate various building structures leading to increased porosity, structural weakening of surface layers and unattractive appearance. Though conventional treatments are done by applications of synthetic agents such as epoxies and surface treatments with water repellents such as silanes or siloxanes, or with pore blockers but all these suffer from several disadvantages, such as different thermal expansion, degradation with age and the need for constant maintenance. So, there is need for self healing materials which can overcome all these problems. The process of microbially induced calcium carbonate precipitation (MICCP) seems to offer potential for consolidation of various building materials.

Though there are different mechanisms involved for carbonate precipitation in various microorganisms, but production of carbonates via ureolytic pathway in bacteria represents a novel biotechnology for various technical applications. The major factors responsible for making this pathway favorable are: common occurrence of urease positive bacteria and low cost of urea substrate, hydrolysis of urea truly satisfies the conditions for carbonate precipitation i.e. simultaneous increase of pH and dissolved inorganic carbon and it does not leave any toxic hazardous by - product. All these benefits broaden the applications of these ureolytic bacteria. The hydrolysis of urea by the widely distributed enzyme urease is also special because it is one of the few biologically occurring reactions that can generate carbonate ions without an associated production of protons. When this hydrolysis occurs in a calcium-rich environment, calcium carbonate precipitates from solution forming a solid-crystalline material.

The present study is divided into two sections. The first part deals with the isolation and characterization of several ureolytic bacterial isolates from alkaline soils along with the study of fundamental principles governing the precipitation process including different enzymes and optimum conditions for the enzyme production while the second part focused on the applications of carbonate precipitating bacteria in various building materials.

As the calcifying bacteria face the conditions of high pH formed during carbonate precipitation upon urea hydrolysis, only those bacterial isolates can work effectively in those environments which harbor the capability to survive the alkaline conditions. So, we explored the microbial diversity from alkaline soil sites for isolation of efficient carbonate precipitating bacteria. The bacterial isolation was done by enrichment method where the growth medium was supplemented with urea. Eight potential isolates were selected which harbored the capability to produce urease as well as precipitate the carbonates. The bacterial isolates in the present study were able to use urea as an energy source, resulting in the production of ammonia and carbonate. This increases the pH and the carbonate concentration near the cells, triggering Ca^{2+} and CO_3^{2-} to precipitate as CaCO_3 . All the bacterial isolates were morphologically, biochemically and molecularly (16S rDNA sequence analysis) characterized. Sequence data of the isolates was analyzed by BLAST (<http://blast.ncbi.nlm.nih.gov/Blast.cgi>) and phylogenetic tree was constructed based on 16S rDNA sequences by neighbor-joining method using MEGA software (v 5.0). Seven isolates were associated with the genera *Bacillus* while one was associated with *Staphylococcus* sp. The isolates were identified as *Bacillus megaterium* SS3, *Bacillus cereus* SS5, *Bacillus subtilis* SS13, *Bacillus thuringiensis* SS15, *Lysinibacillus fusiformis* SS18, *Staphylococcus* sp. SS20, *Bacillus anthracis* SS21 and *Bacillus cereus* SS22. Both SS20 and SS22 were less than 96% similar to previously known bacterial isolates and therefore regarded new bacterial isolates for carbonate precipitation studies.

The ureolytic and biocementation capability of all the strains was compared with *Sporosarcina pasteurii*, a well known urease producer. Urease production in different media, urea concentrations, calcium and nickel were studied. Nutrient broth with 2% urea and 25 mM CaCl_2 was found to be optimal for urease production and carbonate

precipitation. Production of EPS and biofilms was also noticeably significant in all the carbonate precipitating bacterial isolates. Role of urease and another enzyme carbonic anhydrase (CA) in carbonate precipitation was investigated by enzyme inhibition studies to check their effect in carbonate crystal formation. It was firstly reported that along with urease, carbonic anhydrase also plays an important role in bacterial CaCO_3 precipitation process as it works synergistically with urease. The production of CA by all ureolytic bacterial isolates suggested the presence of this enzyme in all carbonate precipitating bacteria. Though role of bovine and microbial CA has been reported in various CO_2 sequestration studies, but our work has made the first step in understanding the role of bacterial CA in CaCO_3 studies for applications in building materials.

The next section targeted the characterization of various carbonate polymorphs formed by all the isolates by Scanning electron microscopic (SEM) studies, Energy dispersive X ray (EDX) spectrum, X ray diffraction (XRD) analysis and Fourier transmission infra red (FT-IR) analysis. This study found that bacterial carbonate precipitation is strain specific. Recognizably different CaCO_3 precipitates under similar conditions were formed by different bacterial isolates i.e. all the carbonates were found to be morphologically as well as chemically distinct. As different technical applications require different carbonate polymorphs, the importance of this work will serve as a useful tool in various industries associated with carbonate biominerals and in depth research studies on these biominerals. After confirming the efficient precipitation of carbonates by different ureolytic isolates, the most efficient ureolytic and calcifying bacterial isolate *Bacillus megaterium* SS3 was selected to investigate its effect on durability properties of different building materials.

In the next part of the work, application of carbonate producing builder bacteria on varying grain sizes and densities sand columns was evaluated to elucidate the effect of microbial calcite on these columns for various commercial applications. Various physical and chemical characteristics of the sand particles upon treatment by calcifying bacteria were evaluated by SEM, EDX, XRD, Mercury intrusion porosimetry (MIP), pH and electrical conductivity (EC) analysis. This study demonstrated the positive potential of carbonate binders in improving the characteristics of varying grains sizes and densities sand columns.

0.5 mm grain size and 1.70 g/cc density of sand columns was found to be optimal for maximum carbonate precipitation leading to significant improvement of these materials.

As production of all conventional building materials like cement, concrete, bricks etc. involves large amounts of energy and CO₂ emissions which is damaging the environment due to continuous exploration and depletion of natural resources, soil – cement blocks have been developed as one of the most energy efficient building materials (Reddy and Jagadish 2003). But due to certain shortcomings of higher permeability and cracking, they have not been encouraged much at commercial level. A barrier layer on their surface that impedes moisture ingress would significantly improve their usefulness. In the subsequent part of the work, the applications of bacterial carbonates were investigated for enhancing the strength and durability of these low energy building materials. The specimens were prepared as per Reddy and Gupta (2005) along with bacterial treatment. Compressive strength, water absorption, linear expansion, rate of moisture absorption, porosity, freeze thaw and weight loss tests were conducted as per IS 3495, ASTM C 67 and Reddy and Gupta (2005) upon bacterial treated as well as control blocks. It was found that the bacterial treated specimens performed better than the control specimens. The supplementation of calcifying bacterial cells revealed positive effect on strength (23% increase), porosity (30% decrease), permeability and durability (18% increase) of low energy building materials. The carbonate layer formed by calcifying bacterial isolates on the surface of these building materials and consolidation of carbonate binders within the loose porous particles resulted in a decrease of the permeation properties, water absorption and porosity leading to enhanced strength. Durability results proved that the carbonate layer was highly coherent and provided greater physico-chemical resistance to these structures. This study offered an interesting and unique concept in improving the durability of low carbon buildings by applications of coherent calcite binders for a wide range of potential applications. This is the first report of application of calcifying bacterial cells on the improved properties of low energy building materials. The effect of bacterial carbonates on affecting the strength properties of ash bricks generated from industrial by - products fly ash as well as rice husk was also investigated as a surface layer treatment. In this case also, it was established that microbially induced calcite precipitation (MICP) effectively impedes percolation of water in the surface of different

building materials, form carbonate binders within the porous materials and effectively consolidates these materials leading to their improved strength. MICCP is highly desirable as the production of these calcite binders is pollution free, natural and highly coherent.

After investigating the potential of carbonate binders in various building materials, the next aim was to produce the formulations of these calcifying bacterial cells in cheap carrier material. For applications of these calcite binder producing bacterial cultures, different expensive carrier materials have been used but their high costs have come in the way of their successful commercialisation. So, in the present study we explored the potential of cheap industrial by-product fly ash as carrier material for bacterial cells and investigated the viability of three calcifying bacterial isolates: *Bacillus megaterium* SS3, *Bacillus cereus* SS5 and *Lysinibacillus fusiformis* SS18 in fly ash carrier at varying temperatures and moisture conditions along with biomineralization efficacy of these formulations. All the three calcifying bacterial isolates were grown in nutrient broth media and mixed with fly ash to achieve 5×10^8 cfu/g at moisture of 30, 40 and 50% and subjected to temperature of 4, 25 and 37°C for 1 year. The viability of these formulations was evaluated at regular intervals by plate count method. We also used laser scanning confocal microscopy to analyze the viability of bacteria by florescent dye 5-cyano-2,3-ditolyl tetrazolium chloride (CTC) along with plate count method. The use of fluorescent dye for investigating the survival of bacterial cells within the formulations has been reported for the first time. Results revealed that fly ash successfully served as effective carrier material and bacterial formulations stored at 4°C provided longer shelf life than those stored at higher temperatures. Up to 10^6 cfu/g was found to sustain in all formulations at 4°C compared to 10^4 - 10^5 cfu/g in case of higher temperatures up to 1 year. For 4°C, higher moistures (50%) were found to provide better survivability while for higher temperatures, lower moistures (30%) favoured higher viability. The biomineralization capability of fresh and formulated bacterial cells was compared on the basis of precipitation of carbonates and it was found that carbonate precipitation efficacy of formulated bacterial cells was comparable to fresh bacterial cells. The present study has for the first time proved the potential of fly ash as carrier for calcifying bacterial cells for commercial purposes.

The next part of the work investigated the optimization of medium for urease production, major enzyme involved in carbonate production by the application of Response surface methodology in *Bacillus megaterium* SS3. In this part, 3 significant factors which effect the production of urease by Placket burman design were found to be concentration of urea, glucose and NaHCO₃. The optimal concentration of these most important factors governing the production of urease was found to be 21.1 g urea, 21.7 g glucose and 1.9 g NaHCO₃ which led to 1.2 fold increase in the urease activity within optimized media which also led to 1.7 times increase in the carbonate production.

As microbial carbonates have numerous applications in various fields including restoration of building materials, the present study has provided “proof of concept” for potential applications of applied microbiology in the civil structures. This study has shed light on importance of various enzymes, extra polymeric substances and conditions for optimal precipitation of carbonate crystals. The results of strain specific precipitation of different polymorphs opined that the carbonate precipitating bacterial isolates are suitable for nano technological applications. The unique ability of the microbial systems to control structure, phase and topography of inorganic crystals makes them suitable candidates for producing durable carbonate binders. Present study has undoubtedly demonstrated the potential of bacterial carbonates in improving the durability of various building materials. This work has demonstrated the improvement in consolidation of loose sand particles in varying grain sized and density sand columns. This is also the first published study to achieve effective consolidation of low energy building materials and building materials from industrial by products. The work has conclusively established that high strength economical cementation can be achieved using MICCP via urea hydrolysis through the applications of indigenous bacterial isolates. Viability studies of calcifying bacterial cells by fluorescent dyes and plate counts in fly ash formulations has further paved the way for commercial applications of these calcifying bacterial isolates for various technical applications. In conclusion, *Applied Microbiology and Biotechnology* has led to generation of cost-efficient and eco-friendly cementation technology by utilizing ureolytic capability of bacteria for improving the properties of different building materials.

References:

- Abbate F, Winum J-Y, Potter BVL, Casini A, Montero J-L, Scozzafava A, Supuran CT (2004). Carbonic anhydrase inhibitors: X-ray crystallographic structure of the adduct of human isoenzyme II with EMATE, a dual inhibitor of carbonic anhydrases and steroid sulfatases. *Bioorg Med Chem Lett* 14: 337 – 341.
- Abou-Zeid MN, Meggers D, McCabe SL (2003). Parameters affecting the rapid chloride permeability test. *Concr Inter* 25: 61 - 66.
- Achal V, Mukherjee A, Basu PC, Reddy MS (2009a). Lactose mother liquor as an alternative nutrient source for microbial concrete production by *Sporosarcina pasteurii*. *J Ind Microbiol Biotechnol* 36: 433 - 438.
- Achal V, Mukherjee A, Basu PC, Reddy MS (2009b). Strain improvement of *Sporosarcina pasteurii* for enhanced urease and calcite production. *J Ind Microbiol Biotechnol* 36: 981-988.
- Achal V, Mukherjee A, Reddy MS (2010). Biocalcification by *Sporosarcina pasteurii* using corn steep liquor as nutrient source. *J Ind Microbiol Biotechnol* 6:170 – 174.
- Achal V, Mukherjee A, Reddy MS (2011a). Microbial Concrete: A Way to Enhance the Durability of Building Structures. *J Mater Civ Eng* 23: 730 - 734.
- Achal V, Mukherjee A, Reddy MS (2011b). Effect of calcifying bacteria on permeation properties of concrete structures. *J Ind Microbiol Biotechnol* 38: 1229 - 1234.
- Achal V, Pan X, Zhang D (2011c). Remediation of copper-contaminated soil by *Kocuria flava* CR1, based on microbially induced calcite precipitation. *Ecol Eng* 37: 1601 – 1605.
- Achal V, Pan X (2011). Characterization of Urease and Carbonic Anhydrase Producing Bacteria and their role in calcite precipitation. *Curr Microbiol* 62: 894 - 902.
- Achal V, Pan X, Fu Q, Zhang D (2012). Biomineralization based remediation of As(III) contaminated soil by *Sporosarcina ginsengisoli*. *J Hazard Mater* 201: 178 – 184.
- Adler L, Brundell J, Falkbring SO, Nyman PO (1972). Carbonic anhydrase from *Neisseria sicca* strain 6021. I. Bacterial growth and purification of the enzyme. *Biochim Biophys Acta* 284: 298–310.
- Al Qabany A (2011). Microbial carbonate precipitation in soils. Doctoral dissertation, Univ. of Cambridge, Cambridge, U.K.
- Al Thawadi SM (2011). Ureolytic bacteria and calcium carbonate formation as a mechanism of

strength enhancement of sand. *Journal of Advance Science and Engineering Research* 1: 98 -114.

Alber BE, Ferry JG (1994). A carbonic anhydrase from the archaeon *Methanosarcina thermophila*. *Proceedings of the National Academy of Sciences USA* 91: 6909 – 6913.

Altalo K, Gashe BA (1993). Protease production by a thermophilic *Bacillus* species (P-001A) which degrade various kinds of fibrous protein. *Biotechnol Lett* 15: 1151-1156.

Al-Thawadi SM (2008). High Strength In-Situ Biocementation of Soil by Calcite Precipitating Locally Isolated Ureolytic Bacteria. PhD thesis. Murdoch University, Western Australia.

Altman FP (1976). Tetrazolium salts and formazans. *Prog Histochem Cytochem* 9: 1 – 56.

Altschul SF, Madden TL, Schaffer AA, Zhang S, Zhang Z, Miller W, Lipman DJ (1997). Gapped BLAST: a new generation of protein database search programs. *Nucleic Acid Research* 25: 3389 - 3402.

Amann RI, Ludwig W, Schleifer KH (1995). Phylogenetic identification and in situ detection of individual microbial cells without cultivation. *Microbiol Molecular Biol Rev* 59: 143-169.

Anderson S, Appanna VD, Huang J, Viswanatha T (1992). A novel role for calcite in calcium homeostasis: *FEBS* 308: 94–96.

Andrews WH, June GA, Sherrod PS, Hammack TS, Amaguana RM (1995). FDA Bacteriological analytical manual, 8th ed. AOAC International, Gaithersburg, MD.

Aono R, Horikoshi K (1991) Carotenes produced by alkaliphilic yellow pigmented strains of *Bacillus*. *Agric Biol Chem* 55: 2643 – 2645.

Aono R, Ito M, Machida T (1999). Contribution of cell wall component teichuronopeptide to pH homeostasis and alkaliphily in the alkaliphile *Bacillus lentus* C-125. *J Bacteriol* 181: 6600-6606.

Archer GL (1998). *Staphylococcus aureus*: a well-armed pathogen. *Clin Infect Dis* 26:1179-81.

Arp G, Reiner A, Reiner J (2001). Photosynthesis-induced biofilm calcification and calcium concentration in Phanerozoic oceans. *Science* 292:1701-1704.

Arunachalam KD, Sathyanarayanan KS, Darshan BS, Raja RB (2010). Studies on the characterisation of Biosealant properties of *Bacillus sphaericus*. *Int J Eng Sci Technol* 2: 270-277.

Aubert JE, Husson B, Sarramone N (2006). Utilization of Municipal Solid Waste Incineration (MSWI) Fly Ash in Blended Cement: Part 1: Processing and Characterization of MSWI Fly Ash. *J Hazardous Mater* 136: 624 - 631.

- Bachmeier KL, Williams AE, Warmington JR, Bang SS (2002). Urease activity in microbiologically-induced calcite precipitation. *J Biotechnol* 93: 171– 181.
- Bagno A, Comuzzi C, Scorrano G (1994). Site of Ionization of Hydroxamic Acids Probed by Heteronuclear NMR Relaxation Rate and NOE Measurements. An Experimental and Theoretical Study. *J Am Chem Soc* 116: 916-24.
- Balan SS, Fazila F, Jayalakshmi S (2012). Characterization of urease enzyme from marine bacterium *Klebsiella* species. *Afr J Microbiol Res* 6: 5914 – 5923.
- Banfield JF and Zhang H (2001). Nanoparticles in the environment, *Rev Mineral Geochem* 44: 1 - 58.
- Bang SS, Galinat JK, Ramakrishnan V (2001). Calcite precipitation induced by polyurethane-immobilized *Sporosarcina pasteurii*. *Enzyme Microb Tech* 28: 404 – 409.
- Bang SS, Ramakrishnan V (2001). Microbiologically-enhanced crack remediation (MECR). Proceedings of the International Symposium on Industrial Application of Microbial Genomes, Daegu, Korea, 3-13.
- Barabesi C, Galizzi A, Mastromei G, Rossi M, Tamburini E and Perito B (2007). *Bacillus subtilis* gene cluster involved in calcium carbonate biomineralization. *J Bacteriol* 189: 228–235.
- Baskar S, Baskar R, Mauclaire L, Mckenzie JA (2005). Role of microbial community in stalactite formation, Sahastradhara caves, Dehradun, India. *Curr Sci* 88: 1305–1308.
- Bäuerlein E (2003). Biomineralization of unicellular organisms: An unusual membrane biochemistry for the production of inorganic nano- and microstructures. *Angew Chem Int* 42: 614-641.
- Bazylinski DA, Frankel RB (2003). Biologically induced mineralization by bacteria. *Reviews in Mineralogy and Geochemistry* 54: 95 – 114.
- Bazylinski DA, Frankel RB (2004). Magnetosome formation in prokaryotes. *Nat Rev Microbiol* 2: 217–230.
- Beijerinck M (1913). De Infusies en de Ontdekking der Backterien, Jaarboek van de Koninklijke Akademie v. Wetenschappen. Muller, Amsterdam.
- Ben Chekroun K, Rodriguez-Navarro C, Gonzalez-Muñoz MT, Arias JM, Cultrone G, Rodriguez-Gallego M (2004). Precipitation and growth morphology of calcium carbonate induced by *Myxococcus xanthus*: implications for recognition of bacterial carbonates. *J Sedimentary Res* 74: 868-876.
- Ben Omar N, González-Muñoz MT, Peñalver JMA (1998). Struvite crystallization on *Myxococcus*

- cells. *Chemosphere* 36: 475 – 481.
- Ben Omar N, Martínez - Cañamero M, González-Muñoz MT, Maria Arias J, Huertas F (1995). *Myxococcus xanthus* killed cells as inducers of struvite crystallization Its possible role in the biomineralization processes. *Chemosphere* 30: 2387 – 2396.
- Benini S, Rypniewski W, Wilson KS, Miletti S, Ciurli S, Mangani S (1999). A new proposal for urease mechanism based on the crystal structures of the native and inhibited enzyme from *Bacillus pasteurii*: why urea hydrolysis costs two nickels. *Structure* 7: 205-216.
- Benzerara K, Menguy N, López-García P, Yoon TH, Kazmierczak J, Tyliszczak T, Guyot F, Brown GE (2006). Nanoscale detection of organic signatures in carbonate microbialites. *PNAS* 103: 9440-9445.
- Berg J, Tymoczko J, Stryer L (2002). *Biochemistry*. WH Freeman and Company, New York.
- Bergdale TE, Pinkelman RJ, Hughes SR, Zambelli B, Ciurli S, Bang SS (2012). Engineered biosealant strains producing inorganic and organic biopolymers. *J Biotech* 161: 181-189.
- Beveridge TJ (1989). Role of cellular design in bacterial metal accumulation and mineralization. *Annu Rev Microbiol* 43: 147-171.
- Beveridge TJ, Meloche JD, Fyfe WS, Murray RGE (1983). Diagenesis of metals chemically complexed to bacteria: laboratory formation of metal phosphates, sulfides, and organic condensates in artificial sediments. *Appl Environ Microbiol* 45: 1094-1108.
- Bhattacharya S, Nayak A, Schiavone M, Bhattacharya SK (2004). Solubilization and concentration of carbon dioxide: novel spray reactors with immobilized carbonic anhydrase. *Biotechnol Bioeng* 86: 37 – 46.
- Bhattacharya S, Schiavone M, Chakrabarti M, Bhattacharya SK (2003). CO₂ hydration by immobilized carbonic anhydrase. *Biotechnol Appl Biochem* 38: 111–117.
- Bodek I, Lyman W, Reehl W, eds. (1988). *Environmental Inorganic Chemistry-properties, Processes, and Estimation Methods*. Pergamon Press, New York. pp. 6.7-1 to 6.7-9.
- Bond GM, Stringer J, Brandvold DK, Simsek FA, Medina MG, Egeland G (2001). Development of integrated system for biomimetic CO₂ sequestration using the enzyme carbonic anhydrase. *Energy Fuels* 15: 309-316.
- Bond GM, Stringer J, Brandvold DK, Simsek FA, Medina MG, Egeland G (1999). Enzymatic catalysis and CO₂ sequestration. *World Res Rev* 11: 603–618.

- Boquet E, Boronat A, Ramos-Cormenzana A (1973). Production of calcite (calcium carbonate) crystals by soil bacteria is a general phenomenon. *Nature* 246: 527–529.
- Botre C, Botre F (1989). Carbonic anhydrase and urease: an investigation in vitro on the possibility of a synergic action. *Biochimica et Biophysica Acta* 997: 111-4.
- Breeuwer P, Abee T (2004). Assessment of the membrane potential, intracellular pH and respiration of bacteria employing fluorescence techniques. *Molecular Microbial Ecology Manual, Second Edition* 8: 1563–1580.
- Braissant O, Decho AW, Przekop KM, Gallagher KL, Glunk C, Dupraz C, Visscher PT (2009). Characteristics and turnover of exopolymeric substances in a hypersaline microbial mat. *FEMS Microbiol Ecol* 67: 293–307.
- Braissant O, Verrecchia E and Aragno M (2002). Is the contribution of bacteria to terrestrial carbon budget greatly underestimated. *Natur wissens chaften* 89, 366–370.
- Braus-Stromeyer S, Schnappauf G, Braus GH, Gobner A, Drake HL (1997). Carbonic anhydrase in *Acetobacterium woodii*. *J Bacteriol* 179: 7197–7200.
- Buchanan AB, Honey BG (1994). Energy and carbon dioxide implications of building construction. *Energy and Buildings* 20: 205–217.
- Buczynski C, Chafetz HS (1991). Habit of bacterially induced precipitates of calcium carbonate and the influence of medium viscosity on mineralogy. *J Sedimentary Petrol* 61: 226–233.
- Burne RA, Chen RE (2001). Bacterial ureases in infectious diseases. *Microbes Infect* 2: 533-542.
- Burne RA, Marquis RE (2000). Alkali production by oral bacteria and protection against dental caries. *FEMS Microbiol Lett* 193: 1-6.
- Burnham L, Dollimore D, Alexander K (2001). Calculations of the Vapor Pressure-Temperature Relationship Using Thermogravimetry for the Drug Allopurinol. *Thermochimica Acta* 367-368: 15-22.
- Buzolyova LS, Somov G (1999). Autotrophic assimilation of CO₂ and C₁ compounds by pathogenic bacteria. *Biochem (Moscow)* 64: 1357 – 1361.
- Cappitelli F, Zanardini E, Ranalli G, Mello E, Daffonchio D, Sorlini C (2006). Improved methodology for bioremoval of black crusts on historical stone artworks by use of sulfate - reducing bacteria. *Appl Environ Microbiol* 72 : 3733 – 3737.
- Cappitelli F, Toniolo L, Sansonetti A, Gulotta D, Ranalli G, Zanardini E, Sorlini, C (2007).

- Advantages of using microbial technology over traditional chemical technology in removal of black crusts from stone surfaces of historical monuments. *Appl Environ Microbiol* 73: 5671–5675.
- Castanier S, Le Metayer-Levrel G, Perthuisot JP (1999). Ca-carbonates precipitation and limestone genesis - the microbiogeologist point of view. *Sediment Geol* 126: 9 - 23.
- Castanier S, LeMétayer-Levrel G, Perthuisot JP (2000). Bacterial roles in the precipitation of carbonate minerals. In Riding RE, Awramik SM (eds), *Microbial sediments*. Heidelberg: Springer-Verlag, 32 - 39.
- Chafetz HS and Buczynski C (1992). Bacterally induced lithification of microbial mats. *Palaios*, 7: 277 – 293.
- Chandrasekhar S, Pramada PN, Majeed J (2006). Effect of calcination temperature and heating rate on the optical properties and reactivity of rice-husk ash. *J Material Sci* 41: 7926 - 7933.
- Chaturvedi S, Chandra R, Rai V (2006). Isolation and characterization of *Phragmites australis* (L.) rhizosphere bacteria from contaminated site for bioremediation of colored distillery effluent. *Ecol Eng* 27: 202 – 207.
- Choudhury B, Aggarwal P, Gothwal RK, Mantri R, Mohan MK, Ghosh P (2006). Biobleaching of non-woody pulps using xylanase enzyme of *Bacillus brevis* BISR-062. *Appl Biochem Biotechnol* 128: 159 - 170.
- Chen L, Shen Y, Xie A, Huang B, Jia R, Guo R, Tang W (2009). Bacteria-Mediated Synthesis of Metal Carbonate Minerals with Unusual Morphologies and Structures. *Cryst growth des* 9: 743 - 754.
- Chen YY, Clancy KA, Burne RA (1996). *Streptococcus salivarius* urease: genetic and biochemical characterization and expression in a dental plaque streptococcus. *Infect Immun* 64: 585 – 592.
- Cheng L, Cord-Ruwisch R (2012). *In situ* soil cementation with ureolytic bacteria by surface percolation. *Ecol Eng* 42: 64 - 72.
- Chin WT, Kroontje W (1962). Conductivity Method for Estimation of Urease Activity. *Agricultural and Food Chemistry* 10: 347 - 348.
- Chirica L, Peteresson C, Hurtig M, Jonsson BH, Boren T & Lindskog S (2002). Expression and localization of α and β Carbonic anhydrase in *Helicobacter pylori*. *Biochemica and Biophysica Acta* 160:192 – 199.

- Chu J, Ivanov V, Naeimi M, Li B, Stabnikov V (2011). Development of microbial geotechnology in Singapore. *Proc. Geofrontiers 2011: Advances in Geotechnical Engineering, Dallas, TX, ASCE Geotechnical Special Publication 211*: 4070 – 4078.
- Cigdem K, Merih K (2005). Effect of formulation on the viability of biocontrol agent, *Trichoderma harzianum* conidia. *African J Biotechnol* 85: 483 – 486.
- Ciurli S, Marzadori C, Benini S, Deiana S, Gessa C (1996). Urease from the soil bacterium: *Bacillus pasteurii* immobilization on Ca-polygalacturonate. *Soil Biol Biochem* 28: 811 - 817.
- Claus D, Berkeley RCW (1986). Genus *Bacillus* in Bergeys manual of systematic bacteriology. Sneath PH (ed), The Willams and Wikins company, Baltimore.
- Coleman JE (1967). Mechanism of action of carbonic anhydrase. Substrate, sulfonamide, and anion binding. *J Biol Chem.* 242: 5212 – 5219.
- Collins CM, D'Orazio SE (1993). Bacterial ureases: structure, regulation of expression and role in pathogenesis. *Mol Microbiol.* 9: 907 – 913.
- Davey ME, O'Toole GA (2000). Microbial biofilms: from ecology to molecular genetics. *Microbiology and Molecular Biology Reviews* 64: 847 - 867.
- Daza A, Santamaria C, Rodrigues-Navarro DN, Camach M, Orive R, Temprano F (2000). Perlite as a carrier for bacterial inoculants. *Soil Biol Biochem* 32: 567 – 572.
- De Belie N, De Muynck W (2008). Crack repair in concrete using biodeposition. *In: Proc. of ICCRR*, Cape Town, South Africa.
- De Jong JT, Fritzges MB, Nusstein K (2006). Microbially induced cementation to control sand response to undrained shear. *J Geotech Geoenviron Eng* 32: 1381 – 13.
- De Jong JT, Soga K, Kavazanjian E, Burns S, Van Paassen LA, Al Qabany A, Aydilek A, Bang SS, Burbank M, Caslake LF, Chen CY, Cheng X, Chu J, Ciurli S, Esnault-Filet A, Fauriel S, Hamdan N, Hata T, Inagaki Y, Jefferis S, Kuo M, Laloui L, Larrahondo J, Manning DAC, Martinez B, Montoya BM, Nelson DC, Palomino A, Renforth P, Santamarina JC, Seagren EA, Tanyu B, Tsesarsky M, Weaver T (2013). Biogeochemical processes and geotechnical applications: progress, opportunities and challenges. *Geotechnique* 63: 287–301.
- De Martin Llano JJ, Segura JMG, Gavilanes JG (1989). Selective silver staining of urease activity in polyacrylamide gels. *Anal Biochem* 177: 37-40.
- De Muynck W, Belie N, Verstraete W (2010). Microbial carbonate precipitation in construction

- materials: a review. *Ecol Eng* 36: 118–136.
- De Muynck W, Cox K, De Belie N, Verstraete W (2008a). Bacterial carbonate precipitation as an alternative surface treatment for concrete. *Constr Build Mater* 22: 875–885.
- De Muynck W, Debrouwer D, De Belie N, Verstraete W (2008b). Bacterial carbonate precipitation improves the durability of cementitious materials. *Cem Concr Res* 38: 1005 – 1014.
- De Muynck W, De Belie N, Verstraete W (2009). Influence of Urea and Calcium Dosage on the Effectiveness of Bacterially Induced Carbonate Precipitation on Limestone. *Ecol Engg* doi:10.1016/j.ecoleng.2009.03.025.
- De Muynck W, Leuridan S, Van Loo D, Verbeken K, Cnudde V, De Belie N, Verstraete W (2011). Influence of pore structure on the effectiveness of a biogenic carbonate surface treatment for limestone conservation. *Appl Environ Microbiol* 77: 6808 – 6820.
- De Siano T, Padhi S, Schaffner DW, Montville TJ (2006). Growth characteristics of Virulent *Bacillus anthracis* and potential surrogate strains. *J Food Protec* 69: 1720 - 1723.
- Debnath A, Singh SV, Singh YP (1995). Comparative assessment of energy requirements for different types of residential buildings in India, *Energy and Buildings* 23: 141 – 146.
- Decho AW (2009). Overview of biopolymer-induced mineralization: What goes on in biofilms. *Ecol Eng* 30: 1 – 8.
- Deepak V, Kalishwaralal K, Ramkumarpandian S, Venkatesh Babu S, Senthilkumar SR, Sangiliyandi G (2008). Optimization of media composition for Nattokinase production by *Bacillus subtilis* using response surface methodology 17: 8170 - 8174.
- DeJong JT, Fritzges MB, Nusslein K (2006). Microbially induced cementation to control sand response to undrained shear. *J Geotech Geoenviron Eng* 132: 1381 – 1392.
- DeJong JT, Mortensen B, Martinez M, Nelson DC (2010). Bio-Mediated Soil Improvement. *Ecol Eng* 36: 197 - 210.
- DeJong JT, Soga K, Banwart SA, Whalley WR, Ginn TR, Nelson DC, Mortensen BM, Martinez BC, Barkouki R (2011). Soil engineering in vivo: harnessing natural biogeochemical systems for sustainable, multi-functional engineering solutions. *JR Soc Interface* 8: 1 - 15.
- Dick J, De Windt W, De Graef B, Saveyn H, Van der Meeren P, De Belie N, Verstraete W (2006). Bio-deposition of a calcium carbonate layer on degraded limestone by *Bacillus* species. *Biodegradation* 17: 357 – 367.

- Dittrich M, Sibling S (2010). Calcium Carbonate Precipitation by Cyanobacterial Polysaccharides. Peley KM and Rogerson (eds) *Tufas and Speleothems: Unravelling the Microbial and Physical Controls*. Geological Society, London, Special Publications, 336: 51 – 63.
- Dittrich M, Vasconcelos C, Dorozhkin P (2010). Microbe-mineral interfaces in biofilms as seen by Atomic Force Microscopy combined with Raman and X-ray Spectroscopy. *Geochimica et Cosmochimica Acta* 74: A236 - A236.
- Dixon NE, Riddles PW, Gazzold C, Blakeley RL, Zerner B (1980). Jack bean urease (EC 3.5.1.5) V. on the mechanism of action of urease on urea, formamide, acetamide, N-methylurea and related compounds. *Canadian J Biochem* 58: 1335 - 1344.
- Douglas E, Bilodeau A, Malhotra VM (1992). Properties and durability of alkali-activated slag concrete. *ACI Mater J* 89: 509-516.
- Douglas S, Beveridge TJ (1998). Mineral formation by bacteria in natural microbial communities. *FEMS Microbiol Ecol* 26: 79–88.
- Drew GH (1910). The action of some denitrifying bacteria in tropical and temperate seas, and the bacterial precipitation of calcium carbonate in the sea. *J Mar biol ass* 9: 142-155.
- Drew GH (1914). On the precipitation of calcium carbonate in the sea by marine bacteria. Carnegie Publication 182: 7 - 45, Washington.
- Dunn BE, Grütter MG (2001). *Helicobacter pylori* springs another surprise. *Nature Struc Biol* 8: 480 - 482.
- Dupraz S, Menez B, Gouze P, Leprovost R, Benezeth P, Pokrovsky O, Guyot F (2009). Experimental approach of CO₂ biomineralization in deep saline aquifers. *Chem Geol* 265: 54–62.
- Durham DR (1987). Utility of subtilisin GX as a detergent additive. *J Appl Bacteriol* 63: 381-386.
- Ehrlich HL (1996). How microbes influence mineral growth and dissolution, *Chem Geol* 132: 5–9.
- El-Shora HM (2001). Properties and immobilization of urease from *Chenopodium album* (C3). *Botanical Bull Academia Sinica* 42: 251-258.
- Ercole C, Bozzelli P, Altieri F, Cacchio P, Gallo MD (2012). Calcium Carbonate Mineralization: Involvement of Extracellular Polymeric Materials Isolated from Calcifying Bacteria. *Microscopy Microanal* 18: 829-839.
- Ercole C, Cacchio P, Botta AL, Centi V, Lepidi A (2007). Bacterially induced mineralization of calcium carbonate: The role of exopolysaccharides and capsular polysaccharides. *Microsc*

Microanal 13: 42–50.

- Eschenhagen M, Schuppler M, Roske I (2003). Molecular characterization of the microbial community. *Water Res* 37: 3224-32.
- Evans DJ Jr, Evans DG, Kirkpatrick SS, Graham DY (1991). Characterization of the *Helicobacter pylori* urease and purification of its subunits. *Microb Pathog* 10: 15-26.
- Falkinham III JO, Hoffman PS (1984). Unique developmental characteristics of the swarm and short cells of *Proteus vulgaris* and *Proteus mirabilis*. *J Bacteriol* 158: 1037-1040.
- FAO Statistical Database (2002) <http://apps.fao.org>.
- Favre N, Christ ML, Pierre AC (2009). Biocatalytic capture of CO₂ with carbonic anhydrase and its transformation to solid carbonate. *J Mol Catal* 60: 3-4.
- Feldmann M (1997). Geomicrobial processes in the subsurface: a tribute to Johannes Neher's work. *FEMS Microbiol Rev* 20: 181-189.
- Ferrer MR, Quevedo-Sarmiento J, Rivadeneyra MA, Bejar V, Delgado R, Ramos-Cormenzana A (1988). Calcium carbonate precipitation by two groups of moderately halophilic microorganisms at different temperatures and salt concentrations. *Curr. Microbiol.* 17: 221-227.
- Ferris FG, Beveridge TJ (1985). Binding of a paramagnetic metal cation to *Escherichia coli* K-12 outer membrane vesicles. *FEMS Microbiol Lett* 24: 43-46.
- Ferris FG, Beveridge TJ, Fyfe WS (1986). Iron-silica crystallite nucleation by bacteria in a geothermal sediment. *Nature* 320: 609-611.
- Ferris FG, Fyfe WS, Beveridge TJ (1987). Bacteria as nucleation sites for authigenic minerals in a metal-contaminated lake sediment. *Chem Geol* 63: 225–232.
- Ferris FG, Phoenix V, Fujita Y, Smith RW (2003). Kinetics of calcite precipitation induced by ureolytic bacteria at 10 to 20 °C in artificial groundwater. *Geochim Cosmochim Acta* 67: 1701–1722.
- Ferris FG, Stehmeier LG (1992). Bacteriogenic mineral plugging, United States Patent 5143155.
- Fishbein WN, Carbone PP (1965). Urease Catalysis: Inhibition of the Enzyme by Hydroxyurea, Hydroxylamine, and Acetohydroxamic Acid. *J Biol Chem* 240: 2407–2414.
- Flemming HC (2002). Biofouling in water systems – cases, causes, countermeasures . *Appl Environ Biotechnol* 59 : 629–640.

- Flood JA, Ashbolt NJ, Pollard PC (1999). Complementary independent molecular, radioisotopic and fluorogenic techniques to assess biofilm communities in two wastewater wetlands. *Water Sci Technol* 39: 65-70.
- Folk R (1993). SEM imaging of bacteria and nanobacteria in carbonate sediments and rocks, *J Sedim Petrol* 63: 990–999.
- Foppen JWA, Schijven JF (2006). Evaluation of data from the literature on the transport and survival of *Escherichia coli* and thermotolerant coliforms in aquifers under saturated conditions. *Water Res* 40: 401 – 426.
- Fortin D, Ferris FG, Beveridge TJ (1997). Surface-mediated mineral development by bacteria. *Rev Mineral* 35: 161-180.
- Friedman LE, de Passerini Rossi BN, Messina MT, Franco MA (2001). Phenotype evaluation of *Bordetella bronchiseptica* cultures by urease activity and congo red affinity. *Lett Appl Microbiol* 33: 285-290.
- Friedrich B, Magasanik B (1977). Urease of *Klebsiella aerogenes*: control of its synthesis by glutamine synthetase. *J Bacteriol* 28: 313-322.
- Fry J (2000). Bacterial diversity and unculturables. *Microbiol Today* 27: 186-188.
- Fujita Y, Ferris FG, Lawson RD, Colwell FS, Smith RW (2000). Calcium carbonate precipitation by ureolytic subsurface bacteria. *Geomicrobiol J* 17: 305-318.
- Fujita Y, Redden GD, Ingram JC, Cortez MM, Ferris FG, Smith RW (2004). Strontium incorporation into calcite generated by bacterial ureolysis, *Geochim Cosmochim Acta* 68: 3261–3270.
- Gaind S, Gaur AC (1990). Influence of Temperature on the Efficiency of Phosphate Solubilizing Microorganisms. *Indian J Microbiol* 30: 305 - 310.
- Gaind S, Gaur AC (2004). Evaluation of fly ash as carrier material for diazotrophs and phosphobacteria. *Bioresour Technol* 95: 187-190.
- Gauckler LJ, Graule TJ, Baader FH (1999). Ceramic forming using Enzyme catalyzed reactions. *Materials Chemistry and Physics* 61: 78-102.
- Gavrilescu M, Chisti Y (2005). Biotechnology—a sustainable alternative for chemical industry. *Biotechnol Adv* 23: 471–499.
- Gebauer D, Gunawidjaja PN, Ko JYP, Bacsik S, Aziz B, Liu L, Hu Y, Bergtröm L, Tai CW, Sham TK, Edén M, Hedin N (2010). Proto-calcite and proto-vaterite in amorphous calcium carbonates.

Angew Chem Int Ed 49: 8889 - 8891.

Geesey G, Jang L (1990). Extracellular polymers for metal binding p. 223–247. In H. L. Ehrlich and C. L. Brierley (ed.), *Microbial mineral recovery*. McGraw Hill, New York, NY.

Ghiorse WC (1984). Biology of iron- and manganese-depositing bacteria. *Ann Rev Microbiol* 38: 515-550.

Ghosh P, Mandal S, Chattopadhyay BD, Pal S (2005). Use of microorganisms to improve the strength of cement mortar. *Cem Concr Res* 35: 1980 – 1983.

Gillis PBM, De Leg J (1992). The genus *Aquaspirillum*. In the prokaryotes: A handbook on the biology of bacteria: ecophysiology, isolation, identification, and applications, Balows A *et al.* (eds), Springer-Verlag, New York, 2569-2582.

Gohel V, Singh A, Vimal M, Ashwini P, Chhatpar HS (2006). Bioprospecting and antifungal potential of chitinolytic Microorganisms. *Afr J Biotechnol* 5: 54-72.

Gollapudi UK, Knutson CL, Bang SS, Islam MR (1995). A new method for controlling leaching through permeable channels. *Chemosphere* 30: 695 – 705.

González - Munoz M, Arias JM, Montoya E, Rodriguez - Gallego M (1993). Struvite production by *Myxococcus coralloides* D. *Chemosphere* 26: 1881 – 1887.

González - Munoz MT, Omar NB, Martínez-Cañamero M, Rodríguez-Gallego M, Galindo AL, Arias J (1996). Struvite and calcite crystallization induced by cellular membranes of *Myxococcus xanthus*. *J Cryst Growth* 163: 434 – 439.

González-Muñoz MT, Rodríguez-Navarro C, Martínez-Ruiz F, Arias JM, Merroun ML, Rodríguez-Gallego M (2011). Bacterial biomineralization: new insights from *Myxococcus* - induced mineral precipitation. *Geol Soc London Sp Pub* 336: 31-50.

Gower LB (2008). Biomimetic model systems for investigating the amorphous precursor pathway and its role in biomineralization. *Chem Rev* 108:4551-4627.

Groneberg RD, Burns CJ, Morrissette MM., Ullrich JW, Morris RL, Darnbrough S, Djuric SW, Condon SM, McGeehan GM, Labaudiniere R, Neuenschwander K, Machel HG (2001). Bacterial and thermochemical sulfate reduction in diagenetic settings: old and new insights. *Sediment Geol* 140: 143-175.

Ha N, Oh ST, Sung JY, Cha KA, Lee MH, Oh BH (2001). Supramolecular assembly and acid resistance of *Helicobacter pylori* urease. *Nature Struct Biol* 8: 505-509.

- Hajduk PJ, Sheppard G, Nettesheim DG, Olejniczak ET, Shuker SB, Meadows RP, Steinman DH, Carrera Jr. GM, Marcotte PA, Severin J, Walter K, Smith H, Gubbins E, Simmer R, Holzman TF, Morgan DW, Davidsen SK, Summers JB, Fesik SW (1997). Discovery of Potent Nonpeptide Inhibitors of Stromelysin using SAR by NMR. *J Am Chem Soc* 119: 5818-27.
- Haltrich D, Preiss M, Steiner W (1993). Optimization of a culture medium for increased xylanase production by a wild strain of *Schizophyllum commune*. *Enzyme Microb Tech* 15: 854-860.
- Hammad IA, Talkhan FN, Zoheir AE (2013). Urease activity and induction of calcium carbonate precipitation by *Sporosarcina pasteurii* NCIMB 8841. *J Appl Sci Res* 9: 1525-1533.
- Hammes F (2003a). Ureolytic microbial calcium carbonate precipitation (PhD thesis). Ghent, Ghent University.
- Hammes F, Boon N, De Villiers J, Verstraete W, Siciliano SD (2003b). Strain-specific ureolytic microbial calcium carbonate precipitation. *Appl Environ Microbiol* 69: 4901 – 4909.
- Hammes F, Seka A, de Knijf S, Verstraete W (2003c). A novel approach to calcium removal from calcium-rich industrial wastewater. *Water Res* 37: 699-704.
- Hammes F, Verstraete W (2002). Key roles of pH and calcium metabolism in microbial carbonate precipitation. *Rev Environ Sci Biotechnol* 1: 3–7.
- Harkes MP, van Paassen LA, Booster JL, Whiffin VS, van Loosdrecht MCM (2010). Fixation and distribution of bacterial activity in sand to induce carbonate precipitation for ground reinforcement. *Ecol Eng* 36: 112–117.
- Heck RW, Tanhauser SM, Manda R, Tu C, Laipis PJ, Silverman DN (1994). Catalytic properties of mouse carbonic anhydrase. *J Biol Chem* 26940: 24742–24746.
- Heydorn A, Ersbøll BK, Hentzer M, Parsek MR, Givskov M, Molin S (2000). Experimental reproducibility in flow-chamber biofilms. *Microbiol* 146: 2409-2415.
- Higashibata A, Fujiwara T, Fukumori Y (1998). Studies on the respiratory system in alkaliphilic *Bacillus*; a proposed new respiratory mechanism. *Extremophiles* 2: 83–92.
- Himabindu M, Ravichandra P, Vishalakshi K, Annapurna J (2006). Optimization of critical medium components for the maximal production of gentamicin by *Micromonospora echinospora* ATCC 15838 using response surface methodology. *Appl Biochem Biotechnol* 134: 143–154.
- Hirayama C, Sugimura M, Saito H, Nakamura M (2000). Purification and properties of urease from the leaf of mulberry *Morus albus*. *Phytochem* 53: 352-330.

- Ho C, Sturtevant JM (1963). The kinetics of the hydration of carbon dioxide at 25°C. *J Biol Chem* 238: 3499-501.
- Horner-Devine MC, Carney KM, Bohannon BJM (2004). An ecological perspective on bacterial biodiversity. *Proc R Soc Biol Sci B* 271: 113–122.
- Hou WC, Chen HJ, Lin YH (2000). Dioscorins from different *Dioscorea* species all exhibit both carbonic anhydrase and trypsin inhibitor activities. *Bot Bull Acad Sin* 41: 191–196.
- Huang S, Xue Y, Sauer-Eriksson E, Chirica L, Lindskog S (1998). Crystal structure of carbonic anhydrase from *Neisseria gonorrhoeae* and its complex with the inhibitor acetazolamide. *J Mol Biol* 283: 301–10.
- Ikedo-Saito M, Shelley DA, Lu L, Booth KS, Caughey WS, Kimura S (1991). Salicylhydroxamic Acid Inhibits Myeloperoxidase Activity. *J Biol Chem* 266: 3611-16.
- Ivanov V, Chu J (2008). Applications of microorganisms to geotechnical engineering for bioclogging and biocementation of soil in situ. *Rev Environ Sci Biotechnol* 7: 139 – 153.
- Ivey DM, Ito M, Gilmour R, Zemsky J, Guffanti AA, Sturr MG, Hicks DB, Krulwich TA (1998). Alkaliphile bioenergetics. In Horikoshi K, Grant WD (eds.), *Extremophiles: Microbial life in extreme environments*. Wiley-Liss New York: 181-210.
- Jagadish KS (1988). The progress of stabilised soil construction in India, in: *Proceedings of National Seminar on Application of stabilised mud blocks in Housing and Building*, Bangalore, India, 17–43.
- Jahns T (1996). Ammonium/urea-dependent generation of a proton electrochemical potential and synthesis of ATP in *Bacillus pasteurii*. *J Bacteriol* 178: 403-409.
- Jargeat P, Gay G, Debaud JC, Marmeisse R (2000). Transcription of a nitrate reductase gene isolated from the symbiotic basidiomycete fungus *Hebeloma cylindrosporum* does not require induction by nitrate. *Mol Gen Genet* 263: 948 – 56.
- Jargeat P, Rekanalt D, Verner MC, Gay G, Debaud JC, Marmeisse R, Fraissinet – Tachet L (2003). Characterisation and expression analysis of a nitrate transporter and nitrite reductase genes, two members of a gene cluster for nitrate assimilation from the symbiotic basidiomycete *Hebeloma cylindrosporum*. *Curr Genet* 43: 199 – 205.
- Jonkers H (2007). Self healing concrete: a biological approach. In: *van der Zwaag, S. (Ed.), Self Healing Materials: An alternative Approach to 20 Centuries of Materials Science*, Springer,

Netherlands, 195–204.

- Jonkers HM, Schlangen E (2007). Crack repair by concrete-immobilized bacteria. In: Schmets, A.J.M., Van der Zwaag, S. (Eds.), *Proc. of First International Conference on Self Healing Materials*, Noordwijk, The Netherlands.
- Jonkers HM, Thijssen A, Muyzer G, Copuroglu O, Schlangen E (2010). Application of bacteria as self-healing agent for the development of sustainable concrete. *Ecol Eng* 36: 230-235.
- Jorand F, Boue´-Bigne´ F, Block JC, Urbain V (1998). Hydrophobic/hydrophilic properties of activated sludge exopolymeric substances. *Water sci technol* 37: 307 – 315.
- Kaltwasser H, Kramer J, Conger WR (1972). Control of urease formation in certain aerobic bacteria. *Archiv fur Mikrobiologie* 81: 178-196.
- Kantzas A, Ferris FG, Jha KN, Mourits FM (1992). A novel method of sand consolidation through bacteriogenic mineral plugging. In: Proc. of CIM Annual Technical Conference, Calgary.
- Kantzas A, Ferris FG, Stehmeier L, Marentette DF, Jha KN, Mourits FM (1992). A novel method of sand consolidation through bacteriogenic mineral plugging (CIM 92-46). In Proceedings of the CIM Annual Technical Conference 1992, Vol. 2, 1-15, Petroleum Society of CIM, Calgary, Canada.
- Karlsson J, Clarke AK, Chen ZY, Huggins SY, Park YL, Husic HD, Moroney JV, Samuelsson G (1998). A novel β -type carbonic anhydrase associated with the thylakoid membrane in *Chlamydomonas reinhardtii* is required for growth at ambient CO₂. *EMBO J* 17: 1208–1216.
- Karner M, Fuhrman JA (1997). Determination of active marine bacterioplankton: A comparison of universal 16S rRNA probes, autoradiography, and nucleoid staining. *Appl Environ Microbiol* 63: 1208–1213.
- Kassen R, Rainey PB (2004). The ecology and genetics of microbial diversity. *Annu Rev Microbiol* 58: 207-231.
- Kawaguchi T, Decho AW (2002). A laboratory investigation of cyanobacterial extracellular polymeric secretions (EPS) in influencing CaCO₃ polymorphism. *J Cryst Growth* 240: 230-235.
- Keefe WE (1976). Formation of crystalline deposits by several genera of the family *Enterobacteriaceae*. *Infect Immun* 14: 590–592.
- Kerr PS, Blevins DG, Rapp BJ, Randall DD (1983). Soybean leaf urease: comparison with seed urease. *Physiologia plantarum* 57: 339-345.

- Khandelwal AK, Nigam VK, Choudhury B, Mohan MK, Ghosh P (2007). Optimization of nitrilase production from a new thermophilic isolate. *J Chem Technol Biotechnol* 82: 646-651.
- Khuri AI, Cornell JA (1987). Response Surfaces: Design and Analysis. Marcel Dekker, New York.
- Kitamura M (2002). Controlling factor of polymorphism in crystallization process. *J Cryst Growth* 237-239: 2205-2214.
- Klein C, Hurlbut CS Jr (1999). Manual of Mineralogy, 21st ed., John Wiley & Sons, Inc., New York.
- Knoll AH (1985). The distribution and evolution of microbial life in the late proterozoic era. *Ann Rev Microbiol* 39: 391-417.
- Knorre H, Krumbein KE (2000). Bacterial calcification. In: Riding, E.E., Awramik, S.M. (Eds.), *Microbial Sediments*. Springer-Verlag, Berlin, 25-31.
- Kokare CR, Chakraborty S, Khopade AN, Mahadik KR (2009). Biofilm: importance and applications. *Indian Journal of Biotechnology* 8: 159-168.
- Krishnamurthy P, Parlow M, Zitzer JB (1998). *Helicobacter pylori* containing only cytoplasmic urease is susceptible to acid. *Infect Immun* 66:5060-6.
- Krulwich TA, Guffanti A (1989). The Na⁺ cycle of extreme alkalophiles: A secondary Na⁺/H⁺ antiporter and Na⁺/solute symporters. *J Bioenerget Biomembr* 21: 663-677.
- Krumbein WE (1974). On the precipitation of aragonite on the surface of marine bacteria. *Naturwissenschaften* 61:167.
- Krumbein WE (1975). Biogenic monohydrocalcite spherules in lake sediments of Lake Kivu (Africa) and the Solar Lake (Sinai). *Sedimentology* 22:631-634.
- Krumbein WE (1979). Photolithotrophic and chemoorganotrophic activity of bacteria and algae as related to beachrock formation and degradation (Gulf of Aqaba, Sinai), *Geomicrobiol J* 1:139-203.
- Kumar D, Palit A (1994). Proceeding of American Power Conference, Chicago 471-476.
- Kumar V, Gupta P (2010). Studies on Shelf-life of Fly-ash Based Azotobacter Chroococcum Formulation and its Bio-efficacy in Wheat. *Res J Agric & Biol Sci* 6: 280-282.
- Kunamneni A, Kumar KS, Singh S (2005). Response surface methodological approach to optimize the nutritional parameters for enhanced production of α -amylase in solid state fermentation by *Thermomyces lanuginosus*. *Afric J Biotechnol* 4: 708-716.
- Kuo ST (1994). A Review on the Research Experience of Coal Ash Artificial Reef in Taiwan.

- Taipower engineering 547, 22-31.
- Kurzak B, Kozlowski H, Farkas E (1992). Hydroxamic and amino hydroxamic acids and their complexes with metal ions. *Coord Chem Rev* 114: 169-200.
- Laguerre G, Maringui P, Allard MR, Charnay MP, Houvrier P, Mazurier SI, Rigottier-Gois H, Amarger N (1996). Typing of rhizobia by PCR DNA fingerprinting and PCR-restriction fragment length polymorphism analysis of chromosomal and symbiotic gene regions: application to *Rhizobium leguminosarum* and its different biovars. *Appl Environ Microbiol* 62: 2029–2036.
- Lai CI (1994). Characteristics of High Volume Fly Ash Concrete. *Taipower engineering* 551: 60-70.
- Lambert JWM, Novakowski K, Blauw M, Latil MN, Knight L, Bayona L (2010). Pamper bacteria, they will help us: Application of biochemical mechanisms in geo-environmental engineering. *ASCE Geotechnical Special Publication* 199: 618-627.
- Lappin-Scott HM, Cusack F, Costerton JW (1988). Nutrient resuscitation and growth of starved cells in sandstone cores: a novel approach to enhanced oil recovery. *Appl Environ Microbiol* 54: 1373-1382.
- Le Metayer - Levrel G, Castanier S, Oriol G, Loubiere JF, Perthuisot JP (1999). Applications of bacterial carbonatogenesis to the protection and regeneration of limestones in buildings and historic patrimony. *Sediment Geol* 126: 25 – 34.
- Lee SG, Calhoun DH (1997.) Urease from a potentially pathogenic coccoid isolate: purification, characterization, and comparison to other microbial ureases. *Infect Immun* 65: 3991-3996.
- Leuko S, Legat A, Fendrihan S, Stan-Lotter H (2004). Evaluation of the LIVE/DEAD *BacLight* Kit for Detection of Extremophilic Archaea and Visualization of Microorganisms in Environmental Hypersaline Samples. *Appl. Environ. Microbiol.* 70: 116884-6886.
- Li M, Guo H, Cheng X (2011). Application of Response Surface Methodology for Carbonate Precipitation Production Induced by Mutant Strain of *Sporosarcina pasteurii*. *Geo-Frontiers* 4079- 4088. Doi: 10.1061/41165(397)417.
- Li W, Liu LP, Chen W, Yu LJ, Li W, Yu H (2010). Calcium carbonate precipitation and crystal morphology induced by microbial carbonic anhydrase and other biological factors. *Proc Biochem* 45: 1017–1021.
- Li W, Liu LP, Zhou PP, Cao L, Yu LJ, Jiang SY (2011). Calcite precipitation induced by bacteria and bacterially produced carbonic anhydrase. *Curr Sci* 100: 502-508.

- Lian B, Hu Q, Chen J, Ji J, Teng HH (2006). Carbonate biomineralization by soil bacterium *Bacillus megaterium*. *Geochim Cosmochim Acta* 70: 5522-5535.
- Lian B, Hu QN, Chen J, Ji JF, Teng HH (2006). Carbonate biomineralization induced by soil bacterium *Bacillus megaterium*. *Geochim Cosmochim Acta* 70: 5522–5535.
- Liang ZP, Feng YQ, Meng SX, Liang ZY (2005). Preparation and properties of Urease Immobilized onto Glutaraldehyde Cross-linked Chitosan Beads. *Chin Chem Letters* 16: 135-138.
- Lippmann F (1973). Sedimentary carbonate minerals. Springer-Verlag, Berlin.
- Liu N, Bond GM, Abel A, McPherson BJ, Stringer J (2005). Biomimetic sequestration of CO₂ in carbonate form: Role of produced waters and other brines. *Fuel Process Technol* 86: 1615– 1625.
- Lowe CR (2000). Nanobiotechnology: the fabrication and applications of chemical and biological nanostructures. *Curr Opin Struct Biol* 10: 428-34.
- Lowenstam HA, Weiner S (1989). On Biomineralization. Oxford University Press, New York.
- Lv GY, Wang P, He JY, Li XN (2008). Medium Optimization for L-Cysteine Production by *Pseudomonas* sp. *Food Technol Biotechnol* 46: 395–401.
- MacLeod FA, Lappin-Scott HM, Costerton JW (1988). Plugging of a model rock system by using starved bacteria. *Appl Environ Microbiol* 54: 1365-1372.
- Malhotra VM (1999). *Making Concrete “Greener” With Fly Ash*, ACI Concrete International, 21 (5): 61-66.
- Manachini PL, Fortina MG (1998). Production in seawater of thermostable alkaline protease by a halotolerant strain of *Bacillus licheniformis*. *Biotechnol Lett* 20: 565-568.
- Mann S (2001). Biomineralization: Principles and Concepts in Bioinorganic Materials Chemistry. Oxford University Press, New York.
- Mann S (2001). Biomineralization: Principles and concepts in bioinorganic materials chemistry. Oxford University Press, Oxford.
- Marshall BJ, Barrett LJ, Prakash C, McCallun RW, Guerrant RL (1990). Urea protects *Helicobacter (Campylobacter) pylori* from the bacterial effect of acid. *Gastroenterology* 99: 697-702.
- Mc Connaughey TA, Whelan JF (1997). Calcification generates protons for nutrient and bicarbonate uptake. *Earth Sci Rev* 42: 95–117.
- McGenity TJ, Sellwood BW (1999). New approaches to studying the microbial precipitation of carbonate minerals. *Sediment Geol* 126: 5-8.

- McKay DS, Gibson EK, Thomas-Keprta KL, Vali H, Romanek CS, Clement S, Chiller XDF, Maechling CR, Zare RN (1996). Search for past life on Mars: Possible relic biogenic activity in Martian meteorite ALH84001. *Science* 273: 924–930.
- Meldrum F, Cölfen H (2008). Controlling mineral morphologies and structures in biological and synthetic systems. *Chem Rev* 108: 4332-4432.
- Merz-Preiss M, Riding R (1999). Cyanobacterial tufa calcification in two freshwater streams: ambient environment, chemical thresholds and biological processes. *Sediment Geol* 126 (1–4): 103-124.
- Mirjafari P, Asghari K, Mahinpey N (2007). Investigating the application of Enzyme carbonic anhydrase for CO₂ sequestration purposes. *J Indus Engn Chem* 46: 921-926.
- Mitchell AC, Dideriksen K, Spangler L, Cunningham A, Gerlach R (2010). Microbially enhanced carbon capture and storage by mineral-trapping and solubility-trapping. *Environ Sci Technol* 44: 5270 – 5276.
- Mitchell JK, Santamarina JC (2005). Biological considerations in geotechnical engineering. *J Geotech Geoenviron Eng* 131: 1222 – 1233.
- Mitchell AC, Ferris FG (2006). The influence of *Bacillus pasteurii* on the nucleation and growth of calcium carbonate. *Geomicrobiol J* 23: 213-226.
- Mitchell JK, Santamarina JC (2005). Biological considerations in geotechnical engineering. *J Geotech Geoenviron Eng* 131: 1222–1233.
- Mobley HLT, Hausinger RP (1989). Microbial urease: Significance, regulation and molecular characterization. *Microbiol Rev* 53: 85-108.
- Mobley HLT, Island MD, Hausinger RP (1995). Molecular biology of microbial ureases. *Microbiol Rev* 59: 451-480.
- Monger HC, Daugherty LA, Lindemann WC, Liddell CM (1991). Microbial precipitation of pedogenic calcite. *Geology* 19: 997–1000.
- Montgomery DC (1991). Design and Analysis of Experiments. 3 New York: John Wiley & Sons. Response surface methods and designs 521–563.
- Morita RY (1980). Calcite precipitation by marine bacteria. *Geomicrobiol J* 2: 63-82.
- Mörsdorf G, Kaltwasser H (1989). Ammonium assimilation in *Proteus vulgaris*, *Bacillus pasteurii* and *Sporosarcina ureae*. *Arch Microbiol* 152: 125-131.
- Morse JW (2003). Formation and Diagenesis of Carbonate Sediments. *In Treatise on GeoChemistry* 7:

- Sediments, Diagenesis and Sedimentary Rocks. Mackenzie FT (ed), Elsevier Press.
- Mortensen BM, Haber M, DeJong JT, Caslake LF, Nelson DC (2011). Effects of environmental factors on microbial induced calcite precipitation. *J Appl Microbiol* 111: 338–349.
- Mukerji K (1986). Soil block presses, Report on Global Survey, German Appropriate Technology Exchange, Dag-Hammerxjold-Weg 1, 6236 Eschborn.
- Mulrooney S, Zakharian T, Schaller RA, Hausinger RP (2001). Dual effects of ionic strength on *Klebsiella aerogenes* urease: pH dependent activation and inhibition. *Arch Biochem Biophys* 394: 280-282.
- Muñoz-Caro C, Niño A, Senent ML, Leal JM, Ibeas S (2000). Modeling of Protonation Processes in Acetohydroxamic Acid. *J Org Chem* 65: 405-10.
- Murthy MSRC, Swaminathan T, Rakshit SK, Kosugi Y (2000). Statistical optimization of lipase catalyzed hydrolysis of methyl oleate by response surface methodology. *Bioproc Bioeng* 22, 35 – 39.
- Myers RH, Montgomery DC (1995). Response Surface Methodology: Process and Product Optimization Using Designed Experiments. 1st ed., Wiley Interscience, New
- Nemati M, Voordouw G (2003). Modification of porous media permeability, using calcium carbonate produced enzymatically *in situ*. *Enzyme Microb Tech* 33: 635-642.
- Ng WS, Lee ML, Hii SL (2012). An Overview of the Factors Affecting Microbial-Induced Calcite Precipitation and its Potential Application in Soil Improvement. *WASET* 62: 723-729.
- Nielsen AT, Tolker-Nielsen T, Barken KB, Molin S (2000). Role of commensal relationships on the spatial structure of a surface-attached microbial consortium. *Environ Microbiol* 2: 59-68.
- Nielsen JL, de Muro MA, Nielsen PH (2003). Evaluation of the Redox Dye 5-Cyano-2,3-Tolyl-Tetrazolium Chloride for Activity Studies by Simultaneous Use of Microautoradiography and Fluorescence In Situ Hybridization. *Appl Environ Microbiol* 69: 641–643.
- Nielsen TH, Bonde TA, Sørensen J. (1998). Significance of microbial urea turnover in N cycling in three Danish agricultural soils. *FEMS Microbiol Ecol* 25: 147-157.
- Nilsson Ö, Sternbeck J (1999). A mechanistic model for calcite crystal growth using surface speciation. *Geochim Cosmochim Acta* 6: 217–225.
- Niño A, Muñoz-Caro C, Senent ML (2000). Suitability of different Levels of Theory for Modelling of Hydroxamic Acids. *J Mol Struct (Theochem)* 530: 291-300.

- Novitsky JA (1981). Calcium carbonate precipitation by marine bacteria. *Geomicrobiol J* 2: 375-388.
- Obst M, Dynes JJ, Lawrence JR, Swerhone GDW, Benzerara K, Karunakaran C, Tyliczszak T, Hitchcock AP (2009). Precipitation of amorphous CaCO₃ (aragonite-like) by cyanobacteria: A STXM study of the influence of EPS on the nucleation process. *Geochim Cosmochim Acta* 73: 4180-4198.
- Ogino T, Suzuki T, Kawada K (1987). The formation and transformation mechanism of calcium carbonate in water. *Geochim Cosmochim Acta* 51: 2757-2767.
- Okwadha G, Li J (2010). Optimum conditions for microbial carbonate precipitation. *Chemosphere* 81: 1143 – 1148.
- Ozgurel HG, Vipulanandan C (2005). Effect of Grain Size and Distribution on Permeability and Mechanical Behavior of Acrylamide Grouted Sand. *J Geotech Geoenviron* 131: 1457-1465.
- Packman JJ, Comings KJ, Booth DB (1999). Using turbidity to determine total suspended solids in urbanizing streams in the Puget Lowlands. *Confronting Uncertainty: Managing Change in Water Resources and the Environment*, 27-29.
- Papke RT, Ward DM (2004). The importance of physical isolation to microbial diversification. *FEMS Microbiol Ecol* 48: 293-303.
- Park IS, Hausinger RP (1995). Requirement of carbon dioxide for in vitro assembly of urease nickel metallocenter. *Sci* 267: 1156–1158.
- Park Sung-Jin, Park Yu - Mi, Chun Woo-Young, Kim Wha-Jung, Ghim Sa -Youl (2010). Calcite-Forming Bacteria for Compressive Strength Improvement in Mortar. *J Microbiol Biotechnol* 20: 782 – 788.
- Pedrozo HA, Schwartz Z, Dean DD, Harrison JL, Campbell JW, Wiederhold ML (1997). Evidence for the Involvement of Carbonic Anhydrase and Urease in Calcium Carbonate Formation in the Gravity-Sensing Organ of *Aplysia californica*. *Calcif Tissue Int* 61: 247-255.
- Pentecost A, Bauld J (1988). Nucleation of calcite on the sheaths of cyanobacteria using a simple diffusion cell. *Geomicrobiol J* 6: 129-135.
- Pettit NM, Smith SRJ, Freedman RB, Burns RG (1976). Soil urease: activity, stability and kinetic properties. *Soil Biol Biochem* 8:479-484.
- Plackett RL, Burman JP (1946). The design of optimum multifactorial experiments. *Biometrika* 33: 305–325.

- Prabhu C, Wanjari S, Puri A, Bhattacharya A, Pujari R, Yadav R, Das S, Labhsetwar N, Sharma A, Satyanarayan T, Rayalu S (2011). Region Specific Bacterial Carbonic Anhydrase for Biomimetic Sequestration of Carbon Dioxide. *Energy and Fuels* 25: 1327 – 1332.
- Prescott LM, Harley JP, Klein DA (1993). Microbiology, 2nd edn. Wm. C. Brown Publishers, Dubuque.
- Provorov NA, Vorobyov NI (2000). Population genetics of rhizobia: Construction and analysis of an "infection and release" model. *J Theor Biol* 205: 105-119.
- Purva Soni SK, Gupta LK, Gupta JK (1998). Thermostable alkaline protease from alkalophilic *Bacillus* sp. IS-3. *Indian J Microbiol* 38: 149-152.
- Pushkas LG, Inui M, Zahan K & Yukawa H (2000). A periplasmic α - type carbonic anhydrase from *Rhodospseudomonas palustris* is essential for bicarbonate uptake. *Microbiol* 146:2957–2966
- Qian C, Wang R, Cheng L, Wang J (2010). Theory of microbial carbonate precipitation and its application in restoration of cement-based materials defects. *Chin J Chem* 28: 847 – 857.
- Raiders RA, Knapp RM, McInerney MJ (1989). Microbial selective plugging and enhanced oil recovery. *J Indust Microbiol* 4: 215–230.
- Ramachandran SK, Ramakrishnan V, Bang SS (2001). Remediation of concrete using microorganisms. *American Con Inst Mat J* 98: 3-9.
- Ramakrishnan V (2007). Performance characteristics of bacterial concrete—a smart biomaterial. *In: Proceedings of the First International Conference on Recent Advances in Concrete Technology*, Washington, DC, 67 – 78.
- Ramakrishnan V, Bang SS, Deo KS (1998a). A novel technique for repairing cracks in high performance concrete using bacteria, *Proc Int Conf on High Performance High Strength Concrete*, Perth, Australia, 597–618.
- Ramakrishnan V, Panchalan R, Bang SS (1998b). Bacterial Concrete- A Self Remediating Biomaterial. *Proceedings of 10th International Congress on the Polymers in Concrete, Hawaii*.
- Ramanan R, Kannan K, Sivanesan SD, Mudliar S, Kaur S, Tripathi AK (2009). Bio-sequestration of carbon dioxide using carbonic anhydrase enzyme purified from *Citrobacter freundii*. *World J Microbiol Biotechnol* 25: 981–987.
- Randolph AD, Larson MA (1988). Theory of Particulate Processes, 2nd ed., Academic Press.
- Rao SS, Reddy BVV, Jagadish KS (1995). Strength characteristics of soil–cement block masonry. *The Indian Concrete Journal* 69: 127–131.

- Rastogi G, Muppidi GL, Gurram RN, Adhikari A, Bischoff KM, Hughes SR, Apel WA, Bang SS, Dixon DJ, Sani RK (2009). Isolation and characterization of cellulose-degrading bacteria from the deep subsurface of the Homestake gold mine, Lead, South Dakota, USA. *J Ind Microbiol Biotechnol* 36: 585-598.
- Rathi P, Goswami VK, Sahai V, Gupta R (2002). Response surface methodology for improving production of hyperthermostable lipase from *Burkholderia cepacia*. *J Appl Microbiol* 93: 930–936.
- Rawat M, Moroney JV (1995). The regulation of carbonic anhydrase and ribulose 1,5 biphosphate carboxylase / Oxygenase activase by light and CO₂ in *Chlamydomonas reinhardtii*. *Plant Physiol* 109: 937–944.
- Rebata-Landa V. 2007. Microbial activity in sediments: Effects on soil behavior. Ph.D. dissertation, Georgia Institute of Technology.
- Reddy BVV (1991). Studies on static soil compaction and compacted soil–cement blocks for walls, Ph.D. thesis, Department of Civil Engineering, Indian Institute of Science, Bangalore, India.
- Reddy BVV (2002). Long-term strength and durability of stabilised mud blocks. Proceedings 3rd International Conference on Non-Conventional Materials and Technologies, Construction Publishing House, 12 - 13 March, Hanoi, Vietnam, 422 - 431.
- Reddy BVV, Jagadish KS (1989). Properties of soil–cement block masonry, *Masonry International* 3: 80–84.
- Reddy BVV, Jagadish KS (2003). Embodied energy of common and alternative building materials and technologies. *Energy and Buildings* 35: 129 – 137.
- Rieger J, Frechen T, Cox G, Heckmann W, Schmidt C, Thieme, J. (2007). Precursor structures in the crystallization / precipitation processes of CaCO₃ and control of particle formation by polyelectrolytes. *Farad Discuss* 136: 265-277.
- Rivadeneira M.A, Delgado R, Delgado G, Moral A, Ferrer MR, Ramos-Cormenzana A (1993). Precipitation of carbonate by *Bacillus* sp. isolated from saline soils. *Geomicrobiol J* 11: 175-184.
- Rivadeneira MA, Delgado G, Ramos-Cormenzana A, Delgado R (1998). Biomineralization of carbonates by *Halomonas eurihalina* in solid and liquid media with different salinities: crystal formation sequence. *Res Microbiol* 149: 277–287.
- Rivadeneira MA, Delgado R, Quesada E, Ramos-Cormenzana A (1991). Precipitation of calcium

- carbonate by *Deleya halophila* in media containing NaCl as sole salt. *Cur Microbiol* 22: 185-190.
- Rivadeneira MA, Parraga J, Delgado R, Ramos-Cormenzana A, Delgado G (2004). Biomineralization of carbonates by *Halobacillus trueperi* in solid and liquid media with different salinities. *FEMS Microbiol Ecol* 48: 39–46.
- Rivadeneira MA, Ramos-Cormenzana A, Delgado G, Delgado R (1996). Process of carbonate precipitation by *Deleya halophila*. *Cur Microbiol* 32: 308 - 313.
- Rivadeneira MA, Delgado G, Soriano M, Ramos-Cormenzana A, Delgado R (2000). Precipitation of carbonates by *Nesterenkonia halobia* in liquid media. *Chemosphere* 41: 617–624.
- Rivadeneira MA, Delgado R, Del-Moral A, Ferrer MR, Ramos-Cormenzana A (1994). Precipitation of calcium carbonate by *Vibrio* sp. From an inland saltern. *FEMS Microbiol Ecol* 13: 197–204.
- Rivadeneira MAG, Delgado A, Ramos-Cormenzana, Delgado R (1998). Biomineralization of carbonates by *Halomonas eurihalina* in solid and liquid media with different salinities: crystal formation sequence. *Res Microbiol* 149: 277–287.
- Roche (2001). Specialty enzymes for industry. Roche Diagnostics GmbH.
- Rodríguez – Navarro C, Jroundi F, Schiro M, Ruiz-Agudo E, González –Muñoz MT (2012). Influence of substrate mineralogy on bacterial mineralization of calcium carbonate: Implications in stone conservation. *Appl Environ Microbiol* 78: 4017–4029.
- Rodríguez - Navarro C, Rodríguez-Gallego M, Ben Chekroun K, Gonzalez-Muñoz MT (2003). Conservation of ornamental stone by *Myxococcus Xanthus* induced carbonate biomineralization. *Appl Environ Microbiol* 69: 2182-2193.
- Rodríguez - Navarro, C., Jimenez-Lopez, C., Rodríguez-Navarro, A., González-Muñoz, M. T. and Rodríguez - Gallego, M. (2007). Bacterially mediated mineralization of vaterite. *Geochim Cosmochim Acta* 71: 1197 – 1213.
- Rodríguez GG, Phipps D, Ishiguro K, Ridgway HF (1992). Use of a fluorescent redox probe for direct visualization of actively respiring bacteria. *Appl Environ Microbiol* 58: 1801– 1808.
- Rodríguez-Navarro C, Rodríguez-Gallego M, Ben Chekroun K, Gonzalez-Munoz MT (2003). Conservation of ornamental stone by *Myxococcus xanthus*-induced carbonate biomineralization. *Appl Environ Microbiol* 69: 2182-2193.
- Ruiz C, Monteoliva-Sanches M, Huertas F, Ramos-Cormenzana A (1988). Calcium carbonate precipitation by several species of *Myxococcus*. *Chemosphere* 17: 835-838.

- Sadowsky MJ, Kinkel LL, Bowers JH, Schottel JL (1996). Use of repetitive intergenic DNA sequences to classify pathogenic and disease suppressive *Streptomyces* strains. *Appl Environ Microbiol* 62: 3489-3493.
- Sahrawat K (1984). Effects of temperature and moisture on urease activity in semi-arid tropical soils. *Plant and Soil* 78: 401-408.
- Samonin VV, Elikova EE (2004). A study on the absorption of bacterial cells on porous materials. *Microbiol* 73: 696-701.
- Sánchez-Navas A, Martín-Algarra A, Rivadeneyra MA, Melchor S, Martín-Ramos JD (2009). Crystal-growth behaviour in Ca-Mg carbonate bacterial spherulites. *Cryst Growth Des* 9:2690-2699.
- Sarda D, Choonia HS, Sarode DD, Lele SS (2009). Biocalcification by *Bacillus pasteurii* urease: a novel application. *J Ind Microbiol Biotechnol* 36: 1111 - 1115.
- Satyanarayana T, Raghukumar C, Shivaji S (2005). Extremophilic microbes: Diversity and perspectives. *Current Sci* 89: 78-90.
- Sawada K (1997). Mechanisms of crystal growth of ionic crystals in solution. Formation, transformation, and growth inhibition of calcium carbonates, in *Crystallization Processes*, Ohtaki, H. (Ed.), Wiley, England.
- Saxena S, Saxena RK (2004). Statistical optimization of tannase production from *Penicillium variable* using fruits (chebulic myrobalan) of *Terminalia chebula*. *Biotechnol. Appl Biochem* 39: 99-106.
- Scholl MA, Mills AL, Herman JS, Hornberger GM (1990). The influence of mineralogy and solution chemistry on the attachment of bacteria to representative aquifer materials. *J Contam Hydrol* 6: 321-336.
- Schultze-Lam S, Fortin D, Davis BS, Beveridge TJ (1996). Mineralisation of bacterial surfaces. *Chem Geol* 132: 171-181.
- Scotese AC, Kline JA (1999). Dual Inhibition of Phosphodiesterase 4 and Matrix Metalloproteinases by an (Arylsulfonyl) Hydroxamic Acid Template. *J Med Chem* 42: 541-44.
- Selenska-Pobell S, Gigova L, Petrova N (1995). Strain-specific fingerprints of *Rhizobium galegae* generated by PCR with arbitrary and repetitive primers. *J Appl Bacteriol* 79: 425-431.
- Senthilkumar SR, Kumar AB, Chandra RK, Gunasekaran P (2005). Optimization of medium composition for alkali-stable xylanase production by *Aspergillus fischeri* Fxn 1 in solid state fermentation using central composite rotary design. *Bioresour Technol* 96: 1380-1386.

- Shaffer G. (2010). Long-term effectiveness and consequences of carbon dioxide sequestration. *Nat Geosci* 3: 464-467.
- Sharma A, Bhattacharya A (2010). Enhanced biomimetic sequestration of CO₂ into CaCO₃ using purified carbonic anhydrase from indigenous bacterial strains. *J Mol Catal B* 67: 122–128.
- Sharma A, Bhattacharya A, Pujari R, Shrivastava A (2008a). Characterization of Carbonic Anhydrase from Diversified Genus for Biomimetic Carbon- dioxide Sequestration. *Indian J Microbiol* 48: 365-371.
- Sharma A, Bhattacharya A, Singh S (2009). Purification and characterization of an extracellular carbonic anhydrase from *Pseudomonas fragi*. *Proc Biochem* 44: 1293–1297.
- Sharma V, Chaudhary R, Khurana JM, Muralidhar K (2008b). In-gel detection of urease activity by nitroprusside–thiol reaction. *Phytochem Anal* 19: 99 – 103.
- Sharp RJ, Munster MJ (1986). In *Microbes in external environments*, Herbert RA, Codd GA (eds), Academia press, London, pp. 233.
- Sherr BF, Giorgio PD, Sherr EB (1999). Estimating abundance and single-cell characteristics of respiring bacteria via the redox dye CTC. *Aquat Microb Ecol* 18: 117-131.
- Shirakawa MA, Cincotto MA, Atencio D, Gaylarde CC, John VM. (2011). Effect of culture medium on biocalcification by *Pseudomonas putida*, *Lysinibacillus sphaericus* and *Bacillus subtilis*. *Braz J Microbiol* 42: 499: 507.
- Shuyun Wang, Xiaobing Lu, Zhongmin Shi (2010). The Effects of Grain Size Distribution and Structure on Mechanical Behavior of Silty Sand. *The Open Ocean Engineering Journal* 3: 82-85
- Silver S, Toth K, Scribner H (1975). Facilitated transport of calcium by cells and subcellular membranes of *Bacillus subtilis* and *Escherichia coli*. *J Bacteriol* 12: 880–885.
- Silverman D, Lindskog S (1988). The Catalytic Mechanism of Carbonic Anhydrase: Implications of a Rate-Limiting Protolysis of Water. *Acc Chem Res* 21: 30-36.
- Simon MA, Bonner JS, Page CA, Townsend RT, Mueller DC, Fuller CB, Autenrieth RL (2004). Evaluation of two commercial bioaugmentation products for enhanced removal of petroleum from a wetland. *Ecol Eng* 22: 263– 277.
- Singh A, Bishnoi NR (2012). Enzymatic hydrolysis optimization of microwave alkali pretreated wheat straw and ethanol production by yeast. *Biores Technol* 108: 94-101.
- Singh P, Cameotra SS (2004). Enhancement of metal bioremediation by use of microbial

- surfactants. *Biochem Biophys Res Commun* 319: 291-297.
- Sloan JJ, Anderson WB (1995). Calcium chloride and ammonium thiosulphate as ammonia volatilization inhibitors for urea fertilizer. *Commun Soil Sci Plant Anal* 26: 2425-2447.
- Smith KS, Ferry JG (1999). A plant-type (β -Class) carbonic anhydrase in the thermophilic methanoarchaeon *Methanobacterium thermoautotrophicum*. *J Bacteriol* 181: 6247–6253.
- Smith KS, Ferry JG (2000). Prokaryotic Carbonic anhydrases. *FEMS Microbiol Rev* 24: 335-66.
- Smith KS, Jakubzick C, Whittam TS, Ferry JG (1999). Carbonic anhydrase is an ancient enzyme widespread in prokaryotes. *Proc Natl Acad Sci USA* 96: 15184–15189.
- Sondi I, Matijevic E (2001). Homogeneous precipitation of calcium carbonates by enzyme catalyzed reaction. *J Colloid Interface Sci* 238: 208-214.
- Southam G (2000). Bacterial surface-mediated mineral formation. In: Environmental Microbe-Mineral Interactions. Lovley DR (ed) ASM Press, Washington, DC, pp 257-276.
- Spanos N, Koutsoukos PG (1998). The transformation of vaterite to calcite: effect of the conditions of the solution in contact with the mineral phase. *J Cryst Growth* 191:783-790.
- Spencer RC (2003). Bacillus anthracis. *J Clin Pathol* 56: 182-187.
- Stahler MF, Ganter L, Katherin L, Manfred K, Stephen B (2005). Mutational analysis of *Helicobacter pylori* carbonic anhydrases. *FEMS Immunol Medical Microbiol* 44: 183–189.
- Stellmach J (1984). Fluorescent redox dyes . 1 . Production of fluorescent formazan by unstimulated and phorbol ester- or digitonin-stimulated Ehrlich ascites tumor cells. *Histochem* 80: 137–143.
- Stemmler AJ, Kampf JW, Kirk ML, Pecoraro VL (1995). A Model for Inhibition of Urease by Hydroxamates. *J Am Chem Soc* 117: 6368-69.
- Stocks - Fischer S, Galinat JK, Bang SS (1999). Microbiological precipitation of CaCO₃. *Soil Biol Biochem* 31: 1563–1571.
- Stoodley P, Dodds I, Boyle JD, LappinScott HM (1999). Influence of hydrodynamics and nutrients on biofilm structure. *J Appl Microbiol* 85:19S–28S.
- Stoodley P, Sauer K, Davies DG, Costerton JW (2002). Biofilms as complex differentiated communities. *Ann Rev Micro* 56: 187-209.
- Sullivan DM, Havlin JL (1988). Agronomic use of ammonium thiosulfate to improve nitrogen fertilizer efficiency. *J Fert* 5: 37–44.
- Sumner JB (1926). The Isolation and Crystallization of the Enzyme Urease. *J Biol Chem* 69:435-441.

- Supuran CT (1994). Carbonic anhydrase inhibitors. In: Puscas, I. (Ed). Carbonic anhydrase and modulation of physiologic and pathologic processes in the organism. Timisoara (Romania): Helicon, pp 29-111.
- Supuran CT, Scozzafava A (2000b). Carbonic anhydrase inhibitors and their therapeutic potential. *Expert Opinion on Therapeutic Patents* 10: 575-600
- Supuran CT, Scozzafava A (2001). Carbonic anhydrase inhibitors. *Curr Med Chem* 1: 61-97.
- Supuran CT, Scozzafava A (2002). Applications of carbonic anhydrase inhibitors and activators in therapy. *Expert Opin Ther Patents* 12:217–242.
- Sutherland IW (2001). Biofilm exopolysaccharides: a strong and sticky framework. *Microbiol* 147: 3-9.
- Sutherland IW (2001). Biofilm exopolysaccharides: a strong and sticky framework. *Microbiology* 147: 3–9
- Suzuki M, Oka T, Okada K (1995). The estimation of energy consumption and CO₂ emission due to housing construction in Japan. *Energy and Buildings* 22: 165–169.
- Szacilowski K, Wanat A, Barbieri A, Wasielewska E, Witko M, Stochel G, Stasicka Z (2002). Reactions of the [Fe(CN)₅NO]²⁻ complex with biologically relevant thiols. *New J Chem* 26: 1495–1502.
- Tai C, Chen FB (1998). Polymorphism of CaCO₃ precipitated in a constant composition environment. *AIChE J* 44: 1790-1798.
- Tamura K, Peterson D, Peterson N, Stecher G, Nei M, Kumar S (2011). MEGA5: Molecular Evolutionary Genetics Analysis Using Maximum Likelihood, Evolutionary Distance, and Maximum Parsimony Methods. *Mol Biol Evol* 28: 2731-2739.
- Thomas-Keprta KL, McKay DS, Wentworth SJ, Stevens TO, Taunton AE, Allen C, Coleman A, Gibson EK, Romanek CS (1998). Bacterial mineralization patterns in basaltic aquifers: Implications for possible life in Martian meteorite ALH84001. *Geology* 26: 1031–1034.
- Thompson JD, Higgins DG, Gibson TJ (1994). Improved sensitivity of profile searches through the use of sequence weights and gap excision. *Comput Appl Biosci* 10:19–29.
- Tiano P, Biagiotti L, Mastromei G. (1999). Bacterial bio-mediated calcite precipitation for monumental stones conservation: methods of evaluation. *J Microbiol Methods* 36: 139 –145.
- Torsvik V, Ovreas L (2002). Microbial diversity and function in soil: From genes to ecosystems. *Curr*

- Opin Microbiol* 5: 240-245.
- Torsvik V, Sorheim R, Gokoyr J (1996). Total bacterial diversity in soil and sediment communities – a review. *J Ind Microbiol* 17: 170-178.
- Trask PD (1959). Effect of grain size on strength of mixtures of clay, sand, and water. *Geo Science World* 70: 569-580.
- Tripp BC, Smith KS, Ferry JG (2001). Carbonic anhydrase: new insights for an ancient enzyme. *J Biol Chem* 276: 48615– 48618.
- Tsuneda S, Aikawa H, Hayashi H, Yuasa A, Hirata A (2003). Extracellular polymeric substances responsible for bacterial adhesion onto solid surface. *FEMS Microbiol. Lett.* 223 (2) 287-292.
- Tsuneda S, Jung J, Hayashi H, Aikawa H, Hirata A, Sasaki H (2003). Influence of extracellular polymers on electrokinetic properties of heterotrophic bacterial cells examined by soft particle electrophoresis theory. *Colloid Surface B* 29: 181-188.
- Tyler B (1978). Regulation of the assimilation of nitrogen compounds. *Annual Rev Biochem* 47: 1127-1162.
- Van Lith Y, Warthmann R, Vasconcelos C, McKenzie JA (2003). Sulphate-reducing bacteria induce low-temperature Ca-dolomite and high Mg-calcite formation. *Geomicrobiol J* 1: 71–79.
- Van Paassen LA (2009). Biogrout: Ground Improvement by Microbially Induced Carbonate Precipitation. PhD Delft: Delft University of Technology.
- Van Paassen LA, Daza CM, Staal M., Sorokin DY, van der Zon W, van Loosdrecht MCM (2010). Potential soil reinforcement by biological denitrification. *Ecol Engn* 36: 68 - 75.
- Vasconcelos C, McKenzie JA, Bernaconi S, Grujic D, Tien AJ (1995). Microbial mediation as a possible mechanism for natural dolomite formation at low temperatures, *Nature* 377: 220–222.
- Veitch FP, Blankenship LC (1963). Carbonic anhydrase in bacteria. *Nature* 197: 76–77.
- Venter JC, Remington K, Heidelberg JF, Halpern AL, Rusch D, Eisen JA, Wu DY, Paulsen I, Nelson KE, Nelson W, Fouts DE, Levy S, Knap AH, Lomas MW, Nealson K, White O, Peterson J, Hoffman J, Parsons R, Baden-Tillson H, Pfannkoch C, Rogers YH, Smith HO (2004). Environmental genome shotgun sequencing of the Sargasso Sea. *Science* 304: 66-74.
- Ventura ON, Rama JB, Turi L, Dannenberg JJ (1993). Acidity of Hydroxamic Acids: An ab Initio and Semiempirical Study. *J Am Chem Soc* 115: 5754-61.

- Vohra A, Satyanarayana T (2002). Statistical optimization of the medium components by response surface methodology to enhance phytase production by *Pichia anomala*. *Proc Biochem* 37: 999–1004.
- Wakabayashi Y, Takamiya R, Mizuki A, Kyokane T, Goda N, Yamaguchi T, Takeoka S, Tsuchida E, Suematsu M, Ishimura Y (1999). Carbon monoxide overproduced by heme oxygenase-1 causes a reduction of vascular resistance in perfused rat liver. *Am J Physiol Gastrointest Liver Physiol* 277: G1088-G1096.
- Walker P, Reddy BVV, Mesbah A, Morel J-C (2000). The case for compressed Earth block construction, in: Proceedings of 6th International Seminar on Structural Masonry for Developing Countries, Allied Publishers Ltd., Bangalore, India, pp. 27–35.
- Walker R, Rossall S, Asher MJC (2004). Comparison of application methods to prolong the survival of potential biocontrol bacteria on stored sugar-beet seed. *J Appl Microbiol* 97: 293–305.
- Wang CY (2008). Control the polymorphism and morphology of calcium carbonate precipitation from a calcium acetate and urea solution. *Mater Lett* 62: 2377–80.
- Wang ML, Peng KW, Wen SB (1994). The study of treating fly ash as raw material of ceramic”, Proc. 9th Conf. On Waste Management Technology in Republic of China, Nov, pp.403-412.
- Wang S, Lu X, Shi Z (2010). The Effects of Grain Size Distribution and Structure on Mechanical Behavior of Silty Sand. *The Open Ocean Engineering Journal* 3: 82-85.
- Wanjari S, Prabhu C, Yadav R, Satyanarayana T, Labhsetwar N, Rayalu S (2011). Immobilization of carbonic anhydrase on chitosan beads for enhanced carbonation reaction. *Proc Biochem* 46: 1010–1018.
- Ward OP (1983). Proteinases. In Fogarty WM (ed) *Microbial enzymes and biotechnology*. Applied Science Publishers, London, England, 251-305.
- Warren LA, Ferris FG (1998). Continuum between sorption and precipitation of Fe (III) on microbial surfaces. *Envir Sci Technol* 32: 2331-2337.
- Warren LA, Haack EA (2001). Biogeochemical controls on metal behaviour in freshwater environments. *Earth Sci Rev* 54: 261–320.
- Warren LA, Maurice PA, Ferris FG (2001). Microbially mediated calcium carbonate precipitation: implications for interpreting calcite precipitation and for solid-phase capture of inorganic contaminants. *Geomicrobiol J* 18: 93-115.

- Warren LA, Maurice PA, Parmar N, Ferris FG (2001). Microbially mediated calcium carbonate precipitation: implications for interpreting calcite precipitation and for solid-phase capture of inorganic contaminants. *Geomicrobiol J* 18: 93 – 125.
- Warthman R, van Lith Y, Vasconcelos C, Mckenzie JA, Karpoff AM (2000). Bacterially induced dolomite precipitation in anoxic culture experiments. *Geol* 28:1091–1094.
- Watabe N, Sharp DG, Wilbur KM (1958). Studies on shell formation. VIII. Electron microscopy of crystal growth of the nacreous layer of the oyster *Crassostrea virginica*. *Biophys Biochem Cytol* 4: 281-286.
- Watabe N, Wilbur KM (1960). Influence of the organic matrix on crystal type in mollusks. *Nature* 188:334.
- Watanabe T, Fududa I, Isa Y, China K (2003). Molecular analyses of protein components of the organic matrix in the exoskeleton of two scleractinian coral species. *Comp Biochem Physiol B – Biochem Mol Biol* 136: 767–774.
- Whiffin VS (2004). Microbial CaCO₃ precipitation for the production of biocement [PhD thesis]. Perth: Murdoch University.
- Whiffin VS, Van Paassen L, Harkes MP (2007). Microbial carbonate precipitation as a soil improvement technique, *Geomicrobiol J* 24: 417–423.
- Whiteley CG, Lee DJ (2006). Enzyme technology and biological remediation. *Enzyme Microb Technol* 38: 291–316.
- Whitman WB, Coleman DC, Wiebe WJ (1998). Prokaryotes: The unseen majority. *Proc Natl Acad Sci* 95: 6578-6583.
- Wingard LB, Brody TM, Larner J, Schwartz A (1991). Human Pharmacology: Molecular to Clinical. St. Louis, Missouri: Mosby Year Book.
- Woese C, Kandler O, Wheelis M (1990). Towards a natural system of organisms: proposal for the domains Archaea, Bacteria, and Eucarya. *Proc Natl Acad Sci* 87: 4576-4579.
- Wolfram L, Bauerfeind P (2009). Activities of urease and nickel uptake of *Helicobacter pylori* proteins are media- and host-dependent. *Helicobacter* 14: 264-270.
- Worrell E, Price L, Martin N, Hendricks C, Ozawa Meida L (2001). Carbon Dioxide Emissions from the Global Cement Industry. *Ann Rev EnerEnviron* 26: 303-29.
- Wright DT (1999). The role of sulphate-reducing bacteria and cyanobacteria in dolomite formation in

- distal ephemeral lakes of the Coorong region, South Australia. Sediment. *Geol* 126: 147–157.
- Xin C, Yin L, Guocheng D, Jian C (2005). Application of response surface methodology in medium optimization for spore production of *Coniothyrium minitans* in solid state fermentation. *World J Microbiol Biotechnol* 21: 593–599.
- Xiong YH, Liu JZ, Song HY, Ji LN (2004). Enhanced production of extracellular ribonuclease by optimization of culture conditions using response surface methodology. *Biochem Eng J* 21: 27-32.
- Yadav R, Labhsetwar N, Kotwal S, Rayalu S (2011). Single enzyme nanoparticle for biomimetic CO₂ sequestration. *J Nanopart Res* 13: 263–271.
- Yang KI (1997). Utilization of Granulated Blast-Furnace Slag in Cement and Concrete. *Technology and Training* 22: 118-132.
- Yang L, Wang S, Tian Y (2008). Purification, Properties, and Application of a Novel Acid Urease from *Enterobacter* sp. *Appl. Biochem. Biotechnol.*, DOI .1007/s12010-008-8159-6.
- Yates KK, Robbins LL (1999). Radioisotope tracer studies of inorganic carbon and Ca in microbially derived CaCO₃. *Geochim Cosmochim Acta* 63: 129-136.
- Yoshida N, Higashimura E, Saeki Y (2010). Catalytic biomineralization of fluorescent calcite by the thermophilic bacterium *Geobacillus thermoglucosidasius*. *Appl Environ Microbiol* 75:7322-7327.
- Zamarreno DV, Inkpen R, May E (2009). Carbonate crystals precipitated by freshwater bacteria and their use as a limestone consolidant. *Appl Environ Microbiol* 75: 5981 - 5990.
- Zhang Z, Lian B, Hou W, Chen M, Li X, Shen W, Li Y (2011). Optimization of nutritional constituents for carbonic anhydrase production by *Bacillus mucilaginosus* K02. *Afr J Biotechnol* 42: 8403-8413.

Appendix I

(A) Nutrient broth

Ingredient	Quantity (g/l)
Peptone	5.0
Beef extract	1.5
Yeast extract	1.5
Sodium chloride	5.0

Boiled to dissolve the medium completely, sterilized by autoclaving at 15 lbs pressure (121°C) for 15 min, pH 7.4 ± 0.2

(B) Nutrient Broth – Urea Media (NB-U)

Ingredient	Quantity (g/l)
Peptone	5.0
Beef extract	1.5
Yeast extract	1.5
Sodium chloride	5.0
Urea	20

The pH of the media was adjusted to 6.5 with 1 N HCl prior to autoclaving without urea. Filter-sterilized urea was added later. The final pH was adjusted to 8.0 by adding 1N HCl.

(C) Nutrient Broth – Urea CaCl₂ Media (NBUC)

Ingredient	Quantity (g/l)
Peptone	5.0
Beef extract	1.5
Yeast extract	1.5
Sodium chloride	5.0
Urea	20
CaCl ₂	25 mM

The pH of the media was adjusted to 6.5 with 1 N HCl prior to autoclaving without urea and CaCl₂. Filter-sterilized urea and CaCl₂ was added later. The final pH was adjusted to 8.0 by adding 1N HCl.

(D) Tryptic soya media

Ingredient	Quantity (g/l)
Casein enzyme hydrolysates	17.0
Papaic digest of soyabean meal	3.0
Sodium chloride	5.0
Dipotassium phosphate	2.5
Dextrose	2.5

(E) Yeast extract media

Ingredient	Quantity (g/l)
Yeast extract	20g
(NH ₄) ₂ SO ₄	10g
Tris-HCl (pH 9.0)	130 mM

(F) B4 Media

Ingredient	Quantity (g/l)
Yeast extract	1 g
Glucose	1 g
Calcium acetate monohydrate	5g

(G) 295 Medium

Ingredient	Quantity (g/l)
-------------------	-----------------------

Nutrient Broth	3g
Sodium bicarbonate	12 g
Urea	10g
CaCl ₂	7.5g

(H) EPS Basal Media

Ingredient	Quantity (g/l)
Beef extract	3 g
Glucose	10 g
Peptone	10 g
NaCl	5 g

pH adjusted to 7.5 with 1N HCl.

(I) Precipitation Agar Medium

Ingredient	Quantity (g/l)
Nutrient broth	3 g
Urea	20g
NaHCO ₃	2.12 g
NH ₄ Cl	10 g
CaCl ₂ . 2H ₂ O	25 mM

pH adjusted to 8.0 with 1N HCl

(J) Luria-Bertani (LB) Medium

Ingredient	Quantity (g/l)
NaCl	10.0
Beef extract	5.0
Tryptone	10.0
Agar	10.0

pH adjusted to 8.0 with 1N NaOH, sterilized by autoclaving at 15 lbs pressure (121 °C) for 15 min, added filtered ampicillin 50 µg/ml to prepare LB - Ampicillin plates

(K) Nitrate agar

Ingredient	Quantity (g/l)
Agar	12.0
Beef extract	3.0
Peptic digest of animal tissue	5.0
Potassium nitrate	1.0

Boiled to dissolve the medium completely, sterilized by autoclaving at 15 lbs pressure (121°C) for 15 min

(L) Starch Agar

Ingredient	Quantity (g/l)
Peptic digest of animal tissue	5.0
Meat extract	3.0
Starch (soluble)	2.0
Agar	15.0

Final pH was adjusted to 7.2 ± 0.1

(M) LB/amp+ agar plates

Prepared LB broth as above, added agar (15 g/l), autoclaved, and cooled to 50°C, added ampicillin 50 µg/ml, Poured plates and stored at 4°C

(N) IPTG stock solution (0.1M)

1.2 g IPTG

Added water to 50 ml final volume, filtered and stored at 4°C

(O) X-Gal (2ml)

100 mg 5-bromo, 4 chloro, 3-indolyl, D galactoside dissolved in 2ml N,N-dimethylformamide, covered with aluminum foil and stored at 20°C

(P) LB plates with Ampicillin/IPTG/X-Gal

Prepared LB plates with ampicillin as above; 100 μ l of 100 mM IPTG and 20 μ l of 50 mg/ml X-Gal spread over the surface of LB ampicillin plate and allowed to absorb for 30 minutes at 37°C prior to use

(Q) TBE Buffer (10x)

Tris-HCl	0.09 M (pH 8)
Boric acid	0.9 M
EDTA	0.02 M (pH 8)

(R) Plasmid Extraction Solution I (10X)

Tris-HCl	25 mM (pH 8.0)
Glucose	50 mM
Na ₂ EDTA	10 mM

(S) Plasmid Extraction Solution II

NaOH	5M
SDS	10%

(T) Plasmid Extraction Solution III

5.0 M K-acetate (pH 4.5)

(U) Agarose Gel Loading Dye (6X)

Bromophenol blue	0.25%
Xylene cyanol FF	0.25%
Glycerol in water	30.0%

(V) Primers

M13 forward primer	5'-GTAAAACGACGGCCAGT-3'
M13 reverse primer	5'-CAGGAAACAGCTATGAC-3'

Rep forward primer	5'-IIICGICGICATCIGGC -3'
Rep reverse primer	5'-ICGICTTATCIGGCCTAC - 3'
BoxA1R PCR	5'CTACGGCAAGGCGACGCTGACG-3'
16S rDNA forward primer	5'-AGAGTTTGATCCTGGCTCAG-3'
16S rDNA reverse primer	5'-ACGGGCGGTGTGTTC-3'

(W) Recipes for SDS/PAGE gels and buffers

Acrylamide stock solution (30%)

Acrylamide	29.2%
N, N-methylelenebisacrylamide	0.8%

Stored in amber colored bottle at 4°C

1.5M Tris-Cl (pH 8.8)	18.5 g/100 ml
0.5M Tris-Cl (pH 6.8)	3 g/50 ml

Stacking gel (4.5%)

5 ml

Acrylamide	800 µl
Milli-Q water	2.85 ml
Tris-HCl (0.5M and pH 6.8)	1.25 ml
SDS (10%, W/V)	50 µl
TEMED	2.5 µl
APS (10%, W/V)	50 µl

Resolving Gel (12 %)

10 ml

Acrylamide	4 ml
Milli-Q water	3.35 ml
Tris-HCl (1.5M and pH 8.8)	2.5 ml
SDS (10%, W/V)	70 µl
TEMED	5 µl
APS (10%, W/V)	70 µl

Tank Buffer (1 L)

Tris-HCl	6.05 g
----------	--------

Glycine	28.8g
SDS (10%, W/V)	10 ml
2× Sample Buffer	
0.5M Tris-HCl (pH 6.8)	2.5 ml
2-mercaptoethanol	0.8 ml
SDS (10%, W/V)	2 ml
Glycerol	2 ml
Bromophenol blue	0.006 g
Final volume	10 ml

(X) Buffer Solutions

a) Phosphate buffer

0.5L of 1M K_2HPO_4 at 174.18g mol⁻¹ = 87.09g

0.5L of 1M KH_2PO_4 at 136.09g mol⁻¹ = 68.045g

Mixed an appropriate volume (ml) of A and B as shown in the table below and diluted to a total volume of 1000 ml, a 0.1 M phosphate buffer of the required pH at room temperature.

A (mL)	B (mL)	pH
13.2	86.8	6.0
19.2	80.0	6.2
27.8	72.2	6.4
38.1	61.9	6.6
49.7	50.3	6.8
61.5	38.5	7.0

b) Tris HCl 7-9 buffer

pH	Volume (L)	TrisBase (g)	HCl (ml)
7.0	2	24.2	15.0-15.5
7.5	2	24.2	12.0-12.5

8.0	2	24.2	8-8.5
8.5	2	24.2	5-5.5
9.0	2	24.2	3-3.5

c) Carbonate and bicarbonate buffer (pH 10)

Stock solution A

0.1 M Sodium carbonate. 10.599 g anhydrous Na_2CO_3 are dissolved in water and diluted to 1 L.

Stock solution B

0.1 M Sodium bicarbonate. 8.4 g NaHCO_3 are dissolved in water and diluted to 1 L.

Solution A and B were mixed in following way:

A (mL)	B (mL)	pH
5	5	9.90
6	4	10.14
7	3	10.28
8	2	10.53
9	1	10.83

d) Glycine NaOH buffer (pH 10)

(a) 0.1 M Glycine; 7.5 g/l (M.W.: 75.0)

(b) 0.1 M Sodium hydroxide; 4.0 g/l (M.W.: 40.0)

Mixed 50 ml of glycine and added given volume of sodium hydroxide solution and adjusted the final volume to 200 ml with deionized water.

pH	ml Sodium hydroxide
8.6	4.0
9.0	8.8
9.4	16.8
9.8	27.2
10.0	32.0
10.4	38.6
10.6	45.5

(Y) Chemicals and Media

All chemicals and reagents used for microbiological and chemical determinations were of the highest analytical grade and purchased from Sigma unless otherwise specified. Standard media components were purchased from Fisher Scientific (USA) or Sigma Aldrich (USA) and Hi-Media (Mumbai, India). Enzymes, Restriction enzymes and other chemicals of molecular biology grade were procured from New England Biolabs, UK.

Appendix II

16S rRNA sequences of bacterial isolates

Bacillus megaterium strain SS3 16S ribosomal RNA gene, complete sequence

GenBank: KC121060.1

[FASTA Graphics](#)

[Go to:](#)

LOCUS KC121060 1543 bp DNA linear BCT

27-JAN-2013

DEFINITION Bacillus megaterium strain SS3 16S ribosomal RNA gene, complete sequence.

ACCESSION KC121060

VERSION KC121060.1 GI:443404545

KEYWORDS .

SOURCE Bacillus megaterium

ORGANISM [Bacillus megaterium](#)

Bacteria; Firmicutes; Bacilli; Bacillales; Bacillaceae;

Bacillus.

REFERENCE 1 (bases 1 to 1543)

AUTHORS Reddy,S.M., Dhami,N.K. and Mukherjee,A.

TITLE Biomineralization of calcium carbonate by bacterial isolates from calcareous soils

JOURNAL Unpublished

REFERENCE 2 (bases 1 to 1543)

AUTHORS Reddy,S.M., Dhami,N.K. and Mukherjee,A.

TITLE Direct Submission

JOURNAL Submitted (02-NOV-2012) Biotechnology, Thapar University, Bhadson Road, Patiala, Punjab 147004, India

COMMENT ##Assembly-Data-START##

Sequencing Technology :: Sanger dideoxy sequencing

##Assembly-Data-END##

FEATURES Location/Qualifiers

source 1..1543

/organism="Bacillus megaterium"

/mol_type="genomic DNA"

/strain="SS3"

/isolation_source="calcareous soil"

/db_xref="taxon:[1404](#)"

rRNA

/country="India"
1..1543
/product="16S ribosomal RNA"

ORIGIN

```
1 agagtttgat cctggctcag gatgaacgct ggcggcgtgc ctaatacatg caagtcgagc
61 gaactgatta gaagcttgct tctatgacgt tagcggcgga cgggtgagta acacgtgggc
121 aacctgcctg taagactggg ataacttcgg gaaaccgaag ctaataccgg ataggatcct
181 ctccctcatg ggagatgatt gaaagatggt ttcggctatc acttacagat gggcccacgg
241 tgcattagct agttggtgag gtaacggctc accaaggcaa cgatgcatag ccgacctgag
301 agggtgatcg gccacactgg gactgagaca cggcccagac tcctacggga ggcagcagta
361 gggaatcttc cgcaatggac gaaagtctga cggagcaacg ccgcgtgagt gatgaaggct
421 ttcgggtcgt aaaactctgt tgtagggaa gaacaagtac aagagtaact gcttgtacct
481 tgacggtacc taaccagaaa gccacggcta actacgtgcc agcagccgcg gtaatacgt
541 ggtggcaagc gttatccgga attattgggc gtaaagcgcg cgcagcgggt ttcttaagtc
601 tgatgtgaaa gcccacggct caaccgtgga gggtcattgg aaactgggga acttgagtgc
661 agaagagaaa agcgggaattc cacgtgtagc ggtgaaatgc gtagagatgt ggaggaacac
721 agtggcgaag gcggtttttt ggtctgtaac tgacgctgag gcgcgaaagc gtggggagca
781 aacaggatta gataccctgg tagtccacgc cgtaaacgat gagtgctaag tgttagaggg
841 tttccgccct ttagtgctgc agctaacgca ttaagcactc cgcctgggga gtacggtcgc
901 aagactgaaa ctcaaaggaa ttgacggggg cccgcacaag cggtgaggca tgtggtttaa
961 ttcgaagcaa cgcaagaac cttaccaggc cttgacatcc tctgacaact ctagagatag
1021 agcgttcccc ttcgggggac agagtgacag gtggtgcatg gttgtcgtca gctcgtgctc
1081 tgagatggtg ggtaagtcc cgcaacgagc gcaacccttg atcttagttg ccagcattta
1141 gttgggcact ctaagggtgac tgccggtgac aaaccggagg aagggtggga tgacgtcaaa
1201 tcatcatgcc cttatgacc tgggctacac acgtgctaca atggatggta caaagggctg
1261 caagaccgcg aggtcaagcc aatcccataa aaccattctc agttcggatt gtaggctgca
1321 actcgectac atgaagctgg aatcgctagt aatcgcggat cagcatgccg cgggtaatac
1381 gttcccgggc cttgaacaca ccgcccgtca caccacgaga gtttgtaaca cccgaagtgc
1441 gtggagtaac cgtaaggagc tagccgccta aggtgggaca gatgattggg gtgaagtcgt
1501 aacaaggtag ccgtatcgga aggtgcggtt ggatcacctc ctt //
```

Bacillus cereus strain SS5 16S ribosomal RNA gene, complete sequence

GenBank: KC121061.1

[FASTA Graphics](#)

[Go to:](#)

LOCUS KC121061 1470 bp DNA linear BCT
27-JAN-2013
DEFINITION Bacillus cereus strain SS5 16S ribosomal RNA gene,
complete sequence.
ACCESSION KC121061
VERSION KC121061.1 GI:443404546
KEYWORDS .
SOURCE Bacillus cereus
ORGANISM [Bacillus cereus](#)
Bacteria; Firmicutes; Bacilli; Bacillales; Bacillaceae;
Bacillus; Bacillus cereus group.
REFERENCE 1 (bases 1 to 1470)
AUTHORS Reddy,S.M., Dhami,N.K. and Mukherjee,A.
TITLE Biomineralization of calcium carbonate by bacterial
isolates from calcareous soils
JOURNAL Unpublished
REFERENCE 2 (bases 1 to 1470)
AUTHORS Reddy,S.M., Dhami,N.K. and Mukherjee,A.
TITLE Direct Submission
JOURNAL Submitted (02-NOV-2012) Biotechnology, Thapar University,
Bhadson Road, Patiala, Punjab 147004, India
COMMENT ##Assembly-Data-START##
Sequencing Technology :: Sanger dideoxy sequencing
##Assembly-Data-END##
FEATURES Location/Qualifiers
source 1..1470
/organism="Bacillus cereus"
/mol_type="genomic DNA"
/strain="SS5"
/isolation_source="calcareous soil"
/db_xref="taxon:[1396](#)"
/country="India"
[rRNA](#) 1..1470
/product="16S ribosomal RNA"

ORIGIN

1 agagtttgat cctggctcag gatgaacgct ggcggcgtgc ctaatacatg caagtcgagc
61 gaatggatta agagcttgct cttatgaagt tagcggcgga cgggtgagta acacgtgggt
121 aacctgcca taagactggg ataactccgg gaaaccgggg ctaataccgg ataacatttt
181 gaaccgcatg gttcgaaatt gaaaggcggc ttcggctgtc acttatggat ggaccgcgt
241 cgcattagct agttggtgag gtaacggctc accaaggcaa cgatgcgtag ccgacctgag
301 agggtgatcg gccacactgg gactgagaca cggcccagac tcctacggga ggcagcagta
361 gggaatcttc cgcaatggac gaaagtctga cggagcaacg ccgcgtgagt gatgaaggct
421 ttcgggtcgt aaaactctgt tgttaggaa gaacaagtgc tagttgaata agctggcacc
481 ttgacggtac ctaaccagaa agccacggct aactacgtgc cagcagccgc ggtaatacgt
541 aggtggcaag cgttatccgg aattattggg cgtaaagcgc gcgcaggtgg tttcttaagt
601 ctgatgtgaa agcccacggc tcaaccgtgg agggtcattg gaaactggga gacttgagtg
661 cagaagagga aagtggaatt ccatgtgtaa cggtgaaatg cgtagagata tggaggaaca
721 ccagtggcga aggcgacttt ctggtctgta actgacactg aggcgcgaaa gcgtggggag
781 caaacaggat tagataccct ggtagtccac gccgtaaacg atgagtgcta agtgttagag
841 ggtttccgcc ctttagtgct gaagttaacg cattaagcac tccgcctggg gagtacggcc
901 gcaaggctga aactcaaagg aattgacggg ggcccgcaca agcgggtggag catgtggttt
961 aattcgaagc aacgcgaaga accttaccag gtcttgacat cctctgacaa ccctagagat
1021 agggcttctc cttcgggagc agagtgacag gtggtgcatg gttgtcgtca gctcgtgctc
1081 tgagatggtg ggtaagtcc cgcaacgagc gcaacccttg atcttagttg ccatcattta
1141 gttgggcaact ctaagggtgac tgccgggtgac aaaccggagg aagggtggga tgacgtcaa
1201 tcatcatgcc cttatgacc tgggctacac acgtgctaca atggacggta caaagagctg
1261 caagaccgcg aggtggagct aatctcataa aaccgttctc agttcggatt gtaggctgca
1321 actcgcttac atgaagctgg aatcgctagt aatcgcgat cagcatgccg cgggtgaatac
1381 gttcccgggc cttgaacaca ccgccgtca caccacgaga gtttgtaaca cccgaagtcg
1441 gtggggtaac cttttggagc cagccgccta//

Bacillus subtilis strain SS13 16S ribosomal RNA gene, complete sequence

GenBank: KC121062.1

[FASTA Graphics](#)

[Go to:](#)

LOCUS KC121062 1456 bp DNA linear BCT
27-JAN-2013
DEFINITION Bacillus subtilis strain SS13 16S ribosomal RNA gene,
complete sequence.
ACCESSION KC121062
VERSION KC121062.1 GI:443404547
KEYWORDS .
SOURCE Bacillus subtilis
ORGANISM [Bacillus subtilis](#)
Bacteria; Firmicutes; Bacilli; Bacillales; Bacillaceae;
Bacillus.
REFERENCE 1 (bases 1 to 1456)
AUTHORS Reddy,S.M., Dhami,N.K. and Mukherjee,A.
TITLE Biomineralization of calcium carbonate by bacterial
isolates from calcareous soils
JOURNAL Unpublished
REFERENCE 2 (bases 1 to 1456)
AUTHORS Reddy,S.M., Dhami,N.K. and Mukherjee,A.
TITLE Direct Submission
JOURNAL Submitted (02-NOV-2012) Biotechnology, Thapar University,
Bhadson Road, Patiala, Punjab 147004, India
COMMENT ##Assembly-Data-START##
Sequencing Technology :: Sanger dideoxy sequencing
##Assembly-Data-END##
FEATURES Location/Qualifiers
source 1..1456
/organism="Bacillus subtilis"
/mol_type="genomic DNA"
/strain="SS13"
/isolation_source="calcareous soil"
/db_xref="taxon:[1423](#)"
/country="India"
rRNA 1..1456
/product="16S ribosomal RNA"

ORIGIN

1 agagtttgaa tggctcagga cgaacgcacc cgggcgtgcc taatacatgc aagtcgagcg
61 aattgatggg agcttgctcc ctgatgtag acggcggacg tgagtaacac gtgggtaccg
121 cgggtgcctg taagactggg ataactccgg gaaaccgggg ctaataaccgg atgcttgttt
181 gaaccgcatg gttcagacat aaaaggtggc ttgccggcta ccacttacag atggaccgc
241 ggcgcataag gtagttggg aggtaacgaa gtcaccagc ggcaacgatg cgtagccgac
301 ctgagggggg gatcggccac actgggactg agacacggcc cagactccta ggggaggcag
361 cagtaggggt aatcttccgc aatggacgaa agcctgacgg agcaacgccg caagagtgat
421 gaaggttttc ggtccgtaaa gctctgttgt tagggaagaa caagtgccgt tcaaataggg
481 cggcaccttg acggtaccta ccagaaacac ggctaactac ttgccacacc cgcggtaata
541 cgtaggtggc aagcgttgtc cggatttatt gggcgtaagg gctcgcaggc ggtttcttag
601 tctgatggga aagccccgg ctcaaccggg gagggtcatt ggaaactggg gcacttgagt
661 gcagaagagg agagtggaat tccacgtgta gcggtgaaat gcgtagagat gtggaggaac
721 accagtggcg aaggcgactc tctggtctgt aactgacgct gaggagcgaa agcgtgggag
781 cgaacaggat tagataccct ggtagtccac gccgtaaacg atgagtgcta agtggtaggg
841 ggtttccgcc ctttagtgct gcagetaacg cattaagcac tccgcctggg gagtacggtg
901 gcttaagact gaaactcaaa ggaattgacg ggggcccgca caagcgggtg agcatgtggt
961 ttaattcgaa gcaacgcgaa gaaccttagg tcttgacatc ctctgacaat cctagagata
1021 ggacgtcccc ttcgggggca gagtaggtgg tgcattggtg gcgtcagctc gtgtcgtgag
1081 atgttgggtt aagtcccgca acgagcgcaa cccttgatca tatttgccag cattcagttg
1141 ggcactctaa ggtgactgcc ggtgacaaac cggaggaagg tggggatgac gtcaaatcat
1201 catgcccctt atgacctggg ctacacacgt gctacaatgg gcagaacaaa gggcagcgaa
1261 cgcgagggta aagccaaccc cacaaaatct gttctcgttc ggatcgcagt ccgctgcaac
1321 tcgactgctg gaagctggaa tcgctagtaa tcgcggatca gcatgccgcg gtgaatacgt
1381 tcccgggcct tgtacacacc gcccgtcaca ccacgagagt ttgtaacacc cgaagtcggt
1441 gaggtaacct ttatgg //

Bacillus thuringiensis strain SS15 16S ribosomal RNA gene, complete sequence

GenBank: KC121063.1

[FASTA Graphics](#)

[Go to:](#)

LOCUS KC121063 1475 bp DNA linear BCT
27-JAN-2013
DEFINITION Bacillus thuringiensis strain SS15 16S ribosomal RNA gene,
complete sequence.
ACCESSION KC121063
VERSION KC121063.1 GI:443404548
KEYWORDS .
SOURCE Bacillus thuringiensis
ORGANISM [Bacillus thuringiensis](#)
Bacteria; Firmicutes; Bacilli; Bacillales; Bacillaceae;
Bacillus; Bacillus cereus group.
REFERENCE 1 (bases 1 to 1475)
AUTHORS Reddy,S.M., Dhami,N.K. and Mukherjee,A.
TITLE Biomineralization of calcium carbonate by bacterial
isolates from calcareous soils
JOURNAL Unpublished
REFERENCE 2 (bases 1 to 1475)
AUTHORS Reddy,S.M., Dhami,N.K. and Mukherjee,A.
TITLE Direct Submission
JOURNAL Submitted (02-NOV-2012) Biotechnology, Thapar University,
Bhadson Road, Patiala, Punjab 147004, India
COMMENT ##Assembly-Data-START##
Sequencing Technology :: Sanger dideoxy sequencing
##Assembly-Data-END##
FEATURES Location/Qualifiers
source 1..1475
/organism="Bacillus thuringiensis"
/mol_type="genomic DNA"
/strain="SS15"
/isolation_source="calcareous soil"
/db_xref="taxon:[1428](#)"
/country="India"
rRNA 1..1475
/product="16S ribosomal RNA"

ORIGIN

1 agagtttgat cctggctcag gatgaacgct ggcgggggtgc ctaatacatg caagtcgagc
61 gaatgaatta agagcttgct cttatgaagt tagcggcgga cgggtgagtt acacgtgggt
121 aacctgcccc taagactggg ataactccgg gaaaccgggg ctaataccgg ataacatttt
181 gaaccgcatg gttcaaaatt gaaaggcggc ttcggctgtc acttatggat ggacccgctg
241 cgcattagct agttggtgag gtaacggctc accaaggcaa cgatgcgtag ccgacctgag
301 agggtgatcg gccacactgg gactgagaca cggcccagac tcctacggga ggcagcagta
361 gggaatcttc cgcaatggac gaaagtctga cggagcaacg ccgcgtgagt gatgaaggct
421 ttcgggtcgt aaaactctgt tgttagggaa gaacaagtgc tagttgaata agctggcacc
481 ttgacggtac ctaaccagaa agccacggct aactacgtgc cagcagccgc ggtaatacgt
541 atgtggcaag cgttatccgg aattattggg cgtaagcgcg cgcacgtggg ttcttaagtc
601 tgatgtgaag cccacggctc aaccgtggag ggtcattgga aactgggaga cttgagtgca
661 gaagaggaaa gtggaattcc atgtgtagcg gtgaaatgcy tagagatatg gaggaacacc
721 agtggcgaaa gcgactttct ggtctgtaac tgacactgag gcgcgaaagc gtggggagca
781 aacaggatta gataccctgg tagtccccgc cgtaaacgat gagtgctaag tgttagaggg
841 ttcccgccct ttagtgctga agttaacgca ttaagcactc cgcttgggga gtacggccgc
901 aaggctgaaa ctcaaaggaa ttgacggggg cccgcacaag cgggtggagca tgtggtttaa
961 ttcgaagcaa cgcgaagaac cttaccaggt cttgacatcc tctgacaacc ctagagatag
1021 ggcttctcct tcgggagcag agtgacaggt ggtgcatggt tgtcgtcagc tcgtgtcgtg
1081 agatgttggg ttaagtcccg caacgagcgc aacccttgat cttagttgcc atcatttagt
1141 tgggcactct aagggtgactg ccggtgacaa accggaggaa ggtggggatg acgtcaaac
1201 atcatgcccc ttatgacctg ggctacacac gtgctacaat ggacggtaca aagagctgca
1261 agaccgagag gtggagctaa tctcataaaa ccgttctcag ttcggattgt aggctgcaac
1321 tcgcctacat gaagctggaa tcgctagtaa tcgcggatca gcatgccgcy gtgaatacgt
1381 tcccgggcct tgaacacacc gcccgtcaca ccacgaccgt ttgtaacacc agtcggtggg
1441 gtaacctttt gccggtagcc gcctgtggga cagat //

Lysinibacillus fusiformis strain SS18 16S ribosomal RNA gene, complete sequence

GenBank: KC121064.1

[FASTA Graphics](#)

[Go to:](#)

LOCUS KC121064 1407 bp DNA linear BCT
27-JAN-2013
DEFINITION Lysinibacillus fusiformis strain SS18 16S ribosomal RNA
gene, complete sequence.
ACCESSION KC121064
VERSION KC121064.1 GI:443404549
KEYWORDS .
SOURCE Lysinibacillus fusiformis
ORGANISM [Lysinibacillus fusiformis](#)
Bacteria; Firmicutes; Bacilli; Bacillales; Bacillaceae;
Lysinibacillus.
REFERENCE 1 (bases 1 to 1407)
AUTHORS Reddy,S.M., Dhami,N.K. and Mukherjee,A.
TITLE Biomineralization of calcium carbonate by bacterial
isolates from calcareous soils
JOURNAL Unpublished
REFERENCE 2 (bases 1 to 1407)
AUTHORS Reddy,S.M., Dhami,N.K. and Mukherjee,A.
TITLE Direct Submission
JOURNAL Submitted (02-NOV-2012) Biotechnology, Thapar University,
Bhadson Road, Patiala, Punjab 147004, India
COMMENT ##Assembly-Data-START##
Sequencing Technology :: Sanger dideoxy sequencing
##Assembly-Data-END##
FEATURES Location/Qualifiers
source 1..1407
/organism="Lysinibacillus fusiformis"
/mol_type="genomic DNA"
/strain="SS18"
/isolation_source="calcareous soil"
/db_xref="taxon:[28031](#)"
/country="India"
rRNA 1..1407
/product="16S ribosomal RNA"

ORIGIN

1 agagtttgat cctggctcag gacgaacgct ggcggcgtgc ctaatacatg caagtcgagc
61 gaacagaaaa ggagcttgct cctttgacgt tagcggcgga cgggtgagta acacgtgggc
121 aacctaccct atagtttggg ataactccgg gaaaccgggg ctaataaccga ataactctct
181 ttgcttcatg gtgaaagact gaaagacggt ttcggctgtc gctataggat gggcccgcgg
241 cgcattagct agttggtgag gtaacggctc accaaggcgg cgacgcgtag ccgacctgag
301 agggatgatc gccacactgg gactgagaca cggcccagac tcctacggga ggcagcagta
361 gggaatcttc cacaatgggc gaaagcctga tggagcaacg ccgcgtgagt gaagaaggtt
421 ttcggatcgt aaaactctgt tgtaagggaa gaacaagtac agtagtaact ggctgtacct
481 tgacgggtacc ttattagaaa gccacggcta actacgtgcc agcagccgcg gtaatacgta
541 tgtggcaagc gttgtccgga attattgggc gtaaagcgcg cgcagcggtc ctttaagtct
601 gatgtgaagc ccacggctca accgtggagg gtcattggaa actgggggac ttaagtgcag
661 aagaggaaag tgggaattcca agtgtagcgg tgaaatgcgt agagatttgg aggaacacca
721 gtggcgaagg cgactttctg gtctgtaact gacgctgagg cgcgaaagcg tggggagcaa
781 acaggattag ataccctggt agtccacgcc gtaaacgatg agtgctaagt gttagagggt
841 ttccgcccct tagtgetgca gctaacgcat taagcactcc gcctggggag tacggtcgca
901 agactgaaac tcaaaggaat tgacgggggc ccgcacaagc ggtggagcgt gtggtttaat
961 tcgaagcaac gcgaagaacc ttaccaggtc ttgacatccc gttgaccact gtagagatat
1021 agtttcccct tcgggggcaa cgggtgacagg tgggtgcatgg ttgtcgtcag ctctgtcgt
1081 gagatgttgg gttaagtccc gcaacgagcg caacccttga tcttagttgc catcatttag
1141 ttgggcactc taaggtgact gccggtgaca aaccggagga aggtggggat gacgtcaaat
1201 catcatgccc cttatgacct gggctacaca cgtgctacaa tggacgatac aaacggttgc
1261 caactcgcga gagggagcta atccgataaa gtcgttctca gttcggattg taggctgcaa
1321 ctcgcctaca tgaagccgga atcgctagta atcgcggatc agcatgccgc ggtgaatagc
1381 ttcccgggcc ttgaacacac cgcccgt //